# Cortical regulation of sleep




Dr Lukas Bernhard Krone

Hertford College, University of Oxford

Department of Anatomy, Physiology and Genetics

Trinity Term 2021

*Thesis submitted for the degree of*
*Doctor of Philosophy*

*"If sleep does not serve an absolutely vital function, then it is the biggest mistake the evolutionary process has ever made"*

Allan Rechtschaffen

# Abstract

Sleep is vital but the regulation of sleep is poorly understood. Over the past decades, several subcortical regions in the mammalian brain have been identified, which promote wakefulness or sleep and constitute a 'sleep switch'. The neurophysiology of the circadian clock, with the suprachiasmatic nucleus of the hypothalamus at its centre, has also been elucidated. However, it is still unclear how the brain tracks the accumulating sleep debt during wakefulness and adjusts the duration and intensity of sleep accordingly. This core process of sleep regulation, termed 'sleep homeostasis', remains enigmatic. The cortex engages in characteristic oscillations during sleep that serve as electroencephalographic (EEG) markers of rapid eye movement (REM) and non-rapid eye movement (NREM) sleep. Slow waves, the hallmark of NREM sleep, indicate the depth of sleep and are used to determine the level of the homeostatic process. The aim of my DPhil project was to probe in mice whether cortex, and in particular neocortical layer 5 pyramidal neurons, contribute to the regulation of slow waves and sleep.

This project was divided into three subprojects. First, I present laminar recordings of neocortical activity during sleep in wild type mice, which suggest that layer 5 actively drives slow waves. Next, I describe the validation of a chemogenetic tool, which I initially planned to use for the manipulation of layer 5 pyramidal neurons. These experiments revealed unexpected effects of the chemogenetic actuators clozapine-N-oxide (CNO) and Compound 21 (Cmpd21) on sleep in wild type mice, which do not express designer receptors exclusively activated by designer drugs (DREADDs). Finally, I present extensive work on 'cortical SNAP25-ablated' (*Rbp4-Cre;Ai14;Snap25*$^{fl/fl}$) mice, which served as a model for chronic silencing of neocortical layer 5 pyramidal and archicortical dentate gyrus granule cells. These mice displayed changes in neocortical dynamics during NREM sleep, a strong increase in wakefulness, and a reduced homeostatic response to sleep deprivation, while circadian measures were unaltered.

Together, my work suggests that the cortex may play an essential role in the regulation of sleep oscillations, architecture, and homeostasis. Further investigation into the cortical regulation of sleep could reveal neural circuits and molecular mechanisms underlying sleep homeostasis and identify novel targets for the manipulation of sleep in the clinic.

Thesis word count: ~47,500

# Acknowledgements

First and foremost, I would like to express my deep gratitude to my supervisors Prof Vladyslav Vyazovskiy, Prof Zoltán Molnár, and Prof Colin Akerman. To Vlad, thank you for being such an incredible supervisor and mentor, for your immense patience and unyielding support, for all you have taught me as a scientist and as a person. To Zoltán, thank you for your enthusiasm, encouragement, and support in all matters of life. Your trust, optimism, and wisdom have been crucial at so many critical stages of my DPhil, during our paper revisions, and during my Cortex Club presidency. To Colin, thank you for all your great support and advice. Your input has been invaluable and you have always helped me redirect my projects in the right direction.

I am very grateful to my postdoc supervisors. To Tomoko, thank you for setting the foundations for this project and for all your patience in teaching me electrophysiology. To Anna, thank you for your relentless support and for sharing not only your vast knowledge and skills, but also your delicious homegrown courgettes, pumpkins and plums.

To all the friendly staff members at DPAG, the BSB, and the university who go out of their way to make things work. Particular thanks to Sarah Noujaim and Dr Deborah Clarke who helped me break through Oxford's administrative jungle, to the IT experts Jen, Simon, and Sean who fixed various computer issues and kept my data safe, to the animal care and veterinary teams who ensured the welfare of our animals, to Pamela Stanworth for helping me with Microsoft Word, and to Carl Wenczek who taught me graphics design and created the mouse illustrations which are included in this thesis.

To all my colleagues and friends in the lab in particular Laura, Martin, Cristina, Mathilde, Linus, and Prius– I wish I could name you all! Having won your friendship has been the most valuable award of this degree. Thank you for sharing all the joy and disappointments of research and for so many great moments outside the lab, especially on our trips to Sienna, Prague, Lucca, Galveston, Basel, London, Vancouver, and Ascona. Many thanks to Laura, Sian, and Christian for proofreading parts of this thesis. To my Cortex Club friends, in particular Tai-Ying, Raf, Marta, Paula, Nicole, and Abishek. The countless events we organised together have taught me more about neuroscience than any university course ever could. I deeply enjoyed being part of such an inspiring, creative, and mutually supportive society. To the boys in the boat, in particular Lukas, Mantas, and Sam, thank you for keeping

me afloat throughout all these years. You have taught me to keep the rhythm when it hurts most and to push hard at the critical moments. If it was not for our friendship and our shared goals, I would have never cycled through the sleet to Abingdon at 5 am, slept a whole week with sore muscles and blistery hands on a 1.80 m long bunk bed in Amsterdam, or endured the hypothermia and fatigue on our 160 km row from Oxford to London.

To Anna, Sam & Maria, Yuri & Rebecca, Jason, Michael, Lilly & Christian, Liisa & Axel, Mimi, Ivo & Ele, Divya & Edwin, Leonie, Teele, Marysia & Brian who made me feel home here in Oxford. I am hugely grateful for our friendship and all your support. You have kept me sane over the course of my DPhil and brought colour to the many grey and rainy days in this country. To Franny, without you I would not be here.

Special thanks go to all my friends back home who have been immensely loyal and supportive throughout these years, in particular to Katha & Benni, Markus, Lisa, Jakob, Jan and Betsy & Chris who repeatedly arranged their holidays around my experiments, conferences, and deadlines. Constanta, thank you for bringing so much happiness into my life throughout three lockdowns, weeks of uncertainty, and months of paper revisions. I am most grateful to my parents, Verena & Andreas, my brother Manuel, his wife Silja, and their wonderful children. You have always been there when I needed you most. You are my core and I truly could not have done this without you!

I would also like to thank everyone who invested into my education – I am committed to give back in future years. To the German taxpayers for more than two decades of free education from elementary school to my medical doctorate. To the Max-Weber Programm Bayern, the Studienstifung des Deutschen Volkes, Hertford College Oxford and the Wellcome Trust for the generous studentships, which allowed me to study free of financial worries. To the German Neurological Society, German Association for Psychiatry, Psychotherapy and Psychosomatics, European Sleep Research Society, World Sleep Society, the Medical Sciences Division and Merton College Oxford, who sponsored my attendances at conferences and summer schools.

Finally, I would like to thank all those who committed their time to teach me and grow my interest in science. Special thanks go to Prof Gero Miesenböck, Prof Adam Packer, Prof David Dupret, and Prof David Bannerman for their stimulating feedback on this project during my transfer and confirmation of status examinations as well as to Prof Irene Tracey and Prof Nick Franks for agreeing to examine this thesis.

# Declaration and attributions

I declare that no part of this thesis has been, or is being, submitted for any qualification other than the degree of Doctor of Philosophy at the University of Oxford.

Parts of this thesis, mostly presented in chapters 2, 3 and 5, have recently been published in *Nature Neuroscience* (Krone et al. 2021). Several figure panels and text elements, which were my own work, overlap between this publication and the thesis presented here. The surgeries and recordings, which provided the dataset for my laminar analysis presented in chapter 3, were conducted in collaboration with Dr Martin Kahn. The project presented in chapter 5 was performed with relevant support from several colleagues. Pilot experiments were conducted by Dr Tomoko Yamagata and two of the animals included in the analysis were recorded by her. Dr Tomoko Yamagata, Dr Cristina Blanco, Dr Mathilde Guillaumin, Dr Martin Kahn, and Dr Laura McKillop supervised my initial implant surgeries and recordings. The general liner model to compare the change in slow wave activity per wake duration between genotypes was created by Dr Vincent van der Vinne. All histological work was closely supervised by Dr Anna Hoerder-Suabedissen. Our histological work to determine the Cre-expression pattern in the cortical SNAP25-ablated mouse model was later expanded and optimised by her and I am grateful for her permission to include some of her histological images in subchapter 5.3.1 of this thesis. The figure legends clearly indicate histological images, which were not my own work. The circadian screen was supervised by Prof Stuart Peirson, Dr Eric Tam and Dr Vincent van der Vinne. Dr Eric Tam, Dr Vincent van der Vinne, Dr Laura McKillop and Dr Mathilde Guillaumin advised me on the statistical analysis presented chapters 3 and 5.

Some parts of the introduction and discussion chapters have been published in a book chapter (Krone and Vyazovskiy 2019) and in a scientific commentary in *Brain* (Krone and Vyazovskiy 2020), which I have written jointly with Prof Vladyslav Vyazovskiy.

# Table of contents

**Abstract** ..... **II**

**Acknowledgements** ..... **III**

**Declaration and attributions** ..... **V**

**Table of contents** ..... **VI**

**Table of figures** ..... **VIII**

**Abbreviations** ..... **X**

**Chapter 1: Introduction** ..... **1**

1.1 Sleep as an essential behaviour ..... 1

1.2 What is sleep and how can it be measured? ..... 1

1.3 Sleep wake circuitry – the subcortical sleep switch ..... 6

1.4 Circadian and homeostatic regulation of sleep ..... 10

1.5 Electrophysiological markers of sleep homeostasis ..... 14

1.6 Local use-dependent sleep – a cortical phenomenon ..... 17

1.7 Hypothesis and project aims ..... 26

**Chapter 2: General methods** ..... **28**

2.1 Mouse breeding and husbandry ..... 28

2.2 Surgical procedures ..... 29

2.3 Experimental procedures for sleep experiments ..... 34

2.4 Electrophysiological recordings ..... 36

2.5 Statistical procedures ..... 38

2.6 Histological methods ..... 40

**Chapter 3: Laminar profile of neocortical activity during NREM sleep** ..... **43**

3.1 Introduction ..... 43

3.2 Methods ..... 48

3.3 Results ..... 49

3.4 Discussion ..... 63

**Chapter 4: Validating tools for the manipulation of layer 5 pyramidal neurons in chronic sleep experiments ..... 66**

4.1 Introduction ..... 66

4.2 Methods ..... 74

4.3 Results ..... 82

4.4 Discussion ..... 105

**Chapter 5: Cortical dynamics, sleep, and circadian regulation in a 'cortical SNAP25-ablated' mouse model ..... 116**

5.1 Introduction ..... 116

5.2 Methods ..... 117

5.3 Results ..... 123

5.4 Discussion ..... 146

**Chapter 6: General discussion and future directions ..... 153**

6.1 Summary of key findings ..... 155

6.2 Subcortical vs. cortical regulation of sleep homeostasis ..... 156

6.3 How to study sleep homeostasis? ..... 166

6.4 Neural circuits linking cortex with subcortical sleep-control centres ..... 169

6.5 Putative molecular mechanisms of cortical sleep regulation ..... 173

6.6 Clinical implications of cortical sleep regulation ..... 176

**Bibliography ..... 179**

# Table of figures


Figure 1: Electrophysiological markers of vigilance states in mammals ..... 4

Figure 2: Active and inactive states in neocortex during NREM sleep ..... 5

Figure 3: The 'center for brain regulation' identified by Constantin von Economo ..... 7

Figure 4: The 'sleep switch': a flip-flop model of sleep-wake control ..... 9

Figure 5: Timecourse of the homeostatic (S) and circadian (C) processes of sleep regulation after regular and extended waking periods ..... 12

Figure 6: Relationship between slow wave amplitude and sleep depth ..... 14

Figure 7: Slow wave activity reflects the time course of the homeostatic process ..... 15

Figure 8: Population firing patterns in neocortex reflect sleep homeostasis ..... 17

Figure 9: Local sleep phenomena in neocortex ..... 20

Figure 10: Electrophysiological implants and recording setup ..... 32

Figure 11: Location of implantation in primary motor cortex and dimensions of a 16-channel laminar probe ..... 50

Figure 12: Initial issues encountered with the analysis of laminar probe histology and detection of electrical microlesions ..... 52

Figure 13: Laminar probe histology after optimisation ..... 54

Figure 14: Histological and electrophysiological assignment of laminar probe channels ..... 55

Figure 15: Examples of EEG, EMG, and laminar recordings during wakefulness, NREM, and REM sleep ..... 57

Figure 16: Neuronal firing rates in layers 2/3 and 5 across vigilance states ..... 58

Figure 17: Laminar profile of neocortical firing dynamics around OFF-ON transitions in C57BL/6J mice ..... 60

Figure 18: Laminar profile of neocortical slow wave dynamics in C57BL/6J mice ..... 61

Figure 19: Laminar response to sleep deprivation ..... 62

Figure 20: Expression of AAV2 & AAV8 in layer 5 pyramidal neurons of the Rbp4-Cre driver line. ..... 71

Figure 21: Implant schematic of wild type mice used for CNO and Cmpd21 injections ..... 76

Figure 22: CNO injection in one *Rbp4-Cre:hM4Di* pilot animal modulates sleep under undisturbed baseline conditions ..... 83

Figure 23: CNO injection in one *Rbp4-Cre:hM4Di* pilot animal affects sleep after sleep deprivation ..... 85

Figure 24: Time course of NREM sleep slow wave activity (SWA) after sleep deprivation in one 'layer 5 DREADD' pilot animal ..... 86

Figure 25: Clozapine modulates sleep in rats ..... 88

Figure 26: Time spent in wakefulness, NREM, and REM sleep after CNO and saline injections ..... 91

Figure 27: Sleep architecture following CNO and saline injections ..... 94

Figure 28: EEG power spectra of wakefulness, NREM, and REM sleep following injections of saline and 5 mg/kg CNO ..... 97

Figure 29: Relative EEG spectra of NREM sleep and measures of sleep continuity following injections of saline and CNO ..... 99

Figure 30: Time spent in wakefulness, NREM, and REM sleep after Cmpd21 and saline injections ..... 101
Figure 31: Relative EEG spectra of NREM sleep, measures of sleep continuity, and sleep architecture parameters following injections of saline and Cmpd21 ..... 103
Figure 32: Control data for CNO effects on sleep in wild type mice ..... 111
Figure 33: Identification of cortical layers in a representative coronal brain slice covering primary motor and sensory cortex. ..... 123
Figure 34: Comparison of Cre-expression in the Rbp4-Cre mouse line between neocortical layer 5, dentate gyrus and hypothalamus. ..... 126
Figure 35: The suprachiasmatic nucleus of the hypothalamus is void of Cre+ cells and spared of fibre tracts in the Rbp4-Cre mouse line ..... 127
Figure 36: No overlap between orexin or melanin concentrating hormone-expressing cells with Rbp4-Cre+ cells but dense fibre tracts in lateral hypothalamus ..... 127
Figure 37: Laminar firing patterns during NREM sleep in cortical Snap25-ablated mice ..... 129
Figure 38: Laminar profile of LFP slow waves and LFP power spectra during NREM sleep in cortical Snap25-ablated mice ..... 130
Figure 39: Sleep profile of cortical SNAP25-ablated mice ..... 131
Figure 40: Genotype differences in the amount of time spent in wake, NREM, and REM sleep during undisturbed baseline recordings are more pronounced in the dark period. ..... 132
Figure 41: EEG power spectra from the frontal and occipital derivations during waking and NREM sleep at baseline show no differences between genotypes. ..... 133
Figure 42: The EEG theta peak during REM sleep is shifted towards lower frequencies in cortical SNAP25-ablated mice. ..... 133
Figure 43: Sleep architectural and electrophysiological measures during baseline recordings indicate reduced homeostatic sleep drive ..... 135
Figure 44: Diminished electrophysiological response to sleep deprivation in cortical SNAP25-ablated mice ..... 136
Figure 45: Laminar and regional aspects of sleep homeostasis ..... 137
Figure 46: Relative EEG power spectra during sleep deprivation show attenuation of theta increase in cortical SNAP25-ablated animals. ..... 138
Figure 47: Sleep amount and architecture following sleep deprivation between ZT 0-6 ..... 139
Figure 48: Circadian characterisation of cortical SNAP25-ablated mice ..... 142
Figure 49: Sleep assessment of cortical SNAP25-ablated mice based on PIR recordings replicates sleep phenotype detected in EEG recordings ..... 143
Figure 50: Sleep-wake profile of cortical SNAP25-ablated mice remains stable in constant darkness ..... 144
Figure 51: The effects of sleep deprivation on sleep amount depend on circadian timing ..... 145

# Abbreviations

| | |
|---|---|
| **AAV** | adeno-associated virus |
| **AD** | anterodorsal thalamus |
| **ANOVA** | analysis of variance |
| **AP** | anterior-posterior brain axis |
| **BDNF** | brain derived neurotrophic factor |
| **BNU** | Behavioural Neuroscience Unit, University of Oxford |
| **BSB** | Biomedical Sciences Building, University of Oxford |
| **CING** | cingulate cortex |
| **cKO** | conditional knockout, i.e. 'cortical SNAP25-ablated' mice (*Rbp4-Cre;Ai14;Snap25$^{fl/fl}$*) |
| **CMOS** | complementary metal-oxide semiconductor |
| **Cmpd21** | compound 21 |
| **CMT** | centromedial thalamus |
| **CNO** | clozapine-N-oxide |
| **CSD** | cortical spreading depression |
| **CSF** | cerebrospinal fluid |
| **CT** | circadian time |
| **CTR** | control mice (Cre-negative controls to cKO mice) |
| **DAPI** | 4′,6-diamidino-2-phenylindole |
| **DiI®** | 1,1'-Dioctadecyl-3,3,3',3'-Tetramethylindocarbocyanine Perchlorate |
| **dnSNARE** | dominant-negative SNARE |
| **DREADDs** | designer receptors exclusively activated by designer drugs |
| **DV** | dorsal-ventral brain axis |
| **EEG** | electroencephalography |
| **EMG** | electromyography |
| **GABA** | γ-aminobutyric acid |
| **GPRC** | G protein-coupled receptors |
| **HPA** | hypothalamic-pituitary-adrenal axis |
| **IL1β** | interleukin-1 beta |
| **LD** | light/dark |
| **LED** | light-emitting diode |
| **LFP** | local field potential |
| **LH** | lateral hypothalamus |
| **LPO** | lateral preoptic nucleus |
| **MANOVA** | multivariate analysis of variance |
| **MCH** | melanin-concentrating hormone |
| **mEPSP** | miniature excitatory postsynaptic potential |
| **ML** | medial-lateral brain axis |
| **MnPO** | median preoptic nucleus |

| | |
|---|---|
| **MSLT** | multiple sleep latency test |
| **MUA** | multi-unit activity |
| **NK1** | neurokinin 1 receptor |
| **nNOS** | neuronal nitric oxide synthetase |
| **NREM sleep** | non-rapid eye movement sleep |
| **OFF period** | brief episode without neuronal spikes across cortical layers |
| **ON period** | brief episode with active neuronal firing across cortical layers |
| **ORX** | orexin/hypocretin |
| **PBS** | phosphate buffered saline |
| **PFA** | paraformaldehyde |
| **PIR** | passive infrared recordings |
| **PV** | parvalbumin |
| **REM sleep** | rapid eye movement sleep |
| **SCN** | suprachiasmatic nucleus |
| **SNAP25** | synaptosomal-associated protein 25kDa |
| **SNARE** | soluble N-ethylmaleimide attachment protein receptor |
| **SOM** | somatostatin |
| **SRS** | sleep regulatory substances |
| **SWA** | slow wave activity (0.5 - 4.0 Hz) |
| **tDCS** | transcranial direct current stimulation |
| **TDT** | Tucker-Davis Technologies Inc. |
| **TMS** | transcranial magnetic stimulation |
| **VGAT** | vesicular GABA transporter |
| **VLPO** | ventrolateral preoptic nucleus |
| **VMP** | ventral midbrain/pons region |
| **VTA** | ventral tegmental area |
| **WT** | wild type mice (C57BL/6J) |

# Chapter 1: Introduction

## 1.1 Sleep as an essential behaviour

Our entire life is structured around the alternating pattern of wakefulness and sleep. Although sleep reduces an individual's ability to interact with the environment and increases the risk of predation, all organisms studied so far sleep (S. S. Campbell and Tobler 1984; Anafi, Kayser, and Raizen 2019). Sleep further appears to be an essential behaviour, because sleep deficits are readily compensated and loss of sleep has detrimental consequences (Cirelli and Tononi 2008).

When animals are continuously deprived of sleep nearly all organ systems suffer damage before the lack of sleep, or the consequences thereof, ultimately leads to death (Rechtschaffen et al. 1983). However, the earliest effects of sleep deprivation are found in brain functions (Krause et al. 2017; Nir et al. 2017) and the need for sensory disconnection during sleep further suggests that sleep is primarily needed by the brain (Krone and Vyazovskiy 2019). It has been suggested that the function of sleep is to allow prophylactic maintenance of individual neurons (Vyazovskiy and Harris 2013). While a thorough discussion of the function(s) of sleep would go beyond the scope of this thesis and has been reviewed elsewhere (Krone and Vyazovskiy 2019; Frank and Heller 2019), it should be highlighted that the search for sleep regulatory mechanisms is intimately intertwined with the quest to identify the core function of sleep. Understanding *how* sleep is regulated will ultimately tell us *why* sleep is needed.

## 1.2 What is sleep and how can it be measured?

In order to investigate sleep experimentally, it is crucial to clarify the defining criteria of sleep. In mammals, sleep can be either defined behaviourally or by its characteristic brain activity.

Behaviourally, sleep can be defined as a rapidly reversible state of reduced responsiveness to external stimuli, which is typically accompanied by immobility and spent in a characteristic posture at a specific sleeping site (Piéron 1913). Another defining behavioural feature of sleep is its homeostatic compensation (Tobler 1983), which means that if sleep is prevented the organism will subsequently respond with an increase in sleep depth and duration. The behavioural definition of sleep is particularly useful in the context of invertebrate sleep research, where the measurement of locomotor activity and the response to sensory stimulation allows for a simple and effective quantification of sleep duration and depth even in the absence of electrophysiological readouts (Hendricks et al. 2000; Shaw et al. 2000; Tobler 1983; Tobler and Stalder 1988).

Recordings of brain and muscle activity by means of electroencephalography (EEG) and electromyography (EMG) in mammals and birds enable a purely electrophysiological definition of sleep (Figure 1)(Adamantidis, Gutierrez Herrera, and Gent 2019). EEG allows to record electrical brain activity from the scalp. Due to their cytoarchitectural geometry, cortical structures contribute most strongly to the spatiotemporally smoothed fluctuations in the electric potential differences detected by the EEG (Buzsáki, Anastassiou, and Koch 2012). EMG records muscle movements by detecting the electric potential differences generated by active muscle cells. During wakefulness, the EEG signal is characterised by fast, irregular, and low amplitude fluctuations reflecting a complex pattern of neuronal activity across brain regions. The EMG shows high muscle activity. Once an animal falls asleep, EMG activity drops, reflecting the fading of skeletal muscle tone at the transition to sleep. Whilst the EEG displays a more regular pattern of high amplitude ‘slow waves’ (<4.0 Hz) and ‘sleep spindles’ (~10-15 Hz), which together define the state of non-rapid eye movement (NREM) sleep (Adamantidis, Gutierrez Herrera, and Gent 2019; Fernandez and Lüthi 2019). This sleep state alternates in regular intervals with the state of rapid-eye movement (REM) sleep. During REM sleep, the

eyes perform saccadic movements behind closed lids and the EEG displays the characteristic ‘theta rhythm’ (5-8 Hz). The EMG shows a further drop in muscle tone reflecting the muscle paralysis that occurs during REM sleep. Often, the heart beat becomes visible in the EMG in the absence of skeletal muscle tone and this very regular low amplitude pattern is only occasionally interrupted by short twitches. Due to the astonishing dissociation between very active EEG rhythms and simultaneous muscle atonia, this state is historically also described as ‘paradoxical sleep’ (Jouvet 1967).

The combination of EEG and EMG measurements has become the standard approach to measure sleep in mammals because it allows sleep to be distinguished from quiet wakefulness, to identify the two states of sleep, and to gain deeper insights into the brain activity during sleep and wakefulness (Figure 1).

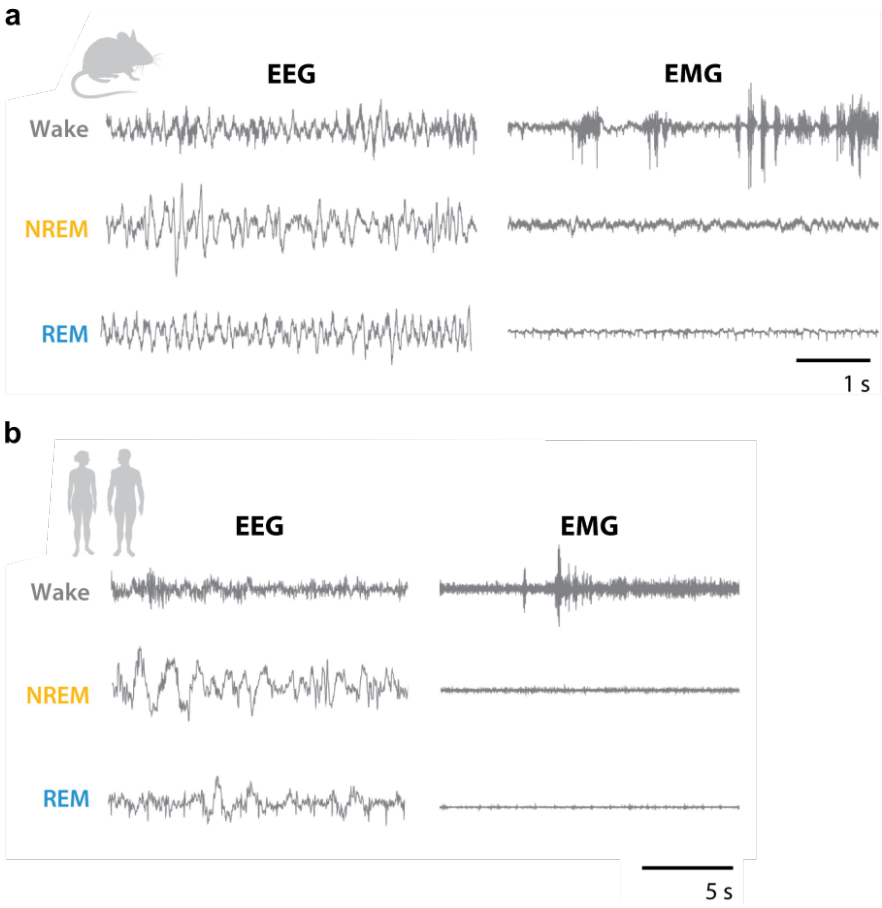



**Figure 1: Electrophysiological markers of vigilance states in mammals**

Representative electroencephalography (EEG) and electromyography (EMG) traces from mice (a) and humans (b) illustrate the considerable similarity in the electrophysiological signature of vigilance states between different mammalian species. Figure modified from (Liu and Dan, 2019).

Another electrophysiological signal, which discriminates NREM sleep from wakefulness and REM sleep, is the firing pattern of neurons in the neocortex (Figure 2). Slow waves observed in the EEG and in local field potentials (LFP), arise from the highly synchronised bistable pattern of population firing in neocortical neurons (Vyazovskiy and Harris 2013). Every few hundred milliseconds, cortical neurons transition between a state of burst firing ('ON') and inactivity ('OFF'), which corresponds to states of depolarisation ('UP') and hyperpolarisation ('DOWN') in the membrane potential of individual neurons, respectively (Steriade 2003). This bistable firing pattern is thought to be largely generated by layer 5 pyramidal neurons in

neocortex (Neske 2016) in interaction with reticular thalamic and thalamocortical neurons (Steriade, Nuñez, and Amzica 1993). The active states are thought to be triggered in layer 5 pyramidal neurons either by an intrinsic pacemaker mechanism (Le Bon-Jego and Yuste 2007; Lőrincz et al. 2015) or by spontaneous vesicle release (Chauvette, Volgushev, and Timofeev 2010; Timofeev et al. 2000) and then propagated in a sequential structure through neocortex (Luczak et al. 2007; Massimini et al. 2004). In contrast, the inactive states are thought to arise from activity-dependent $K^+$ conductances (Steriade, Nuñez, and Amzica 1993; Sanchez-Vives et al. 2000) or from active inhibition (Beltramo et al. 2013) and are synchronised by thalamocortical projections (Hay et al. 2021). Independent of the mechanism, the bistable neocortical firing patterns are characteristic of the NREM sleep state and provide important insights into the functional state of the neocortical network (Noda and Ross Adey 1970).

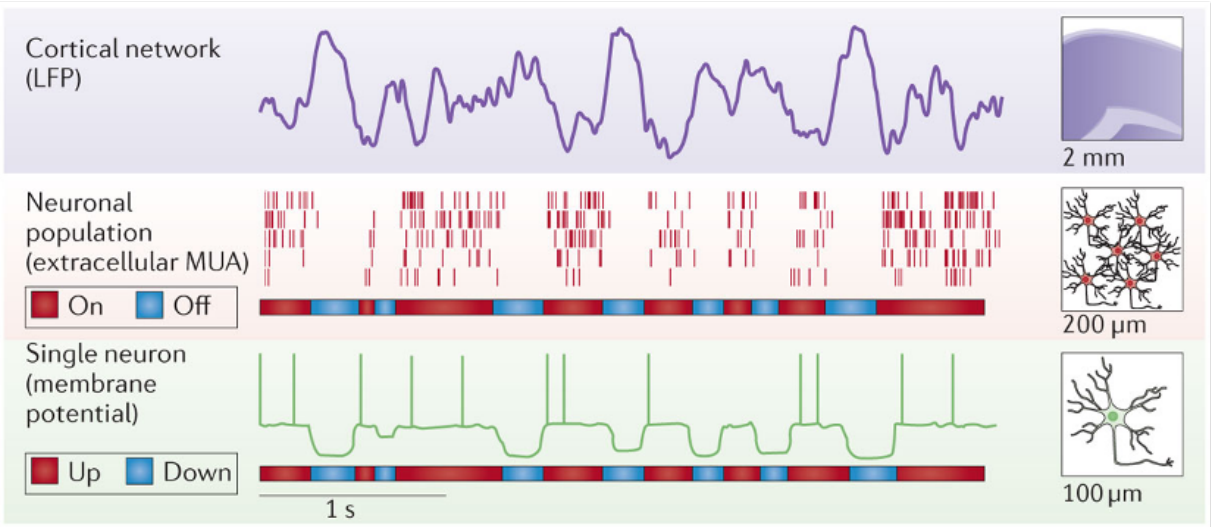



**Figure 2: Active and inactive states in neocortex during NREM sleep**

The characteristic pattern of slow wave pattern during NREM sleep observed in electroencephalography (EEG) recordings is also found in local field potentials (LFP) from neocortex (top row), generated by synchronised alternations between active and inactive states in neuronal populations. Brief episodes of burst firing ('On' states), and quiescence ('Off' states) in neocortical population activity measured in multiunit recordings (MUA) reflect synchronised fluctuations between depolarised ('Up' states) and hyperpolarised ('Down' states) levels of the membrane potential of individual neurons. Figure from (Vyazovskiy and Harris, 2013).

## 1.3 Sleep wake circuitry – the subcortical sleep switch

From the perspective of a 21st century neuroscientist, it appears self-evident that the regulation of sleep in the mammalian brain can be studied by targeted manipulation of neural circuits combined with electrophysiological readouts of vigilance states in rodent models. However, the possibility to study the neurophysiology of sleep only gained widespread attraction about a century ago through the work of the Viennese neurologist Constantin von Economo on 'sleep as a problem of localization' (Economo 1930). Based on careful clinical observation of patients who survived the *lethargic epidemic encephalitis* with localised inflammatory brain lesions, von Economo concluded that damage to the anterior part of the hypothalamus leads to insomnia, while damage to the upper part of the brainstem causes hypersomnolence or coma (Figure 3)(Economo 1930).

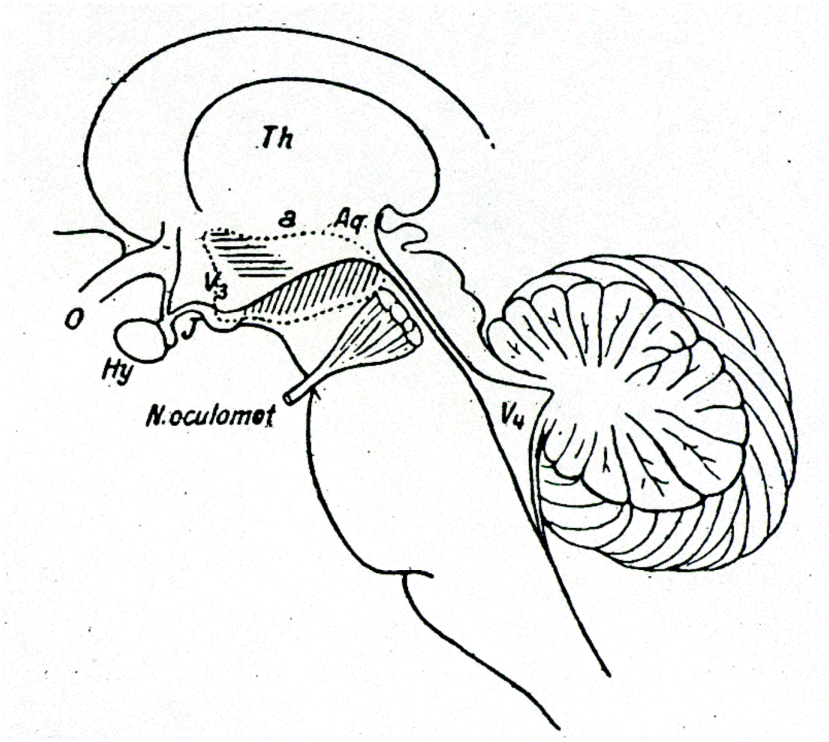



**Figure 3: The 'center for brain regulation' identified by Constantin von Economo**

The brain region, which Constantin von Economo identified as relevant for sleep-wake control (area marked with dotted line) on a hemisection of the diencephalon, brainstem, and cerebellum. Note that the horizontal stripes in the anterior hypothalamus indicate the subregion where von Economo suspected a sleep centre based on the insomnia symptoms of patients with lesions in this area. Conversely, the diagonal stripes at the junction between the midbrain and the diencephalon indicate the subregion where the damage was often found when patients presented with hypersomnia or coma. The anatomical landmarks are: o: optic nerve. Hy: hypophysis. Th: thalamus. Aq: aqueduct. V3 and V3: third and fourth ventricle. N. occulomot: oculomotor nerve. Figure from (von Economo, 1930).

Lesion experiments in rodents later confirmed the existence of sleep and wake regulatory centres and pathways in the anatomical structures, which von Economo had proposed as the ‘center for brain regulation’ (Nauta 1946). The subsequent description of an ascending arousal system in the brainstem (Moruzzi and Magoun 1949) and the findings that an inhibitory cell group in the ventrolateral preoptic nucleus (VLPO) sends projections to several wake-promoting structures (Sherin et al. 1998) and VLPO lesions through microinjections of ibotenic acid cause profound insomnia in rats (Lu et al. 2000) provided the basis for the concept of a

sleep-wake switch (Saper, Chou, and Scammell 2001). According to this model, there are two sets of sleep and wake active nuclei, mostly located in the hypothalamus, brainstem, and basal forebrain (Figure 4). Wake active nuclei are thought to promote activation of the forebrain, in particular through monoaminergic neurotransmitter release in the cortex and cholinergic signalling to the thalamus (Saper, Scammell, and Lu 2005). Monoaminergic release from the raphe nucleus (serotonin), tuberomammillary nucleus (histamine) and locus coeruleus (noradrenaline) is high during wakefulness and low during sleep, while acetylcholine release from the pedunculopontine nucleus and laterodorsal tegmentum is high during wakefulness and REM sleep, and low during NREM sleep (Nir and Tononi 2010). In contrast, the VLPO is thought to represent the major sleep-promoting centre, inhibiting the wake-promoting system through γ-aminobutyric acid (GABA) and galanin neurotransmission. A special role is assigned to orexinergic neurons in the lateral hypothalamus, which contribute to the regulation arousal (Yamanaka et al. 2003) and are critically involved in the pathophysiology of narcolepsy (Hara et al. 2001; Chemelli et al. 1999; Bassetti et al. 2019). Their action is thought to be wake promoting and, importantly, state-stabilizing preventing sudden onset of NREM sleep and immediate transitions into REM sleep (Saper, Scammell, and Lu 2005).

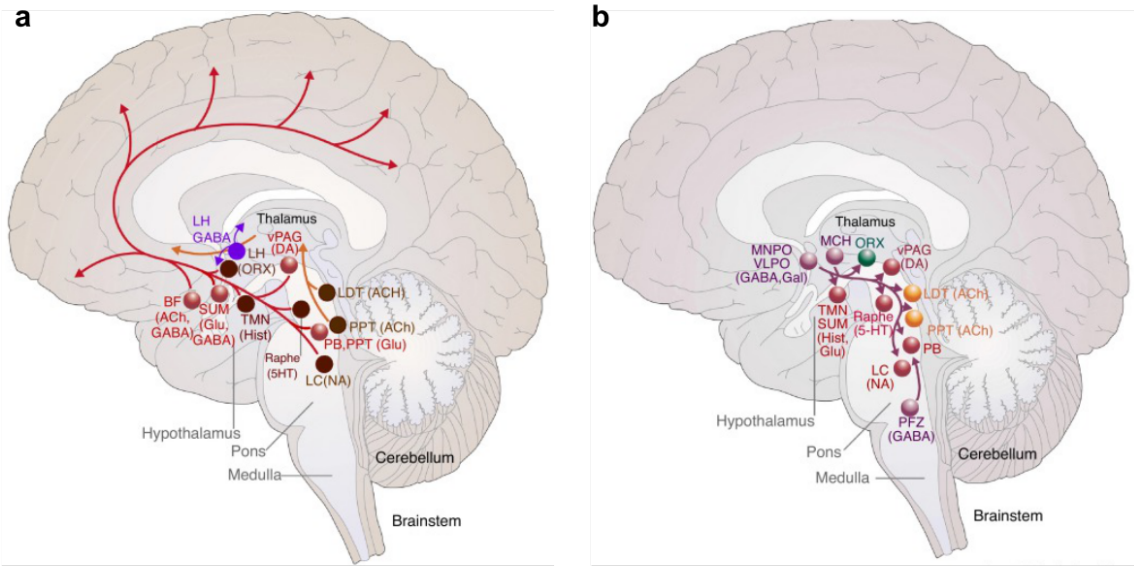



**Figure 4: The 'sleep switch': a flip-flop model of sleep-wake control**

The influential concept of a sleep-switch by Clifford Saper classifies nuclei in the brainstem, hypothalamus, and basal forebrain according to their role in promoting wakefulness (a) or sleep (b). During wakefulness, arousal nuclei activate cortex and thalamus. During sleep, a small set of inhibitory nuclei suppress the arousal system. Note that in this concept cortex is not considered a structure with sleep- or wake-regulating properties. Figure modified from (Saper and Fuller, 2017).

Until the beginning of the 21st century, the discovery of sleep-wake regulating nuclei was largely based on histological staining for the immediate early gene cFOS, recording of discharge patterns from candidate regions as well as on their mechanical or toxin-induced lesioning. The advent of advanced methods for spatiotemporal control of neuronal activity, such as optogenetics (Miesenböck 2009; Lima and Miesenböck 2005) and chemogenetics (Roth 2016; Alexander et al. 2009) has rapidly accelerated the search for sleep- and wake-promoting neurons and advanced our understanding of sleep-wake circuitry in the mammalian brain. Many of the previous assumptions on the role of sleep- and wake-regulatory nuclei have been confirmed (Adamantidis et al. 2007), but in several instances novel facets have also been discovered. For example, sleep regulatory effects of some nuclei might depend on their firing patterns (Carter et al. 2010; Oikonomou et al. 2019), while other cell populations have been

found to link sleep regulation with other core physiological processes such as thermoregulation (Harding et al. 2018; Kroeger et al. 2018). In addition, the set of subcortical nuclei contributing to sleep regulation has been greatly expanded, especially due to the discovery of several nuclei, which use the fast-acting neurotransmitters GABA and glutamate (Saper and Fuller 2017). Most recently the basal ganglia circuitry has been implicated in sleep regulation, providing an interesting neurophysiological link between locomotor control, emotional state, sleep and arousal (Liu et al. 2020; Yu et al. 2020; 2019; Eban-Rothschild et al. 2016; Taylor et al. 2016). Another fascinating development is the gradual delineation of REM regulating circuitry (Lu et al. 2006; Weber et al. 2015).

The decades since von Economo's initial work have provided many insights into the neuronal circuitry which performs the transition between vigilance states. Detailed knowledge about the sleep switch enables us to now investigate the circuits through which the brain regulates the timing, duration, and intensity of sleep, and ultimately address the question: *What operates the sleep switch?*

## 1.4 Circadian and homeostatic regulation of sleep

A theoretical framework for how timing, duration, and intensity of sleep are regulated is provided by the two process model of sleep regulation (Borbély 1982; Daan, Beersma, and Borbély 1984). According to the model, a sleep-independent circadian process (Process C) and a sleep-dependent homeostatic process (Process S) represent the two major determinants of sleep regulation (Figure 5).

The homeostatic process reflects the build-up of sleep debt during waking and its dissipation during sleep. In mammals, EEG power density in the low frequency range, typically defined as slow wave activity (SWA, 0.5 – 4 Hz), during NREM sleep is the principal marker of the

homeostatic process (Borbély et al. 2016; Borbély 1982). The initial level of SWA after sleep onset is determined by the duration of prior waking and the decline of SWA during sleep reflects the discharge of sleep debt (Borbély et al. 1981; Tobler and Borbély 1986). Importantly, SWA also reflects sleep intensity. SWA is closely correlated with the arousal threshold to external stimuli (Neckelmann and Ursin 1993) and the frequency of spontaneous awakenings during sleep (Franken et al. 1991). It is thought that this intensity domain of sleep, which ensures that a sleep deficit can be recovered without a major increase in subsequent sleep time, is essential to keep the sleep-wake rhythm aligned with the circadian environment (Borbély 1982).

The circadian process reflects the rhythmic fluctuation of sleep propensity in a near 24-h rhythm (Borbély 1982). The circadian rhythm is entrained to the external day/night cycle by 'zeitgebers' such as light, but continues to orchestrate physiological processes even in the absence of external timing cues (Dibner, Schibler, and Albrecht 2010; Aschoff 1965). The fluctuation of sleep propensity across day and night ensures that sleep is facilitated in a time window that is most appropriate for the ecological requirements of a respective species. Melatonin and core body temperature are physiological makers of the circadian process (Borbély et al. 2016).

The two processes engage in a dynamic interaction, which explains many phenomena related to sleep in our daily lives. For example, the model explains why we are more tired in the evening after an early start in the morning, but also why it is typically more difficult to sleep on the morning after a night shift compared to our usual bed time, despite the increased sleep debt.

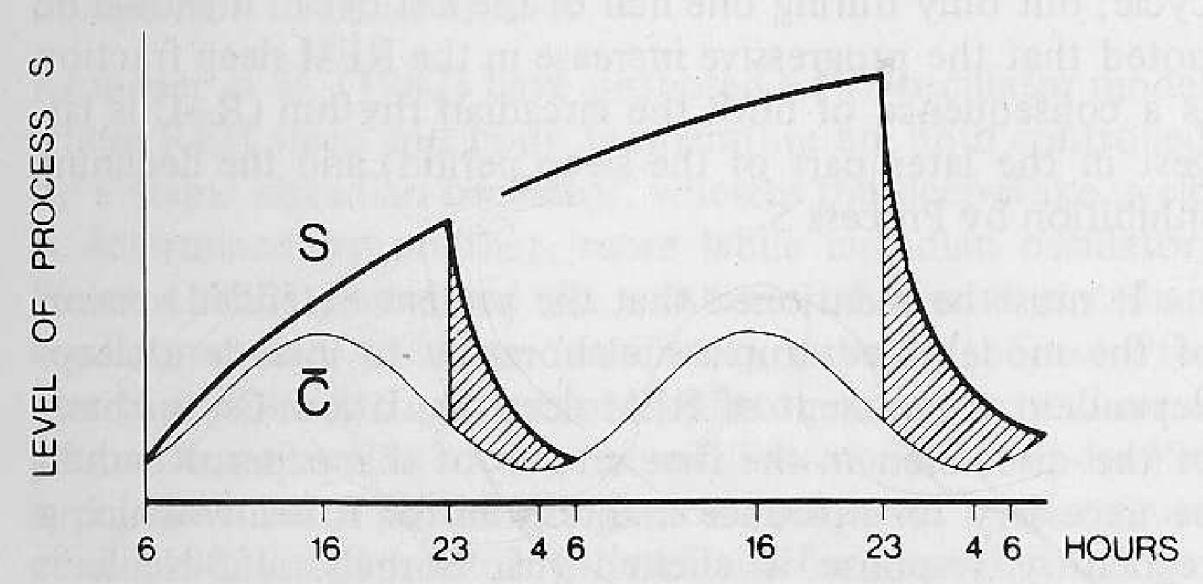



**Figure 5: Timecourse of the homeostatic (S) and circadian (C) processes of sleep regulation after regular and extended waking periods**

According to the two-process model of sleep regulation, the homeostatic process (S) reflects the accumulating sleep debt during wakefulness, while the inverse ($\bar{C}$) of the circadian process reflects the wake propensity at any given time point. The initial formulation of the model suggests that sleep propensity represents the difference between these two processes. Figure from (Borbély, 1982).

While the two-process model has been extensively validated and extended experimentally and computationally (Dijk and Czeisler 1995; Dijk, Beersma, and Daan 1987; Achermann and Borbély 2003; Guillaumin et al. 2018) the search for the biological implementation of the two processes is still ongoing. It is well-established that circadian rhythms, generated in transcriptional-translational oscillators throughout the body, are coordinated by a 'master-clock' in the suprachiasmatic nucleus (SCN) of the hypothalamus (Dibner, Schibler, and Albrecht 2010). Although the molecular regulation of the circadian process has been delineated in great detail (Partch, Green, and Takahashi 2014), it is only partially understood how the output of the circadian pacemaker(s) affects the sleep-wake regulating system. On one hand, neuronal pathways connecting the SCN and the VLPO have been found (Chou et al. 2003). On the other hand, even transplantation of SCN tissue into the third ventricle can effectively

reinstate a regular sleep-wake rhythm in an arrhythmic animal (Ralph et al. 1990), suggesting that humoral factors also play an important role.

The neurobiological implementation of the homeostatic process in the mammalian brain is far less understood than that of the circadian process. A strong case can be made for an involvement of adenosine in the homeostatic process, not only because the adenosine antagonist caffeine reduces the electrophysiological signature of elevated sleep need (Landolt et al. 2004) and counteracts some of the behavioural and cognitive effects of sleep deprivation (Urry and Landolt 2015). Genetic manipulations of adenosine metabolism in glial cells and adenosine sensing in neurons profoundly affects the homeostatic process (Bjorness et al. 2016), and adenosine levels, at least in the basal forebrain and the neocortex, reflect the time course of the homeostatic process during sleep deprivation and recovery sleep (Porkka-Heiskanen, Strecker, and McCarley 2000). It remains, however, under debate through which receptor and at which site in the brain adenosine exerts its influence on the homeostatic regulation of sleep (Lazarus et al. 2019). Some evidence suggests that cortical manipulations of adenosine signalling can affect EEG delta activity and sleep (Van Dort, Baghdoyan, and Lydic 2009). Other work has demonstrated that the firing pattern of sleep-active neurons in the median preoptic nucleus (MnPO) and VLPO reflects the homeostatic process and their activity can be suppressed by adenosine application (Alam et al. 2013). However, it is still not clear whether this region that plays an important role in sleep-switching, also regulates sleep homeostasis. Ablation of galaninergic neurons in the VLPO attenuates the rebound of both delta activity and sleep time after sleep deprivation, but increases the amount of sleep at baseline (Ma et al. 2019), which suggests that this subcortical region is involved in the homeostatic regulation of sleep, but other structures also strongly contribute to titrating the right amount of sleep.

## 1.5 Electrophysiological markers of sleep homeostasis

While the molecular and anatomical underpinnings of homeostatic sleep regulation in the mammalian brain are still largely elusive, much progress has been made in discovery of electrophysiological correlates of sleep homeostasis.

Shortly after the introduction of the EEG by Hans Berger (Berger 1929), it was found that EEG recordings not only provide a non-invasive readout of the sleep-wake state, but also reflect the depth of sleep. In 1937 Blake and Gerard performed overnight EEG recordings and repeatedly played a tuning fork through a loudspeaker while asking their study participants 'are you awake?'. This experiment demonstrated that the declining amplitude of slow waves during sleep (REM sleep was only discovered in 1953 by Aserinsky and Kleitman) mirrors the decreasing arousal threshold over the course of a night (Figure 6)(Blake and Gerard 1937). This finding, which first indicated that slow frequency oscillations in the EEG reflect the depth of sleep, was later confirmed with more refined methods (Rechtschaffen, Hauri, and Zeitlin 1966; Neckelmann and Ursin 1993).

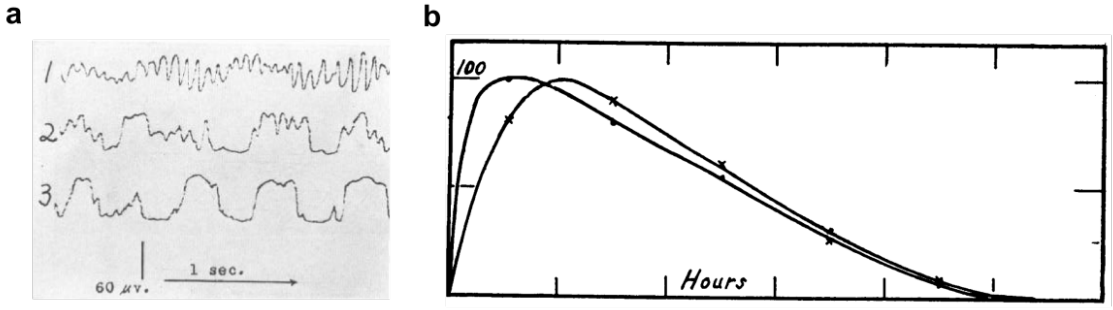



**Figure 6: Relationship between slow wave amplitude and sleep depth**

a) Wakefulness (1), light sleep (2), and deep sleep (3) are characterised by different wave patterns in 'crystograph' recordings of the electroencephalogram (EEG) of human volunteers. During deep sleep high amplitude slow waves occur. b) Systematic assessment of sleep depth (crosses), as defined by auditory awakening thresholds, and slow wave amplitudes (dots). Figure modified from (Blake and Gerard, 1937).

With the arrival of automated EEG signal analysis, SWA became the primary marker of the homeostatic process and the time course of process S in the two-process model was derived from EEG spectral analysis (Borbély 1982). It was later demonstrated in great detail that SWA during NREM declines exponentially during sleep and its initial level reflects the duration of preceding wakefulness (Figure 7)(Dijk 1995; Dijk, Beersma, and Daan 1987).

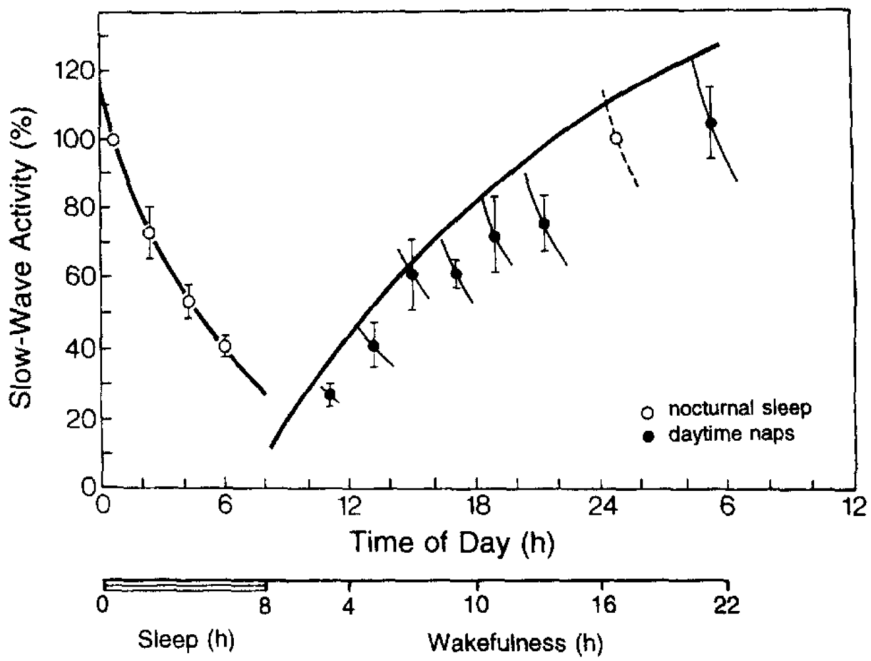



**Figure 7: Slow wave activity reflects the time course of the homeostatic process**

Electroencephalogram (EEG) slow wave activity (SWA) during non-rapid eye movement (NREM) sleep declines exponentially during sleep, here shown for healthy human sleepers. The measurement of NREM sleep SWA during naps at different times of the day and after sleep deprivation suggests that a saturating exponential function describes the relationship between the level of SWA and the previous wake duration. Figure from (Dijk, 1995).

However, SWA is not the only EEG marker of the homeostatic process. The rising level of sleep debt is reflected in elevated theta power of the wake EEG (Cajochen et al. 1995) and the rise rate of theta activity during sleep deprivation corresponds to the increase of SWA between baseline and the first NREM sleep episode of the recovery sleep (Finelli et al. 2000).

Detailed analysis of the cortical firing patterns during NREM sleep later revealed that the homeostatic process is also reflected in the population activity of cortical neurons (Figure 8)(Vyazovskiy et al. 2009). When sleep pressure is high, average firing rates in neocortex are increased independent of the vigilance state. During NREM sleep, when cortical populations engage in the characteristic bistable firing pattern of OFF and ON periods, cortical firing rates are on average lower than during wakefulness or REM sleep. However, the frequency of neuronal firing rates in neocortex during the ON state correlates with the level of SWA during NREM sleep (Vyazovskiy et al. 2009). When the homeostatic sleep drive is high – early during sleep and especially after sleep deprivation – OFF periods are frequent and long. Once the homeostatic sleep drive fades, OFF periods become rarer and shorter (Figure 8b). The synchrony at which populations of cortical neurons switch between the active ON and silent OFF states, and vice versa, also decreases with the dissipation of sleep debt (Figure 8c)(Vyazovskiy et al. 2009). It is thought that the sparseness of OFF periods and the lower synchrony of population activity around their onset and offset is reflected in fewer and smaller slow waves, which in turn reduces SWA in the EEG spectrogram (Vyazovskiy, Cirelli, and Tononi 2011). Together, these findings indicate that the firing patterns in neocortex closely mirror the homeostatic process.

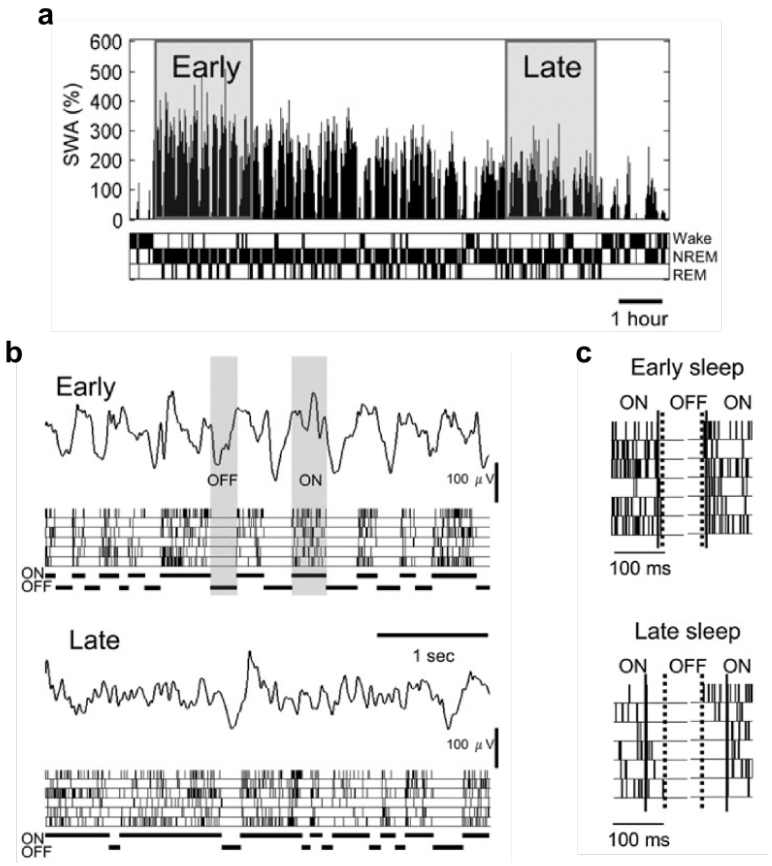



**Figure 8: Population firing patterns in neocortex reflect sleep homeostasis**

a) The time course of slow wave activity (SWA) in the rat electroencephalogram (EEG) during the 12-h light period reflects the dissipation of the homeostatic sleep pressure. As in humans, the level of SWA during late sleep is lower than during early sleep. b) Local field potential (LFP) and corresponding multiunit activity (MUA) in six channels of neocortical implants. During early sleep (top), high homeostatic sleep pressure is not only reflected in the high amplitude of slow waves and their frequent occurrence, but also in the long and frequent OFF periods of neuronal population activity in neocortex. Later during sleep (bottom) OFF periods become shorter and less frequent. c) Synchrony of neuronal firing at the transitions between active ON and inactive OFF states in neocortex decreases when sleep pressure dissipates. Figure modified from (Vyazovskiy et al., 2009).

## 1.6 Local use-dependent sleep – a cortical phenomenon

Slow wave activity during NREM sleep is not only modulated by previous wake duration but also by 'wake intensity', depending on the type of activity performed during wakefulness (Milinski et al. 2021; Hanlon et al. 2009). For example, the amount of exploratory behaviour

during wakefulness correlates with the expression of plasticity-related genes such as BDNF and the subsequent level of SWA during NREM sleep (Huber, Tononi, and Cirelli 2007).

### 1.6.1 Local use-dependent regulation of slow wave activity

The level of SWA during NREM sleep can differ between cortical areas depending on the preceding functional engagement during wakefulness (Kattler, Dijk, and Borbély 1994; Vyazovskiy, Borbély, and Tobler 2000; Huber et al. 2004; 2006; 2007; Hanlon et al. 2009). A first indication for the relationship between use of a cortical area and NREM sleep SWA levels was provided by the findings that vibration of one hand in human participants during wakefulness subsequently leads to higher NREM sleep SWA in the contralateral hemisphere compared to the ipsilateral hemisphere, which receives the sensory input from the unstimulated hand (Kattler, Dijk, and Borbély 1994). Similarly, when the whiskers of rats are cut on one side before the animals engage in exploratory behaviour during wakefulness, SWA during subsequent NREM sleep is higher over the hemisphere which still receives sensory input from intact whiskers compared to the hemisphere deprived of whisker input (Vyazovskiy, Borbély, and Tobler 2000).

The relationship between local cortical activity during wakefulness and SWA during subsequent NREM sleep was further demonstrated in a series of experiments that aimed to elicit an increase or decrease of cortical activation in human volunteers during wakefulness before high-density EEG recordings were performed during sleep. Practicing a visuomotor task, which particularly engages localised regions of the right parietal lobe leads to a subsequent local increase in SWA, the degree of which correlates with improved performance of the task after sleep (Figure 9a)(Huber et al. 2004). Similarly, a local increase of SWA during NREM can also be evoked by inducing localised potentiation of cortical EEG responses using transcranial magnetic stimulation (TMS) during wakefulness (Huber et al. 2007). Conversely,

a local suppression of SWA during NREM sleep can be observed unilaterally over sensorimotor areas as a result of contralateral arm immobilisation (Huber et al. 2006).

### 1.6.2 Local sleep-like events during wakefulness

A local regulation of electrophysiological markers of sleep homeostasis in the neocortex does not only occur during sleep, but it has also been shown that slow waves and neuronal OFF periods can appear in circumscribed neocortical areas during behavioural wakefulness. It was first found serendipitously in rats and macaque monkeys that sleep deprivation or prolonged engagement in a behavioural task can trigger the appearance of slow waves and OFF periods, respectively, even while the animal is still awake (Borbély, Tobler, and Hanagasioglu 1984; Pigarev, Nothdurft, and Kastner 1997). More systematic investigation of neocortical slow waves and OFF periods later revealed that brief occurrences of electrophysiological markers of sleep can be observed locally, restricted to one area, and globally, encompassing frontal and parietal cortex simultaneously, in awake and behaving rats (Figure 9b). These sleep-like events occur more frequently after extended wakefulness accompanied by an increase in the proportion of global events (Vyazovskiy et al. 2011). Importantly, when local OFF periods in the frontal cortex contralateral to the preferred paw of the animal were observed around half a second before trial execution in a pellet reaching task, the attempts to reach the food pellet were typically unsuccessful, indicating that local occurrence of sleep-like activity during wakefulness affects performance (Vyazovskiy et al. 2011). These findings and subsequent work in humans on the relationship between local sleep-like phenomena and behavioural performance (Nir et al. 2017; Andrillon et al. 2021), suggest that local cortical areas can briefly ‘fall asleep’ even while individuals are apparently awake and engaging in a task. They further indicate that cortical bistability foreshadows sleep onset.

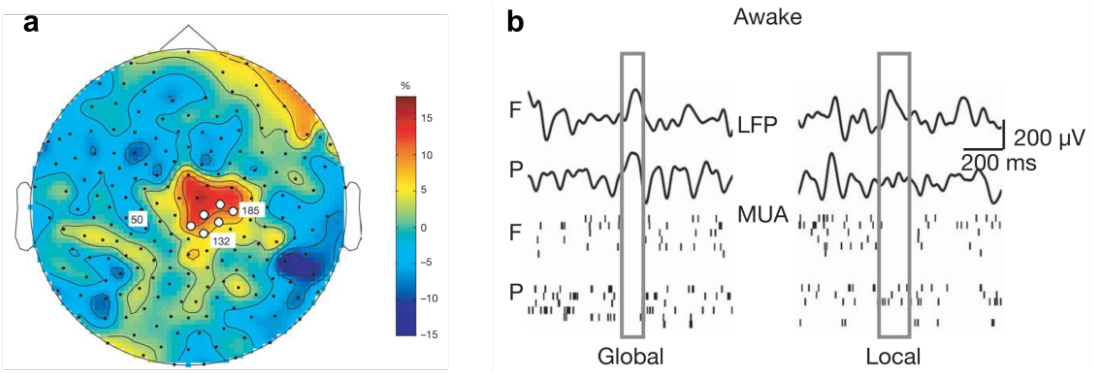



**Figure 9: Local sleep phenomena in neocortex**

a) High density electroencephalogram (EEG) recordings during non-rapid eye movement (NREM) sleep from a human volunteer show local differences in the power of slow wave activity (SWA) between two conditions of a visuomotor learning task, one of which particularly engages circumscribed areas of the right parietal cortex. The locally elevated level of SWA over the most used areas of cortex has been interpreted as indication for local use-dependent sleep. b) Local and global intrusion of slow waves and neuronal OFF periods in a sleep deprived rat indicate that local sleep phenomena can be observed in neocortex during behavioural wakefulness. Figure panel (a) from (Huber et al., 2004) and figure panel (b) from (Vyazovskiy et al., 2004).

### 1.6.3 Molecular drivers of local sleep

It was first suggested by Krueger in 1993 that *"sleep is 'quantal' in nature"* and global sleep arises from the synchronisation of local-networks sleep driven on a molecular level by sleep-regulatory substances (SRS)(Krueger and Obál 1993; Krueger et al. 2008). Several substances have been identified, which (1) enhance sleep, (2) vary with an animals sleep-wake history, (3) act on sleep regulatory circuits, (4) can be blocked to inhibit sleep and sleep rebound, and (5) have altered levels in pathological states of increased sleepiness (Clinton et al. 2011). While a thorough review of these biochemical regulators of sleep and their proposed action would exceed the scope of this introduction and can be found elsewhere (Clinton et al. 2011), it should be pointed out that many SRS have direct effects on neocortical activity and modulate SWA when they are applied to neocortex or their action is locally blocked (Krueger et al. 2019). This suggests that cortex is one of the regions affected by the molecular drivers of sleep. It should

further be highlighted that several molecules, which can elicit local sleep phenomena in cortex, are also markers of inflammation, energy metabolism, or neuronal plasticity providing a putatively interesting link between local sleep and a use-dependent model of sleep homeostasis (Krueger and Tononi 2011). In addition to these humoral signals, one should not omit the recent evidence for intracellular processes, which might also drive sleep homeostasis on a local level. Candidate mechanisms, first partially identified in invertebrates, include oxidative stress (Kempf et al. 2019), endoplasmic reticulum stress (J. A. Williams and Naidoo 2020), and phosphorylation of (synaptic) proteins (Brüning et al. 2019; Noya et al. 2019; Ode and Ueda 2020). Targeted manipulations of these processes in mammalian neocortex will clarify whether they are involved in the regulation of local sleep.

### 1.6.4 Does local sleep affect global sleep?

Despite the growing interest in local sleep phenomena, especially their regulation and relevance for behavioural performance, the question whether local sleep affects global sleep has not yet been addressed systematically. However, some findings on cortical manipulations, which affect subcortical sleep regulatory networks or the global regulation of sleep, could be interpreted as indication for an influence of local cortical on global subcortical sleep regulation.

Unilateral microinjections of interleukin-1 beta (IL1β), one of the most studied SRS, led to increased expression of the neuronal activity marker cFOS not only in the injected cortical area but also in hypothalamic regions of sleep-wake control such as the VLPO of the same side (Yasuda et al. 2007). Another study investigated the effects of the commonly used sleep drug zolpidem on sleep in mice, which are generally zolpidem-insensitive due to a mutation in the $GABA_A$ receptor $\gamma 2$ subunit gene with the exception of selected brain regions where the functional subunit was locally reconstituted (Uygun et al. 2016). The study showed that zolpidem can induce sleep when the relevant receptor subunit is expressed in histaminergic

neurons of the tuberomammillary nucleus, a known wake promoting subcortical region and target of GABAergic projections from the VLPO. However, a reduction of sleep latency, albeit without a significant increase in NREM sleep time, was surprisingly also found when only the frontal neocortex was made sensitive to zolpidem. No sleep modulation effects of zolpidem were found when the superior colliculus was selectively made zolpidem sensitive (Uygun et al. 2016). These findings could be interpreted in favour of a model in which cortex and the subcortical sleep-switch, but not all regions of the mammalian brain, contribute to sleep regulation.

Electrical stimulation experiments also suggest that cortex might take part in the global regulation of sleep. While the electrical stimulation experiments performed by Hess and colleagues in cats first demonstrated that manipulation of various subcortical areas including thalamus can induce sleep (Akert, Koella, and Hess 1952), later work also showed that stimulation of the neocortex can induce sleep, which displays the characteristic pattern of slow waves and can be reversed by sensory stimuli of sufficient intensity (Peñaloza-Rojas, Elterman, and Olmos 1964). Nowadays, non-invasive brain stimulation techniques represent powerful tools to temporarily affect cortical activity in circumscribed areas (Di Lazzaro, Rothwell, and Capogna 2018). During my medical doctorate, I contributed to a study, which found that transcranial direct current stimulation (tDCS), a method which can increase or decrease cortical excitability depending on the polarity of the applied current (Nitsche and Paulus 2000), affects total sleep time in healthy volunteers in a polarity-specific fashion when applied to frontal but not occipital cortical areas (Frase et al. 2016). Based on our findings and other accumulating evidence for the effects of non-invasive brain stimulation on sleep, we postulated a concept of

cortical 'top-down control of arousal and sleep' to challenge the prevailing view that cortex is merely under control of subcortical sleep-wake circuitry (Krone et al. 2016).[1]

Another indication for an influence of local cortical activity on global sleep regulation arises from the study of cortical spreading depression (CSD). CSD describes a wave of depolarisation propagating through cortex in migraine episodes, epileptic seizures, and after cortical trauma – all of which are typically followed by an episode of somnolence and patients' desire to sleep. Experimental induction of CSD in rats leads to a subsequent increase in NREM sleep lasting for several hours (Cui et al. 2008). Interestingly, even unilateral induction of CSD increases NREM sleep duration, while unilaterally elevating the expression of brain derived neurotrophic factor (BDNF) and the level of SWA, specifically during NREM sleep (Faraguna et al. 2010).

Together, these experiments suggest that local cortical manipulations can influence global sleep and provide a strong incentive to directly test whether local (cortical) sleep can affect global (organism) sleep.

### 1.6.5 Layer 5 pyramidal neurons – the neuroanatomical link between local and global sleep?

The cortex is a layered structure and the neocortex is traditionally subdivided into six main layers (K. D. Harris and Shepherd 2015), not considering the structural and functional differences between several sublayers in the primate primary visual cortex (Balaram, Young,

[1] The terminology 'top-down' vs. 'bottom-up' regulation of sleep should be avoided in the future as inconsistent use of these terms between different research groups will inevitably lead to confusion. Krueger and colleagues (Van Dongen, Belenky, and Krueger 2011; Krueger et al. 2019) use the term 'top-down' from an organisational perspective for a model in which sleep is imposed on the brain by subcortical centres in contrast to a 'bottom-up' model in which sleep is initiated through local use-dependent processes in distributed neuronal assemblies. In contrast, I and other authors (Siclari et al. 2014; Uygun et al. 2016; Krone et al. 2016) have used the term 'bottom-up' from an anatomical perspective to describe subcortical regulation of sleep in contrast to 'top-down' regulation of sleep by cortical projections to subcortical structures.

and Kaas 2014), or in mouse and rat cerebral cortex with layer 5a and 5b (Baker et al. 2018; Kim et al. 2015) or layer 6b, which has been less investigated but is potentially an important remnant of the subplate (Hoerder-Suabedissen and Molnár 2015). The diversity of layer 5 pyramidal neuron subtypes with their distinct projection profiles within cortex, to the thalamus, or to other subcortical targets allows for highly complex processing of information (Baker et al. 2018; Kim et al. 2015). However, it is widely thought that layer 5 pyramidal neurons with extrathalamic projections represent the only output pathway through which cortex signals to subcortical structures beyond the thalamus and controls behaviour (Sherman and Usrey 2021). It should, however, be mentioned that a group of long-ranging GABAergic projection neurons has now been described, yet investigations into their network connectivity and functional role are just beginning (Melzer and Monyer 2020). Among the at least 133 cortical cell types (Tasic et al. 2018; Yao et al. 2021), layer 5 pyramidal neurons are hence the best candidate for a cell population, that conveys cortical signals of sleep debt to the subcortical centres of sleep control.

In addition, layer 5 pyramidal neurons have several features that suggest they may engage in the homeostatic regulation of slow wave activity and sleep. In contrast to several other cortical cell types, layer 5 pyramidal neurons are sensitive to adenosine and become hyperpolarised through adenosine $A_1$A receptor signalling and subsequent opening of $K_{ir}3$ channels in particular in the prefrontal cortex (van Aerde, Qi, and Feldmeyer 2015; Radnikow and Feldmeyer 2018). This is of particular interest because pharmacological studies suggest that adenosine signalling in prefrontal cortex modulates EEG delta power, arousal, and sleep (Van Dort, Baghdoyan, and Lydic 2009). In addition, it is thought that layer 5 pyramidal neurons play a driving role in the regulation of slow waves, although most of the work on this topic has been conducted in brain slices or anaesthetised animals (Neske 2016). Initial work in slices of ferret neocortex suggested that the slow oscillation is initiated by layer 5 pyramidal neurons and then propagated to deeper and more superficial cortical layers (Sanchez-Vives and

McCormick 2000a). Subsequent *in vivo* laminar recordings in naturally sleeping and anaesthetised cats supported the proposition that active states of the slow oscillation start in neocortical layer 5 and suggested that the wide dendritic arborisation of deep layer pyramidal neurons makes them well-suited to initiate the active state upon spontaneous neurotransmitter release (Chauvette, Volgushev, and Timofeev 2010). In addition, some subtypes of layer 5 pyramidal neurons, as well as an interneuron subtype called 'Martinotti cells', have intrinsic pacemaker properties (Le Bon-Jego and Yuste 2007; Lőrincz et al. 2015). Optogenetic activation and inhibition of layer 5 pyramidal neurons potently elicit strong network ON and OFF states (Beltramo et al. 2013). This is in contrast to layer 2/3 pyramidal neurons. Among the diverse subcortical targets of layer 5 pyramidal neurons (Kita and Kita 2012), a recent study identified the lateral hypothalamus (LH), a region containing sleep-regulatory orexin (ORX) and melanin-concentrating hormone (MCH) neurons (Prasad, Carroll, and Sherman 2020). A dense terminal field of axons in this the LH arises from prefrontal cortex layer 5 pyramidal neurons, which are under the control of the Rbp4-Cre driver line (Prasad, Carroll, and Sherman 2020). In addition to these neurophysiological and neuroanatomical considerations, non-invasive brain stimulation techniques strongly influence layer 5 pyramidal neurons (S. C. Murphy et al. 2016; Di Lazzaro, Rothwell, and Capogna 2018), which might explain how these techniques can exert effects on sleep-wake regulation.

In summary, several lines of evidence suggest that layer 5 pyramidal neurons might be critical for the regulation of cortical slow waves, although this has not yet been conclusively shown *in vivo* in sleeping animals. Many properties of layer 5 pyramidal neurons such as their sensitivity to adenosine, their projections to subcortical centres of sleep-wake control, and their responsiveness to specific non-invasive brain stimulation techniques make them a compelling target for probing a role for the cortex in the regulation of sleep oscillations and vigilance states.

## 1.7 Hypothesis and project aims

Our brain would be very inefficient if individual cortical areas would often go into local sleep whenever they felt the need and we lost the respective functions for a brief episode of time. Therefore, it appears most likely that cortex presents local sleep only under exceptional circumstances. Instead, cortex might typically sense and integrate the local demands for prophylactic cellular maintenance across its individual areas to prevent their uncoordinated switch off, and broadcast the overall level of cortical sleep debt to the subcortical sleep switch, which controls global sleep.

The main hypothesis being tested in my DPhil project is that cortex, and in particular neocortical layer 5 pyramidal neurons, actively contributes to the regulation of sleep oscillations and sleep-wake states.

Following from this hypothesis, I specified the following aims for my DPhil project:

1) To describe the local spatiotemporal dynamics in neocortex during sleep using laminar recordings in wild type mice.
2) To validate tools for the *in vivo* manipulation of neocortical layer 5 pyramidal neurons in chronic sleep experiments.
3) To investigate the effects of subacute or chronic manipulations of neocortical layer 5 pyramidal neurons on cortical dynamics during sleep and sleep regulation.

My thesis contains three experimental chapters. In chapter 3 I present laminar recordings of neocortical activity during sleep in wild type mice and explore whether layer 5 actively drives slow waves, a hallmark of NREM sleep and marker of sleep depth. In chapter 4 I present an initial pilot experiment using chemogenetic tools to manipulate layer 5 pyramidal neurons. This chapter continues with a description of subsequent experiments, which test the effects of

two commonly used chemogenetic actuators, clozapine-N-oxide (CNO) and compound 21 (Cmpd21), on sleep in mice that do not express the designer receptors required for chemogenetic remote control. In chapter 5 I present an extensive assessment of cortical dynamics, sleep, and circadian regulation in 'cortical SNAP25-ablated' (*Rbp4-Cre;Ai14;Snap25*$^{fl/fl}$) mice, which served as a model for chronic silencing of neocortical layer 5 pyramidal and archicortical dentate gyrus granule cells.

# Chapter 2: General methods

This chapter contains a summary of experimental procedures, materials, and methods, which were used in more than one of the projects presented in my thesis. The general methodology of chronic *in vivo* electrophysiological recordings in freely moving mice is described here. This includes the surgical procedures for the implantation of EEG screws and laminar probes, the experimental setup for chronic electrophysiological recordings, the standard procedure for data acquisition and analysis as well as the histological methods used to localise the laminar implants and determine the cortical layers. A description of specific methods used for individual subprojects can be found in the methods sections of the respective chapters. Details regarding the specific mouse strains as well as the numbers and characteristics of the animals used in each project are also provided there.

All experiments were performed in accordance with the United Kingdom Animal (Scientific Procedures) Act 1986 under personal and project licences granted by the United Kingdom Home Office. Ethical approval was provided by the Ethical Review Panel at the University of Oxford. Animal holding and experimentation was located at the Biomedical Sciences Building (BSB) and the Behavioural Neuroscience Unit (BNU), University of Oxford.

## 2.1 Mouse breeding and husbandry

Mouse breeding was performed on the level 2 breeding unit of the BSB. In preparation for experiments, cages of group-housed mice were transferred to the level 1 experimental unit of the BSB. Animals, which were designated for implantation of cranial recording devices, underwent a thorough health check a few days before surgery and were then single-housed in individually ventilated cages. Two to three days before surgery, mice were habituated to the taste of strawberry jelly in preparation for post-surgical oral analgesia for which the same type

of jelly would be enriched with an oral Metacam® (meloxicam, 5 mg/kg, Boehringer Ingelheim Ltd., Bracknell, UK) preparation. One day before surgery, mice were injected with Dexamethasone (0.2 mg/kg s.c., Boehringer Ingelheim Ltd., Bracknell, UK) to reduce brain swelling and the inflammatory response to the surgical implant. On the day of surgery, mice underwent another thorough health check and weighing and were then transferred to the 'sleep and circadian neurophysiology unit' on level 3 of the BSB for the surgical procedure, which is outlined in the next section. After surgery, mice were returned to level 1 where they underwent close post-operative monitoring at least once per day for at least five days. A standardised scoring sheet was used to assess the health status and evaluate the need for post-operative analgesia. After the recovery period of at least five days, mice were transferred back to the 'sleep and circadian neurophysiology unit' of the BSB, where electrophysiological recordings and passive infrared recordings were performed. Upon completion of the experiments, mice were transferred to the neighbouring BNU for terminal anaesthesia followed by transcardial perfusions and brain collection for the histological processing to reconstruct electrode position and cortical lamination.

## 2.2 Surgical procedures

All animals undergoing electrophysiological *in vivo* recordings were implanted with custom-made cranial head stages for EEG/EMG recordings in an aseptic surgical procedure under isoflurane anaesthesia as described here. A subset of animals received one or two additional intracranial implants during the same surgery session. Details about the additional implants are provided in the methods sections of the respective chapters.

### 2.2.1 Preparation of EEG and EMG implants

In preparation for the surgery, custom-made head stages for EEG/EMG recordings were manufactured using stainless steel screws (shaft diameter 0.86 mm, InterFocus Ltd, Cambridge, UK), stainless steel wires, eight-pin and 90° connectors (Pinnacle Technology Inc, Kansas, USA, model 8415-SM). Connections were soldered and sealed with Simplex Rapid dental acrylic cement (Associated Dental Products Ltd, Swindon, UK). After conductivity testing the head stages were sterilised for aseptic surgery.

### 2.2.2 Preoperative procedures

Immediately before the surgical procedure, mice were anaesthetised in an induction chamber with ~5 % isoflurane at an oxygen flow rate of ~2-3 L/min until righting and pedal reflex were absent. Mice were then transferred to a heat pad, where anaesthesia was maintained through a nose mask using ~2-3 % isoflurane at an oxygen flow rate of ~1-1.5 L/min while the implantation site was shaved and analgesia administered. Metacam® (meloxicam, 5 mg/kg, Boehringer Ingelheim Ltd., Bracknell, UK) and Vetergesic® (buprenorphine, 0.1 mg/kg, Sogeval UK Ltd., York, UK) were administered via s.c. injection. The mice were then transferred to a stereotactic surgery frame (David Kopf Instruments, California, USA; Model 900 Small Animal Stereotaxic Instrument) placed on a heat pad, and fitted with a rectal probe to maintain the core body temperature around 36°C. After fixation of the animal's head in the stereotactic frame, the isoflurane concentration was adjusted based on the breathing rate (target rate 50-90 per min) and was kept stable typically using a isoflurane concentration between 0.6-1.2 % at a flow rate of ~1 L/min throughout the surgery. Regular anaesthesia checks were performed every 15-30 minutes by a surgery assistant. Viscotears Liquid Gel® (Alcon Laboratories Limited, Hemel Hempstead, UK) was applied for eye protection before the implantation site was thoroughly cleaned with povidone-iodine and ethanol.

### 2.2.3 Implantation of electroencephalography and electromyography electrodes

The absence of the pedal reflex was confirmed before the skull was exposed via a midline incision from the level of the eyes to approximately 1.5 cm caudal to the ears. The skin flaps were retracted using bulldog clips or surgical retractors. Connective tissue was removed and the skull surface was cleaned with 3% hydrogen peroxide[2], etched with 37% phosphoric acid etching gel, and rinsed with saline. Using the stereotactic frame, the positioning of the mouse skull was recalibrated to allow no more than 0.2 mm deviation between the dorso-ventral coordinates for Bregma and Lambda. Once the levelled position of the skull was confirmed, implantation sites were marked on the skull using needle-tip with ink attached to the stereotactic arm. The standard positions for EEG screws relative to Bregma were (Figure 10a):

- Frontal EEG: AP +2.0 mm; ML +2.0 mm
- Occipital EEG: AP -3.5 to 4.0 mm; ML +2.5 mm
- Anchor screw: AP -3.5 to 4.0 mm; ML -2.5 mm
- Reference screw: 2 mm behind Lambda; ML ±0.0 mm

[2] This practice was stopped in summer 2018 upon advice of the in house veterinary service due to considerations that accidental exposure of the soft tissue at the incision margins to hydrogen peroxide could potentially impair the wound healing after the surgery.

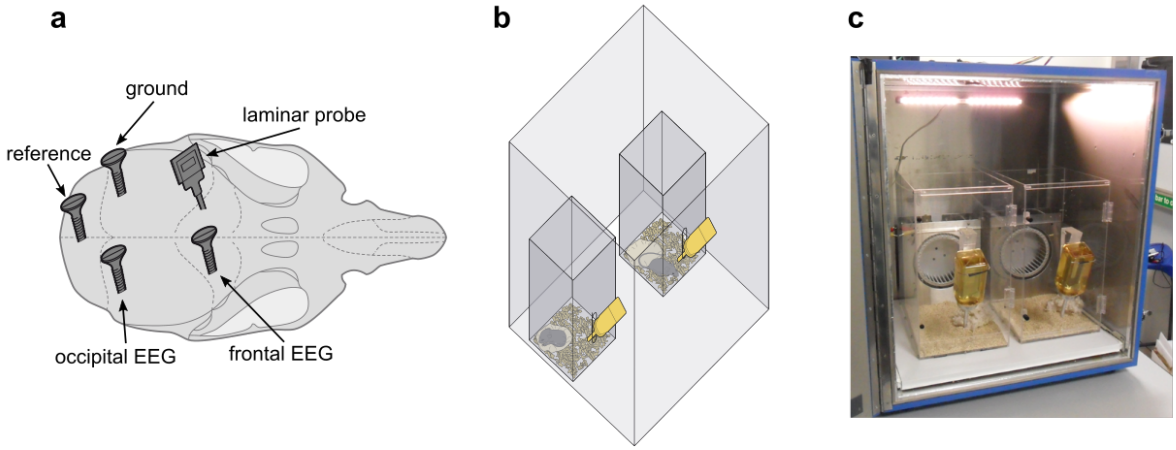



**Figure 10: Electrophysiological implants and recording setup**

a) Schematic of a mouse skull with frontal and occipital electroencephalography (EEG) implants, a laminar probe in the right primary motor cortex as well as ground and reference screws. b) Schematic of the recording setup. Two single-housed mice are placed in a sound-attenuated Faraday chamber. The cables for tethered recordings are inserted from the top. c) Picture of a recording chamber. Note that in the experiments presented in this thesis the running wheels at the back were blocked by a Plexiglas screen. Picture in panel (c) courtesy of Prof Vladyslav Vyazovskiy.

Under microscopic control, a surgical drill with a 0.6 mm diameter carbon steel burr (InterFocus Ltd, Linton, UK) was used to prepare skull holes for the epidural insertion of the stainless steel screws. The exposed dura at the bottom of the holes was kept moist by applying sterile saline to the holes immediately after drilling. All EEG screws were carefully implanted in the designated holes and fixed with dental cement SuperBond® (Prestige Dental Products Ltd, Bradford, UK). Following the stabilisation of the EEG screws, two stainless steel wires were implanted bilaterally into muscle pockets, which were created with the tips of sharp forceps. The implants and wires were then secured with dental cement and the skin in the neck sutured if necessary.

### 2.2.4 Implantation of cortical laminar probes

In a subset of animals, a 16-channel laminar probe (NeuroNexus Technologies Inc., Ann Arbor, MI, USA; model: A1x16-3mm-100-703-Z16) was also implanted to perform intracortical

recordings across cortical layers. To optimise the post-hoc histological assessment of insertion depth the tips of the electrodes were stained with the orange-red fluorescent membrane stain Dil® (1,1'-Dioctadecyl-3,3,3',3'-Tetramethylindocarbocyanine Perchlorate; Thermo Fisher Scientific, Waltham, MA, USA) shortly before the surgery and the probes then immediately protected from light exposure to minimize bleaching. A concentration of approximately 20 mg/ml DiI dissolved in 50/50% acetone/methanol was found to be most suitable to ensure a reliable demarcation of the electrode tract without excessive diffusion of the stain into the surrounding tissue.

The implantation of laminar probes was usually performed after the initial fixation of the EEG screws but before the insertion of the EMG wires. The implant coordinates for the laminar probes in primary motor cortex were: AP +1.1 mm; ML -1.75 mm; tilt 15° left (Figure 10a). The tilt was chosen to allow for an insertion of the laminar probes perpendicular to the cortical surface and to the cortical layers. For the insertion of the laminar probe, the bone around the implantation site was thinned in a circle with a diameter of around 1-1.5 mm under microscopic view using the same drill as for the EEG burr holes. The thinning of the skull around rather than above the implantation site ensured that the implanted cortex remained untouched and remained protected by a small island of skull bone until moments before the probe insertion. Once the dura in the circle around the implantation site had been freed of remaining bone flakes and moisturised with saline, the laminar probe was attached to a ZIF-Clip® 16 channel headstage (Tucker-Davis Technologies Inc., Alachua, FL, USA), fixed to a stereotaxic arm (David Kopf Instruments, California, USA; Model 900 Small Animal Stereotaxic Instrument), and carefully lowered over the implantation site. After the fine calibration of the stereotactic coordinates, the probe was retracted by a few centimetres, so that the bone flap over the implantation site could be removed using a needle tip. Because the dura is attached to the skull bone, removal of the bone flap alone was sufficient to remove the underlying dura. Once the

cortex was exposed, the laminar probe was lowered onto the pial surface and then inserted into the tissue under both stereotactic and microscopic control of the implantation depth. Individual probe channels could usually be seen through the microscope, which facilitated the depth control during the insertion. The highest electrode was typically placed about 50 µm under the cortical surface. In one instance, intraoperative recordings were performed to monitor the neuronal responses during the slow insertion of the probe into cortex. Immediately after implantation, the implantation site was sealed with the silicone elastomer Kwik-Sil® (World Precision Instruments Inc., Sarasota, FL, USA). The electrode shaft was then cemented to the neighbouring implants and the electrode was grounded and referenced to the respective skull screws.

### 2.2.5 Postoperative care

Before termination of the anaesthesia, sterile saline (5 ml/kg per hour surgery time) was administered to compensate for the fluid loss. Following the procedure, animals were closely monitored for about 1 hour in a recovery box (30°C initially, 25°C after regaining the righting reflex). When animals regained the ability to walk and reacted to external stimuli, they were returned to their home cage. During the first 3 days after surgery oral Metacam® in a strawberry jelly was provided for postoperative analgesia and i.p. injections of Vetergesic® and Metacam® were performed if required. Regular checks were performed until full recovery of the animal.

## 2.3 Experimental procedures for sleep experiments

### 2.3.1 Recording conditions

For sleep recordings, mice were transferred to separate custom-made Plexiglas cages (20.3 x 32 x 35 cm), which were placed in sound-attenuated and light-controlled Faraday chambers (Campden Instruments, Loughborough, UK), with each chamber fitting two cages (Figure

10b,c). Animals were allowed free access to food pellets and water at all times and underwent daily health inspection. A 12:12 h light:dark cycle (lights on at 9 am, light levels 120–180 lux) was implemented, temperature maintained at around 22 ± 2 °C, and humidity kept around 50 ± 20 %.

### 2.3.2 Standard experimental timeline

After an acclimatisation period of at least 3 days during which animals were habituated to the tethered recording conditions, continuous recordings were started, which were performed in 24-h blocks starting at light onset. After denoising of the electrophysiological signals, typically achieved through grounding and shielding of sources of electrical noise such as ventilation fans and lights, an undisturbed 24-h recording was performed on a designated baseline day. On the subsequent day, all animals were sleep deprived for 6 hours starting at light onset. Animals were then left undisturbed for the remainder of the 24-h recording period. Animals were typically kept in the recording setup for another 2-3 weeks to perform additional experiments, such as pharmacological manipulations, exposure to altered light-dark cycles, or recordings under access to running wheels.

### 2.3.3 Sleep deprivation

Sleep deprivation was performed for 6 hours from light onset, during the circadian period when mice are typically asleep and thus the homeostatic response to sleep loss can be most reliably elicited (Huber, Deboer, and Tobler 2000a). At light onset, recording chambers were opened, the nesting material removed, and novel objects such as wood blocks, cotton tips, bubble wrap, polystyrene blocks, and LEGO® bricks placed into the mouse cages to encourage exploratory behaviour. Experimenters continuously observed the mice and exchanged the provided objects for new objects when mice stopped exploring. At the end of the 6-h sleep deprivation, all

objects were removed, the nesting material returned, and the recording chambers closed. The animals were then left undisturbed for the remainder of the 24-h recording period.

## 2.4 Electrophysiological recordings

### 2.4.1 Data acquisition

Data was acquired using the 128 Channel Neurophysiology Recording System (Tucker-Davis Technologies Inc., Alachua, FL, USA) and the electrophysiological recording software Synapse (Tucker-Davis Technologies Inc., Alachua, FL, USA), and saved on a local computer. EEG and EMG signals were continuously recorded, filtered between 0.1 - 100 Hz, and stored at a sampling rate of 305 Hz. Extracellular neuronal activity was continuously recorded at a sampling rate of 25 kHz and filtered between 300 Hz - 5 kHz. Whenever the recorded voltage in an individual laminar channel crossed a manually set threshold indicating putative neuronal firing (at least 2 standard deviations above noise level), 46 samples around the event (0.48 ms before, 1.36 ms after) were stored. Concomitantly with the spike acquisition, LFPs were continuously recorded from the same electrodes and processed with the abovementioned settings for EEG signals.

### 2.4.2 Offline signal processing

EEG, EMG, and LFP signals were resampled at a sampling rate of 256 Hz using custom-made code in MATLAB (The MathWorks Inc, Natick, Massachusetts, USA, version v2017a) and converted into the European Data Format (EDF) as previously described (McKillop et al. 2018). Spike wave forms were further processed using a custom-made MATLAB script and events with artefactual wave forms were excluded from further analysis of neuronal activity. Multi-unit activity (MUA) traces for each channel were created using the time points of the first threshold crossing as individual spiking events.

### 2.4.3 Scoring of vigilance states

The software Sleep Sign for Animals (version 3.3.6.1602, SleepSign Kissei Comtec Co., Ltd., Nagano, Japan) was used for manual sleep scoring. EEG, EMG, and LFP recordings were partitioned into epochs of 4 seconds. Vigilance states were assigned manually to each recording epoch based on visual inspection of the frontal and occipital EEG derivations in conjunction with the EMG. Epochs with recording artefacts due to gross movements, chewing or external electrostatic noise were assigned to the respective vigilance state but not included in the electrophysiological analysis. EEG and LFP power spectra were computed using a fast Fourier transform routine (Hanning window) with a 0.25 Hz resolution and exported in the frequency range between 0 and 30 Hz for spectral analysis.

### 2.4.4 Definition of vigilance state episodes

Vigilance state episodes were typically defined as blocks of at least one minute (i.e. fifteen 4-s epochs) scored with the same vigilance state. Unless stated otherwise in the methods section of the respective chapter, interruptions of up to 16 s were allowed. Short intrusions wakefulness lasting up to 16 s during NREM or REM episodes were scored as movement and not counted towards the overall amount of wakefulness but instead analysed separately as brief awakenings.

### 2.4.5 Channel selection for laminar data analysis

If laminar implants were deemed suitable for data analysis following the histological assessment outlined in subchapter 2.6.3, LFP and MUA signals for each individual channel were plotted for visual assessment of the recording quality. Individual channels were only included in the subsequent analysis of LFP data if the average spectrograms of wake, REM, and NREM epochs from the baseline and sleep deprivation days reflected the characteristic profile of the respective vigilance state. Additional requirements were that 24-h plots of SWA

for each 4-s epoch did not indicate relevant signal fluctuations independent of the vigilance state and that no high-amplitude artefacts during NREM or REM sleep were observed. Before the MUA analysis, the average firing rates for each channel were plotted for all 4-s epochs and visually screened for artefacts.

### 2.4.6 Definition of OFF periods

Population OFF periods were defined as periods of total neuronal silence across all electrodes, which lasted at least 50 ms and no more than 4000 ms in accordance with previous work (Vyazovskiy et al. 2009). Subsequently, the top 20% longest OFF periods were included for final analyses. The latency to the first spike after the population OFF-ON transition was calculated separately for MUA recorded in layers 2/3 and layer 5. Only ON periods with at least 1 spike in each of the layers occurring within the first 200 ms were included in this analysis.

## 2.5 Statistical procedures

Data were analysed using MATLAB, SAS JMP (version 7.0; SAS Institute Inc. Cary, NC, USA) and IBM SPSS Statistics for Windows (version 25.0; IBM Corp., Armonk, N.Y., USA). Reported averages are mean±s.e.m. Analyses of variance (ANOVAs) were performed as described by Howell and Lacroix (G. T. Howell and Lacroix 2012). To examine potential differences in firing dynamics between superficial versus deep cortical layers in C57BL/6J mice, repeated-measures ANOVAs were conducted with cortical layers (layer 2/3 versus layer 5) and time bins as within-subject factors. To examine potential differences between genotypes of the cortical SNAP25-ablated mouse line, split-plot ANOVAs were conducted; genotype was entered as a between-subject factor, whereas time bins, EEG spectral bins, and vigilance states (wake, NREM, and REM) were entered as within-subject factors. $\alpha = 0.05$ was

adopted for main effects and interactions. Significant two-way interaction terms were followed up with Bonferroni-adjusted post hoc comparisons with $\alpha_{adjusted} = 0.05/k$, where k represents the total number of pairwise comparisons made (D. C. Howell 2012). In ANOVAs with multiple time points, the total number of post hoc comparisons was minimised in each case, and hence controlling for the increase in familywise error rate, by pooling across multiple time bins. For spectral analysis, EEG/LFP power spectra of individual animals were log-transformed before hypothesis testing. Bonferroni correction was not applied for post hoc comparison of spectral data because ANOVAs consisting of 119 EEG spectral bins would be too conservative and reduce statistical power (Achermann and Borbély 1998); thus, α was kept at 0.05 in these cases. In all figure panels illustrating EEG or LFP spectrograms, frequency bins for which the resulting post-hoc comparison was significant after Bonferroni adjustment are highlighted with black asterisks; bins only significant before Bonferroni adjustment are highlighted with grey asterisks to indicate areas of interest bearing in mind that no correction for multiple comparisons was applied. In the circadian analysis, a multivariate ANOVA (MANOVA) was conducted to examine if the linear combination of multiple circadian response variables (period length, periodogram power, and phase shift) differed between genotypes (Tabachnick and Fidell 2011). Greenhouse-Geisser correction was used when the assumption of sphericity was violated (Mauchly's test of sphericity, $p<0.05$). Mann-Whitney U tests were performed for main analyses instead of one-way ANOVAs if the assumption of normality was violated (Shapiro-Wilk test of normality, $p<0.05$). In all figures, significance levels are indicated with black asterisks: '*' for $0.05 \geq p > 0.01$; '**' for $0.01 \geq p > 0.001$; '***' for $0.001 \geq p$. Grey asterisks indicate post-hoc comparisons with $P < 0.05$, which do not reach significance after Bonferroni correction for multiple comparisons. Panels representing grouped data of durations spent in specific vigilance states show group mean (red line), 95% confidence interval (pink box), and one standard deviation (blue box) with individual data

points overlaid; these plots were generated using the functions notBoxPlot (Rob Campbell (2019). notBoxPlot (https://www.github.com/raacampbell/notBoxPlot), GitHub. Retrieved June 15, 2019) and RGB (Kristjan Jonasson (2019). RGB triple of color name, version 2 (https://www.mathworks.com/matlabcentral/fileexchange/24497-rgb-triple-of-color-name-version-2), MATLAB Central File Exchange. Retrieved June 15, 2019). For key analyses, the effect sizes were calculated as Cohen's d using the MATLAB function computeCohen_d (Ruggero G. Bettinardi (2020). computeCohen_d(x1, x2, varargin) (https://www.mathworks.com/matlabcentral/fileexchange/62957-computecohen_d-x1-x2-varargin), MATLAB Central File Exchange. Retrieved October 4, 2020). Statistical analysis methods in chapter 4 deviated from the procedures described here, as most of the analysis for this chapter was performed using general liner models in Prism (version 9.1.1; GraphPad). Details are provided in the methods section of the respective chapter.

## 2.6 Histological methods

### 2.6.1 Electrical microlesions to localise electrode position

After completion of the experiments, microlesions of selected channels on the laminar probe were performed under terminal pentobarbital anaesthesia using the electroplating device NanoZ$^{TM}$ (White Matter LLC, Seattle, WA, USA). The settings for the microlesion procedure were optimised throughout the project based on histological results as described subchapter 3.3.1. After extensive validation, the optimal microlesion parameters appeared to be 5 µA and 10 seconds of current application and usually four lesions were performed starting at the deepest electrode contact (channel 16), and then lesioning the channels 500 (channel 11), 1,000 (channel 6), and 1,500 µm (channel 1) above. Immediately following microlesioning, mice were perfused with 0.1 M phosphate buffered saline (0.9 %) (PBS) followed by 4 %

paraformaldehyde (PFA) in PBS for tissue preservation for further histological processing and analysis.

### 2.6.2 Tissue preparation and microscopy

It was found that the demarcation of the electrode was best visible, if, instead of extracting the brain immediately after perfusion, the whole head of the mouse was kept in the PFA solution for about 3 days, then transferred to PBSA (0.1M PBS + 0.1-0.05% sodium azide) until the histology could be performed, typically after a few weeks. The brain was then removed from the skull and embedded in 4% agarose for sectioning, staining and microscopy. Tissue damage, especially to the cortical region around the implant, could be avoided by dissecting the brain starting from the skull base. A vibrating microtome (Leica VT1000S) was used to section the brains into 50 μm coronal slices. Fluorescent staining was performed with 4′,6-diamidino-2-phenylindole (DAPI).

### 2.6.3 Assessment of cortical layers and laminar probe position

After fluorescence microscopy, implantation sites were mapped using a mouse brain atlas (Paxinos and Franklin 2019). The anterior-posterior and medio-lateral position of the implant site was determined based on anatomical landmarks. The depth of the laminar implant was assessed by measuring the distance between cortical surface and the electrical current-induced tissue microlesions. The boundaries between cortical layers were identified based on cell density and morphology. Animals were only included in the laminar analysis if the position of the laminar probe in the primary motor cortex could be anatomically confirmed, if there was no relevant cortical damage at the implant site, and if the histological assignment of electrode channels to respective cortical layers matched the electrophysiological profile as described in subchapter 3.3.1. ImageJ (version 1.52a) was used to merge fluorescence images and add scale bars to the histological images (Schindelin et al. 2012). Figures were then created using

Inkscape (version 1.0.2, Inkscape Project. (2020). Inkscape. Retrieved from https://inkscape.org).

# Chapter 3: Laminar profile of neocortical activity during NREM sleep

## 3.1 Introduction

The role of the cortex in sleep-wake regulation can be best investigated by using both observational and perturbational approaches. I hypothesised that cortex, and in particular neocortical layer 5 pyramidal neurons, actively contributes to the regulation of sleep oscillations and sleep-wake states. This chapter focuses on the observational approach. I here describe the implementation of laminar probe recordings in freely moving mice and their application in assessing cortical dynamics of OFF and ON periods during NREM sleep. In the introduction to this chapter, I will explain what (laminar) silicon probes are and how *in vivo* silicon probe recordings have propelled our understanding of the relationship between neuronal dynamics and behaviour particularly in rodent neuroscience. I will further provide examples of how silicon probes have recently been used to investigate cortical dynamics during anaesthesia and REM sleep and why this methodology was appropriate to address my research question. The brief methods section provides information about the experimental animals used for the recordings presented in this chapter and contains cross-references to the detailed description of histological techniques and analysis methods for the laminar recordings provided in the general methods chapter. The results section consists of two parts: The first part summarises the histological work required for the assignment of individual recording channels of the laminar probe to the respective neocortical layer. The second part summarises my initial results from laminar recordings in wild type mice, which underscored the importance of layer 5 in orchestrating cortical dynamics during NREM sleep. In the discussion section, I will outline how my efforts to implement *in vivo* laminar probe recordings were essential to address the role of layer 5 pyramidal neurons in the regulation of sleep oscillations.

### 3.1.1 Silicon probes for chronic *in vivo* recordings in mice

Silicon probes are microscale electrode arrays on a silicon substrate produced in photolithographical microfabrication. The typical shank thickness and width between 10 and 100 µm minimises the tissue damage and the predefined configuration of several electrode contacts on one single array enables the recording of local field potentials and neuronal firing at a high spatiotemporal resolution (Buzsáki, Anastassiou, and Koch 2012). Silicon probe technology is particularly powerful in establishing links between neuronal firing dynamics and animal behaviour, because the size and weight of silicon probes renders the arrays suitable for chronic *in vivo* recordings in freely moving animals (Buzsáki et al. 2015). Laminar probes, a type of silicon probes with individual contacts aligned on one single shaft (Figure 11b), are ideal for recording from cortical structures because individual channels can be assigned to specific cortical layers and long laminar probes can be used to record simultaneously from cortical structures such as neocortex or hippocampus and subcortical structures such as thalamus or striatum. Over the course of this project, complementary metal-oxide-semiconducter (CMOS) technology in Neuropixel probes has brought an order of magnitude increase in the number of recording sites to 960 (Jun et al. 2017) and most recently to 5120 per electrode, with a spacing of 15 µm (Steinmetz et al. 2021). However, the number of simultaneously recorded channels on each individual probe remains at 384 and the immense amount of data generated per time unit limits their use for continuous 24-h recordings. Especially in chronic recordings, the number of simultaneously recorded signals still remains considerably below the numeric count of channels per electrode. I used a Neuronexus 16-channel laminar probe with a spacing of 100 µm, because the length of this probe (electrode contacts spanning 1.5 mm) made it possible to span the entire neocortical depth in the primary motor cortex of a mouse and to have at least one channel in each cortical layer. The choice of a laminar implant was motivated by several factors: First, the extremely small diameter of the

probes and the single-shank design minimise cortical tissue damage. Second, if adequately implanted, the probes are highly resistant to artefacts due to movement or electrostatic noise. Third, the probes have a high recording stability and can be used for several weeks, which is a crucial factor for chronic sleep experiments. Fourth, the electrodes were commercially available and compatible both with our TDT 128 Channel Neurophysiology Recording System used to record EEG and EMG signals and with the NanoZ$^{TM}$ electroplating device used to create microlesions under terminal anaesthesia for the histological assessment of the electrode position. Overall, the Neuronexus 16-channel laminar probes were well suited for the aim of this project to assess neocortical dynamics during sleep, in particular the laminar firing patterns underlying NREM sleep slow waves.

### 3.1.2 Cortical neuronal dynamics associated with slow waves in brain slices and anaesthetized animals

Cortical activity during NREM sleep and under most types of general anaesthesia is characterized by an alternating pattern between active firing and coordinated silence in neocortex, which results in slow waves in LFP and EEG recordings (Steriade, Nuñez, and Amzica 1993; Steriade et al. 1993; M. Murphy et al. 2011; Warnaby et al. 2017). This bistable activity pattern, which is thought to be generated by a corticothalamic interplay during physiological sleep (Steriade, Nunez, and Amzica 1993), can also be observed in brain slices (Sanchez-Vives et al. 2000) and has been extensively studied in anaesthetised animals due to the similar temporal dynamics during general anaesthesia and sleep (Steriade, Nuñez, and Amzica 1993; González-Rueda et al. 2018). Based on cortical deafferentiation experiments it has been postulated that neocortex alone can generate ON-OFF dynamics and slow oscillations of a similar temporal structure to the intact brain, suggesting that the neocortex might be the pacemaker of this activity pattern (Timofeev et al. 2000). Within neocortex, *in vitro*

experiments in ferret neocortex (Sanchez-Vives et al. 2000) and *in vivo* work in cats suggest that layer 5 initiates the transitions from silent OFF to active ON periods (Chauvette, Volgushev, and Timofeev 2010). The assumption that layer 5 pyramidal neurons play an essential role in coordinating these dynamics is supported by optogenetic activation and photoinhibition experiments comparing the population responses after stimulation of pyramidal neurons in layers 2/3 and 5 (Beltramo et al. 2013). Two mechanisms might underlie this functional role of layer 5 pyramidal neurons: an initiation of activity due to intrinsic pacemaker properties of a subclass of neurons (Le Bon-Jego and Yuste 2007; Lőrincz et al. 2015) or the summation of miniature excitatory postsynaptic potentials (mEPSPs) resulting from spontaneous neurotransmitter release (Timofeev et al. 2000). While the neocortical dynamics underlying slow waves *in vitro* and in anaesthetised animals have been extensively studied, much less is known about their spatiotemporal structure during natural sleep.

### 3.1.3 Cortical neuronal dynamics during slow wave sleep

It has been long established that neocortical population activity shows a characteristic bistable pattern during NREM sleep (Noda and Ross Adey 1970). The relationship between the fluctuating UP and DOWN states in the membrane potential of individual neurons, the alternating ON and OFF states of burst firing and neuronal silence in cortical populations, and the oscillating depth negative and positive slow waves in local field potentials has been described in detail (Steriade, Timofeev, and Grenier 2001). However, the temporal change of OFF-periods and slow waves with sleep-wake history (Vyazovskiy et al. 2009) and their occurrence during wakefulness (Vyazovskiy et al. 2011) and REM sleep (Funk et al. 2016) have only been investigated more recently. In brief, the duration and incidence of ON and OFF periods, as well as the neuronal synchrony at the transition between population activity and silence during NREM sleep, all correlate with changes in slow wave activity and reflect the

homeostatic sleep drive in cortex (Vyazovskiy et al. 2009). OFF periods are more frequent and long when sleep debt is high, while ON periods are frequent but short. With dissipating homeostatic sleep drive, OFF periods become shorter and less frequent, while ON periods become longer and less frequent. The synchrony between individual neurons at the transitions between oscillating states of population activity and silence is higher when sleep pressure is elevated and lower when it has dissipated (Vyazovskiy et al. 2009). While these homeostatic changes could merely be driven by the neuromodulatory milieu, the homeostatic change in firing rates within each individual vigilance state indicates that the homeostatic response is implemented directly in cortex rather than imposed on it (Vyazovskiy et al. 2009). This assumption is also supported by the finding that brief periods of population silence can occur in cortex even in awake animals when sleep pressure is high (Vyazovskiy et al. 2011). Interestingly, laminar probe recordings from six different cortical areas led to the observation that slow waves can occur during REM sleep in superficial layers in primary cortical areas and indicated that slow wave activity during NREM sleep might be most pronounced in deep cortical layers (Funk et al. 2016). However, this study did not investigate neuronal dynamics underlying slow waves and the spectral differences between deep and superficial cortical layers were not explored systematically (Funk et al. 2016). Due to a lack of histological or electrophysiological proof of cortical integrity in the study by Funk et al., it remains a possibility that some of the reported patterns in the occurrence of slow waves could be explained by cortical damage as commonly observed during the surgical implantation procedure (Sheroziya and Timofeev 2014), especially as slow waves are known to occur independent of vigilance state when cortical integrity is compromised (personal conversation with Prof. Igor Timofeev in 2018)(Sarasso et al. 2021; Sanchez-Vives and Mattia 2014).

The experiments presented in this chapter had two aims: First, to develop an implantation and histology protocol for laminar probe recordings in mice, which minimises cortical damage and

ensures a precise localisation of individual electrode channels to specific cortical layers. Second, to acquire a laminar dataset from primary motor cortex in wild type mice for a descriptive characterisation of neuronal firing and brain oscillations across the entire thickness of the cortex sampling all cortical layers during wakefulness and sleep and during state transitions.

## 3.2 Methods

In collaboration with Dr Martin Kahn, I performed these experiments in 7 wild type C57BL/6J (C57BL/6JOlaHsdOxuni) mice (age at baseline recording 125±8 days) sourced internally from the Biomedical Services at the University of Oxford. Animals were implanted for EEG, EMG, and laminar recordings from primary motor cortex as described in the general methods chapter (section 2.2) with the exception that each animal was also implanted with a bipolar concentric electrode (PlasticsOne Inc., Roanoke, VA, USA) in the right primary motor cortex, anterior to the frontal EEG screw. To accommodate this additional implant, which was used by Dr Martin Kahn after completion of my experiments to deliver electrical pulses to cortex, the frontal EEG screw was implanted slightly posterior to its usual position. We did not encounter any difficulties with the manual sleep scoring and it should be noted that the laminar data presented in this chapter was recorded from the hemisphere contralateral to the EEG and concentric electrode implants. Therefore, we have no indication that this additional implant affected the laminar recordings presented in this chapter. Electrophysiological data acquisition, sleep scoring, and data analysis were performed as outlined in the general methods (section 2.3). A special focus of the laminar analysis was the assessment of OFF periods. A definition of OFF periods and references for the adopted analysis criteria are provided in the general methods (section 2.4.6). The histological procedures to localise the laminar probe position was refined

as outlined in the results section of this chapter. The final protocol is provided in the general methods chapter (section 2.6).

## 3.3 Results

### 3.3.1 Assignment of laminar probe channels to individual cortical layers

The very first challenge in setting up the laminar probe recordings was to develop a protocol to identify the exact in situ position of the individual electrode contacts on the shank of the laminar probe in relation to the cortical layers at the implantation site. While the stereotactic implantation procedure should in theory ensure that the implants are placed with no more than approximately 100 μm deviation from the optimal implantation depth, the small anatomical differences in the suture landmarks of the mouse's skull, as well as the inevitable expansion and shrinkage of the brain during surgical anaesthesia, make it necessary to validate the correct positioning in primary motor cortex as well as the depth of each individual laminar implant (Buzsáki et al. 2015). In preparation for the laminar probe surgeries, I estimated that by tilting the probe 15° in the anteroposterior axis towards the side of the implant, it should enter the cortex perpendicular to the surface, thereby minimising the tissue damage through lateral sheer forces and, in principle, allowing for recordings from the same cortical column (Figure 11a). The electrodes were inserted to a depth of 1.6 mm, so that the part of the laminar probe shank containing the electrode contacts spans all cortical layers, with the bottom channel reaching into corpus callosum (and occasionally as deep as the striatum) and the top channel lying just under the cortical surface in layer 1 (Figure 11 a,b). The fragility of the probe (entire thickness is 15 μm) and the sensitivity of the brain tissue to mechanical stress forbid any readjustments to the electrode position after insertion and implantation (Figure 11 b,c).

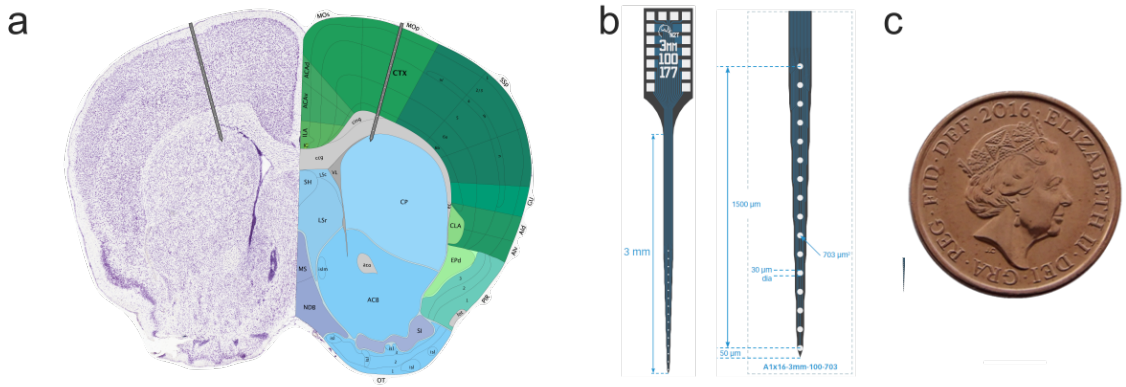



**Figure 11: Location of implantation in primary motor cortex and dimensions of a 16-channel laminar probe**

a) Laminar probe position on a coronal brain section of a young adult (56 day) mouse. Brain section and outline of the brain structures at anterior-posterior position approximately Bregma +1.1mm. Image credit: Allen Institute. Laminar probe superimposed to indicate orientation and relative dimensions. b) Catalogue image of a 16-channel laminar probe (NeuroNexus Technologies Inc). Individual contacts of 30 µm diameter are spaced every 100 µm on a 1.5 mm shank segment (right). Note that the entire shank length is 3 mm to allow for sealing and implantation of the shaft above the cortical surface as depicted in this similar probe design with smaller (15 µm) contacts (left). c) Electrode shank of a laminar probe (lower left in the panel) in relation to a one penny coin. Coin image retrieved from: https://en.wikipedia.org/w/index.php?curid=45219773 on 11/07/2021.

In preparation of my first implants, I consulted previous examples of electrode staining with DiI (1,1'-Dioctadecyl-3,3,3',3'-Tetramethylindocarbocyanine Perchlorate) (Magill et al. 2006; Funk et al. 2016; Sakata and Harris 2009) and microlesions (information provided by Neuronexus). However, the exact preparation of the DiI stain (Magill et al. 2006) and the details of the parameters of the current and time used for the microlesion lesion procedure are rarely reported (Parikh et al. 2007). Similarly, the individual steps of the implantation procedure, especially concerning the craniotomy and durotomy are typically not mentioned, despite reports that it is *"practically impossible to remove the dura without cortical damage in mice."* (Sheroziya and Timofeev 2014). My initial attempts to perform laminar implants highlighted various technical challenges of laminar probe recordings. Using an 80 mg/ml solution of DiI (dissolved in 50/50% acetone/methanol) as suggested by a previous study

(Magill et al. 2006), the electrode tract could be easily visualized in the post-mortem histology, yet only as a thick blurry trace (Figure 12a). Especially in the white matter, the boundaries of the electrode tract could not be delineated due to apparent diffusion alongside the myelinated fibre tracts. In addition, the overlapping emission spectra of DiI and the tdTomato reporter (Ai14) in the transgenic mouse model presented in chapter 5, rendered the DiI stain at this previously published concentration insufficient for precise electrode localisation (Figure 12a). Despite careful durotomy under microscopic control, all initial surgeries resulted in damage to the superficial cortical layers (Figure 12a) and in some animals, the electrode localisation could no longer be performed due to tissue damage, either resulting from surgical complications or from tissue adhesion to the implant during removal of the laminar probe upon brain extraction during the perfusion procedure (Figure 12a).

To facilitate the localisation of the electrode, I then introduced a microlesion procedure using the NanoZ device from White Matter LLC (Figure 12c). Using personal notes, kindly shared by Dr Xudong Wang (NDCN, University of Oxford), I performed the first successful microlesions, yet the parameters required further optimisation as the microlesions were larger than expected and the hole created by current application to the bottom channel of the laminar probe tended to fuse with the lateral ventricle (Figure 12d).

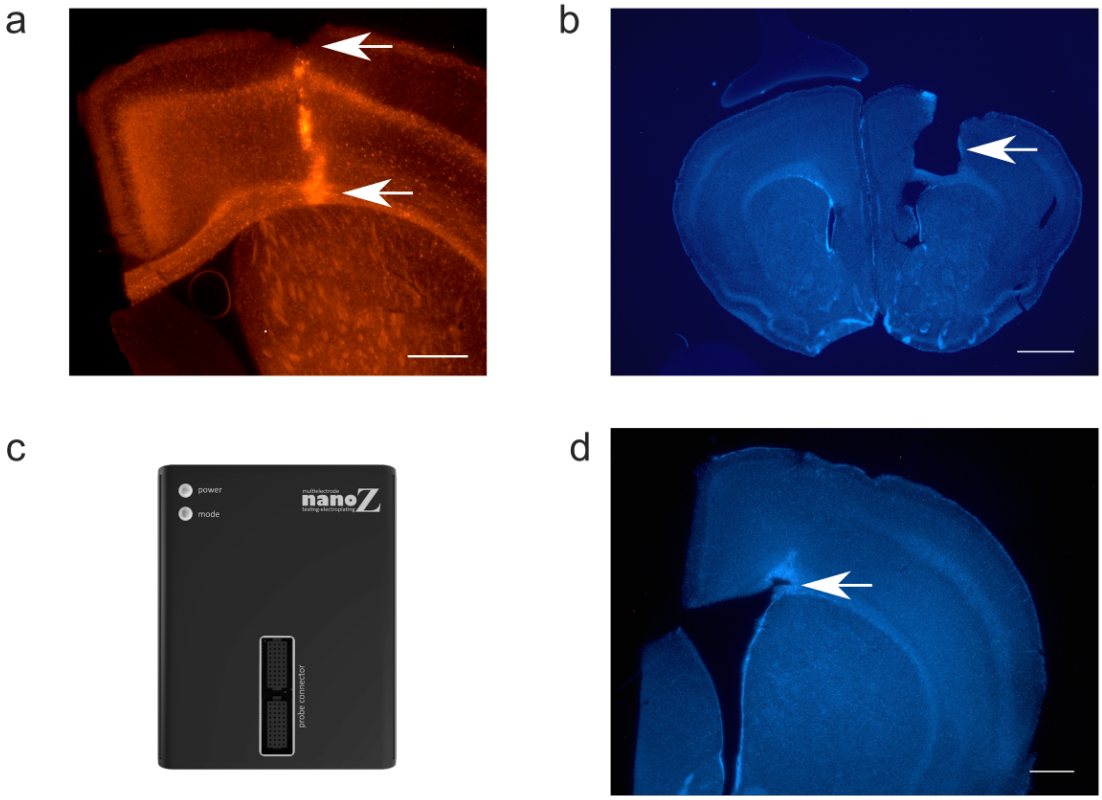



**Figure 12: Initial issues encountered with the analysis of laminar probe histology and detection of electrical microlesions**

a) Coronal section of a laminar probe tract stained with DiI in a *Rbp4-Cre;Ai14;Snap25*$^{fl/fl}$ mouse. Arrows indicate structural damage in superficial cortical layers 1 and 2/3 as well as the diffusion of the DiI stain in the white matter, which makes it impossible to identify the exact position of the implant. Further note that the overlapping emission spectra of the tdTomato reporter Ai14 and the DiI stain make it difficult to distinguish Cre+ cells from stained tissue. b) Structural damage at the implant site, most likely due to adhesion of the brain tissue to the electrode during removal of the headstage. c) NanoZ device from White Matter LLC. d) Oversized microlesion breaking into the left lateral ventricle due to excessive current application. Scale bars in panels a and d: 500 µm. Scale bar in panel b: 1,000 µm. DiI: 1,1'-Dioctadecyl-3,3,3',3'-Tetramethylindocarbocyanine Perchlorate.

After several steps of optimisation of the surgery techniques, microlesion procedure, perfusion, tissue extraction, and histology procedures I was able to implant laminar probes without cortical damage and to precisely localise the electrode tract (Figure 13). In short, the surgery procedure was optimised based on the notion that the periosteal layer of the dura mater is attached to the skull and therefore the dura can be removed by creating a bone island and levering it with a needle tip without touching the dura or the brain. Through this technical

refinement, cortical integrity could be maintained in nearly every single surgery. The microlesion procedure was optimised by reducing the current strength and the duration of current application to 5 µA and 5-25 seconds, which reduced the size of the created microlesions (Figure 13b). The optimal microlesion parameters appeared to be 5 µA and 10 seconds current application and it was most useful for the histological measurements to start from the bottom channel. By electrolesioning the bottom channel first, I could ensure that at least the deepest channel was clearly demarcated even if the current damaged the electrode at some point during the microlesion procedure. Following the first lesion, I typically performed three more lesions 500 (channel 11), 1,000 (channel 6), and 1,500 µm (channel 1) above the deepest channel before the mice were transcardially perfused. In order to stabilise the brain tissue before electrode removal, the entire mouse skull (with the headstage in place) was placed into PFA solution (4%, made up in PBS) for three days and subsequently stored in PBSA for at least four weeks at 4 $^{o}$C before the laminar probe was extracted. By chance, I observed that this extended post-fixation and subsequent storage of the brain with the laminar probe in place typically resulted in very fine marks at the position of most or all individual electrode contacts (Figure 13a and a''), even those which had not been used for microlesions, possibly due to metal deposition.

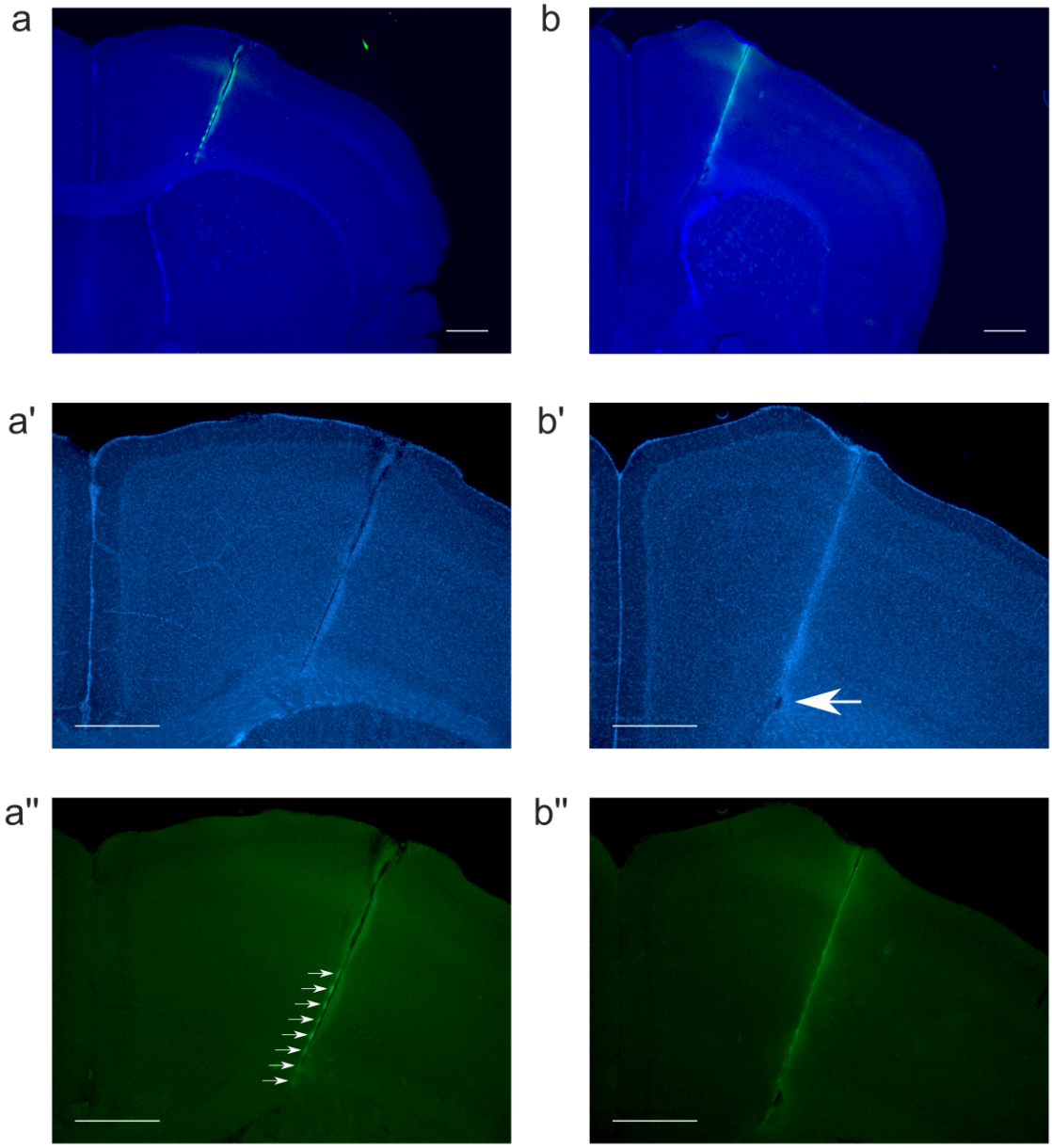



**Figure 13: Laminar probe histology after optimisation**

a-b) Two representative composite images of a coronal brain sections including a laminar probe track. Higher magnification raw images of the blue (') and green (") channels are shown below. Note the fine demarcation of individual channels in panel a'' and the microlesion at the depth of the bottom channel in panel b'. All scale bars: 500 µm.

This optimised histological procedure was used as the primary method to determine the position of individual laminar probe channels. However, in addition, the positioning of each implant was further confirmed using the recorded neuronal signals. Typically, some of the bottom channels were in the corpus callosum, resulting in no or very sporadic and distant

neuronal activity (Figure 14). Similarly, the top channel of the laminar probe was often located on the cortical surface and did not register meaningful neuronal signals. I used these locations as my reference points.

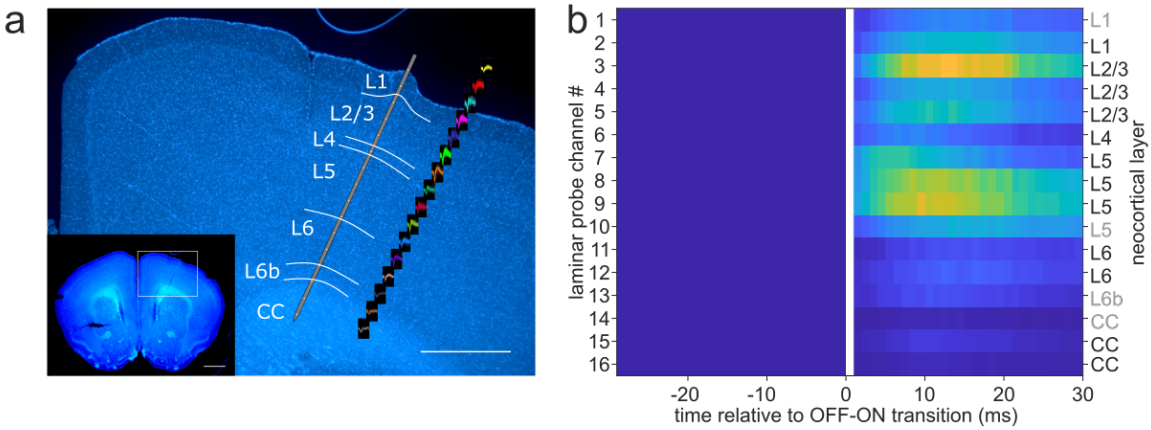



**Figure 14: Histological and electrophysiological assignment of laminar probe channels**

a) Coronal brain section with superimposed schematic of the laminar probe and spike wave forms recorded from individual channels 1-16. Note that according to the histological estimate of the laminar probe position, the top channel is located just on the cortical surface and the bottom three channels in the corpus callosum. This histological assessment is validated by lack of meaningful spike wave forms (inlays in panel a) and the near absence of neuronal firing at the OFF-ON transition (panel b) in the respective channel. b) average neuronal activity in each individual laminar probe channel averaged across all OFF-ON transitions (minimum duration of OFF periods analysed here is 100 ms) during non-rapid eye movement (NREM) in a 24 h baseline recording. Note that the strongest firing is observed in layers 2/3 and 5 and that the boundary between these supra- and infragranular layers is clearly distinguishable in the population firing pattern. CC: Corpus Callosum. L1, L2/3,/ L5, L6, L6b: Neocortical layers 1, 2/3, 5, 6, 6b.

As an additional means to validate the electrode depth, I used the laminar profile of neuronal activity at the OFF-ON transition between population silence and active firing during NREM sleep (Figure 14b). I observed the strongest neuronal activity in supra- and infragranular layers (Figure 14b) with a distinct band of low firing at the boundary between layers 2/3 and 5. As previously reported (Chauvette, Volgushev, and Timofeev 2010), the polarity inversion of large slow waves in the LFP during NREM sleep also occurred at this level (Figure 15b). Only if the histological and electrophysiological depth estimate of the laminar probe channels

matched, and the integrity of all cortical layers was histologically validated, was an animal included in the laminar analysis.

### 3.3.2 Laminar activity across cortical layers illustrates vigilance state-dependent differences in neocortical dynamics

Once the methodological challenges of laminar probe recordings had been overcome, I first asked whether the data acquired in the laminar recordings would reflect the cortical activity patterns described in previous work on neocortical activity during sleep in mice (Vyazovskiy et al. 2009). As expected, the vigilance states were clearly distinguishable based on EEG and EMG recordings. Wakefulness was characterised by low amplitude, high frequency EEG and irregular high and low amplitude EMG signals reflecting voluntary muscle activity (Figure 15a). NREM sleep showed high amplitude slow waves in the EEG accompanied by nearly complete absence of muscle activity in the EMG, with heart beat artefacts visible as regular low amplitude spikes in the EMG (Figure 15b). REM sleep was identified by a regular pattern of theta activity in the EEG accompanied by either muscle atonia reflected in flat EMG with heartbeat artefacts during tonic REM sleep or occasional muscle twitches during phasic REM sleep (Figure 15c). The LFP and MUA traces reflected the cortical activity accompanying these observed EEG patterns. During NREM sleep the characteristic bistable pattern of alternating OFF periods with population silence and ON periods with high population activity was observed in the MUA of all animals. OFF periods were accompanied by large amplitude slow waves, often with positive deflections in infragranular and negative deflections in supragranular layers (Figure 15b). However, it should be noted that this signal inversion during slow waves described in great detail in anaesthetised cats (Contreras and Steriade 1995), and frequently investigated in anaesthetised animals and brain slices (Chauvette, Volgushev, and Timofeev 2010), was not present during all slow waves and local field potentials were

sometimes positive across all layers. This may indicate that the characteristics of slow waves during sleep and anaesthesia differ in some of their characteristic properties (Timofeev and Chauvette 2018) and show a much greater diversity (e.g. in terms of OFF-state duration) during natural sleep than during anaesthesia (Torao-Angosto et al. 2021).

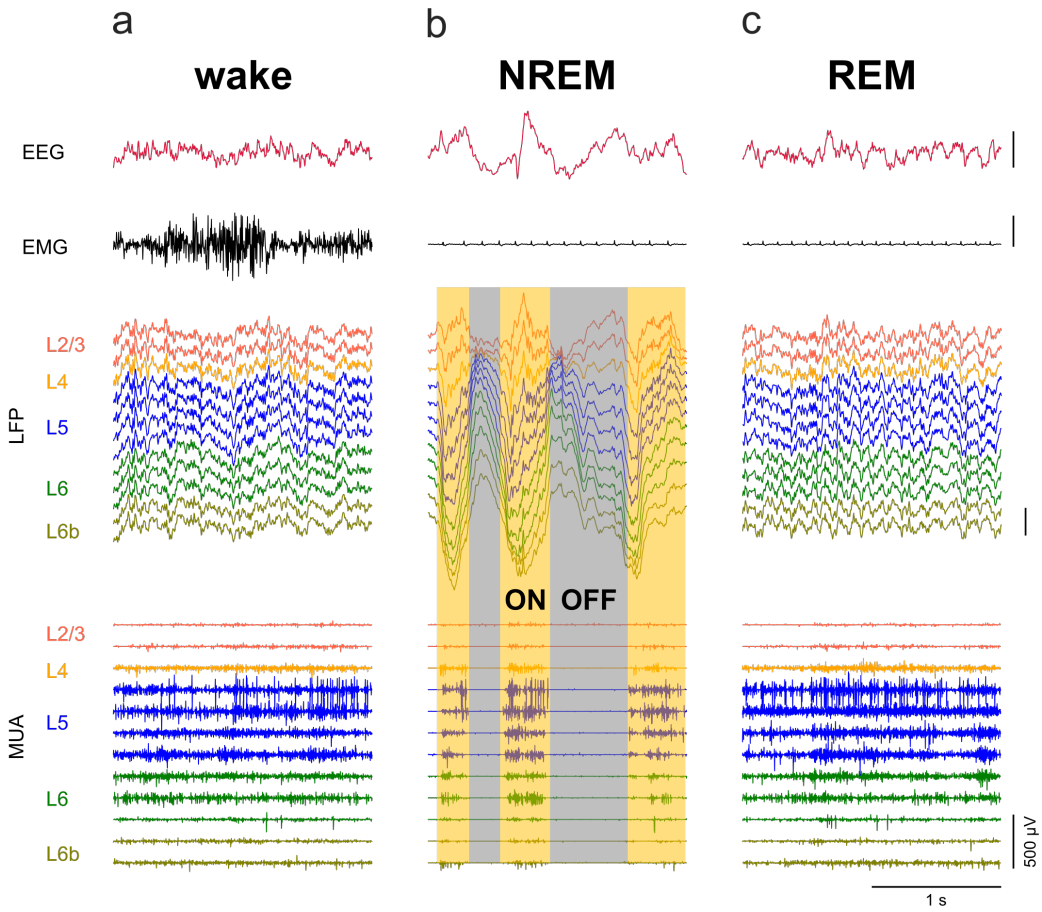



**Figure 15: Examples of EEG, EMG, and laminar recordings during wakefulness, NREM, and REM sleep**

Representative examples of recording signals acquired by simultaneous EEG, EMG, and laminar recordings during wakefulness (a), NREM sleep (b), and REM sleep (c). LFP, and MUA traces are colour coded. Neuronal ON and OFF periods during NREM sleep are highlighted with transparent yellow and grey panels, respectively. All scale bars on y-axis, 500µV. EEG: electroencephalogram. EMG: electromyogram. L2/3, L4, L5, L6, L6b: Neocortical layers 2/3, 4, 5, 6, and 6b. LFP: local field potentials. MUA: multi-unit activity. NREM: non-rapid eye movement sleep. REM: rapid eye movement sleep.

As expected, firing rates were modulated by vigilance state and layer (Figure 16, interaction between vigilance state and layer ($F(2,12) = 16.409$, $p < 0.001$, mixed ANOVA). Cortical

neurons fired at the highest rates during wakefulness, lowest rates during NREM sleep and in between these two values during REM sleep (wake: 23.22 ± 3.45, NREM: 16.79 ± 2.45, REM: 19.78 ± 2.86 Hz, main effect of vigilance state $F(2,12)=17.968$, $p$ <0.001), as previously observed (Vyazovskiy et al. 2009). There was a trend towards layer differences in firing rates (main effect of cortical layer: $F(1,6)=5.709$, $p=0.054$) but none of the post-hoc comparisons between the two layers reached the Bonferroni-corrected significance thresholds.

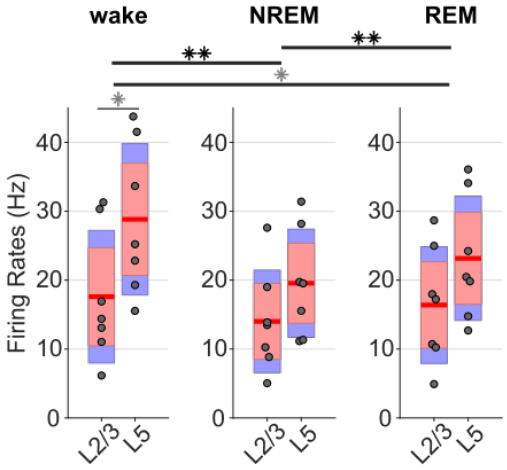



**Figure 16: Neuronal firing rates in layers 2/3 and 5 across vigilance states**

Firing rates in layer 2/3 and 5 during wakefulness, NREM, and REM sleep. Note the modulation of firing rates with vigilance state. Numerical differences between the two layers are only significant for wakefulness and only if no Bonferroni adjustment is applied. Similarly, the post-hoc comparison of firing rates between wakefulness and REM sleep did not reach significance following Bonferroni adjustment of α (grey asterisks). Black asterisks indicate post-hoc contrasts between vigilance states with significant differences (*$p$ < 0.05, **$p$ < 0.01, ***$p$ < 0.001). Panels represent grouped data including group mean (red line), 95% confidence interval (pink box), and one standard deviation (blue box) with individual data points overlaid. L2/3, L5: neocortical layers 2/3 and 5. NREM: non-rapid eye movement sleep, REM: rapid eye movement sleep. wake: wakefulness.

### 3.3.3 Laminar firing patterns during OFF-ON transitions indicate leading role of layer 5 in orchestrating cortical bistability

The putative differences between physiologically regulated sleep slow waves and slow waves during anaesthesia (Torao-Angosto et al. 2021) or in brain slices prompted me to re-evaluate

the assumption that the bistable transitions in cortical neuronal firing underlying slow waves are orchestrated by layer 5 (Chauvette, Volgushev, and Timofeev 2010). I first visually assessed the MUA pattern during OFF-ON transitions between silent and active periods in all seven C57BL/6J mice included in this experiment. As shown in the example in Figure 17a, I consistently observed that neuronal firing was initiated in layer 5 at the OFF-ON transition before other cortical layers would join the population response. To quantify this phenomenon, I analysed the surge of neuronal activity at the OFF-ON transition in layers 2/3 and 5 and observed that the firing rates in layer 5 were higher during the first 10 ms of the ON-period (Figure 17b), indicating that the rise of neuronal activity in layer 5 is earlier and stronger than in layer 2/3 (cortical layer × time interaction $F(29,174) = 9.412$, $p < 0.001$, with L5 > L2/3 in the first 10 ms, $p = 0.008$, mixed ANOVA followed by 3 Bonferroni-adjusted post hoc comparisons of cortical layer in 10-ms bins). In order to correct for a putative influence of the numerically higher firing rates in layer 5, I directly compared the average latency to the first spike for OFF-ON transitions in which the total number of spikes in layer 5 was matched with layer 2/3 for the 200-ms time window after the first spike of every ON period. Independent of the total spike number, the latency to the first spike was consistently shorter in layer 5 (main effect of cortical layer $F(1,6)$ 86.301, $p < 0.001$ and cortical layer × count interaction $F(17,102) = 27.205$, $p < 0.001$, with L5 < L2/3 in all spike count bins, $p$s < 0.001, mixed ANOVA followed by 10 Bonferroni-adjusted post hoc comparisons of cortical layers in 2-spike bins) (Figure 17c). This finding supports the idea that layer 5 has a leading role in driving population activity during the bistable state underlying slow waves in NREM sleep.

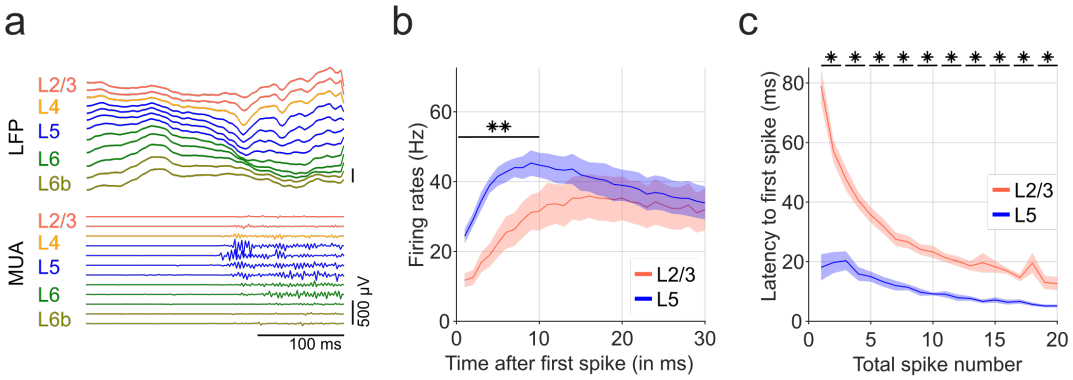



**Figure 17: Laminar profile of neocortical firing dynamics around OFF-ON transitions in C57BL/6J mice**

a) Representative OFF-ON transition illustrating that population activity typically starts in layer 5. Both scale bars on y-axis, 500 µV. b) Average neuronal firing activity at the transitions from population OFF to ON periods during baseline NREM sleep. Note that firing rates at the OFF-ON transition are higher in layer 5 during the first 10 ms after the first spike. c) Latency to the first spike for matched spike numbers during the first 200 ms of the ON period. Note that the latency to the first spike is shorter in layer 5 irrespective of the total number of spikes in a given ON period. Black asterisks indicate post-hoc contrasts with significant differences (*p < 0.05, **p < 0.01, ***p < 0.001). L2/3, L5: Neocortical layers 2/3, 5. NREM: non-rapid eye movement sleep.

### 3.3.4 NREM sleep slow waves and slow wave activity are larger in layer 5 compared to layer 2/3

Transition synchrony of neuronal bistable firing patterns correlate with EEG SWA during natural NREM sleep (Vyazovskiy et al. 2009). However, it has not been tested whether local differences in the OFF-ON dynamics of specific cortical layers are reflected in the characteristics of LFP slow waves and SWA. I therefore analysed the average LFP signal for the 1-s time window centred over OFF-ON transitions and the laminar LFP spectra from layers 2/3 and 5 during NREM sleep. This analysis showed that slow wave amplitudes in layer 5 are consistently higher compared to layer 2/3 (L2/3: 164.15 ± 25.25, range 67.81 – 234.30 µV; L5: 475.14 ± 37.32, range 363.50 – 586.01 µV, $t(6) = -14.606$, $p<0.001$) and that the NREM sleep spectra show a power difference specifically in the slow frequency range, which is defined as

slow wave activity (0.5 – 4.0 Hz) during NREM sleep (L2/3: 2021.83 ± 218.61, range 1386.68 – 2638.82 $\mu V^2$/0.25Hz; L5: 4752.26 ± 533.29, range 3335.03 – 6685.62 $\mu V^2$/0.25Hz, $t(6) = -7.489$, $p<0.001$). Importantly, the differences in slow wave activity during wakefulness and REM sleep, when slow waves are only sporadically observed, were considerably less pronounced.

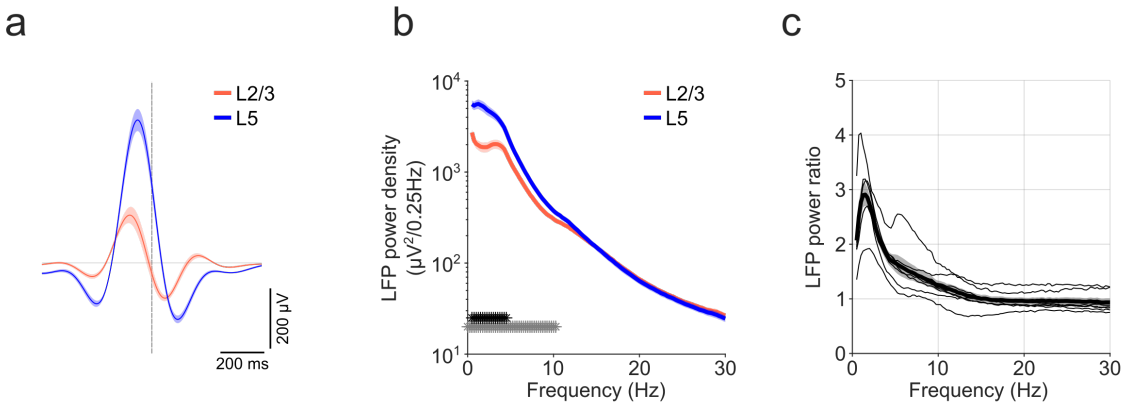



**Figure 18: Laminar profile of neocortical slow wave dynamics in C57BL/6J mice**

a) Average LFP slow waves during non-rapid eye movement (NREM) sleep in layers 2/3 (L2/3) and 5 (L5) of C57BL/6J mice (n=7), centred over the OFF-ON transition (vertical dashed line). Note the layer difference in slow wave amplitudes. b) Local field potential (LFP) power spectra of L2/3 and L5 of cKO and CTR mice during NREM sleep. Note the difference in the spectral power in slow frequencies. Individual asterisks indicate spectral bins with significant differences in post-hoc comparison before (grey) and after (black) Bonferroni adjustment of α. c) Ratio between LFP power spectra are plotted for each individual animal (thin lines) as well as group mean and standard errors of the mean (thick line with shaded area). L2/3 and L5: Neocortical layers 2/3 and 5. NREM: Non-rapid eye movement sleep.

### 3.3.5 Homeostatic response to sleep deprivation is more pronounced in layer 2/3 compared to layer 5

Finally, I asked how the homeostatic response to sleep deprivation is reflected in LFP recordings from L2/3 and L5. I found that spectral power was increases across the entire analysed frequency range between 0.5 – 30 Hz during NREM sleep in the first hour after sleep

deprivation, with a particular elevation in SWA in line with the commonly observed elevation of power in the slow frequency range after sleep deprivation (Figure 19). Interestingly, layer 2/3 presented greater spectral power both in the slow frequencies and over the entire frequency range (first hour after sleep deprivation, SWA: $t(6)=2.986$, $p = 0.024$, full power spectrum: $t(6)=5.172$, $p = 0.002$, Figure 19b). The time course of SWA after sleep deprivation showed an initial elevation and subsequent exponential return to baseline, as previously described for the frontal and occipital EEG derivations (Huber, Deboer, and Tobler 2000a). Layer 2/3 had higher levels of SWA across the six hour rebound period compared to layer 5 (Figure 19c, main effect of time $F(11,176) = 49.333$, $p < 0.001$, main effect of cortical layer: $F(1,16) = 8.036$, $p = 0.12$, no significant interaction between time and layer, mixed ANOVA).

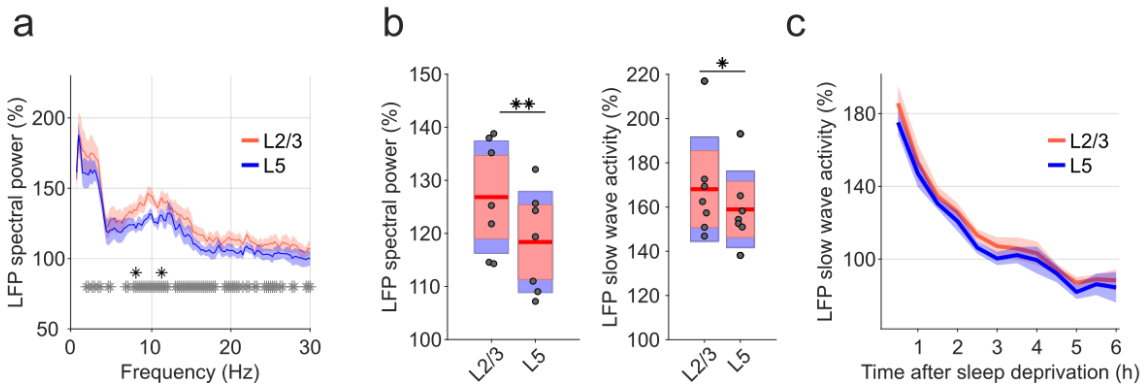



**Figure 19: Laminar response to sleep deprivation**

a) Spectral power in the LFPs from layers 2/3 and 5 during NREM sleep in the first hour (ZT 6-7) after six hours of sleep deprivation relative to baseline NREM average. Individual asterisks indicate frequency bins with significant differences in post-hoc comparison before (grey) and after (black) Bonferroni adjustment of α. b) Average LFP spectral power (left) and slow wave activity (right) from layers 2/3 and 5 for the same time window as shown in panel (a). c) Time course of slow wave activity in LFPs from L2/3 and L5 during NREM sleep after sleep deprivation relative to baseline average. Black asterisks indicate post-hoc contrasts with significant differences (*p < 0.05, **p < 0.01, ***p < 0.001). Panel b represents grouped data including group mean (red line), 95% confidence interval (pink box), and one standard deviation (blue box) with individual data points overlaid. LFP: local field potential. ZT: zeitgeber time.

## 3.4 Discussion

### 3.4.1 Chronic laminar recordings in freely moving mice as central tool in investigating the role of the cortex in sleep-wake regulation

Laminar recordings are widely established. Yet the use of laminar probes for chronic *in vivo* recordings in freely moving mice for sleep research poses technical challenges in particular the need to preserve the cortical integrity during the implantation procedure and to localise the exact *in situ* position of the laminar probe. In this chapter, I showed the feasibility of such long-term laminar recordings and presented some methodological adaptations, which allowed me to successfully record LFP and MUA data across cortical layers. Neuronal firing rates showed the previously reported modulation by vigilance state. I further confirmed that, as previously reported in slice recordings and anaesthetised animals, layer 5 leads the OFF-ON transitions. I further found larger amplitudes of LFP slow waves and greater SWA during NREM sleep in layer 5 compared to layer 2/3. I then presented evidence that LFP spectral power is elevated in LFP recordings from both layers 2/3 and 5 after sleep deprivation, but that the elevation of spectral power and SWA in layer 2/3 is more pronounced than in layer 5. These findings can be interpreted as evidence that layer 5 leads the neuronal population dynamics underlying the generation of slow waves during NREM sleep. However, my analysis provides an indication that layer 2/3 might be more responsive to changes in homeostatic sleep drive. Most of the current knowledge about the electrophysiological features of sleep homeostasis is based on EEG recordings (Franken et al. 1991; Tobler and Borbély 1986; Werth, Achermann, and Borbély 1996; Borbély, Tobler, and Hanagasioglu 1984; Huber, Deboer, and Tobler 2000b). The two process model of sleep regulation was originally developed (Borbély 1982), then mathematically defined (Daan, Beersma, and Borbély 1984) and later refined (Borbély et al. 1989; Achermann and Borbély 2003) and adapted to mice (Guillaumin et al. 2018) based

on EEG SWA during NREM sleep. However, this 'global' SWA is only a reflection of underlying firing dynamics of cortical neurons, which provide a much more fine-scaled 'local' description of the homeostatic process (Vyazovskiy et al. 2009; Thomas et al. 2020). These patterns ought to be investigated using intracortical recordings to approach a mechanistic understanding of the cortical dynamics reflecting, and potentially driving the homeostatic process. The data presented in this chapter illustrates that layers 2/3 and 5 show distinct patterns in slow wave features and NREM spectra at baseline and after sleep deprivation indicating that fine-scale intracortical dynamics contribute to the regulation of sleep oscillations. This notion could be further investigated with additional analysis of this rich dataset. Current source density analysis would allow to assess the temporal dynamics around the initiation of OFF-ON and ON-OFF transitions. Analysis of laminar activity during vigilance state transitions could reveal which layer initiates the bistable firing pattern that foreshadows sleep onset.

### 3.4.2 Layer 5 as primary candidate for the manipulation of cortex in the context of homeostatic regulation of sleep

While still descriptive and preliminary, my laminar analysis of neocortical dynamics during NREM sleep in wild type mice hints at a special role of layer 5 in the regulation of NREM sleep slow waves. As previously postulated based on optogenetic stimulation experiments (Beltramo et al. 2013), slice recordings (Sanchez-Vives and McCormick 2000a) and *in vivo* recordings in anaesthetised animals, mostly cats (Chauvette, Volgushev, and Timofeev 2010), layer 5 appears to fire first and thereby lead the population activity across cortical layers in the transition from silent OFF to active ON states. In addition, the larger amplitudes of individual slow waves and the greater SWA in layer 5 compared to layer 2/3 indicate a potential role as generator of slow waves in the neocortex during physiological NREM sleep. It is somewhat surprising that layer 2/3 showed a larger increase in SWA after sleep deprivation compared to

layer 5. Yet, considering that this layer difference in spectral power increase appeared across the entire frequency range, layer 5 remains the primary candidate for cortical manipulations in the context of slow wave regulation and sleep control. It is essential to complement the observational data presented here with a perturbational approach. In the next two chapters, I will explore how acute and chronic manipulations of layer 5 pyramidal neurons can be used to elucidate a putative contribution of layer 5 pyramidal neurons to local and global sleep oscillations and sleep-wake control.

# Chapter 4: Validating tools for the manipulation of layer 5 pyramidal neurons in chronic sleep experiments

## 4.1 Introduction

Until a century ago, the discovery of brain structures involved in the regulation of sleep relied on 'experiments by nature'. Von Economo's postulation of a 'sleep-regulating center' in the hypothalamus and brainstem, was largely based on careful clinical observation of patients with viral brain lesions resulting from the *lethargic encephalitis*. In his seminal paper on 'sleep as a problem of localization', he further supports his argument by citing reports of patients with Wernicke's and Gayet's disease, brain tumours and haemorrhages in his proposed 'center for brain regulation', who all presented a similar sleep symptomatology to his encephalitis patients (Economo 1930). Transection and electrical stimulation experiments in animals soon provided deeper insights into the functional neuroanatomy of sleep in the mammalian brain (Nauta 1946; Akert, Koella, and Hess 1952). Yet, precise dissection of sleep regulatory circuitry based on genetic targeting of selected cell populations became only possible in the late 1980s through the development of site-specific recombination technology (Sauer and Henderson 1988). More recently, the combination of recombinant technology with powerful tools for acute or chronic manipulation of cellular activity has led to the rapid discovery of many sleep- or wake-promoting nuclei (Saper and Fuller 2017; Adamantidis et al. 2007; Liu and Dan 2019). These novel and powerful tools, most noticeably 'optogenetics' (Miesenböck 2011) and 'chemogenetics' (Roth 2016) have gained considerable popularity due to the possibility of using them to probe the causal relationship between neuronal activity and animal behaviours (Lima and Miesenböck 2005; Alexander et al. 2009; Zhu et al. 2014), including sleep-wake control (Adamantidis et al. 2007; Y. Hayashi et al. 2015). However, many of these tools can elicit strong and unphysiological signals in the brain (E. J. Campbell and Marchant 2018;

Sjulson et al. 2016; Wiegert et al. 2017). The careful choice and validation of the most suitable tool to manipulate neuronal activity for the cell type and scientific question of interest is of uttermost importance to avoid the fate of many researchers, who *"voyaged into the known, and discovered the expected"* (Miesenböck 2009). Therefore, the aim of the experiments presented in this chapter was to carefully validate tools for the *in vivo* manipulation of neocortical layer 5 pyramidal neurons in chronic sleep experiments.

In the introduction to this chapter, I present a small selection of widely used tools for activation and inhibition, invasive and non-invasive stimulation, acute or chronic manipulation of neurons. I discuss the extent to which these technologies are suitable to address the role of the cortex in the regulation of sleep oscillations and vigilance states. I will explain why an approach of non-invasive, subacute or chronic silencing of layer 5 pyramidal neurons appeared most appropriate for the aims of my DPhil project. Such silencing can for example be achieved by crossing the Rbp4-Cre driver line for layer 5 pyramidal neurons with a reporter line expressing chemogenetic designer receptors exclusively activated by designer drugs (DREADDs) in Cre-positive cells. However, at the end of the introduction to this chapter, I will provide a brief review of the literature, which suggested shortly after the start of this project that the 'pharmacologically inert' designer drug clozapine-N-oxide (CNO), used as DREADD actuator, can affect neuronal activity and behaviour through back-metabolism to its parent drug clozapine. I will explain how these findings motivated me to conduct an extensive control experiment aiming to clarify whether CNO and a next-generation DREADD actuator Compound 21 (Cmpd21) modulate sleep in the absence of DREADDs.

The results section starts with initial findings from a chemogenetic pilot experiment conducted in one mouse, which expressed the inhibitory DREADD hM4Di under control of the layer 5 driver line Rbp4-Cre (*Rbp4-Cre:hM4Di*). I will report that after CNO administration, this

mouse displayed a sleep pattern that could be compatible with either a genuine DREADD effect or with sleep-modulating effects of CNO or its parent drug clozapine. The largest part of the results section will then be dedicated to the control experiment – prompted by the growing literature on CNO side effects and my pilot results from the *Rbp4-Cre:hM4Di* mouse – in which I systematically assessed the effects of CNO and Cmpd21 on sleep in wild type mice. My aim was to determine whether CNO would itself affect sleep in the absence of DREADDs. I will report that both CNO and Cmpd21 modulated sleep.

In the discussion section, I will elaborate on putative mechanisms underlying the effects of CNO and Cmpd21 on sleep, highlight potential limitations of my study, assess the implications of my findings for the future use of chemogenetics in sleep research, and outline alternative strategies for subacute or chronic manipulations of layer 5 pyramidal neurons.

### 4.1.1 Invasive vs. non-invasive approaches for neuronal manipulations in cortex

The manipulation of cortex provides a special challenge in sleep research because slow waves are thought to be generated in a corticothalamic interplay (Adamantidis, Gutierrez Herrera, and Gent 2019; Crunelli and Hughes 2010). The physiological regulation of slow waves and SWA, the key marker of sleep homeostasis, depends on integrity of cortex, thalamus, and their reciprocal connections (David et al. 2013; Timofeev et al. 2000; Lemieux et al. 2014; Hay et al. 2021). When the connections between cortex and thalamus are severed the cortex engages in slow waves (Timofeev et al. 2000) and it has been suggested that SWA is the default mode of cortex (Sanchez-Vives and Mattia 2014). Slow waves appear during different types of general anaesthesia (Sleigh et al. 2019; González-Rueda et al. 2018; Warnaby et al. 2017) and can be found in isolated, severed, or damaged cortical areas independent of the vigilance state (Sanchez-Vives and McCormick 2000b; Timofeev et al. 2000; Sheroziya and Timofeev 2014; Sarasso et al. 2021; Russo et al. 2021; Krone and Vyazovskiy 2020; Lemieux et al. 2014) and

even in cortical cell cultures (Hinard et al. 2012). The characteristics of slow waves in these settings can be very different from those observed during sleep (Torao-Angosto et al. 2021; Warnaby et al. 2017; Ni Mhuircheartaigh et al. 2013; Russo et al. 2021; Sarasso et al. 2021; Timofeev and Chauvette 2018; Lemieux et al. 2014). It is known that cortical and thalamic slow wave activity are extremely sensitive to cortical damage in *in vivo* experiments and some experts in intracortical electrophysiological recordings have stated that it is *"practically impossible to remove the dura without cortical damage in mice"* (Sheroziya and Timofeev 2014). I therefore decided that a non-invasive approach would be most suitable for *in vivo* manipulations of cortex in mice, which would avoid confounds associated with cortical damage. In order to avoid damaging the cortex through injections for viral delivery of reporter constructs or through implantation of optic fibres, it appeared preferable to use a Cre-driver line selective for our cell population of interest (S. Gong et al. 2007), e.g. the most commonly used driver line for layer 5 pyramidal neurons 'Rbp4-Cre' (Gerfen, Paletzki, and Heintz 2013), and cross it with a suitable reporter line.

### 4.1.2 Local vs. global manipulations of cortex

In addition to preserving cortical integrity, genetic crosses also make it possible to manipulate layer 5 pyramidal neurons across the entire cortical mantle, whereas virus-based approaches would be predicted to affect a much smaller population of neurons. Based on previous experiments mentioned in the general introduction (see subchapter 1.6.4: Does local sleep affect global sleep?) one could speculate that local manipulation of a circumscribed cortical area could possibly be sufficient to affect sleep oscillations and global sleep-wake control (Yasuda et al. 2007; Uygun et al. 2016; Frase et al. 2016; Faraguna et al. 2010). Some evidence suggests that the prefrontal cortex might be most sensitive to homeostatic sleep pressure (Marzano et al. 2013; Massimini et al. 2004; Werth, Achermann, and Borbély 1997; Huber,

Deboer, and Tobler 2000b; Cajochen, Foy, and Dijk 1999). However, for the aim of my DPhil project to probe a role for the cortex, and in particular layer 5 pyramidal neurons, in the regulation of sleep oscillations and vigilance states, it seemed preferable to start with a more general approach and to attempt cortex-wide manipulation of those cells. My primary concern was that even if my overall hypothesis was correct, local manipulations of layer 5 pyramidal neurons achieved through injection of viral vectors might only elicit local effects on slow waves and not on global sleep parameters. The interpretation of changes in slow wave regulation, however, would be compromised by the structural damage induced by the injection procedure.

To validate these concerns regarding the spatial scale of viral-mediated delivery, I performed pilot experiments to assess how many cortical neurons are transduced following a multi-injection protocol that was optimised for maximum delivery and within the UK Home Office license granted to our laboratory. My calculations, based on the spread of commonly used adeno-associated virus (AAV) vectors, revealed that even after 10 optimally distributed injections of 200 nl AAV serotypes 2 or 8, less than 1 % of the targeted layer 5 pyramidal neuron population across the corticle mantle expressed the AAV construct following viral transduction (Figure 20). These results supported the view that a genetic cross might be more suitable than an injection-based approach to silence layer 5 pyramidal neurons cortex-wide.

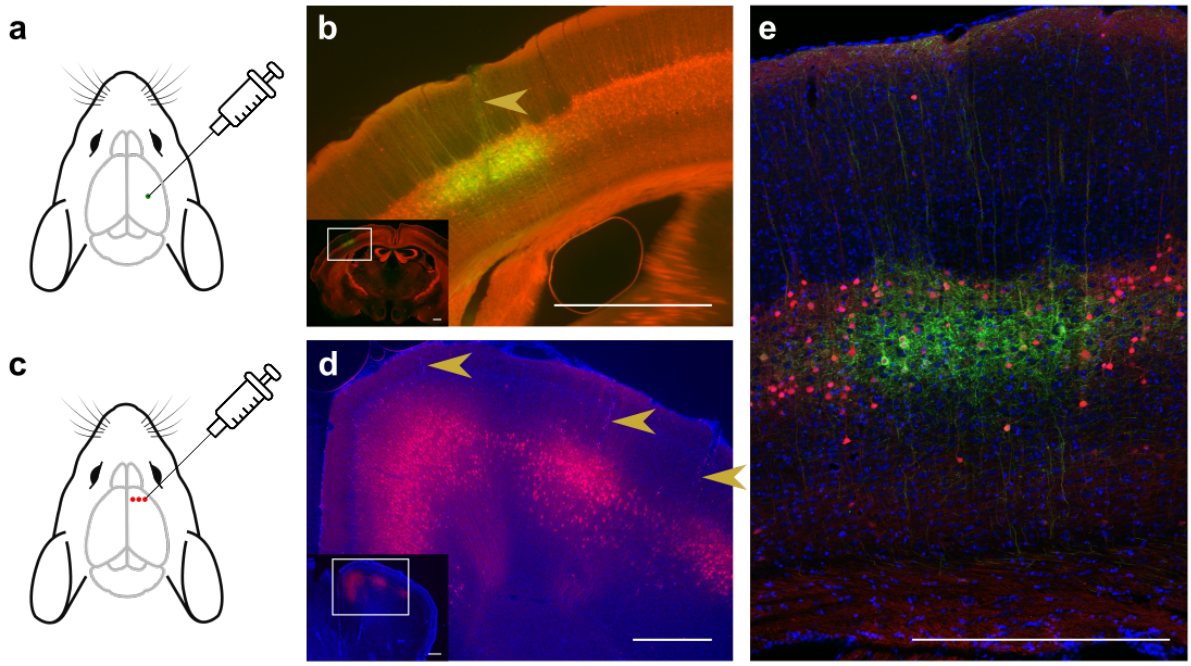



**Figure 20: Expression of AAV2 & AAV8 in layer 5 pyramidal neurons of the Rbp4-Cre driver line.**

a,b) Single virus injection of a green fluorescent AAV2 virus (AAV2-CAG-Flex-ArchT-GFP) in a *Rbp4-Cre;Ai14+/+* mouse. Measured maximal spread ~500 µm. Red: tdTomoato in Cre+ cells, green: GFP. c,d) Multiple virus injections of a red fluorescent AAV8 virus (AAV8-hSyn-DIO-hM4Di-mCherry) in prefrontal cortex of the Rbp4-Cre driver line. The most medial injection tract was used for two injections at different depths. Blue: DAPI, red: mCherry e) Confocal stack image from the same injection as panel b. Blue: DAPI, red: tdTomato; green: GFP. Injection tracts marked with brown arrows. AAV: Adeno associated virus. DAPI: 4′,6-diamidino-2-phenylindole. GFP: green fluorescent protein. All scale bars: 500µm.

### 4.1.3 Acute, subacute, and chronic silencing tools

Another important consideration in the study of sleep homeostasis is the appropriate time scale over which neuronal function should be manipulated. In mice, homeostatic sleep drive accumulates during wakefulness and dissipates during sleep over a time scale of several minutes to a few hours (Huber, Deboer, and Tobler 2000a; Thomas et al. 2020; Guillaumin et al. 2018). These relatively slow dynamics suggest that in order to elicit relevant changes to the physiological processes underlying the build-up, sensing, or integration of homeostatic sleep drive, one would need to manipulate relevant neurons in a subacute or chronic fashion. This

approach is in stark contrast to the more commonly performed optogenetic stimulations used to probe the sleep-wake switching properties of subcortical nuclei (Weber and Dan 2016), where strong acute stimuli are applied and the immediate consequences upon vigilance state transitions or acute changes in electrophysiological parameters are assessed (Herrera et al. 2016). Taking the long time scale of sleep homeostasis into account, it seemed most appropriate to use an approach that would subacutely or chronically silence layer 5 pyramidal neurons, e.g. in form of a DREADD-reporter line (Zhu et al. 2016) or a conditional SNAP25-knockout (Hoerder-Suabedissen et al. 2019), rather than an optogenetic tool. The chemogenetic DREADD approach appeared most suitable because temporary manipulations of neuronal activity can be achieved through simple i.p. injection of a designer drug, the DREADD actuator (Roth 2016), and the technology is widely used in rodent sleep research (Varin and Bonnavion 2019).

### 4.1.4 Concerns about side-effects of 'pharmacologically inert' chemogenetic actuators

Clozapine-N-oxide (CNO) is the most commonly used chemical ligand for DREADD receptors (Roth 2016) and was therefore the logical first choice for my chemogenetic experiments. Originally, CNO was described as pharmacologically inert compound, which exclusively activates DREADDs (Armbruster et al. 2007). It was also long assumed that in mice CNO is not back-converted into the parent drug, clozapine (Guettier et al. 2009). However, during the design of our study, it was first demonstrated that CNO has substantial off-target effects in mice (Gomez et al. 2017) resulting in competitive inhibition of several endogenous receptors, most importantly histaminergic H1, serotoninergic 5-HT2A, muscarinic M1, M3, M4, and dopaminergic D1 and D2 receptors (Gomez et al. 2017). It was proposed in the same study that the *in vivo* mechanism of action of CNO at DREADDs in mice and rats is based on back metabolism of CNO to clozapine, which has a better permeability through the blood brain

barrier and a higher affinity to the excitatory hM3Dq and inhibitory hM4Di DREADD receptors than CNO itself (Gomez et al. 2017). Shortly after this initial study had questioned the pharmacological inertness and mechanism of action of CNO, the CNO back-metabolism to clozapine in mice was directly demonstrated and it was reported that plasma concentrations of clozapine were 7.4% of the measured CNO levels at 30 minutes after s.c. CNO administration, similar to the clozapine/CNO ratio of 7.5% at the same time point after i.p. injection in rats (Manvich et al. 2018). The same study also re-assessed the original data on which the assumption was based that CNO is not back-metabolized (Guettier et al. 2009) and the new analysis revealed a clozapine to CNO ratio of 9.2% in the previous experiment, which had used a very low 1 mg/kg dose of CNO and hence the absolute levels of clozapine had been reported as negligible (Manvich et al. 2018). While it has now been demonstrated that commonly used doses of CNO (Manvich et al. 2018; MacLaren et al. 2016) and very low doses of clozapine (Ilg et al. 2018) can elicit behavioural effects in mice, it should be highlighted that most psychotropic drugs including clozapine evoke characteristic sleep changes (Riemann and Nissen 2012). Clozapine, is an atypical neuroleptic known to profoundly alters sleep architecture in humans (Monti, Torterolo, and Pandi Perumal 2017), rats (Sorge, Pollmächer, and Lancel 2004; Spierings, Dzoljic, and Godschalk 1977), and mice (Grønli et al. 2016). Sedation, fatigue, but also agitation are typical dose-dependent side effects of clozapine treatment in mental health hospitals and are observed in nearly half of the patients during the first month after starting clozapine treatment (Iqbal et al. 2020). I therefore hypothesised that CNO might modulate sleep due to back-metabolism to clozapine might have been overlooked and that the more novel DREADD ligand Cmpd21, which does not convert into clozapine, might represent a more suitable DREADD actuator.

In summary, the project presented in this chapter was initially designed to use CNO activation of an inhibitory DREADDD to investigate the effects of subacute silencing of neocortical

layer 5 pyramidal neurons on sleep oscillations and sleep. Following my first pilot experiments and growing concerns in the literature about the inertness of the designer drugs used to activate DREADDs, this project was later redesigned to answer the research question whether CNO and Cmpd21 affect sleep in the absence of DREADDs.

## 4.2 Methods

A detailed description of the methodology used for the chronic electrophysiological *in vivo* recordings can be found in the general methods section. This brief methods section aims to provide a concise overview of the animals and chemogenetic tools, as well as the experimental design and statistical analysis methods specific to the experiments presented in this chapter.

### 4.2.1 Animals

*Rbp4-Cre:hM4Di mice for DREADD pilot experiment*

In order to acquire chemogenetic control over layer 5 pyramidal neurons, I crossed the layer 5 driver line Rbp4-Cre (Gerfen, Paletzki, and Heintz 2013) with the inhibitory DREADD reporter line B6.129-Gt(ROSA)26Sor$^{tm1(CAG-CHRM4*,-mCitrine)Ute}$/J (R26-LSL-hM4Di-DREADD, The Jackson Laboratory, Stock No: 026219) (Zhu et al. 2016) to generate a recombinant mouse abbreviated as '*Rbp4-Cre:hM4Di*' throughout this chapter. Rbp4-Cre is the most commonly used pan-layer 5 driver line with an expression profile across cortical regions in both layer 5a and 5b pyramidal cell populations (Gerfen, Paletzki, and Heintz 2013). I chose this driver line with the intention of targeting a large subpopulation of layer 5 pyramidal neurons independent of the cortical area or sublayer. A colony of this mouse line was already established in the Molnár laboratory at the outset of my experiment and used in previous studies (Grant, Hoerder-Suabedissen, and Molnár 2016). The R26-LSL-hM4Di-DREADD mouse strain represents a reporter line for Cre-dependent expression of the inhibitory Gi-DREADD hM4Di (Zhu et al.

2016) and I imported this line from the Jackson laboratory in 2019. In this reporter mouse line, Cre-recombinase causes the removal of a floxed-STOP cassette upstream of the Gt(ROSA)26Sor locus, thereby leading to the expression of a CAG promoter-driven HA-hM4Di-pta-mCitrine. The yellow fluorescent protein mCitrine enables identification of the cells expressing the construct, whilst hM4Di activation via local or systemic injection of CNO is predicted to cause neuronal silencing by inducing the canonical $G_i$-pathway in the expressing cells (Zhu et al. 2016). I generated the *Rbp4-Cre:hM4Di* cross because it offered the potential for cortex-wide, non-invasive, and subacute inhibition of neocortical layer 5 pyramidal neurons.

*Wild-type mice for the investigation of CNO/Cmpd21 effects on sleep*

The experiments investigating effects of the DREADD actuators CNO and Cmpd21 on sleep were initially planned as a small control study. In order to reduce the number of animals used in laboratory research, most of the animals included in this experiment had previously been recorded for other sleep studies in the Vyazovskiy laboratory. In total I used 16 male C57BL/6J mice sourced internally from the Biomedical Services at the University of Oxford. Only 3 of these animals were specifically implanted for this study, while 13 mice were implanted by, or in collaboration with, colleagues at the Vyazovskiy laboratory. All 16 animals were implanted with a right frontal EEG screw and EMG wires in the neck muscles, as described in the general methods chapter. The 13 animals used for other experiments had the following implants in addition to the standard headstage configuration:

- Five animals were implanted by Dr Jose Prius Mengual with a frontal left and bilateral occipital EEG screws as well as with a nut centred between and slightly anterior to the frontal EEG screws, which served as a socket for a detachable light-emitting diode

(LED) device. These animals were used to generate pilot data before systematic planning of this study.

- Four animals were implanted by Dr Hannah Alfonsa with a right occipital EEG screw and a cannula (C315I; PlasticsOne) targeted to layer 5 of the primary somatosensory cortex.
- Four animals were implanted in shared surgeries with Dr Jose Prius Mengual with a frontal EEG screw over the left hemisphere as well as a left occipital EEG screw and a right occipital 16-channel laminar probe as well as a nut centred between and slightly anterior to the frontal EEG screws for the detachable LED device.
- Three animals were implanted in collaboration with Dr Jose Prius Mengual exclusively for this study and had a left frontal and bilateral occipital EEG screws in addition to the right frontal EEG screw and the EMG wires in the neck muscles.

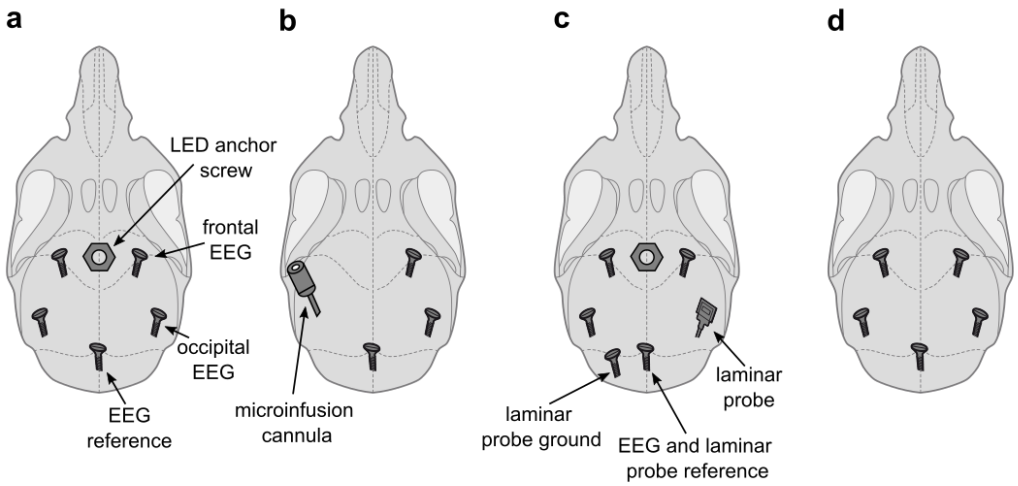



**Figure 21: Implant schematic of wild type mice used for CNO and Cmpd21 injections**

a) LED anchor screw, bilateral frontal and occipital EEG screws, and cerebellar reference screw b) Microinfusion cannula, right frontal and occipital EEG screws, and a cerebellar reference screw. c) LED anchor screw, bilateral frontal and left occipital EEG screws, right occipital laminar probe, and cerebellar reference screw. d) bilateral frontal and occipital EEG screws, and cerebellar reference screw. EEG: electroencephalogram. LED: light-emitting diode.

The 9 animals implanted with a socket for the placement of a detachable LED device received flickering light stimulation to one of the eyes combined with a 4-h sleep deprivation on up to four experimental days before being transferred to this study. All animals had at least 3 rest days without experimental interventions before the first injections of CNO or saline for the study presented here.

The 4 animals implanted with a cannula in the left primary motor cortex received intracortical microinfusions of bumetanide for a transient and localised blockade of the Na-K-2Cl cotransporter NKCC1 (Kahle and Staley 2008), as well as of VU0436271 for a transient and localised blockade of the chloride potassium symporter KCC2 (Sivakumaran et al. 2015). Two of these animals underwent 2 intracortical microinfusions and the other two animals underwent 3 intracortical microinfusions before inclusion in my study. The last infusion took place 12 days before the start of the study presented here. Due to the limit of 5 injection or infusion procedures on the UK Home Office project license under which these experiments were conducted, these animals could only be subjected to 3 and 2 i.p. injections of different CNO doses and saline.

Only seven animals, the four animals implanted with laminar probes and the three animals implanted exclusively for this study, were used for Cmpd21 injections as this condition was added to the experimental protocol after the pilot data from CNO injections had been analysed.

### 4.2.2 Experimental procedures and study design for chemogenetic experiments

*CNO injections in one Rbp4-Cre:hM4Di mouse*

CNO injections in the *Rbp4-Cre:hM4Di* mouse (age: 128 days at first injection, weight: 26.1 g) were performed under two different conditions – an undisturbed condition and a sleep deprivation condition. In the first condition, injections of 5 mg/kg CNO (0.25 mg/ml solution)

and saline (volume matched with CNO injections) were performed at the beginning of the light phase on two days separated by a 72-h rest interval. The injection time at light onset was chosen as mice usually spend a large proportion of time asleep during the first half of the light period and hence changes to sleep architecture or to NREM or REM sleep EEG spectra are most readily observed during interventions at this circadian time point. In the second condition, injections of the same volumes of CNO and saline were performed at the end of a 6-h sleep deprivation on two days separated by a 72-h rest interval. Sleep deprivation started at light onset at 9 am and the injections were performed around 2:45 pm. This time point was chosen because SWA is enhanced after sleep deprivation and a suppression of SWA or a wake-inducing effect of a drug would most easily be observed under this well-controlled condition of elevated sleep pressure.

*CNO and Cmpd21 injections in wild type mice*

All 16 wild type C57BL/6J animals (age: 113±6 days, weight: 25.2±0.5 g) received a medium dose of CNO (5 mg/kg, 0.25 mg/ml solution) and an equivalent volume of saline in a counterbalanced order with a 72-h rest interval between the first two experimental sessions. Of those 16 mice, fourteen also received a 10 mg/kg CNO injection (0.5 mg/ml solution) and twelve a 1 mg/kg CNO (0.05 mg/ml solution). These two injections were counterbalanced as third and fourth injections. Seven animals also received a 3 mg/kg (0.15 mg/ml) Cmpd21 injection in a fifth experimental session. This semi-counterbalanced design was chosen to ensure that at the medium dose condition is counterbalanced with saline injections to circumvent putative habituation or adaptation effects following repeated injection of CNO. Animals were on a regular light-dark cycle (lights on at 9 am) and intraperitoneal (i.p.) injections were performed within 15 minutes after light onset following a brief health check. The delay between light onset and injection was (mean±SEM): saline: 4.19±0.87 min, 1 mg/kg

CNO: 4.58±0.59, 5 mg/kg CNO: 3.52±1.04 min, 10 mg/kg CNO: 4.75±0.59 min, 3 mg/kg Cmpd21: 6.01±0.96 min. Individual recording sessions were separated by a rest interval of at least 72 hours. The recording chambers were kept open for approximately 10-15 minutes after the injection to monitor for potential adverse effects. The chambers were then closed and the animals checked remotely at regular intervals for the first 6-12 hours after injection. For data analysis, all recordings were aligned to the time point of injections.

*Justification of semi-counterbalanced study design*

This study was designed to determine whether commonly used CNO doses would affects sleep. To date, it is unclear whether repeated injections of CNO lead to adaptation effects (E. J. Campbell and Marchant 2018). However, it is known that the sleep modulating effects of clozapine change over the course of chronic administration (Sorge, Pollmächer, and Lancel 2004; Spierings, Dzoljic, and Godschalk 1977; Hinze-Selch et al. 1997). Therfore, I opted for this semi-counterbalanced design to provide a clean comparison between the saline and the medium (5 mg/kg) dose CNO condition. Low (1 mg/kg) and high (10 mg/kg) dose CNO conditions were performed in the second experimental week and the Cmpd21 injection was performed last in all seven animals, which received this drug, because this condition was added to the experimental plan at a later stage of the study, when initial pilot results indicating CNO effects on sleep had already been obtained.

### 4.2.3 Clozapine-N-oxide and Compound 21 products

To avoid back-metabolism to clozapine, I opted for the use a water-soluble salt preparation of CNO, clozapine-N-oxide dihydrochloride (Tocris, Bio-Techne LTD, Abingdon, UK, catalogue no.: 6329). This updated CNO preparation has the further advantage that one can avoid the use of the toxic solvent dimethyl sulfoxide (DMSO), which is typically used for the preparation of

CNO products in concentrations of up to 15% (E. J. Campbell and Marchant 2018). It is important to note that clozapine-N-oxide dihydrochloride has higher bioavailability but considerably less back-metabolism to clozapine compared CNO-DMSO in rhesus macaques (D. C. Allen et al. 2019). Pharmacokinetic analysis of this product in mice has not been performed or is not available at the current date (personal conversation with the Tocris customer support on the 14th of May 2021). For Cmpd21 injections I used the water-soluble version of DREADD agonist 21 (Compound 21 dihydrochloride, Tocris, Bio-Techne LTD, Abingdon, UK, catalogue no.: HB6124). I used this product at a dose of 3 mg/kg because a recent study reported detailed pharmacokinetic assessment of this product at this specific concentration as well as behavioural test results from a 5-choice serial-reaction-time task, which did not reveal any behavioural effects at this dose (Jendryka et al. 2019).

### 4.2.4 Sample size determination

Sample size and power calculations were performed using G*Power 3.1, an open-source statistical power analysis program (Faul et al. 2007). I chose a sample size of 16 animals based on previous experiments in our lab investigating the effects of the sedative diazepam on sleep (McKillop et al. 2021), which indicated an effect size of Cohen's d = 0.90 for the key outcome parameter NREM sleep time. I therefore decided that this control study should be sufficiently powered to detect effects of sizes of d=1 designed between saline and individual CNO treatment conditions with a power of 0.9 at the given α-error probability of 0.05. The estimated sample size from this calculation was 12-13 animals per group. Considering that four animals could only receive three or less injections, I included 16 animals in this study.

### 4.2.5 Data analysis

Data were pre-processed as outlined in the general methods section. For the statistical comparison of CNO and saline injections mixed-effect models were calculated using Prism

(version 9.1.1; GraphPad). Significant main effects of treatment conditions or interaction terms were followed up with Dunnett's adjustment for post hoc comparisons. In mixed-effect models with multiple time points I analysed acute (0-2 hours post injection) and prolonged (0-6 hours post injection) effects separately. For spectral analysis, EEG/LFP power spectra of individual animals were log-transformed before hypothesis testing. Individual spectral bins were compared between individual CNO treatments and saline used two-tailed t-tests. Following the convention in the presentation of EEG power spectra, as mentioned in the general methods subchapter 2.5, no correction was applied for post hoc comparison of spectral data because ANOVAs consisting of 119 EEG spectral bins would be too conservative and reduce statistical power (Achermann & Borbély, 1998); thus, α was kept at 0.05 in these cases. Comparisons between the Cmpd21 and saline condition were performed using one-tailed t-tests to assess whether sleep variables were changed in the same direction as after CNO treatment. For analysis of the percentage of time spent in the three vigilance states, wakefulness and NREM sleep were expressed as the percentage of time in the respective time window, REM was expressed as percentage of total sleep time in the respective time window as in previous work (Huber, Deboer, and Tobler 1999). For sleep architecture analysis, NREM and REM sleep episodes were defined as intervals of at least one minute with allowing an interruption of 4-16 seconds. Brief awakenings are defined as up to 16 second interruptions of sleep by wake-like EEG and EMG patterns (Franken et al. 1991). The sleep scoring was performed by Janine Traut, Dr Elise Meijer, Dr Laura McKillop and Dr Jose Prius Mengual, who were blinded to the experimental condition. Data from one animal had to be partially excluded because of a defective EEG headstage. This animal had to be excluded from the analysis of brief awakenings due to EMG artefacts, which made it difficult to identify a sudden increase of muscle tone during sleep. The same animal futher had to be excluded from the analysis of the 1 mg/kg and 5 mg/kg CNO treatments because of technical issues.

## 4.3 Results

### 4.3.1 Pilot experiment in one *Rbp4-Cre:hM4Di* mouse indicates modulation of sleep after CNO injections

The visual inspection of the hypnograms of one *Rbp4-Cre:hM4Di* pilot mouse after CNO and saline injection indicated that CNO injections evoke changes in sleep parameters in this transgenic 'layer 5 inhibitory DREADD' animal (Figure 22 and Figure 23).

First, I compared the sleep profile during an undisturbed baseline recording and after a saline and a 5 mg/kg CNO injection at light onset plotting slow wave activity for each 4-second recording epoch (Figure 22). As expected, the animal stayed awake for a few minutes after the injection in both the saline and the CNO condition. However, for the subsequent 4-5 hours I observed an unusual sleep architectural pattern in the CNO condition. The animal engaged in largely uninterrupted NREM sleep for the first three hours after injection and only one short REM episode occurred within this time window. Slow wave activity appeared suppressed between hours 2-4 of the recording. A normal pattern of alternating NREM and REM sleep and intermittent wake episodes, as observed in the baseline condition and after saline injection, re-appeared during the fifth hour of the recording. After about 6 hours (the first half of the light period), the sleep-wake pattern and SWA level showed no obvious differences from baseline recordings. Due to a technical issue, the recordings after saline injection were interrupted after approximately 7.5 hours.

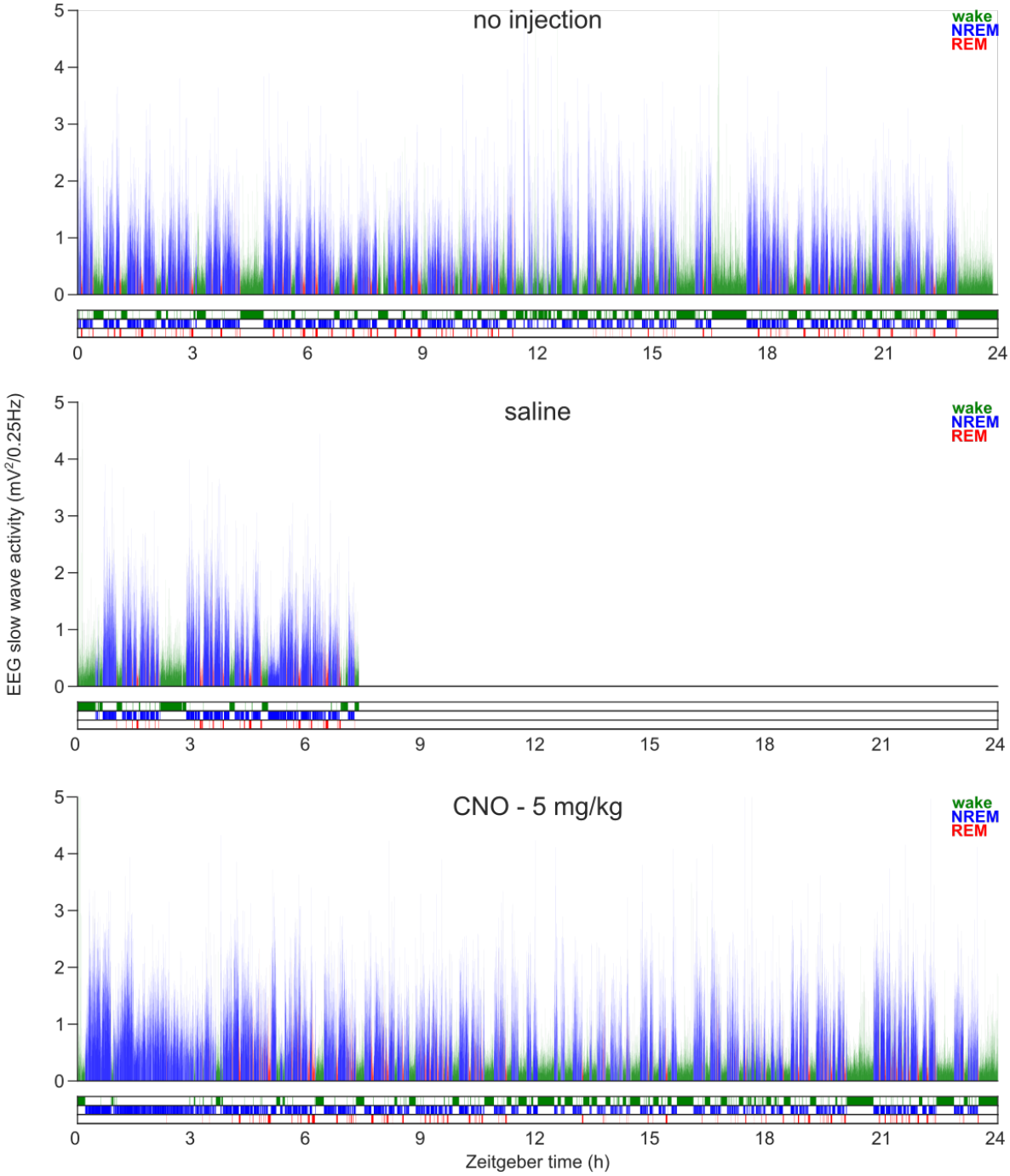



**Figure 22: CNO injection in one *Rbp4-Cre:hM4Di* pilot animal modulates sleep under undisturbed baseline conditions**

Hypnogram and EEG SWA (0.5- 4.0Hz, 4s epochs) of one representative *Rbp4-Cre:hM4Di* animal in undisturbed recordings under baseline conditions (top panel), after saline injection (middle panel) and after injection of 5 mg/kg CNO (bottom panel). All three plots are 24-h recordings with vigilance states colour coded (green: wake; blue: NREM, red: REM). Note that in the saline condition the recording was interrupted after approximately 7.5 hours. Further note that the change in sleep architecture and SWA for the first 4-5 h after CNO injection. CNO: Clozapine-N-oxide. EEG: electroencephalogram. NREM: non-rapid eye movement sleep. REM: rapid eye movement sleep. SWA: slow wave activity.

Next, I repeated the 5 mg/kg CNO and saline injections in combination with sleep deprivation. The mouse was kept awake by exposure to novel objects for the first six hours of the light period as described in the general methods section (subchapter 2.3.3) and approximately 15 minutes before the end of the sleep deprivation, the animal was injected with either saline or with CNO. The saline injection was followed by a brief wake episode before the animal showed the characteristic pattern of sleep after sleep deprivation including consolidated sleep and elevated SWA during NREM sleep. In contrast, the CNO injection was followed by an almost immediate transition to sleep after sleep deprivation and a similar pattern of sleep architectural changes as observed after CNO injections at light onset in undisturbed conditions. In particular, the animal presented highly consolidated NREM sleep with an unusually low number of awakenings. Furthermore, REM sleep appeared suppressed with only two short REM episodes in the first three hours after sleep deprivation (Figure 23). Spectral analysis indicated that NREM sleep SWA following sleep deprivation was initially elevated in both CNO and saline conditions. However, only the saline condition was followed by an exponential decay of NREM sleep SWA, whilst the CNO injection was followed by a U-shaped time course of SWA levels, possibly indicating a temporary suppression and subsequent rebound of SWA during NREM sleep (Figure 24).

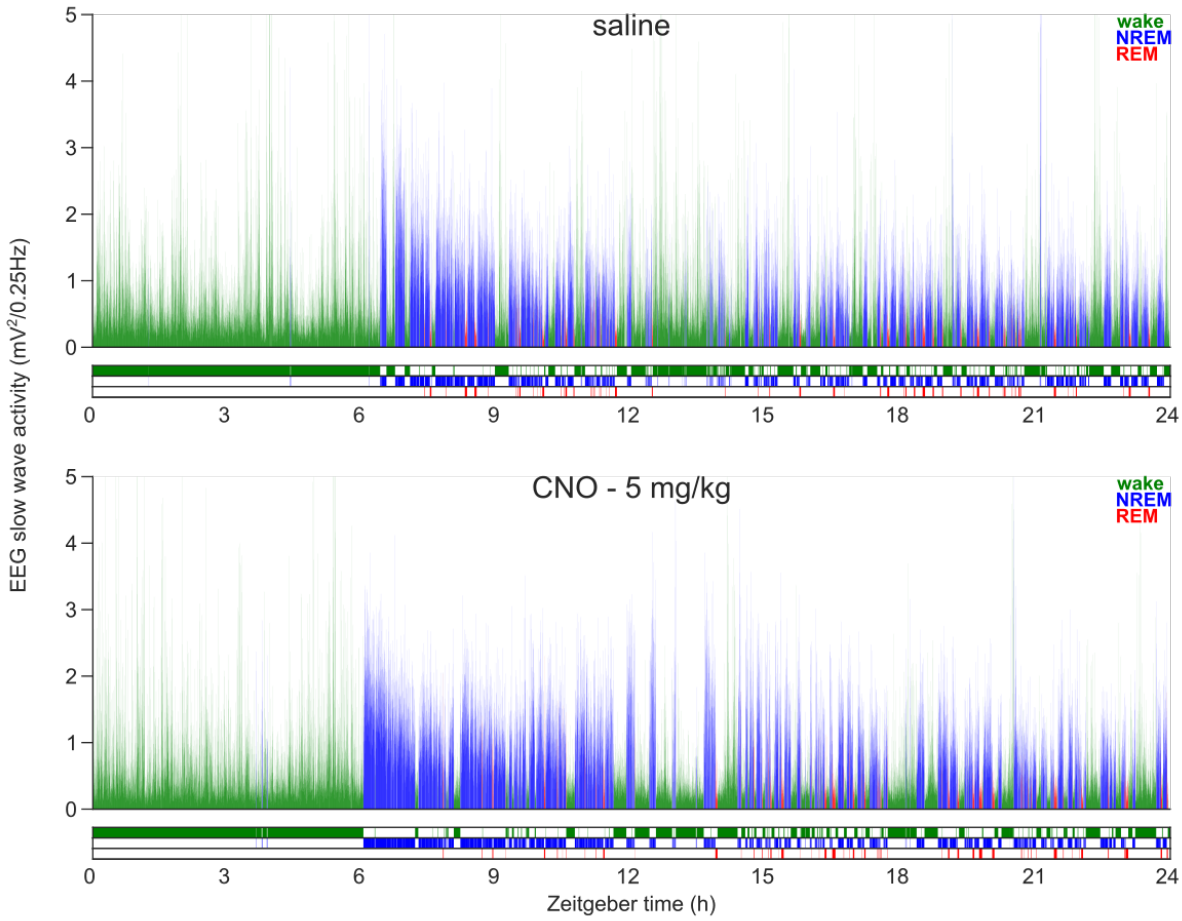



**Figure 23: CNO injection in one *Rbp4-Cre:hM4Di* pilot animal affects sleep after sleep deprivation**

Hypnogram and EEG slow wave activity (0.5- 4.0Hz, 4s epochs) of one representative *Rbp4-Cre:hM4Di* animal in a six-hour sleep deprivation experiment after saline injection (top panel) and after injection of 5 mg/kg CNO (bottom panel) immediately before recovery sleep (ZT 5:45). All three plots represent 24h recordings with vigilance states colour coded (green: wake; blue: NREM, red: REM). Note that CNO affects sleep architecture and slow wave activity for the first 4-5 h after injection. CNO: Clozapine-N-oxide. EEG: electroencephalogram. REM: rapid eye movement sleep. NREM: non-rapid eye movement sleep.

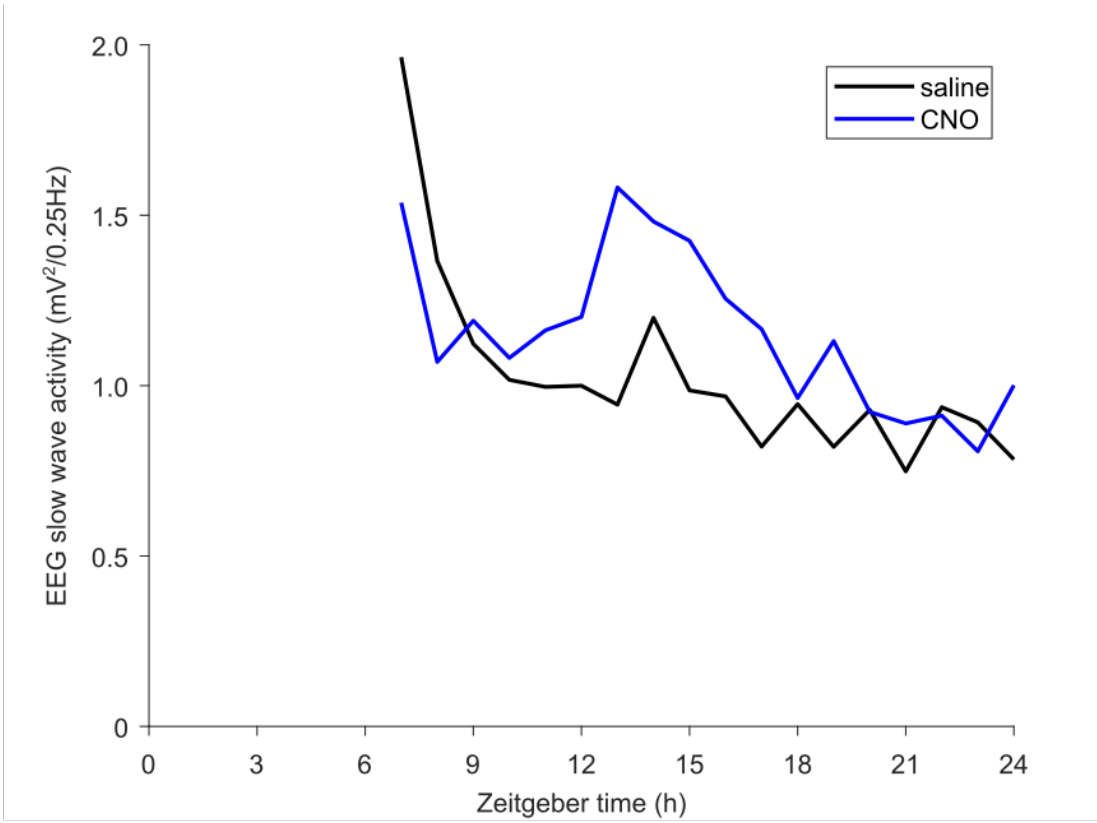



**Figure 24: Time course of NREM sleep slow wave activity (SWA) after sleep deprivation in one 'layer 5 DREADD' pilot animal**

Hourly average of EEG slow wave activity (0.5-4.0 Hz) during NREM sleep of one representative *Rbp4-Cre:hM4Di* animal in a six-hour sleep deprivation experiment after injections of saline (black) and 5 mg/kg CNO (blue) immediately before recovery sleep (ZT 5:45). Note that in the saline condition slow wave activity shows an exponential decline for the first six hours after sleep deprivation, while in the CNO condition an unusual U-shaped course of slow wave activity is observed. CNO: Clozapine-N-oxide. DREADD: Designer Receptors Exclusively Activated by Designer Drugs. EEG: electroencephalogram. NREM: non-rapid eye movement sleep. ZT: zeitgeber time.

The time scale of the sleep effects observed in this pilot experiment was in line with the reported pharmacokinetic and pharmacodynamic properties of CNO (Jendryka et al. 2019; Alexander et al. 2009). Previous work indicates that CNO concentrations in the cerebrospinal fluid (CSF) and brain tissue peak within 15 minutes after i.p. injections and DREADD-modulation of neuronal activity starts around 5-10 minutes after CNO administration (Alexander et al. 2009; Jendryka et al. 2019). The duration of effects was similar to those reported in other sleep studies using DREADDs (Y. Hayashi et al. 2015; Takata et al. 2018), which observed sleep-modulatory effects within the first hour typically lasting for two to six hours. However, it should be mentioned that DREAD-modulation of sleep has been observed for at least 12 hours in individual studies (Yu et al. 2019).

Although the results from one individual animal should not be overinterpreted, the temporary suppression of SWA after DREADD-inhibition of layer 5 pyramidal neurons in this pilot experiment appeared consistent with the assumption, arising from the literature and from my laminar recordings in wild type mice presented in the previous chapter, that layer 5 pyramidal neurons make an essential contribution to the generation of slow waves. However, the consolidation of NREM sleep and the suppression of REM sleep was puzzling. The growing body of literature, which started to question the mechanism of action of DREADD technology (Gomez et al. 2017), demonstrated back-metabolism of CNO to clozapine in mice (Manvich et al. 2018; Jendryka et al. 2019), and challenged the assumption that CNO is a pharmacologically inert ligand by demonstrating off-target binding to endogenous neurotransmitter receptors (Gomez et al. 2017; Jendryka et al. 2019), prompted me to consult the literature on clozapine effects on sleep. Interestingly, previous studies had found that clozapine alters sleep-wake behaviour in rats comparable to the strong sedative effects observed in humans (Figure 25)(Sorge, Pollmächer, and Lancel 2004; Spierings, Dzoljic, and Godschalk 1977). Based on chronic EEG/EMG recordings and i.p. injections of clozapine at light onset, the authors of one

study concluded that *"clozapine increases sleep maintenance in rats"* and leads to a *"suppression of mechanisms of REM sleep initiation"* (Sorge, Pollmächer, and Lancel 2004).

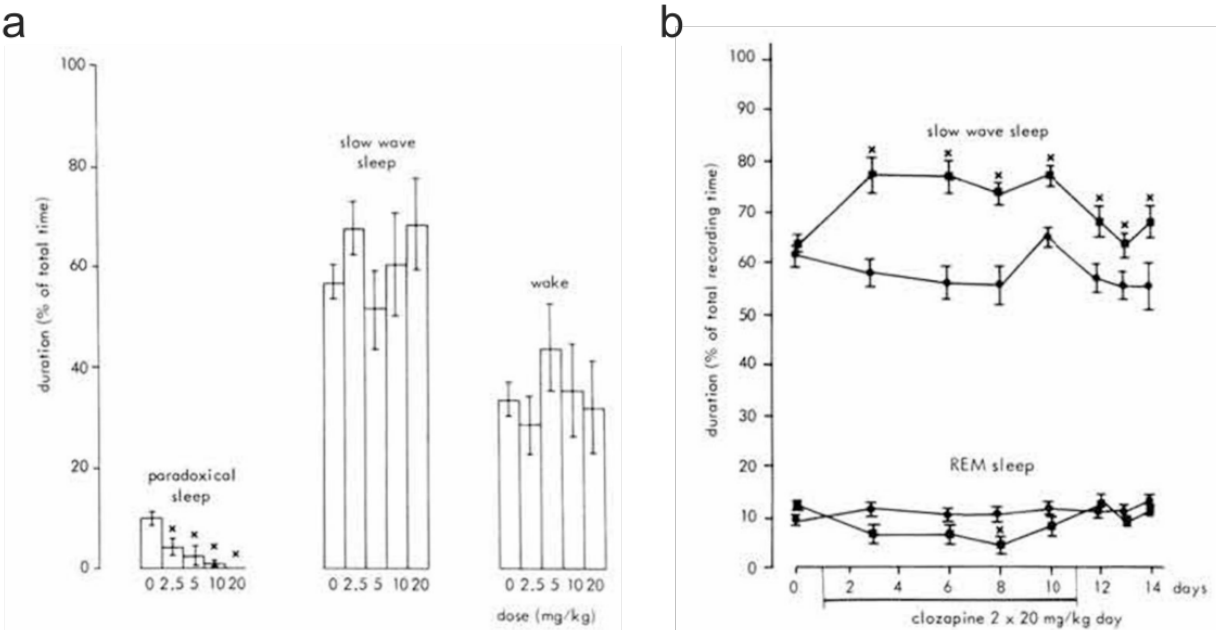



**Figure 25: Clozapine modulates sleep in rats**

a) Dose-dependent effects of clozapine on paradoxical sleep (i.e. rapid eye movement (REM) sleep), slow wave sleep (i.e. non-REM (NREM) sleep) and wakefulness in a 4-h time window following an i.p injections in Wistar albino rats. Note the dose-dependent suppression of REM sleep. b) Effects of twice-daily i.p. administration of 20mg/kg clozapine (squares) compared to propylene glycol vehicle (dots) over two weeks. Note the increase in NREM sleep and suppression in REM sleep for the first 10 days before REM sleep returns to baseline, possibly due to tolerance or homeostatic compensation. Modified from Spierings et al. 1977.

In the light of these reports, I concluded that the pilot results from my first CNO-injected *Rbp4-Cre:hM4Di* DREADD mouse might be confounded by clozapine effects resulting from *in vivo* back-conversion of CNO to clozapine. This prompted me to suspend the DREADD experiments and instead perform an extensive control experiment, systematically examining the effects of CNO on sleep in wild type mice.

### 4.3.2 Systematic investigation of putative CNO effects on sleep in wild type mice

In chemogenetic sleep studies, control data from CNO-injected wild type animals is often not presented or is limited to one sleep parameter, e.g. the amount of time in wakefulness, NREM sleep, and REM sleep in one given time window. Many studies refer to previous papers reporting that CNO itself has no effects on sleep (Funk et al. 2017; Harding et al. 2018; Y. Hayashi et al. 2015; Takata et al. 2018; Fernandez et al. 2018). To be able to interpret the sleep phenotype observed after CNO injection in the *Rbp4-Cre:hM4Di* mouse and to distinguish whether it was caused by DREADD inhibition of layer 5 pyramidal neurons or by CNO, I decided to analyse commonly reported sleep parameters in a batch of five C57BL/6J mice using a low (1 mg/kg), medium (5 mg/kg), and high (10 mg/kg) dose of CNO, which have all been previously used in published sleep studies (Funk et al. 2017; Harding et al. 2018; Y. Hayashi et al. 2015; Takata et al. 2018; Fernandez et al. 2018). Following the results acquired in this batch of five animals and based on sample size estimations, which I had performed at the outset of the study using previous datasets from our research group (McKillop et al. 2021), I then extended the sample size in this control study to 16 C57BL/6J wild type mice in order to have sufficient statistical power to detect biologically relevant effects of CNO on sleep.

*CNO suppresses REM sleep*

I first assessed the percentage of time spent in wakefulness, non-rapid eye movement (NREM) and rapid eye-movement (REM) sleep for the first six hours after injection of CNO or saline at the beginning of the light period (Figure 26). There was no indication that CNO affected the time spent awake. For NREM sleep there was a non-significant trend towards an interaction effect between the time point and treatment condition ($F(6.318,74.55) = 1.872$, $p = 0.093$) and there was a significant main effect of the treatment condition on the percentage of REM sleep ($F$ (2.007, 30.10) = 5.729, $p = 0.008$). To investigate these patterns more closely, I analysed

the acute and prolonged influence of CNO on NREM and REM sleep time. There was a trend towards a treatment effect on NREM sleep in the 'acute' time window (first two hours, $F(1.911,23.57) = 3.054$, $p = 0.068$), while REM sleep was significantly affected both acutely (first two hours, $F(1.783, 21.99) = 8.951$, $p = 0.002$) and over the entire six hour observation period ($F(1.839, 22.68) = 7.525$, $p = 0.004$). The effect sizes for post-hoc comparisons between the individual CNO conditions and saline were consistently larger for REM sleep than for NREM, indicating that CNO more strongly affects REM than NREM sleep (Table 1).

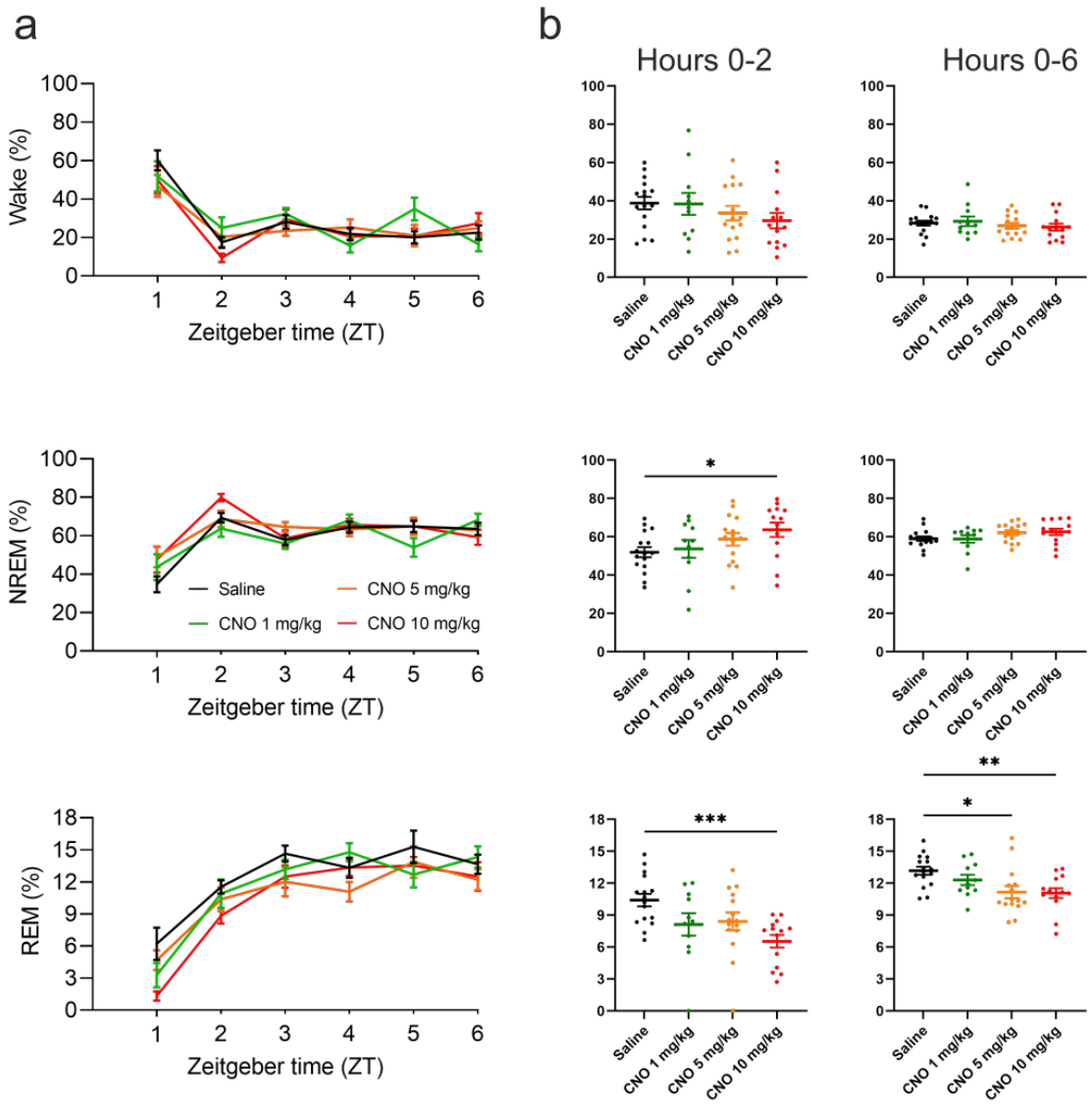



**Figure 26: Time spent in wakefulness, NREM, and REM sleep after CNO and saline injections**

a) Time course of wakefulness, non-rapid eye movement (NREM), and rapid-eye movement (REM) sleep for six hours following injection of clozapine-N-oxide (CNO) or saline at light onset (Zeitgeber time 0, ZT 0). b) Percentage of time spent in the three vigilance states during the first two hours (left column) and over the entire six-hour observation period after saline and CNO injections. The axis labels of panel (a) also indicate the y-axes for the analyses presented the same row in panel (b). n=16 for saline, n=11 for 1 mg/kg, n=15 for 5 mg/kg, n=14 for 10 mg/kg for vigilance state analysis. Asterisks indicate post-hoc contrasts with significant differences (*$P < 0.05$, **$P < 0.01$, ***$P < 0.001$).

**Table 1: Time spent in wakefulness, NREM, and REM sleep after CNO and saline injections**

| | | Treatment condition (mean values ± standard error) | | | | Mixed-effect analysis | | Effect size for post-hoc comparisons (Cohen's d) | | |
|---|---|---|---|---|---|---|---|---|---|---|
| Vigilance state | Parameter | Saline (n=16) | CNO 1 mg/kg (n=11) | CNO 5 mg/kg (n=15) | CNO 10 mg/kg (n=14) | *F* | *p* | low dose | medium dose | high dose |
| **Wake** | | | | | | | | | | |
| | 2-h time window (%) | 38.7813 ±3.2743 | 38.3636 ±5.7692 | 33.5444 ±3.8399 | 29.6429 ±3.9910 | F (1.939, 23.91) = 1.468 | 0.2504 | -0.0234 | -0.3393 | -0.4815 |
| | 6-h time window (%) | 28.3530 ±1.3114 | 29.3232 ±2.5037 | 26.9321 ±1.5278 | 26.2553 ±1.7923 | F (1.730, 21.34) = 0.6888 | 0.4928 | 0.1467 | -0.1715 | -0.2633 |
| **NREM** | | | | | | | | | | |
| | 2-h time window (%) | 51.9896 ±2.6391 | 53.7020 ±4.6576 | 58.7741 ±3.2742 | 63.7103 ±3.7117 | F (1.911, 23.57) = 3.054 | 0.0682 | 0.1157 | 0.4941 | 0.6961 |
| | 6-h time window (%) | 59.0799 ±1.1641 | 58.9074 ±1.9870 | 62.1914 ±1.2667 | 62.6111 ±1.6784 | F (1.531, 18.88) = 2.028 | 0.1661 | -0.0361 | 0.4130 | 0.4630 |
| **REM** | | | | | | | | | | |
| | 2-h time window (%) | 6.1354 ±0.5709 | 5.2121 ±0.8723 | 5.5296 ±0.6426 | 4.3492 ±0.4418 | F (2.366, 29.18) = 2.590 | 0.0839 | -0.3251 | -0.2348 | -0.6559 |
| | 2-h time window (% of sleep) | 10.4160 ±0.5877 | 8.1286 ±1.0534 | 8.4071 ±0.8351 | 6.5371 ±0.5937 | F (1.783, 21.99) = 8.951 | 0.0019 | -0.5802 | -0.5594 | -1.2743 |
| | 2-h time window (% of NREM) | 11.6996 ±0.7374 | 8.9862 ±1.2086 | 9.3021 ±0.9672 | 7.0497 ±0.6714 | F (1.858, 22.91) = 9.140 | 0.0015 | -0.5895 | -0.5673 | -1.2707 |
| | 6-h time window (%) | 8.9329 ±0.2401 | 8.2963 ±0.4838 | 7.8568 ±0.4849 | 7.7619 ±0.3314 | F (2.350, 28.99) = 2.959 | 0.0601 | -0.3718 | -0.5591 | -0.8140 |
| | 6-h time window (% of sleep) | 13.1740 ±0.3774 | 12.3119 ±0.4884 | 11.1629 ±0.5722 | 11.0742 ±0.4606 | F (1.839, 22.68) = 7.525 | 0.0038 | -0.4697 | -0.7724 | -0.9333 |
| | 6-h time window (% of NREM) | 15.2055 ±0.5001 | 14.0760 ±0.6364 | 12.6328 ±0.7455 | 12.4919 ±0.5741 | F (1.788, 22.05) = 7.382 | 0.0045 | -0.4658 | -0.7509 | -0.9430 |

*CNO alters sleep architecture*

Physiological sleep in mammals is typically entered through NREM sleep and characterised by the alternation between NREM and REM sleep episodes. The average timing, duration, and frequency of NREM and REM episodes in mice vary slightly depending on the genetic background, but are kept within tight limits for individual strains (Franken, Malafosse, and Tafti 1999). The effects of psychotropic drugs on sleep are often most prominent in sleep architecture parameters (Riemann and Nissen 2012). Clozapine modulates sleep architecture

in humans (Monti, Torterolo, and Pandi Perumal 2017), rats (Sorge, Pollmächer, and Lancel 2004; Spierings, Dzoljic, and Godschalk 1977), and mice (Grønli et al. 2016). The analysis of sleep architectural parameters was therefore of paramount importance in assessing whether CNO affects sleep in wild-type mice.

NREM and REM sleep latency were significantly affected by CNO treatment (NREM sleep: $F(2.146,26.47)=3.380$, $p = 0.046$); REM sleep: $F(2.308, 28.46) = 6.985$, $p = 0.002$)(Figure 27b,c left panels). Post-hoc analyses showed that the reduction in NREM latency reached statistical significance only in the 1 mg/kg CNO condition, similar to previous observations in rats, which suggested that a low dose of clozapine might produce a more immediate but shorter lasting sleep induction compared to higher doses (Sorge, Pollmächer, and Lancel 2004). REM latency was significantly increased in the 1 mg/kg and 10 mg/kg CNO condition compared to saline injections. CNO also evoked unusually long NREM episodes in the medium (5 mg/kg CNO) and high dose (10 mg/kg CNO) conditions ($F(2.881, 35.53) = 13.24$, $p < 0.001$) while the maximum length of REM episodes remained unchanged. The average number and duration of NREM and REM episodes was also affected by CNO treatment. I observed longer but fewer NREM episodes after CNO administration (NREM episode duration: $F(2.436, 30.04) = 11.64$, $p < 0.001$, Cohen's d for saline vs. 5 mg/kg = 1.14; NREM episode number: $F$ (2.476, 30.54) = 7.796, $p = 0.001$, Cohen's d for saline vs. 5 mg/kg = -1.06)(Figure 27b). A similar, but less pronounced pattern was found for REM episodes (REM episode duration: $F(2.330, 40.39) = 4.509$, $p = 0.013$, Cohen's d for saline vs. 5 mg/kg = 0.39; REM episode number: $F$ (2.665, 32.87) = 2.680, $p = 0.069$, Cohen's d for saline vs. 5 mg/kg = -0.36)(Figure 27c).

Overall, the data suggest that CNO strongly alters sleep architecture in mice (for detailed statistical results see Table 2) in a pattern similar to that previously reported for clozapine in rats (Sorge, Pollmächer, and Lancel 2004) and humans (Hinze-Selch et al. 1997).

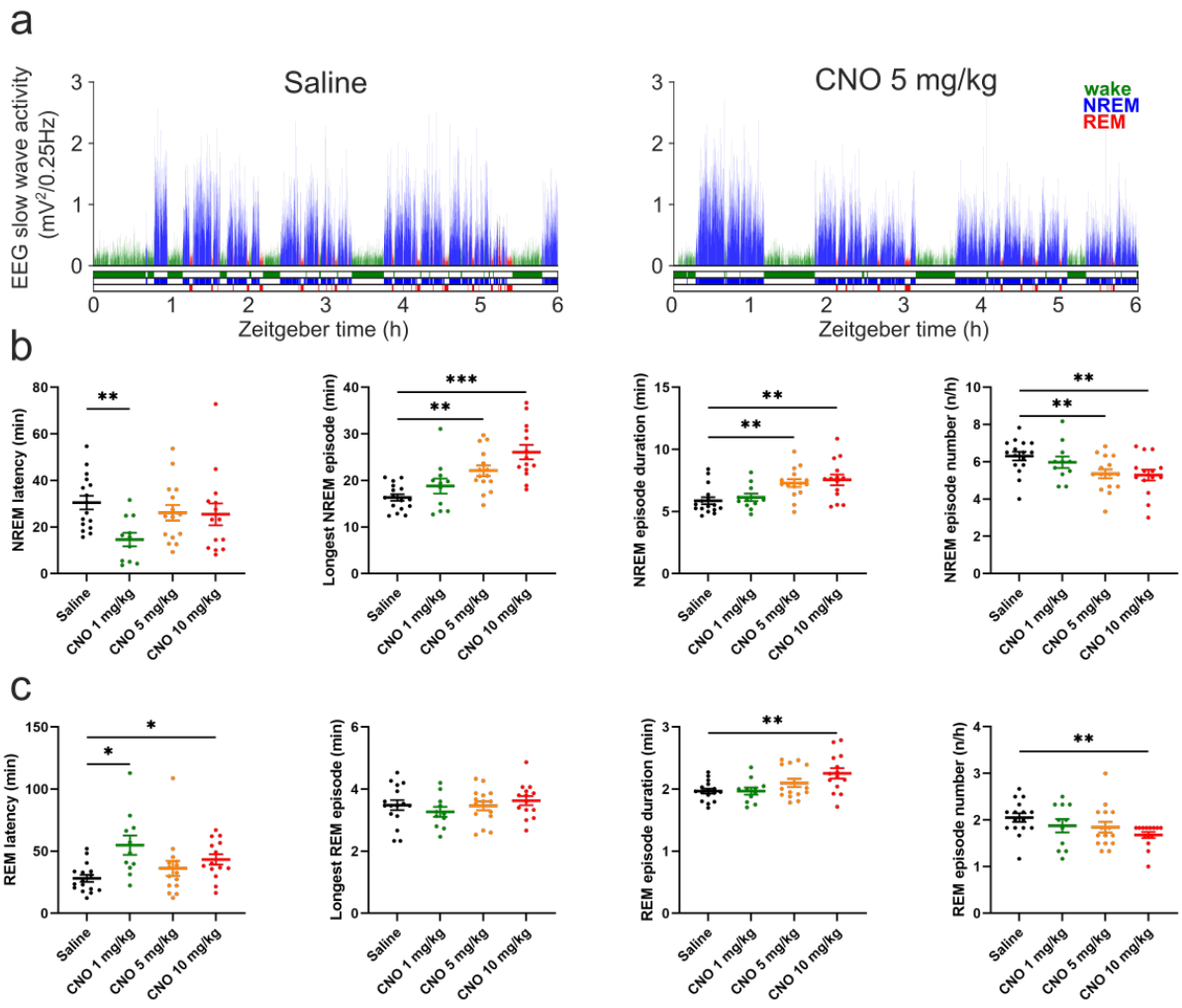



**Figure 27: Sleep architecture following CNO and saline injections**

a) Representative hypnograms and EEG slow wave activity (0.5- 4.0 Hz, 4-s epochs) from one individual mouse after injection of saline (left panel) and 5 mg/kg CNO. Note the reduced latency to NREM sleep, the suppression of REM sleep, and the increased duration of individual NREM sleep episodes. b) NREM sleep architecture following saline and CNO injections. Note that the latency to NREM sleep, the duration of the longest NREM sleep episode, the average duration, and number of NREM sleep episodes over the six hour observation period are significantly altered by CNO treatment. c) REM sleep architecture following saline and CNO injections. Note that the latency to REM sleep as well as the average duration, and number of REM sleep episodes over the six hour observation period are significantly altered by CNO treatment. n=16 for saline, n=11 for 1 mg/kg, n=15 for 5 mg/kg, n=14 for 10 mg/kg for vigilance state analysis in panels b and c. Asterisks indicate post-hoc contrasts with significant differences (*P < 0.05, **P < 0.01, ***P < 0.001). CNO: Clozapine-N-oxide. EEG: electroencephalogram. NREM: non-rapid eye movement sleep. REM: rapid eye movement sleep.

## Table 2: Sleep architecture after CNO and saline injections

| | | Treatment condition (mean values ± standard error) | | | | Mixed-effect analysis | | Effect size for post-hoc comparisons (Cohen's d) | | |
|---|---|---|---|---|---|---|---|---|---|---|
| Vigilance state | Parameter | Saline (n=16) | CNO 1 mg/kg (n=11) | CNO 5 mg/kg (n=15) | CNO 10 mg/kg (n=14) | *F* | *p* | low dose | medium dose | high dose |
| **Wake** | | | | | | | | | | |
| | Longest episode (min) | 31.3292 ±2.3901 | 32.0000 ±3.9528 | 31.6089 ±3.2855 | 31.7952 ±3.5150 | F (2.108, 26.00) = 0.02110 | 0.9825 | 0.0663 | 0.0189 | 0.0298 |
| | Episode duration average (min) | 11.6562 ±0.9793 | 9.6981 ±0.6636 | 11.0855 ±0.8599 | 11.0939 ±0.9275 | F (2.578, 31.80) = 0.8177 | 0.4777 | -0.4160 | -0.1221 | -0.1355 |
| | Episode number (n/h) | 1.5313 ±0.1429 | 1.7727 ±0.1107 | 1.4889 ±0.1254 | 1.4286 ±0.0984 | F (2.338, 40.52) = 1.241 | 0.3036 | 0.3046 | -0.0592 | -0.1694 |
| **NREM** | | | | | | | | | | |
| | Latency (min) | 30.4958 ±2.9506 | 14.6485 ±2.9015 | 26.1378 ±3.3676 | 25.4762 ±4.6781 | F (2.146, 26.47) = 3.380 | 0.0463 | -1.2021 | -0.3744 | -0.2424 |
| | Longest episode (min) | 16.3458 ±0.6994 | 18.8061 ±1.6012 | 22.1067 ±1.1553 | 26.0905 ±1.5547 | F (2.881, 35.53) = 13.24 | <0.000 1 | 0.3562 | 0.9438 | 1.5129 |
| | Episode duration average (min) | 5.8746 ±0.2822 | 6.1381 ±0.2998 | 7.2894 ±0.3127 | 7.5503 ±0.4268 | F (2.436, 30.04) = 11.64 | <0.000 1 | 0.1810 | 1.1430 | 1.1883 |
| | Episode number (n/h) | 6.3021 ±0.2318 | 5.9697 ±0.3113 | 5.3556 ±0.2444 | 5.2857 ±0.2915 | F (2.476, 30.54) = 7.796 | 0.0010 | -0.2938 | -1.0628 | -1.1989 |
| **REM** | | | | | | | | | | |
| | Latency (min) | 28.1375 ±2.8814 | 54.8970 ±7.7841 | 36.1778 ±6.0069 | 43.3667 ±4.1811 | F (2.308, 28.46) = 6.985 | 0.0024 | 0.9798 | 0.3517 | 0.8288 |
| | Longest episode (min) | 3.4833 ±0.1631 | 3.2667 ±0.1585 | 3.4622 ±0.1445 | 3.6286 ±0.1480 | F (2.720, 33.55) = 1.101 | 0.3583 | -0.3224 | -0.0272 | 0.1800 |
| | Episode duration average (min) | 1.9684 ±0.0396 | 1.9699 ±0.0574 | 2.0995 ±0.0662 | 2.2542 ±0.0835 | F (2.330, 40.39) = 4.509 | 0.0132 | 0.0049 | 0.3941 | 1.0034 |
| | Episode number (n/h) | 2.0521 ±0.0922 | 1.8788 ±0.1441 | 1.8444 ±0.1167 | 1.6786 ±0.0664 | F (2.665, 32.87) = 2.680 | 0.0690 | -0.2975 | -0.3630 | -0.9286 |
| **Sleep consoli-dation** | | | | | | | | | | |
| | NREM before REM onset (min) | 20.9500 ±1.8146 | 31.4970 ±3.5462 | 30.0711 ±3.5065 | 35.9095± 3.5029 | F (2.709, 33.41) = 5.071 | 0.0066 | 0.7346 | 0.5683 | 1.0475 |
| | Brief awakenings (n/h)* | 36.8033 ±3.7206 | 27.6169 ±3.2139 | 20.9897 ±2.7844 | 21.5082± 2.0680 | F (1.968, 23.62) = 10.38 | 0.0006 | -0.6271 | -1.0691 | -1.5760 |

*animal numbers for analysis of brief awakenings: n=15 for saline, n=11 for 1 mg/kg, n=15 for 5 mg/kg, n=13 for 10 mg/kg

*CNO affects the NREM spectrogram and sleep consolidation*

In addition to sleep time and architecture, EEG spectra are typically analysed in sleep studies. I therefore assessed whether CNO affects EEG spectral power during NREM sleep. The focus of my EEG spectral analysis was on the comparison between the medium dose (5 mg/kg) of CNO and saline (Figure 28). I observed that CNO increased spectral power in the range between 0.5-1.25 Hz and suppressed the power in nearly all frequency bins between 6-30 Hz during NREM sleep in the first 2 hours after injection. While the increase in slow frequency bins during NREM sleep appeared to be temporary, the suppression of power above 6 Hz remained significant for the entire six-hour observation period. A comparison of all three CNO conditions with saline injection indicated similar effects in the high dose (10 mg/kg CNO), but no relevant spectral changes in the low dose (1 mg/kg CNO) condition (Figure 29a). Spectral analysis of wakefulness and REM sleep did not reveal any systematic effects of CNO (Figure 28).

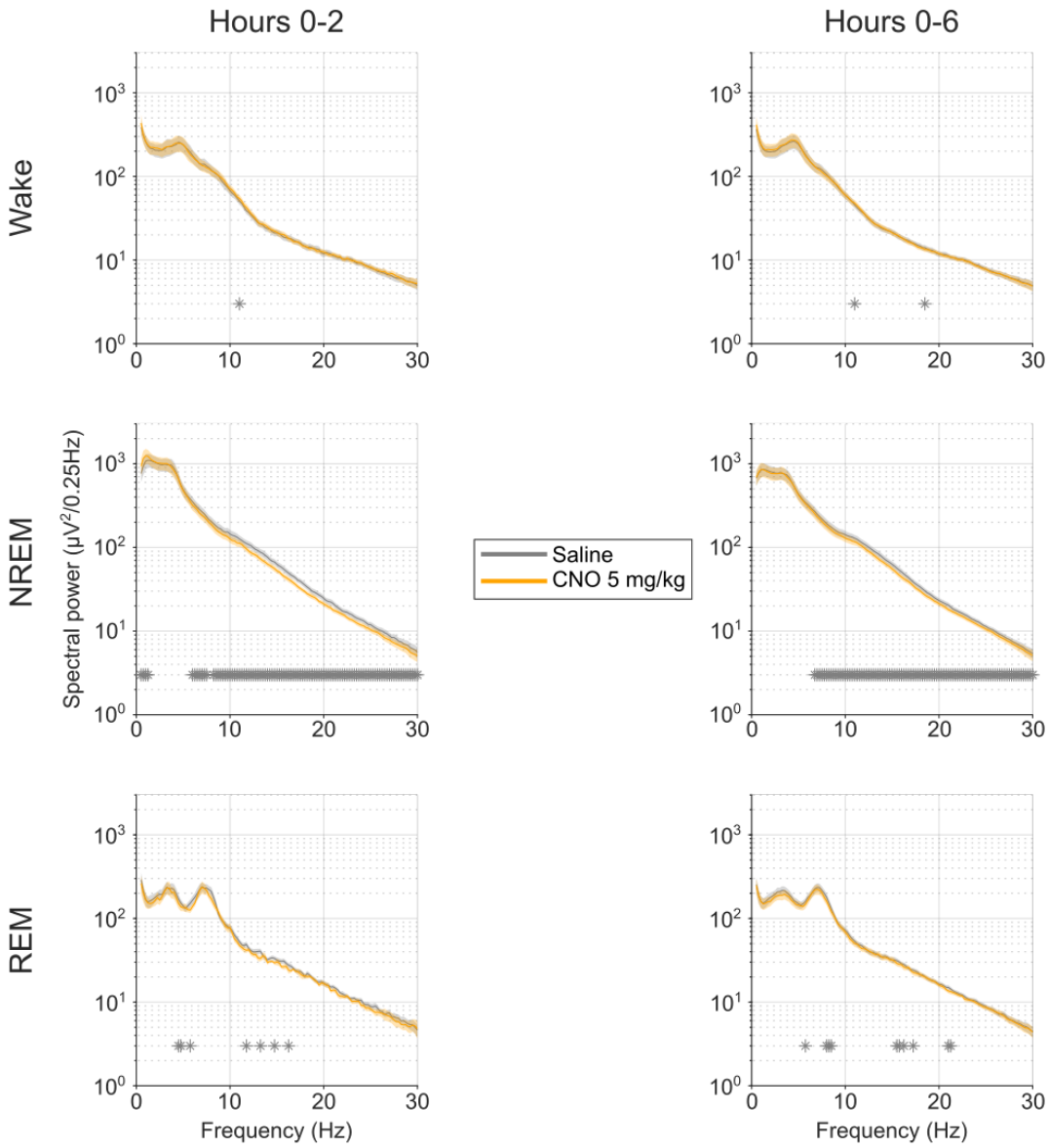



**Figure 28: EEG power spectra of wakefulness, NREM, and REM sleep following injections of saline and 5 mg/kg CNO**

EEG spectral power in 0.25 Hz bins between 0.5 and 30 Hz arranged by vigilance state and time window (left panels: first 2 hours, right panels: first 6 hours). Frequency bins with significant differences in uncorrected post-hoc testing are indicated with grey asterisks. Note the systematic increase of slow frequencies (0-1.25 Hz) in the first 2 hours and the suppression of spectral power in higher frequencies (6.25-30 Hz) in the NREM sleep spectrogram both in the first 2 hours and over the entire observation period. n=10 for saline and for 5 mg/kg in spectral analysis. CNO: Clozapine-N-oxide. EEG: electroencephalogram. NREM: non-rapid eye movement sleep. REM: rapid eye movement sleep.

As consolidated NREM sleep, elevated spectral power in slow frequencies, and suppressed REM sleep might indicate an increase in sleep pressure or pharmacologically induced sedation,

I assessed the cumulative amount of NREM sleep before the first REM episode (1 min or longer of REM sleep), as well as the frequency of brief awakenings (4-16 second intrusions of wake-like EMG and EEG during sleep), which is a behavioural marker of sleep continuity (Franken et al. 1991). I found that both measures were significantly changed after CNO injection (NREM before REM: $F(2.709, 33.41) = 5.071$, $p = 0.007$; brief awakenings: $F(1.968, 23.62) = 10.38$, $p < 0.001$). Effect size calculations indicated medium-to-large effects even for the low dose condition, which did not reach statistical significance in the post-hoc tests (Cohen's d for saline vs. 1 mg/kg for increase of NREM sleep before the first REM episode d = 0.73 and for reduction of brief awakenings d = - 0.63). The observed effects of CNO on sleep continuity were consistent with a previously described increase of quiet wakefulness after clozapine administration in mice (Grønli et al. 2016), decreased sleep fragmentation in rats (Sorge, Pollmächer, and Lancel 2004), and a pattern of increased sleep continuity reported in humans (Hinze-Selch et al. 1997; Riemann and Nissen 2012; Monti, Torterolo, and Pandi Perumal 2017).

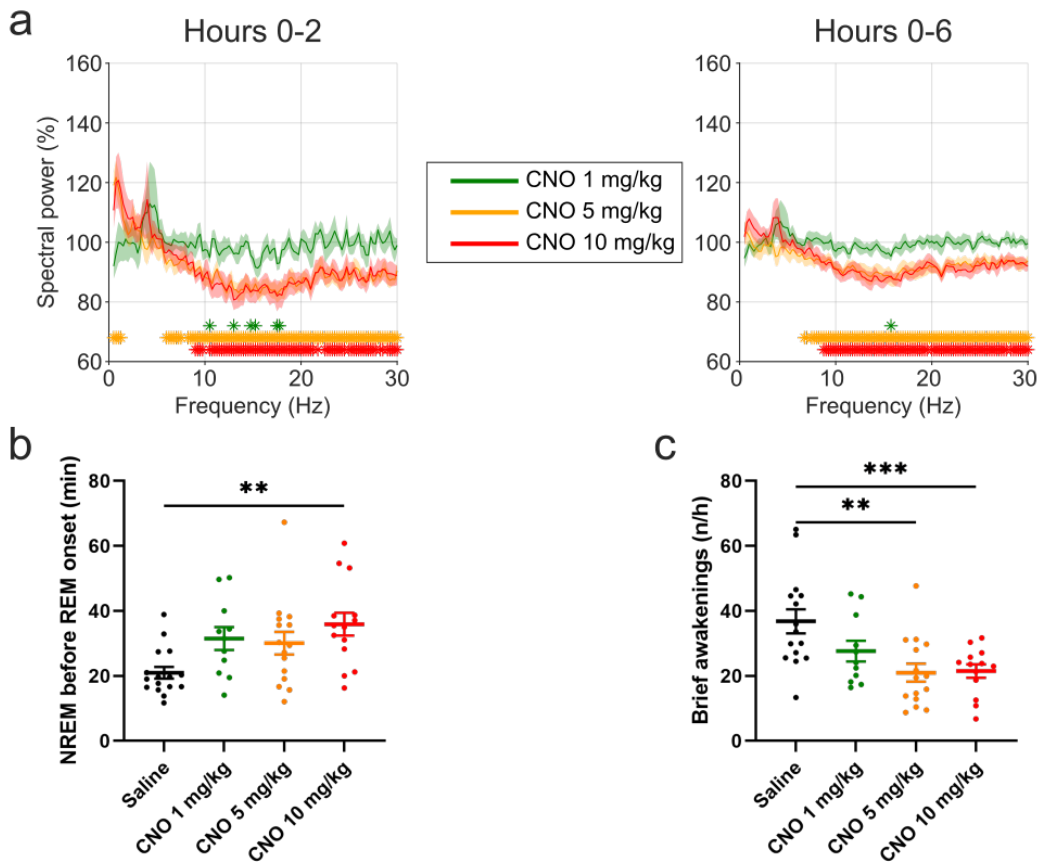



**Figure 29: Relative EEG spectra of NREM sleep and measures of sleep continuity following injections of saline and CNO**

a) Spectral power during NREM sleep relative to saline injections for the acute (first 2 hours) and full (6 hours) observation period. b) Cumulative amount of NREM sleep before the first REM sleep episode. c) Frequency of brief awakenings (4-16 sec) per hour of sleep for the first 2 hours after injections. n=10 for saline, n=6 for 1 mg/kg, n=10 for 5 mg/kg, n=8 for 10 mg/kg for spectral analysis in panel a. n=16 for saline, n=11 for 1 mg/kg, n=15 for 5 mg/kg, n=14 for 10 mg/kg for vigilance state analysis in panels b. n=15 for saline, n=11 for 1 mg/kg, n=15 for 5 mg/kg, n=13 for 10 mg/kg for analysis of brief awakenings in panel c. Asterisks indicate post-hoc contrasts with significant differences (*P < 0.05, **P < 0.01, ***P < 0.001). CNO: Clozapine-N-oxide. EEG: electroencephalogram. NREM: non-rapid eye movement sleep.

### 4.3.3 Compound 21 generates sleep-modulatory effects that are similar to CNO

Based on recent studies indicating that CNO back-metabolism to clozapine causes behavioural effects in rodents (Ilg et al. 2018; Gomez et al. 2017; Manvich et al. 2018; MacLaren et al. 2016), I expected that direct sleep-modulator could be overcome by using alternative DREADD ligands, which do not convert to clozapine *in vivo*. Another possibility, however, is

that off-target binding of CNO to endogenous receptors, which is largely shared between CNO and Cmpd21 (Jendryka et al. 2019), directly causes or contributes to the change in sleep patterns. To test if the CNO effects on sleep are, at least in part, caused by off-target binding to endogenous receptors, I performed intraperitoneal injections of Cmpd21 at a dose of 3 mg/kg as an additional condition in the last batch of seven mice.

Surprisingly, Cmpd21 also modulated sleep when compared to saline injections. I found a strong and statistically significant reduction of REM sleep over the six hour observation period ($t(6)=3.253$, $p = 0.009$, Cohen's d = -1.23) as well as indications for a moderate reduction over the first two hours, which approached statistical significance ($t(6)=1.845$, $p = 0.057$, Cohen's d = -0.70)(Figure 30a,b).

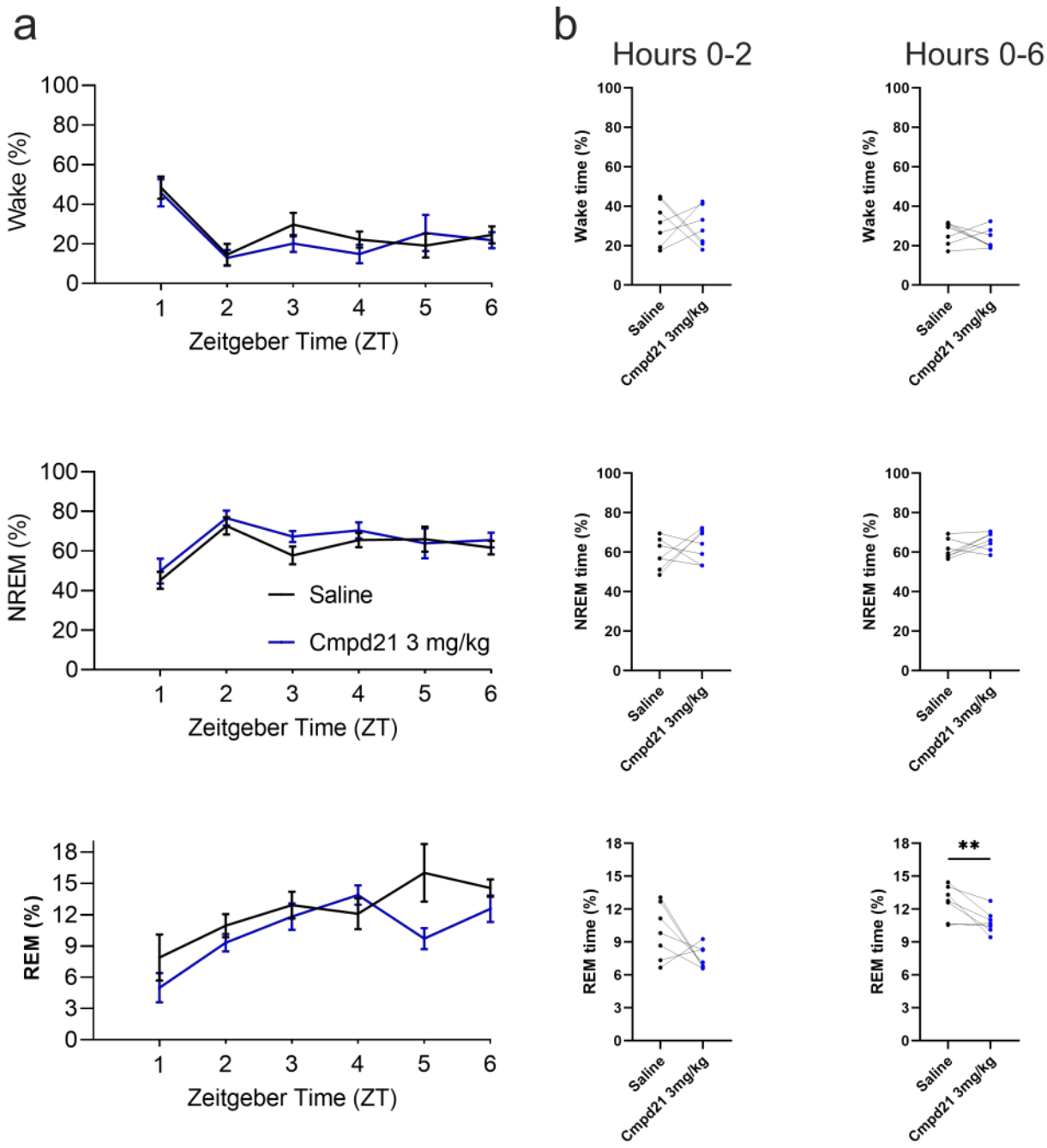



**Figure 30: Time spent in wakefulness, NREM, and REM sleep after Cmpd21 and saline injections**

a) Time course of wakefulness, non-rapid eye movement (NREM), and rapid-eye movement (REM) sleep for six hours following injection of Compound 21 (Cmpd21) or saline at light onset (Zeitgeber time 0, ZT 0). b) Percentage of time spent in the three vigilance states during the first two hours (left column) and over the entire six-hour observation period after saline and CNO injections. n=7. Asterisks indicate post-hoc contrasts with significant differences (*P < 0.05, **P < 0.01, ***P < 0.001).

Only three of the Cmpd21-injected animals had sufficient EEG quality to perform spectral analysis. However, NREM spectra showed a numerical increase in the very slow frequency bins and a suppression of frequencies above 6 Hz, a pattern which resembled that of the medium and high dose CNO injections (Figure 31a). The amount of NREM sleep before the first occurrence of REM sleep was increased (t(6) = 2.252), $p = 0.033$, Cohen's d = 0.85) and brief awakenings were reduced ($t(5) = 2.164$, $p = 0.041$, Cohen's d = -0.52)(Figure 31b,c). All NREM and REM architecture parameters showed the same trend in the group mean as observed after CNO injections (Figure 31d,e). The increase in the duration of the longest NREM sleep episode ($t(6)=2.551$, $p = 0.022$, Cohen's d = 0.96), the increase in the average duration of NREM ($t(6) = 2.462$, $p = 0.025$, Cohen's d = 0.93) and REM episodes ($t(6) = 2.229$, $p = 0.034$, Cohen's d = 0.84), as well as the reduction in the number of NREM episodes ($t(6) = 2.809$, $p = 0.015$, Cohen's d = -1.06) reached statistical significance in this small sample of seven mice (Table 3).

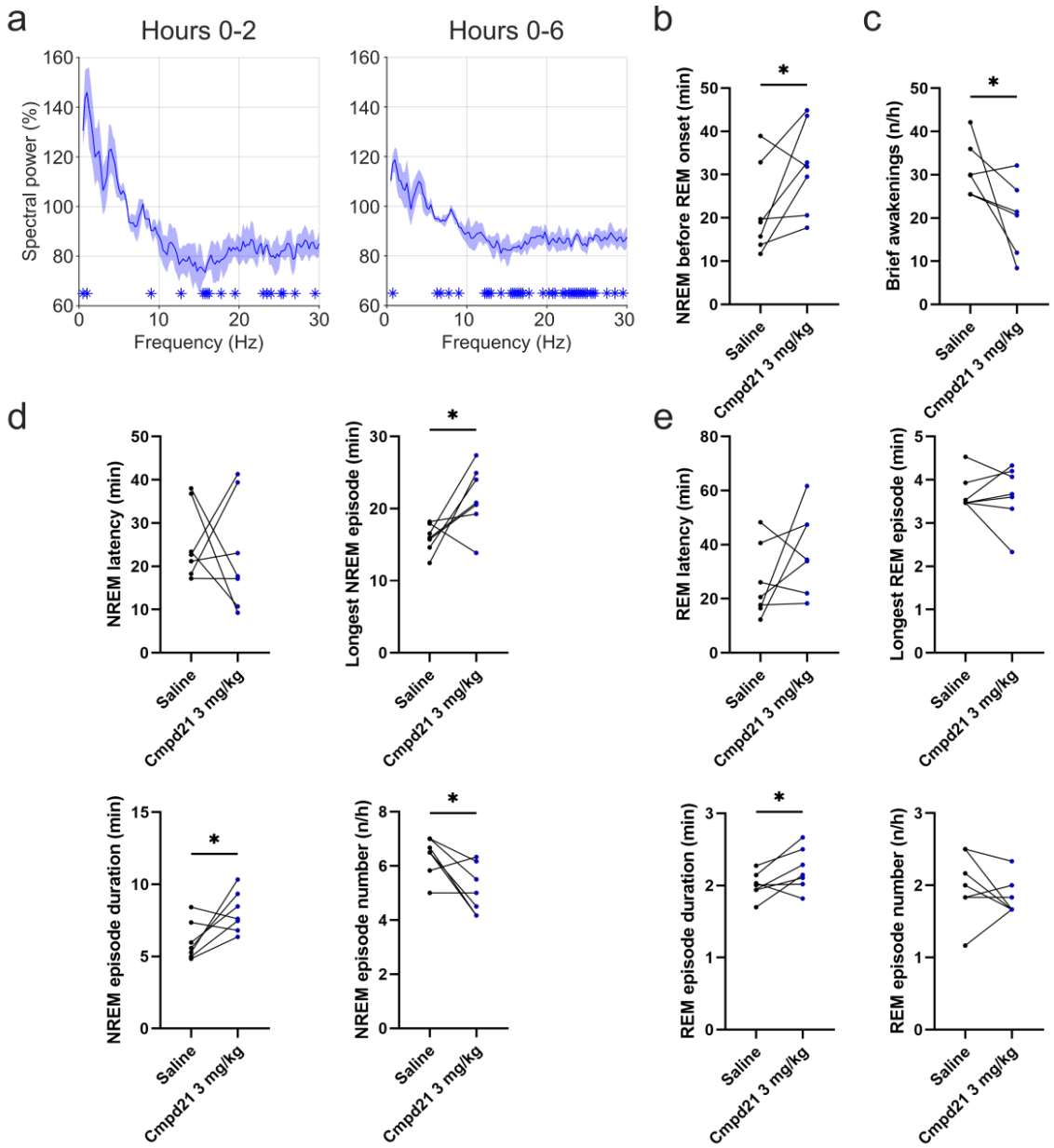



**Figure 31: Relative EEG spectra of NREM sleep, measures of sleep continuity, and sleep architecture parameters following injections of saline and Cmpd21**

a) Spectral power during NREM sleep relative to saline injections for the acute (first 2 hours) and full (6 hours) observation period following CNO injections. b) Cumulative amount of NREM sleep before the first REM sleep episode. c) Frequency of brief awakenings (4-16 sec) per hour of sleep for the first 2 hours after injections. d) NREM sleep architecture following saline and Cmpd21 injections. Note that the duration of the longest NREM sleep episode, the average duration, and number of NREM sleep episodes over the six hour observation period are significantly altered by Cmpd21 treatment in the same direction as observed after CNO injections. c) REM sleep architecture following saline and Cmpd21 injections. Number of animals n=7 mice for vigilance state analysis in panels b, d, e. For spectral analysis in panel a: n=3. For analysis of brief awakenings in panel c: n=6 mice. Asterisks indicate post-hoc contrasts with significant differences (*P < 0.05, **P < 0.01, ***P < 0.001). EEG: electroencephalogram. NREM: non-rapid eye movement sleep. REM: rapid eye movement sleep.

## Table 3: Sleep parameters after saline and Compound 21 injections

| Vigilance state | Parameter | Saline (n=7) | Cmpd21 3 mg/kg (n=7) | *t* | *p* | Effect size (Cohen's d) |
|---|---|---|---|---|---|---|
| **Wake** | | | | | | |
| | 2-h time window (%) | 31.4841 ±4.1581 | 29.3571 ±3.7073 | t=0.2993, df=6 | 0.3874 | -0.1131 |
| | 6-h time window (%) | 26.4153 ±2.1399 | 23.5106 ±1.9486 | t=0.9230, df=6 | 0.1958 | -0.3489 |
| | Longest episode (min) | 27.6286 ±2.5082 | 30.3524 ±4.1173 | t=0.8184, df=6 | 0.2222 | 0.3093 |
| | Episode duration average (min) | 10.4205 ±0.9875 | 10.6269 ±1.8085 | t=0.1339, df=6 | 0.4489 | 0.0506 |
| | Episode number (n/h) | 1.5714 ±0.2463 | 1.4286 ±0.1776 | t=0.4680, df=6 | 0.3281 | -0.1769 |
| **NREM** | | | | | | |
| | 2-h time window (%) | 58.9444 ±2.9443 | 63.2302 ±3.0788 | t=0.8081, df=6 | 0.2249 | 0.3054 |
| | 6-h time window (%) | 61.4603 ± 1.8489 | 65.5873 ±1.6922 | t=1.623, df=6 | 0.0779 | 0.6133 |
| | Latency (min) | 25.3619 ±3.2217 | 22.6571 ±4.8946 | t=0.3844, df=6 | 0.3570 | -0.1453 |
| | Longest episode (min) | 15.9143 ±0.7453 | 21.5429 ±1.6727 | t=2.551, df=6 | 0.0217 | 0.9641 |
| | Episode duration average (min) | 6.0655 ±0.5040 | 8.0568 ±0.5341 | t=2.462, df=6 | 0.0245 | 0.9307 |
| | Episode number (n/h) | 6.3571 ±0.2708 | 5.1190 ±0.3426 | t=2.809, df=6 | 0.0154 | -1.0617 |
| **REM** | | | | | | |
| | 2-h time window (%) | 6.6508 ±0.9090 | 5.2460 ±0.4823 | t=1.050, df=6 | 0.1670 | -0.3970 |
| | 2-h time window (% of sleep) | 9.9182 ± 0.9511 | 7.5927 ±0.3919 | t=1.829, df=6 | 0.0585 | -0.6915 |
| | 2-h time window (% of NREM) | 11.0846 ±1.1739 | 8.2282 ±0.4615 | t=1.845, df=6 | 0.0573 | -0.6972 |
| | 6-h time window (%) | 8.8571 ±0.3862 | 7.9630 ±0.3277 | t=2.086, df=6 | 0.0410 | -0.7885 |
| | 6-h time window (% of sleep) | 12.6278 ±0.5749 | 10.8374 ±0.3969 | t=3.234, df=6 | 0.0089 | -1.2223 |
| | 6-h time window (% of NREM) | 14.4824 ±0.7491 | 12.1680 ±0.5030 | t=3.253, df=6 | 0.0087 | -1.2296 |
| | Latency (min) | 26.0095 ±5.0918 | 37.8952 ±5.8049 | t=1.474, df=6 | 0.0954 | 0.3718 |
| | Longest episode (min) | 3.6952 ±0.1539 | 3.6476 ±0.2573 | t=0.2047, df=6 | 0.4223 | -0.0774 |
| | Episode duration average (min) | 2.0054 ±0.0678 | 2.2206 ±0.1093 | t=2.229, df=6 | 0.0337 | 0.8425 |
| | Episode number (n/h) | 2.0000 ±0.1744 | 1.8333 ±0.0962 | t=1.000, df=6 | 0.1780 | -0.3780 |
| **Sleep consoli-dation** | | | | | | |
| | NREM before REM onset (min) | 21.6762 ±3.8776 | 31.5714 ±3.9007 | t=2.252, df=6 | 0.0326 | 0.8511 |
| | Brief awakenings (n/h)* | 31.5102 ±2.6435 | 20.1852 ±2.6435 | t=2.164, df=5 | 0.0414 | -0.8836 |

*animal numbers for analysis of brief awakenings: n=6

## 4.4 Discussion

I initially set out to perform DREADD manipulations of neocortical layer 5 pyramidal neurons using an *Rpb4-Cre:hM4Di* cross to test the involvement of cortical layer 5 pyramidal neurons in the regulation of sleep oscillations and vigilance states. A pilot experiment using 5 mg/kg CNO in one mouse from this inhibitory DREADD cross indicated a change in the sleep profile after CNO compared to saline injections, both after injections at light onset under undisturbed conditions and after injections at the end of a six hour-long sleep deprivation. In both conditions, CNO injections in the *Rbp4-Cre:hM4Di* mouse were followed by extended NREM sleep episodes with unusually few transitions to wakefulness or REM sleep. REM sleep was nearly abolished for the first three hours and a physiological sleep pattern with regular alternation between NREM and REM sleep only re-established after 4-5 hours. Following sleep deprivation, NREM sleep SWA appeared temporarily suppressed and there was an indication for a rebound of SWA levels following their initial suppression after CNO injection. While the temporary suppression SWA was in line with the hypothesised role of layer 5 pyramidal neurons in the regulation of slow waves and consistent with the results from my laminar analysis presented in the previous chapter, the sleep architecture changes were strikingly similar to previously reported effects of clozapine on sleep in rats (Sorge, Pollmächer, and Lancel 2004). My pilot results and recent reports about CNO back-metabolism to clozapine (Jendryka et al. 2019; Manvich et al. 2018) and concomitant behavioural effects of commonly used CNO doses in rodents (Gomez et al. 2017; MacLaren et al. 2016; Ilg et al. 2018) prompted me to perform a sleep-screen for CNO effects in wild type mice, initially planned as a control experiment. This experiment revealed effects of CNO on sleep. I observed a dose-dependent suppression of REM sleep as well as changes in sleep architecture parameters and EEG spectra of NREM sleep consistent with a sleep-consolidating effect of CNO. To establish whether these effects were caused by CNO back-metabolism to clozapine, I also assessed sleep after injection

of Cmpd21, a next generation DREADD ligand which does not convert to clozapine. Cmpd21 also evoked REM suppression, modulated sleep architecture, and affected the NREM sleep spectrogram.

In the last part of this chapter, I will discuss putative mechanisms of CNO- and Cmpd21-induced sleep modulation, potential limitations of my study, implications for the application of DREADD technology in sleep research, and alternative approaches for subacute and chronic manipulations of neuronal activity in layer 5 pyramidal neurons.

### 4.4.1 Putative mechanisms for sleep-modulatory effects of DREADD ligands

In this study, CNO and Cmpd21 elicited very similar effects on sleep amount, architecture, and oscillations. This is somewhat surprising, because Cmpd21 does not back-metabolise to CNO (Thompson et al. 2018) and the CNO product used in my experiments is optimised for reduced back-metabolism to CNO (D. C. Allen et al. 2019). The most parsimonious explanation for the observed effects is that CNO and Cmpd21 modulate sleep through off-target binding at endogenous neurotransmitter receptors. It is known that CNO is a competitive inhibitor of several neurotransmitter receptors, including histaminergic H1, serotoninergic 5-HT1A, 5-HT1B, 5-HT2A, 5-HT2B, muscarinic M1, M2, M3, M4, adrenergic α1A and α2A, and dopaminergic D1 and D2 receptors (Gomez et al. 2017; Jendryka et al. 2019). In addition, it was recently reported that also Cmpd21 (X. Chen et al. 2015), despite its lack of *in vivo* conversion to clozapine (Thompson et al. 2018), has an off-target binding profile similar to CNO (Jendryka et al. 2019). It was also shown that Cmpd21 increases the firing rate of nigral dopaminergic neurons in wild type rats, indicating that Cmpd21 also elicits direct neuromodulatory effects in rodents (Goutaudier et al. 2020). Among several endogenous receptors relevant for sleep regulation, CNO and Cmpd21 induce a strong competitive inhibition at histamine H1-receptors. This was shown in an enzymatic affinity screen, in which

the inhibition constant ($K_i$, the concentration at which 50% of the receptor are occupied) was 0.03 µM, approximately the CNO concentration measured in mouse brain tissue 15 minutes after a 3.5 mg/kg injection of CNO (Jendryka et al. 2019). H1-receptor knockout and pharmacological antagonism of the H1 receptor in mice results in a reduced number of brief awakenings, fewer but longer NREM sleep episodes, and a reduced latency to NREM sleep after i.p. injections (Huang et al. 2006). In addition, antihistamines which induce drowsiness as a common adverse effect, are known to strongly suppress REM sleep, but can be acutely NREM-promoting at low doses and wake-promoting at high doses, respectively (Ikeda-Sagara et al. 2012). Therefore, it appears plausible that the effects of the two DREADD actuators are mediated by direct antihistaminergic action. However, a contribution of other receptors such as the 5-$HT_{2A}$ receptors, that are shared off-target binding sites of both DREADD ligands (Jendryka et al. 2019) and thought to induce the locomotor suppression after high doses of clozapine (McOmish et al. 2012), should not be excluded.

### 4.4.2 Limitations of the sleep screen after CNO and Cmpd21 injection

It is important to note that this study on sleep-modulating effects of CNO and Cmpd21 was initiated as a control experiment and was not designed to meet the high experimental design standards of a pharmacology study assessing dose-dependent effects of a drug. I will therefore highlight some of the central limitations, which should be considered in the interpretation of my results.

First, the experimental conditions were not perfectly counterbalanced. As described in the methods section of this chapter (section 4.2), the saline and the 5 mg/kg CNO condition were randomised as the first two injections to allow for a direct comparison between saline and the medium dose of CNO, and to avoid potential adaptation effects resulting from repeated CNO injections. Injections of 1 mg/kg CNO and 10 mg/kg CNO were performed in the third and

fourth session and could not be delivered to all animals due to UK Home Office project license restrictions. Cmpd21 injections were performed in a fifth session and only in the last batch of seven animals because the decision to test this alternative DREADD ligand was made once the pilot results from the CNO injections indicated sleep-modulatory effects. I therefore cannot rule out potential contributions resulting from habituation to the injection procedure, or sequence effects due to repeated CNO treatment. This should particularly be considered in the interpretation of the sleep latency experiments as one could expect that the arousal-promoting effect of the intraperitoneal injection procedure would decline with repeated injections.

Second, most of the animals (13 out of 16) had been used in other experiments before they underwent CNO injections. While 9 animals had only received LED flickering light stimulation and sleep deprivation, 4 animals were included from a study investigating the effects of chloride transporter proteins in cortex. The animals from the LED study had received at least 3 rest days before inclusion in this experiment and the animals from the chloride transporter study received 12 rest days before inclusion in this experiment. The type of experiments and the duration of the rest interval before inclusion into the CNO/Cmpd21 study makes it highly unlikely that my findings were confounded by this factor, but effects of these previous experiences on the pharmacological manipulations performed here cannot be fully excluded.

Third, the sample size of Cmpd21-injected animals was small (n=7) and below the sample size initially intended for each experimental condition. Therefore, all analyses concerning Cmpd21 effects should be considered exploratory. It should also be noted that one-sided t-tests were used for the comparison of Cmpd21 and saline injections because the hypothesis was directed towards assessing whether Cmpd21 would alter sleep parameters in the same direction as CNO. To avoid misinterpretation of this null-hypothesis testing, I provided Cohen's d as effect size measure in Table 3.

Fourth, the CNO and Cmpd21 products used in this study are hydrochloride salt preparations of the respective drugs with improved water solubility. These products were chosen to avoid the use of the toxic solvent DMSO, required in concentrations of up to 15% to produce solutions with other CNO products (E. J. Campbell and Marchant 2018), and because the selected CNO product was reported to have reduced back-metabolism to clozapine based on a pharmacokinetic study in rhesus macaques (D. C. Allen et al. 2019). I have contacted the company to regarding the pharmacokinetic properties of these products in mice, but this data is not available. In macaques, Clozapine N-oxide dihydrochloride results in plasma concentrations of free CNO, which are 6-7 higher compared to a comparable CNO product dissolved in 10% DMSO (D. C. Allen et al. 2019). It is therefore conceivable that our CNO product, which had previously been used in other neuroscientific studies in mice (Boender et al. 2021; Chang and Gean 2019) including work on sleep spindles (Fernandez et al. 2018), has a particularly high bioavailability and might therefore more strongly affect endogenous neurotransmitter receptors than other CNO products or preparations. It should be emphasised that my experiment did not include any measurements of plasma, CSF, or brain tissue concentrations of clozapine, CNO, or Cmpd21 and that I did not validate the off-target receptor binding profile of the specific CNO and Cmpd21 products used here. Any conclusions about the mechanism of action discussed in this thesis, in particular regarding the hypothesis that sleep effects of CNO and Cmpd21 might be induced by off-target binding of endogenous receptors rather than or in addition to back-metabolism to clozapine, should therefore be considered speculative.

Despite these limitations, the present study offers a strong indication that CNO and Cmpd21 modulate sleep. To validate these effects and gain further insights into the mechanism of action it would be desirable to repeat this study in a sample of mice that had not undergone other procedures and had been fully habituated i.p. injections, and to fully randomise the conditions

using a latin square design, for example. To gain mechanistic insights, it would further be required to use different CNO and Cmpd21 products and to measure the *in vivo* concentrations of these substances and their metabolites in plasma, CSF, and brain tissue. One could further consider the use of H1 knockout animals to establish whether the effects are indeed modulated by H1 receptor binding.

### 4.4.3 Implications for the use of DREADD technology in basic sleep research

The results presented here suggest that current inconsistencies in the sleep literature and unresolved differences between optogenetic and DREADD studies (Varin and Bonnavion 2019) might have resulted from the assumption that CNO does not affect sleep. Many recent studies show convincing control data, which clearly indicates that the specific CNO concentration and products used do not affect any of the investigated parameters (Erickson et al. 2019; Mondino et al. 2021; Takata et al. 2018; Yu et al. 2019). Some early studies, using doses of less than 1 mg/kg CNO, consistently demonstrated that neither the amount of sleep, nor EEG spectra, nor the duration and number of NREM and REM bouts was affected by the specific CNO preparations used for the respective DREADD experiments (Anaclet et al. 2015; Venner et al. 2016). However, especially older DREADD studies commonly compare CNO injections with saline conditions in DREADD-expressing animals without presenting a CNO-injected DREADD-free controls for some of the core experiments (Y. Hayashi et al. 2015) and other sleep studies have used CNO doses up to 10 mg/kg (Funk et al. 2017). Because neuronal inhibition through hM4Di receptors is typically less effective than neuronal activation through hM3Dq receptors, it is common to use higher doses of CNO for the excitatory than for the inhibitory DREADD experiment when attempting bi-directional modulation of behaviours (E. J. Campbell and Marchant 2018). This practice is also commonly observed in sleep studies and

makes it difficult to differentiate between direct CNO and actual DREADD effects (Varin, Luppi, and Fort 2018; Funk et al. 2017).

A first indication that sleep is affected by CNO doses of 5 mg/kg and above can be found in a recent chemogenetic study (Varin, Luppi, and Fort 2018). The authors, who provide time courses and sleep architectural analysis in their supplementary data (Figure 32), report that in their hands *"[CNO] induced dose-dependent effects on sleep, statistically significant for doses higher than 5 mg/kg"* and speculate that this might have been caused by CNO conversion to clozapine (Varin, Luppi, and Fort 2018). However, this important accidental finding that CNO affects sleep against previous assumptions is not included in the title or abstract of the study and has found surprisingly little attention in the sleep research community as indicated by the observation that currently (27th of July 2021) no other PubMed-listed publication cites the sleep-modulating effects of CNO suggested by this study.

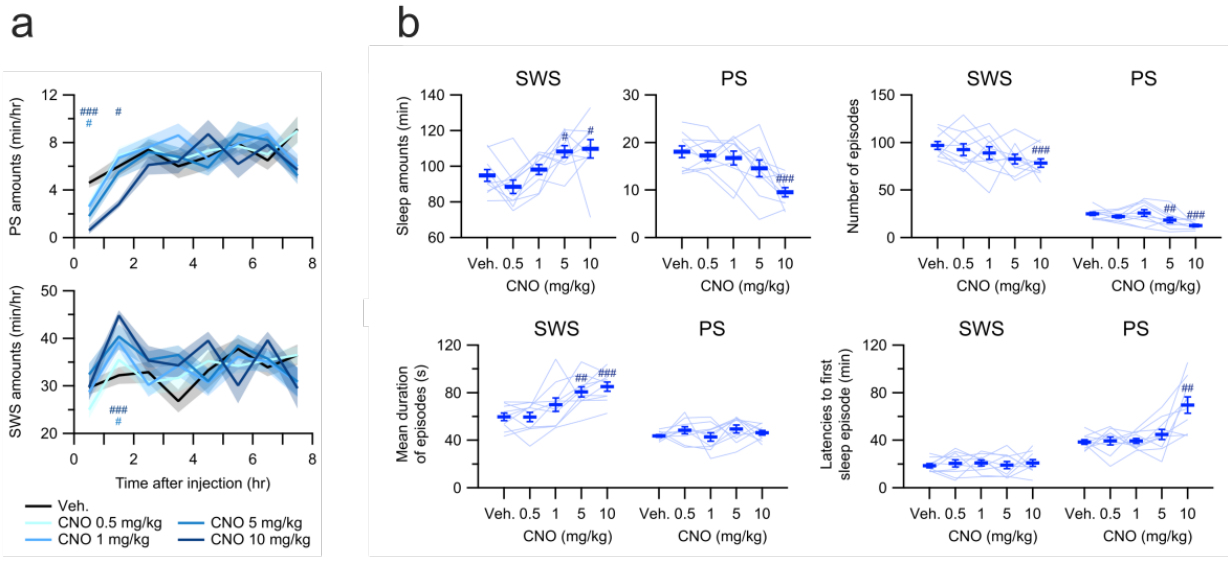



**Figure 32: Control data for CNO effects on sleep in wild type mice**

a) Time course of REM sleep (PS for 'paradoxical sleep') and NREM sleep (SWS for 'slow wave sleep') for six hours after CNO injections in DREADD-free control mice. b) sleep architectural parameters after CNO injections in DREADD-free control mice. PS: paradoxical sleep (i.e. rapid-eye movement (REM) sleep). SWS: slow wave sleep (i.e. non-rapid eye movement (NREM) sleep). Figure modified from Varin et al. 2018.

My experiments presented in this chapter confirm and considerably expand the findings by Varin and colleagues, and suggest that even doses of 1 mg/kg CNO have moderate effects on several sleep parameters and might cause rapid but short-lasting sedation in line with a recent sleep study suggesting that this dose of CNO induced *"a trend to deeper and slower respiration"* (Fleury Curado et al. 2018). A close look at control data and supplementary materials of recent chemogenetic studies provides hints that several different CNO product and concentrations might modulate sleep. For example a study investigating the role of somatostatin-positive cortical interneurons in the generation of sleep slow waves shows time courses of wakefulness, NREM, and REM sleep in which an initial suppression of REM sleep and increase of NREM sleep after 5 mg/kg and 10 mg/kg CNO injections in DREADD negative controls compared to saline-injected controls is visible (Funk et al. 2017). REM spectra are not provided for CNO-injected groups after sleep deprivation, possibly due to the lack of REM sleep in those animals. While the putative sleep modulating effects of CNO in control animals are not statistically analysed in this study, the authors also demonstrate genuine DREADD effects (Funk et al. 2017). In another study investigating the neural circuity linking sleep and thermoregulation, which carefully provides CNO-injected controls for all experiments, there is a non-significant trend towards increased NREM sleep in the control data after 5 mg/kg CNO administration compared to saline (Harding et al. 2018). The amount of REM sleep for both groups is not shown, however the authors report very low amounts of REM sleep (0.0%, 0.2%, 0.1%, and 0.3% of the recording time) over a 3-h time window following 5 mg/kg CNO injections in four CNO-injected animals from different genotypes, suggesting that CNO injections in this study might have suppressed REM sleep independent of whether mice expressed DREADDs and lowered their body temperature or not (Harding et al. 2018). This would be in line with the fine-scale analysis of sleep architecture in a different study, where a non-significant trend towards a reduction in the number and increase in the duration of REM

bouts can be observed for a very low CNO dose of 0.3 mg/kg (Naganuma et al. 2018). It has been highlighted previously that the off-target effects of CNO vary between individual animals and the susceptibility might vary dependent on several factors such as age, sex, species and strain of the experimental animals (Manvich et al. 2018), possibly due to differences in the activity of the cytochrome P450 enyme, which converts CNO to clozapine (Mahler and Aston-Jones 2018). In addition, CNO products and solvents used in the preparation of the injected solution differ in their pharmacokinetic properties (D. C. Allen et al. 2019). Together, these factors underline the paramount importance of using the lowest possible does of CNO required to activate DREADDS, including CNO-injected DREADD-negative animals as controls, and performing bidirectional modulation with the same dose of CNO.

In addition to previously raised concerns about CNO back-metabolism to clozapine, my findings indicate that CNO side effects cannot simply be overcome through the use of DREADD actuators that do not convert to clozapine. Considering that another next generation DREADD agonist, perlapine, which is structurally similar to Compound 21 (X. Chen et al. 2015; Thompson et al. 2018) is a REM-suppressing sedative and muscle relaxant used in the treatment of insomnia (Ando et al. 1970; S. R. Allen and Oswald 1973; Stille et al. 1973) and that atypical antipsychotics such as olanzapine have similar sleep-modulatory effects (Monti, Torterolo, and Pandi Perumal 2017), it should be discussed whether chemogenetic approaches that do not require actuators with high chemical similarity to clozapine could provide a better alternative for basic and translational neuroscience research (Magnus et al. 2019). The optimisation of DREADD ligands based on comparison between the binding affinity to hM1Dq, hM3Dq or hM4Di DREADDs versus wild type hM1, hM3, or hM4 receptors might not be the best way forwards as this strategy cannot exclude high binding affinity of the ligands to other endogenous receptors (Thompson et al. 2018; X. Chen et al. 2015), which are not part of the human muscarinic acetylcholine receptor family.

In addition, my results provide a basis for technical refinements of animal research as they indicate that systematic sleep analysis might be a sensitive tool to assess the pharmacological inertness of DREADD ligands *in vivo* due to the many neurotransmitter systems involved in sleep control. It should also be noted that sample sizes of control groups are usually small and power analysis of our study showed that medium (5 mg/kg) and high (10 mg/kg) doses of CNO induced changes in the amount of NREM and REM sleep of similar magnitude to those observed after administration of the established hypnotic diazepam (McKillop et al. 2021) indicating the importance of including power calculations if non-significant trends are observed in control experiments with small sample sizes.

In conclusion, DREADD technology remains an invaluable tool in sleep neuroscience. However, findings solely based on comparison of higher CNO doses and saline injections alone should be carefully reassessed, especially if the results are controversial and inconsistent with those obtained using other tools for neuronal remote control. In some circumstances, direct CNO effects might have been attributed to DREADD activation and in other cases relevant DREADD effects might have been masked by direct CNO action.

### 4.4.4 Alternative approaches for subacute and chronic manipulations of neuronal activity in layer 5 pyramidal neurons

While chemogenetic manipulations in principle appeared the most elegant option for subacute and non-invasive manipulations of layer 5 pyramidal neurons in chronic sleep experiments, it became evident that other approaches might provide more suitable alternatives to address the question whether the cortex contributes to the regulation of sleep oscillations and vigilance states. The search for the most suitable approach for subacute or chronic non-invasive silencing of selected neurons had already pointed me to the seminal work on synaptic neurotransmitter release by Südhof and colleagues (Südhof and Rizo 2011). Initial studies showed that that

neurotransmitter secretion from synaptic vesicles can be completely abolished by deletion of key proteins of the synaptic release machinery, yet even null mutants of the protein Munc18-1 present normal layering, path finding, and synaptic morphology indicating that even abolition of evoked transmitter release throughout development does not prevent normal brain assembly (Verhage et al. 2000). Detailed neuroanatomical work in the constitutive *Snap25* knockout, where only evoked synaptic transmission is blocked, and found normal neurodevelopment (Molnár et al. 2002; Washbourne et al. 2002). A conditional knockout mouse model (*Rbp4-Cre;Ai14;Snap25*$^{fl/fl}$) was available in the Molnár lab at Oxford and this research group had previously performed extensive neuroanatomical work from the onset of Cre-expression at E16.5 (Leone et al. 2014) and found normal neurodevelopment, in particular cortical layering and axonal pathfinding (Hoerder-Suabedissen et al. 2019; Grant, Hoerder-Suabedissen, and Molnár 2016). Because several studies on this specific mechanism (blockade of evoked synaptic vesicle release through ablation of SNAP25) (Washbourne et al. 2002; Molnár et al. 2002; Blakey, Wilson, and Molnár 2012) and on this specific mouse model (*Rbp4-Cre;Ai14;Snap25*$^{fl/fl}$) (Washbourne et al. 2002; Molnár et al. 2002) showed normal development and axonal path finding (Hoerder-Suabedissen et al. 2019), this mouse strain appeared suitable to investigate laminar neocortical dynamics and global sleep-wake regulation in the context of chronically silenced layer 5 pyramidal neurons. In the next chapter, I will present laminar analysis of cortical dynamics during sleep, EEG assessment of vigilance states, as well as circadian phenotyping of this mouse model based on passive infrared recordings.

# Chapter 5: Cortical dynamics, sleep, and circadian regulation in a 'cortical SNAP25-ablated' mouse model

## 5.1 Introduction

In the previous chapters I presented laminar recordings from wild type mice, which indicated that the bistable OFF-ON dynamics during NREM sleep are led by neocortical layer 5. I further presented pilot EEG experiments aiming at manipulating Rbp4-Cre expressing layer 5 pyramidal and archicortical dentate gyrus granule cells using the chemogenetic DREADD technology. These experiments provided a tentative hint that inhibition of the targeted cortical neurons might reduce EEG SWA during NREM sleep. However, I found that the DREADD actuators CNO and Cmpd21 have direct sleep modulatory effects and concluded that the originally planned DREADD approach could not resolve the question whether layer 5 pyramidal neurons play a role in the regulation of sleep oscillations and vigilance states. In this chapter, I will present a detailed characterisation of cortical dynamics, sleep and circadian regulation in a 'cortical SNAP25-ablated' mouse model *Rbp4-Cre;Ai14;Snap25*$^{fl/fl}$, a transgenic mouse line in which a subpopulation of layer 5 pyramidal and dentate gyrus granule cells is chronically silenced due to removal of the t-SNARE protein SNAP25.

The methods section will provide information about the mice used in each part of the experiment and cross-references to the methods chapter, where the relevant techniques are introduced. The results section first includes an anatomical characterisation of Cre-expression in the cortical SNAP25-ablated mouse model and then summarises three types of sleep assessment (1) laminar recordings of neocortical dynamics during sleep, (2) EEG-based analysis of sleep architecture and sleep oscillations, and (3) circadian phenotyping using passive infrared (PIR) recordings. In the discussion section, I will argue that this mouse line

represents a valuable experimental model to probe an involvement of cortex in the regulation of sleep. I will further discuss the limitations of this study, present implications of our findings, and conclude with an assessment of what can be learnt from this mouse model and what needs to be further tested with different approaches.

## 5.2 Methods

### 5.2.1 The 'cortical Snap25-ablated' (*Rbp4-Cre;Ai14;Snap25$^{fl/fl}$*) mouse model

*Chronic cell-type specific silencing by Cre-Lox mediated disruption of the Snap25 gene*

*Rbp4-Cre;Ai14;Snap25$^{fl/fl}$* is a triple transgenic mouse line, which was designed as a model for functional silencing of cortical layer 5 pyramidal and dentate gyrus granule cells. *Ai14* is a Cre-reporter allele with a lox-P flanked STOP cassette. Because the red fluorescent tdTomato reporter is expressed continuously once the STOP cassette has been removed by Cre-recombinase, this indicator labels all cells expressing Cre-recombinase at any stage of development or during adulthood. *Snap25$^{fl/fl}$* is a transgene with lox-P sites flanking the alternatively spliced exons 5a and 5b of the t-SNARE (target membrane soluble N-ethylmaleimide-sensitive factor attachment protein (SNAP) receptor) gene *Snap25.* Cre-dependent excision of exon 5a/5b leads to a reduced length gene transcript and non-detectable levels of SNAP25 protein, and cessation of $Ca^{2+}$-dependent evoked synaptic vesicle release (Hoerder-Suabedissen et al. 2019). This chronic t-SNARE disruption allows cortex-wide silencing of selected cell types while avoiding a mechanical manipulation of cortex.

*Nomenclature*

Although the primary incentive to use this mouse model was to silence layer 5 pyramidal neurons, we decided to term this mouse 'cortical SNAP25-ablated' instead of 'layer 5

silenced', because both neocortical layer 5 pyramidal neurons and archicortical dentate gyrus granule cells express Cre-recombinase under the *Rbp4* driver and because the SNAP25-ablation is a very specific silencing mechanism and we found it important to avoid confusion with other silencing tools such as optogenetics or chemogenetics. I will use the following abbreviation for the two genotypes used for the *in vivo* recordings: *Rbp4-Cre;Ai14;Snap25*$^{fl/fl}$ mice will be termed 'cKO' to indicate the conditional knockout of SNAP25; Cre-negative littermates (*Ai14;Snap25*$^{fl/fl}$) used as controls will be abbreviated as 'CTR'. The anatomical work validating the Cre-expression under the Rbp4-Cre promotor was performed in heterozygous *Rbp4-Cre;Ai14;Snap25*$^{fl/+}$ mice.

*Neuroanatomical, behavioural and physical features of the cortical Snap25-ablated mice*

Extensive neurodevelopmental work has been performed to characterise the effects of disrupted evoked neurotransmitter release through ablation of SNARE proteins (Verhage et al. 2000; Washbourne et al. 2002; Molnár et al. 2002) and specifically in the *Rbp4-Cre;Ai14;Snap25*$^{fl/fl}$ mouse line (Hoerder-Suabedissen et al. 2019). These studies consistently report that brain development, in particular cortical layering and axonal pathfinding, is unaffected by ablation of SNAP25 (Washbourne et al. 2002; Hoerder-Suabedissen et al. 2019). It was reported in a previous study that most cKO mice develop a hindlimb clasp from around 4-5 months of age and that by 8 months of age, cortical Cre+ cell density is decreased. All of my experiments were therefore conducted in young adult mice to avoid confounding effects of neurodegeneration. In addition, I only used male mice because gender and the oestrus cycle affect sleep. In all of my cohorts spontaneous behaviour appeared indistinguishable between genotypes, but conditional knockout mice have a lower body weight compared to Cre-negative controls (cortical SNAP25-ablated: 21.3±0.6 g, controls: 24.4±0.6 g, $t(18)=2.94$, $p=0.009$, unpaired t-test), as reported previously (Hoerder-Suabedissen et al. 2019).

*Breeding scheme*

Animals were retrieved from the breeder colony upon availability. Breeder pairs consisted of *Rbp4-Cre/+;Ai14/Ai14;Snap25*$^{fl/+}$ females and *Ai14/Ai14;Snap25*$^{fl/fl}$ males. This particular breeding scheme was chosen for two reasons. First, *Rbp4-Cre/+;Ai14/Ai14;Snap25*$^{fl/fl}$ females have a habit of abandoning their pups and develop neurological problems from 4-5 months of age, rendering those animals unsuitable for breeding. Second, Cre becomes deregulated in the male germline of Cre-positive males and can subsequently be unspecifically expressed throughout the brain and body of the pups (personal communication from Dr. Hoerder-Suabedissen, DPAG, University of Oxford). Based on this breeding scheme on average only 1/8 of the animals in each litter were male *Rbp4-Cre;Ai14;Snap25*$^{fl/fl}$. As soon as animals of the desired genotype reached adulthood, they were included in the study and the recording capacities were filled with randomly selected Cre-negative controls from the colony, preferably littermates.

*Age and number of animals*

Electrophysiological, circadian, and anatomical work was performed on different batches of animals. For EEG/EMG experiments and laminar implants I used a total of 12 cKO mice (age at baseline recording 90±5 days) and 8 CTR mice (age at baseline recording 85±4 days). For circadian experiments, I used 10 cKO (age at baseline recording 84±1 days) and 7 CTR mice (age at baseline recording 83±1 days). Anatomical work was performed on 6 *Rbp4-Cre;Ai14;Snap25*$^{fl/+}$ mice (age at perfusion date 57±6 days). No animals were excluded from the study, but only a subset of animals had suitable recordings for specific EEG and laminar analyses. The number of animals used for each individual analysis is stated in the respective figure legend.

### 5.2.2 Sleep recordings in 'cortical SNAP25-ablated mice'

Surgical implantation of EEG/EMG devices and laminar probes in primary motor cortex was performed as described in the general methods chapter (section 2.2). A detailed description of the general procedure for electrophysiological data acquisition, sleep scoring, and data analysis can also be found in the general methods chapter (section 2.3).

The analyses criteria for vigilance state episodes differed slightly from those used in the previous chapter. For analyses of mean and maximum duration of sustained wake episodes in the EEG dataset, I included wake episodes, which were at least 1 min long allowing brief intrusions of sleep of 1 min or less. For the analysis of mean duration of NREM episodes, I included NREM episodes, which were at least 1 min long allowing brief intrusions of REM sleep or brief awakenings of 1 min or less. I allowed interruptions of up to 1 minute because longer time spans of immobility are typically used to define sleep when the measurement is based on behavioural assessment (Brown et al. 2016) and I originally considered analysing the sleep-wake profile over several days based on EMG variance. To investigate the change in NREM sleep SWA across prolonged wake episodes under undisturbed conditions, I used the EEG dataset from the baseline day and included consolidated periods of waking lasting at least 15 min, whereby short episodes of sleep <1 min were not considered as interruptions. I then analysed NREM sleep SWA in the 15-min time window immediately preceding and following prolonged (>15 min) wake episodes, if both time windows included at least 10 min of artefact-free NREM sleep and no more than 3 min of wakefulness. These time criteria were chosen arbitrarily yet they seemed adequate to identify consolidated wake episode preceded and followed by consolidated sleep.

### 5.2.3 Circadian screen in 'cortical SNAP25-ablated'

For the assessment of the circadian characteristics of this mouse model, I performed PIR camera recordings. This dataset was also used to validate the sleep phenotype detected in electrophysiological recordings. For these recordings mice were housed in light-isolated chambers, in which the light-dark cycle can be flexibly set using a timer switch and which fit up to six mouse cages. The mice were individually housed and placed under a passive infrared motion detector that continuously recorded activity in time intervals of 100 ms. Individual readings were pooled into one minute bins for all analyses as it has previously been validated that periods of inactivity of >40 s provide a reliable measure of behaviourally defined sleep (Brown et al. 2016). Initially mice were kept under a stable 12:12 h light:dark cycle for at least 7 days before being released into constant darkness. The circadian period and amplitude were assessed over an interval of 7-10 days in the constant dark condition by chi-square periodogram analysis using ActogramJ (Schmid, Helfrich-Förster, and Yoshii 2011). After at least 10 days in constant darkness, all mice were exposed to a 2-h light pulse provided around Circadian Time (CT) 13.5 h. The resulting phase delay of the circadian rhythm was quantified in all animals by extrapolating the onsets of activity to the day of the light pulse (Albrecht and Foster 2002).

### 5.2.4 Histological work in 'cortical SNAP25-ablated' mice

The position and depth of the laminar probes was assessed as described in the general methods section 2.6. In addition, the Cre expression in different brain regions under the *Rbp4-Cre* driver was assessed using DAPI-histology as described for the laminar probe localisation.

The immunohistochemistry protocol for the identification of hypothalamic neurons expressing orexin (ORX) and melanin-concentrating hormone (MCH) consisted of the following steps: the sections were stained with rabbit anti-MCH antibody (1:2000; H-070-47; Phoenix

Pharmaceuticals) or rabbit anti-Hcrt antibody (1:500, kind gift from Anthony Van den Pol, Yale University). The sections were subsequently incubated in blocking solution (3% or 10% donkey serum [Hcrt or MCH respectively] and 0.3% Triton-X100 in 0.1M PBS) for one hour at room temperature before incubation with the primary antibody in blocking solution at 4°C overnight (MCH) or for 72h (Hcrt). The primary antibody was revealed by incubating with donkey anti-rabbit-AlexaFluor488 (1:500) antibody in blocking solution for two hours at room temperature. Finally, the sections were counterstained with DAPI.

To identify the position and morphology of Cre-expressing neurons, greater microscopy resolution was required than for the localisation of the laminar probe. Therefore, laser scanning confocal microscope images were acquired (Zeiss LSM710) and image stacks created to assess the cellular morphology across the z-plane of the brain section. The cytoplasmic tdTomato expressed from the Ai14 reporter gene allows reliable identification of Cre+ neurons based on native tdTomato fluorescence (Grant, Hoerder-Suabedissen, and Molnár 2016; Hoerder-Suabedissen et al. 2019). The native fluorescence is detectable even in thin neurites and synapses, which can be used to visualise the dendritic and axonal morphology of labelled neurons. While the figures in this chapter present representative sections, the Cre-expression was assessed in six *Rbp4-Cre;Ai14;Snap25*$^{fl/+}$ mice and the results across all animals were similar to those presented in the representative images. The histological work was closely supervised by Dr. Anna Hoerder-Suabedissen and it is stated in the figure legends, which of the raw images were acquired by her.

## 5.3 Results

### 5.3.1 Cre-expression in cortical Snap25-ablated mice

The validation of the previously reported Cre-expression pattern in the Rbp4-Cre driver line was of paramount importance to ensure that the cell-specific disruption of the *Snap25* gene and subsequent removal of the SNAP25 protein was restricted to cortical cells. The Tg(Rbp4-Cre)KL100Gsat (short: Rbp4-Cre) line was created as part of the Gene Expression Nervous System Atlas (GENSAT) project (S. Gong et al. 2007), and is neuroanatomically classified as a layer 5 driver line (Gerfen, Paletzki, and Heintz 2013; J. A. Harris et al. 2014). Expression of Cre-recombinase is driven by gene *Rbp4* encoding the retinol binding protein 4. I first assessed the Cre-expression in primary motor and sensory cortex of an *Rbp4-Cre;Ai14;Snap25*$^{fl/+}$ mouse and confirmed that Cre-expression in neocortex is largely restricted to layer 5 pyramidal neurons (Figure 33).

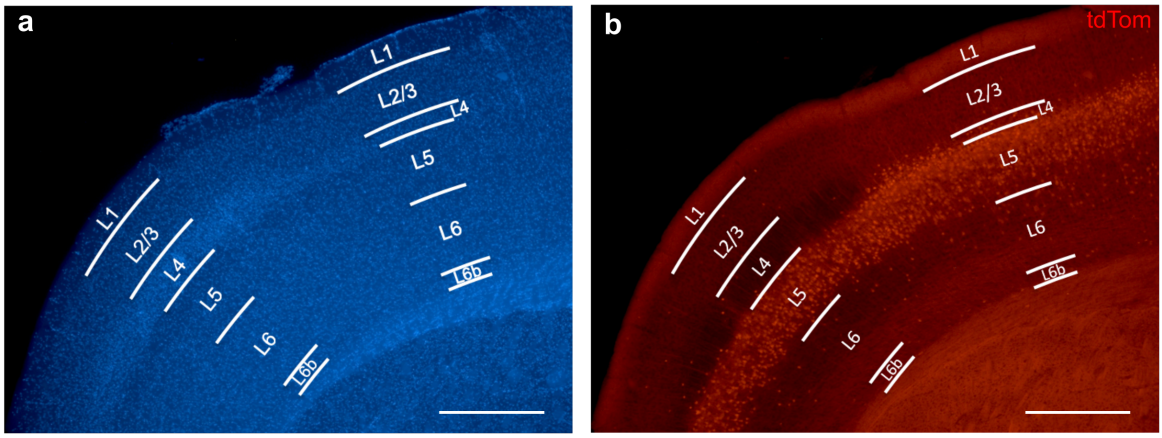



**Figure 33: Identification of cortical layers in a representative coronal brain slice covering primary motor and sensory cortex.**
a) Cortical layers were determined using DAPI staining and identification of characteristic anatomical features of specific layers such as cell density and nuclear size. b) Expression of the red fluorescent protein tdTomato is restricted to layer 5 in both primary motor and sensory cortex. The selective Cre-expression was driven by a Rbp4 promoter that cleaved the STOP-floxed site in the tdTomato reporter Ai14 mouse. Anterior-posterior position: approximately Bregma +0.75 mm. DAPI: 4′,6-diamidino-2-phenylindole. Scale bars: 500 µm.

In subsequent neuroanatomical work lead by Dr. Anna Hoerder-Suabedissen (DPAG, University of Oxford), we then set out to quantify the percentage of layer 5 pyramidal neurons and dentate gyrus granule cells, which are Cre-expressing. In line with previous reports (Beltramo et al. 2013), we found that approximately 21% of layer 5 pyramidal neurons expressed Cre-recombinase as indicated by expression of the red fluorescent reporter tdTomato (Figure 34a,b). Because tdTomato generates a reliable signal both in cell bodies and in dendrites and axons, the morphology of tdTomato+ cells including their extensive dendritic branches in neocortical layer 1 and their long subcortical projections can be seen in epifluorescence and confocal microscopy images (Figure 33, Figure 34a,b). Turning to the hippocampus, the second brain region with relevant Cre-expression in the Rbp4-Cre driver line (Gerfen, Paletzki, and Heintz 2013), we found that approximately 39% of all dentate gyrus granule cells were tdTomato-positive (Figure 34d,e). In contrast, the hypothalamus and especially the ventrolateral preoptic nucleus (VLPO), which is classically considered a sleep promoting centre (Saper, Chou, and Scammell 2001) albeit wake-promoting neurons are intermingled (Szymusiak et al. 1998; Chung et al. 2017), contains only about 1% of very sparse and scattered tdTomato+ neurons (Figure 34c). Interestingly, the suprachiasmatic nucleus of the hypothalamus (SCN), which represents the master clock in the mammalian brain (Ralph et al. 1990; Mistlberger 2005), appeared void of tdTomato+ cells and even fibre tracts. We finally wanted to assess whether the few tdTomato+ neurons in the hypothalamus of our cortical SNAP25-ablated mouse line systematically overlap with the well described set of hypocretin/orexin (ORX) neurons, known to be essential for arousal stability (Adamantidis et al. 2007), or melanin-concentrating hormone (MCH) expressing neurons, which are thought to stabilize REM and NREM sleep (Jego et al. 2013; Konadhode et al. 2013). Confocal laser scanning microscopy following ORX and MCH immunohistochemistry showed no co-expression of tdTomato and either of the two markers (Figure 36). Together, this anatomical

work indicates that the Rpb4-Cre mouse line strongly labels the cortical cell types of interest while ectopic Cre-expression is sparse, and importantly does not overlap with the two major sleep-regulatory cell populations or the circadian control centre in the hypothalamus. Therefore, the cortical SNAP25-ablated mouse appears suitable to test the effects of chronic silencing of neocortical layer 5 pyramidal and archicortical dentate gyrus granule cells on sleep.

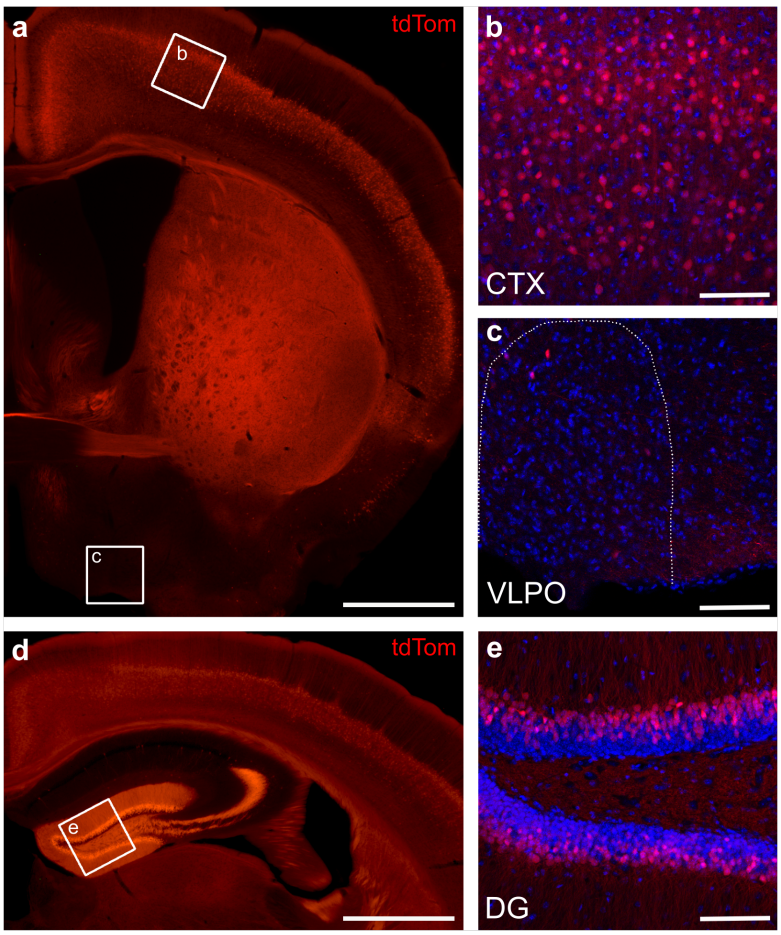



**Figure 34: Comparison of Cre-expression in the Rbp4-Cre mouse line between neocortical layer 5, dentate gyrus and hypothalamus.**

a) Coronal section of an *Rbp4-Cre;Ai14;Snap25*$^{fl/+}$ mouse brain indicating areas, which were further examined for Cre-expression using confocal imaging of DAPI stained slices. b,c) Laser scanning confocal microscope images from neocortex (CTX, b) and ventrolateral preoptic hypothalamus (VLPO, c) of DAPI stained (blue) sections, showing the distribution of tdTomato+ cells in the two regions. The VPLO region is outlined with a white, dotted line. Cell counts on corresponding coronal sections in three brains revealed that 20.53±0.98% (480/2342) of cortical L5 cells were tdTomato+, while only 1.15±0.40% (35/3006) of hypothalamic cells expressed the red fluorescent indicator. d) Coronal section of an *Rbp4-Cre;Ai14;Snap25*$^{fl/+}$ mouse brain indicating the area of the dentate gyrus which was further examined for Cre-expression. e) Laser scanning confocal microscope image of dentate gyrus (DG) in a DAPI stained (blue) section. TdTomato+ cells were quantified in both the top and bottom blades of DG in three images, each from three different brains, and comprise 39.39±3.72% of cells in the granule layer. As evident from the boxed regions in (a,d), the tdTomato+ cells in different brain regions vary in their fluorescence intensity, therefore the images in panels (b,c,e) were acquired with settings optimised to show the tdTomato+ cells in each brain region. CTX: neocortex. DAPI: 4′,6-diamidino-2-phenylindole. DG: dentate gyrus. VLPO: ventrolateral preoptic hypothalamus. Scale bars: 1mm (a,d), 100 µm (b,c,e) Images acquired by Dr. Anna Hoerder-Suabedissen.

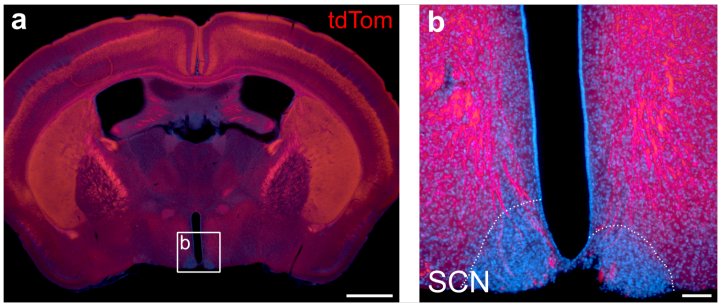



**Figure 35: The suprachiasmatic nucleus of the hypothalamus is void of Cre+ cells and spared of fibre tracts in the Rbp4-Cre mouse line**

a) Epifluorescence image of an *Rbp4-Cre;Ai14;Snap25fl/+* brain section at the level of the suprachiasmatic nucleus (SCN). The section was counterstained with DAPI (blue). Box indicates approximate region from which image in (b) was taken. (b) High-magnification epifluorescence image of the SCN region. Rbp4-Cre;Ai14 axons are shown in red, cell nuclei stained with DAPI in blue. Note that there are no tdTomato+ cells located within the SCN (outlined with white dotted lines), and very few of the dense axon bundles pass through the SCN. DAPI: 4′,6-diamidino-2-phenylindole. SCN: suprachiasmatic nucleus. Scale bars: 1mm (a), 100 µm (b). Images acquired by Dr. Anna Hoerder-Suabedissen.

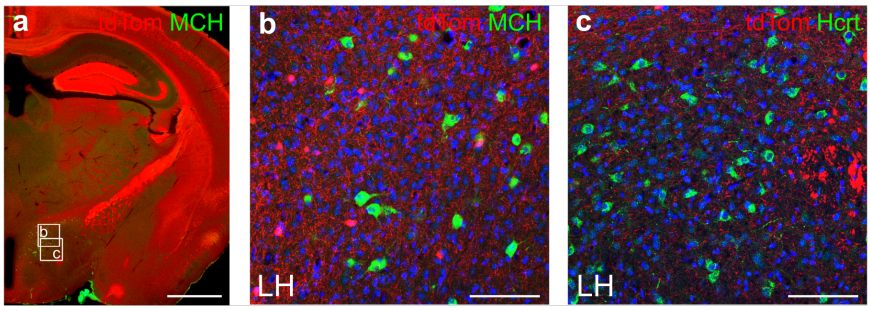



**Figure 36: No overlap between orexin or melanin concentrating hormone-expressing cells with Rbp4-Cre+ cells but dense fibre tracts in lateral hypothalamus**

(a) Epifluorescence image of an *Rbp4-Cre;Ai14;Snap25$^{fl/+}$* brain hemisection at the level of the lateral hypothalamic area (LH), stained for melanin concentrating hormone (MCH) in green. Boxes indicate approximate regions from which images in (b,c) were taken. (b,c) Laser scanning confocal microscope images of two representative sections of LH of the same brain as shown in (a) stained for MCH (b) or orexin/hypocretin (Hcrt; c). Rbp4-Cre;Ai14 cells and processes are shown in red, and nuclei are counterstained with DAPI (blue). Note that no MCH+ cell was tdTom+ (n=3 brains, 692 MCH+ cells), and no Hcrt+ cell was tdTom+ (n=3 brains, 469 Hcrt+ cells). Note the dense fine fibres surrounding cell bodies in LH, consistent with an axonal terminal field in that region. DAPI: 4′,6-diamidino-2-phenylindole. Hcrt: orexin/hypocretin. LH: lateral hypothalamus. MCH: melanin concentrating hormone. tdTom: tdTomato. Scale bars: 1mm (a), 100 µm (b,c). Images acquired by Dr. Anna Hoerder-Suabedissen.

Prompted by a recent report about a terminal field of projections from layer 5 pyramidal neurons in prefrontal cortex (Prasad, Carroll, and Sherman 2020), we made the additional observation that the LH area is enriched in tdTomato-positive axonal projections (Figure 36b,c). While further tracing studies are necessary to identify the exact origin of these fibre tracts, this finding could hint at a potentially relevant projection, most likely from subcortically projecting pyramidal neurons in layer 5b, to a major sleep-control area in the hypothalamus.

### 5.3.2 Neocortical laminar dynamics

To assess whether cortical SNAP25-ablation affects cortical neocortical dynamics during sleep, I first analysed the firing rates in layers 2/3 and 5 and subsequently the neuronal dynamics at OFF-ON transitions during NREM sleep. Analysis of MUA during NREM sleep found no significant genotype difference in the firing rates of layer 2/3 and layer 5 (genotype x layer interaction: $F(1,8) = 0.946$, $p = 0.359$, mixed ANOVA, post-hoc comparisons for the two layers: $p$s > 0.1, see Figure 37a). Furthermore, there was no significant genotype difference in the latency to the first spike in layer 5 at OFF-ON transitions (genotype x count interaction: $F(15,120) = 0.750$, $p = 0.730$, bins 17-20 excluded from ANOVA due to insufficient data in one CTR animal, no significant effect of genotype in any of the 16 spike count bins, $p$s > 0.1, see Figure 37b), in line with previous publications about the silencing mechanism used in this mouse model, which indicate that SNAP25 ablation does not prevent the depolarisation of 'silenced' neurons (Washbourne et al. 2002; Bronk et al. 2007; Marques-Smith et al. 2016). However, the surge of neuronal firing at OFF-ON transitions in layer 5 was significantly reduced and the peak time delayed in cKO mice (genotype x time interaction: $F(29,232) = 4.326$, $p < 0.001$, mixed ANOVA, post-hoc comparisons of Genotype in 10-ms bins: CTR > cKO in the first 10 min, $p = 0.009$; surge time: $F(1,8)=10.081$, $p = 0.013$, one-way ANOVA,

see Figure 37c), which is in line with previous work showing that layer 5 pyramidal neurons provide strong local monosynaptic excitation to one another (Markram et al. 1997; Lefort et al. 2009).

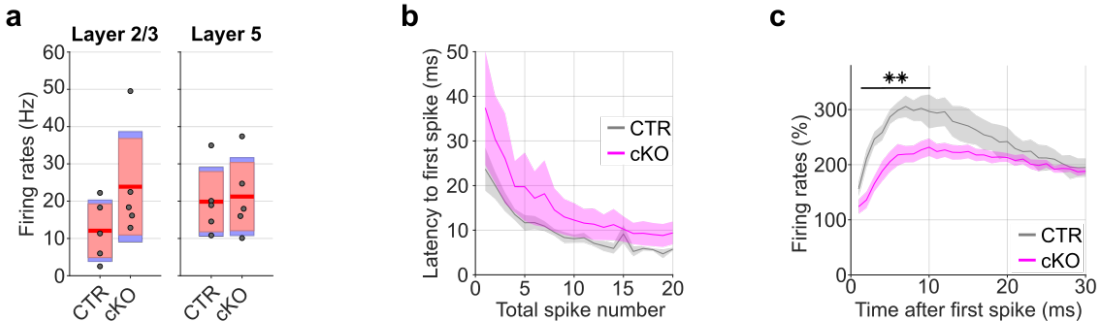



**Figure 37: Laminar firing patterns during NREM sleep in cortical Snap25-ablated mice**

a) Firing rates across neocortical layers 2/3 and 5 of both genotypes during non-rapid eye movement (NREM) sleep. b) Latency to the first spike at OFF-ON transitions in layer 5 of cKO and CTR animals. c) Neuronal activity in layer 5 (L5) at OFF-ON transitions in cKO and CTR animals relative to NREM sleep average. n=5 CTR and n=5 cKO for laminar analysis. Data in panel a represent grouped data including group mean (red line), 95% confidence interval (pink box), and one standard deviation (blue box) with individual data points overlaid. Data in panels b and c are presented as mean ± SEM (shaded areas). cKO: conditional knockout animals. CTR: control animals. NREM: Non-rapid eye movement sleep. Scale bar histology image 500µm.

Having confirmed the assumptions about laminar dynamics in the cortical SNAP25-ablated mouse model, I addressed the question whether LFP slow waves or slow wave activity were altered in a layer-specific fashion. I found a significant interaction effects between genotype and cortical layer for both slow wave amplitudes ($F(1,8)=95.17$, $p<0.001$, mixed ANOVA) and SWA ($F(1,8)=114.82$, $p<0.001$, mixed ANOVA). The amplitude of LFP slow waves in layer 5 was decreased ($t(8)=3.70$, $p=0.006$, $d=2.34$, paired t-test) and the levels of slow wave activity were reduced ($t(8)=2.87$, $p=0.021$, $d=1.81$, paired t-test). The opposite pattern was observed in layer 2/3, where a trend towards increased slow wave amplitudes ($t(8)=-2.21$, $p=0.058$, $d=-1.40$, paired t-test) and elevated slow wave activity ($t(8)=3.07$, $p=0.15$, $d=-1.94$, paired t-test) was observed (Figure 38). The differential regulation of layer 5 and 2/3 slow waves in cortical

SNAP25-ablated mice results in a significantly reduced ratio of slow wave amplitudes ($F(1,8) = 10.84$, $p = 0.011$, one-way ANOVA) and SWA in cortical SNAP25-ablated mice ($F(1,8) = 53.68$, $p < 0.001$, one-way ANOVA, see inlays on Figure 38). These layer-specific changes to intracortical dynamics are consistent with a reduction of local monosynaptic excitation between layer 5 pyramidal neurons (Lefort et al. 2009) and diminished disynaptic inhibition of layer 2/3 pyramidal neurons (Vecchia et al. 2020).

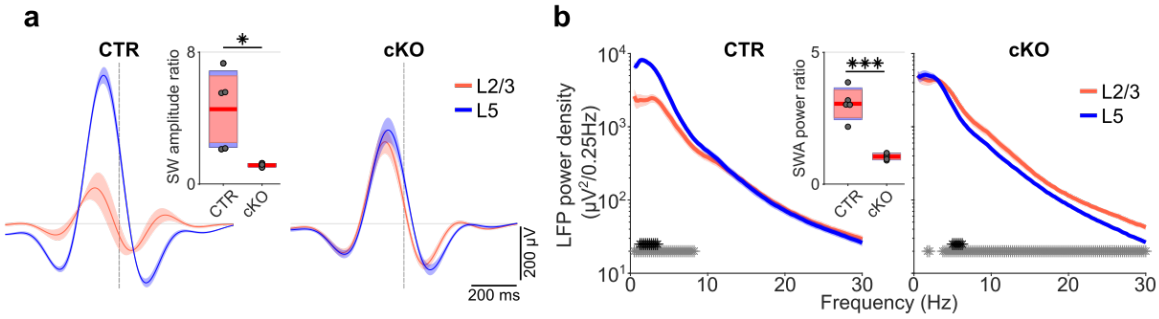



**Figure 38: Laminar profile of LFP slow waves and LFP power spectra during NREM sleep in cortical Snap25-ablated mice**

a) Average LFP slow wave in layers 2/3 (L2/3) and 5 aligned to the OFF-ON transition (vertical dashed line) in cKO and CTR mice. Inset: slow wave (SW) amplitude ratio between L2/3 and L5. b) LFP spectra of L2/3 and L5 of cKO and CTR mice during NREM sleep. Asterisks indicate frequency bins with significant differences in post-hoc comparison before (grey) and after (black) Bonferroni adjustment of α. Inset: slow wave activity (SWA) ratio between L2/3 and L5. n=5 CTR and n=5 cKO for laminar analysis. Black asterisks on insets indicate post-hoc contrasts with significant differences (*$p < 0.05$, **$p < 0.01$, ***$p < 0.001$). Data on panels a and b are presented as mean ± SEM (shaded areas). Insets in panels represent grouped data including group mean (red line), 95% confidence interval (pink box), and one standard deviation (blue box) with individual data points overlaid. cKO: conditional knockout animals. CTR: control animals. L2/3, L5: Neocortical layers 2/3, 5. LFP: local field potentials.

### 5.3.3 Sleep in cortical SNAP25-ablated mice

To probe whether cortical SNAP25-ablation merely alters local neocortical dynamics during NREM sleep or also affects vigilance state regulation and the EEG patterns, I next assessed the sleep-wake profile and EEG spectra in cortical SNAP25-ablated mice. Cortical SNAP25-ablated mice presented increased wakefulness and reduced NREM sleep (genotype x vigilance

state interaction: Greenhouse-Geisser $F(1.056,13.732) = 33.008$, $p < 0.001$, mixed ANOVA, see Figure 39a,b). The sleep phenotype was more pronounced during the dark period (Figure 39a,c), when also REM sleep was significantly reduced (Figure 40). The increase in the amount of wakefulness in cKO mice was on average approximately three hours per day (cKO: 13.83±0.39 h, CTR: 10.57±0.42 h, $t(13)=5.55$, $p<0.001$, $d=2.96$, t-test for independent samples) and all individual cKO mice included in this experiment spent more time awake compared to all individual CTR mice, underscoring the robustness of the sleep phenotype.

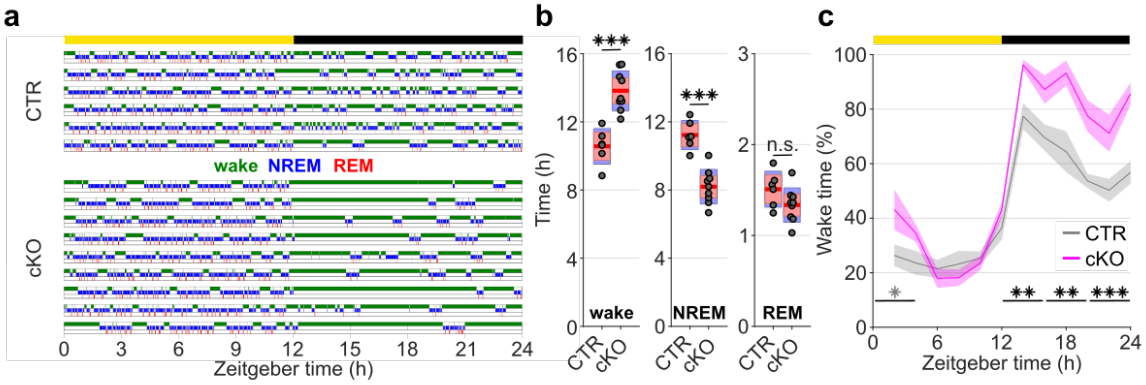



**Figure 39: Sleep profile of cortical SNAP25-ablated mice**

a) Hypnograms from all individual Cre-negative control (CTR) and cortical SNAP25-ablated (cKO) animals under undisturbed baseline conditions. Note the increased amount of wakefulness and long wake episodes in cKOs. Vigilance states are colour coded: wake=green, NREM=blue, REM=red. c) Time spent in vigilance states (wake, NREM, and REM) during 24h baseline recordings. d) Time course of wakefulness over 24h baseline recordings, showing that the differences between genotypes mostly occur during the dark period (ZT12-24). Number of animals: n=6 CTR and n=9 cKO for vigilance state analysis. Black asterisks indicate post-hoc contrasts with significant differences (*P < 0.05, **P < 0.01, ***P < 0.001), grey asterisk indicates post-hoc comparison with P < 0.05, which does not reach significance after Bonferroni correction for multiple comparisons. Yellow and black bars above panels a, c indicate light and dark periods, respectively. Panels b represents grouped data including group mean (red line), 95% confidence interval (pink box), and one standard deviation (blue box) with individual data points overlaid. cKO: conditional knockout animals. CTR: control animals. NREM: non-rapid eye movement sleep. REM: rapid eye movement sleep.

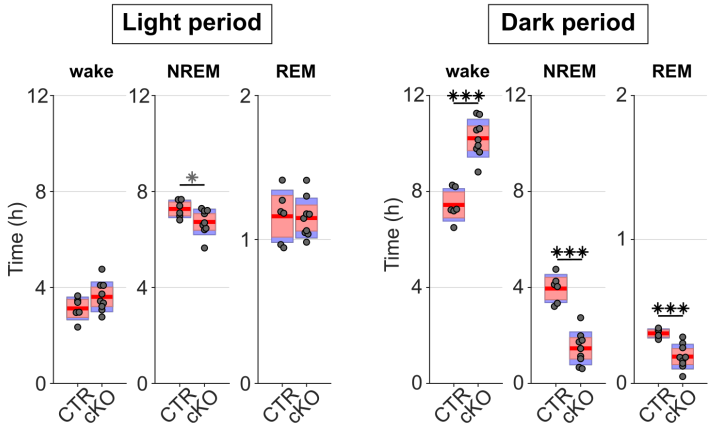



**Figure 40: Genotype differences in the amount of time spent in wake, NREM, and REM sleep during undisturbed baseline recordings are more pronounced in the dark period.**

During the light period, the distribution between vigilance states is similar between genotypes with only a trend towards increased wakefulness and reduced NREM and REM sleep, while strong differences occur during the dark period. Black asterisks indicate post-hoc contrasts with significant differences (*p < 0.05, **p < 0.01, ***p < 0.001), grey asterisks indicate post-hoc comparisons with P < 0.05, which do not reach significance after Bonferroni correction for multiple comparisons. Data is presented as group mean (red line), 95% confidence interval (pink box), and one standard deviation (blue box) with individual data points overlaid. Number of animals: n=6 CTR and n=9 cKO for vigilance state analysis. cKO: conditional knockout animals. CTR: control animals. NREM: Non-rapid eye movement sleep. REM: Rapid eye movement sleep.

Next, I compared the EEG spectra during wakefulness and NREM sleep in undisturbed 24-h baseline recordings between the two genotypes. There were no significant genotype difference in either of the two, frontal and occipital, EEG derivations (Figure 41a,b). I also assessed the wake spectrogram separately for the dark period, when mice are mostly wake, and the light period, when mice are mostly asleep, and found no significant differences either. However, there was a significant leftwards shift of the theta peak in the EEG spectra of both EEG derivations during REM sleep (main effect of genotype: $F(1,11) = 33.532$, $p < 0.001$, mixed ANOVA, see Figure 42). The absence of genotype differences in the NREM spectra show that the differential regulation of LFP SWA during NREM sleep in layers 2/3 and 5 do not result in an overall effect on EEG SWA during NREM sleep.

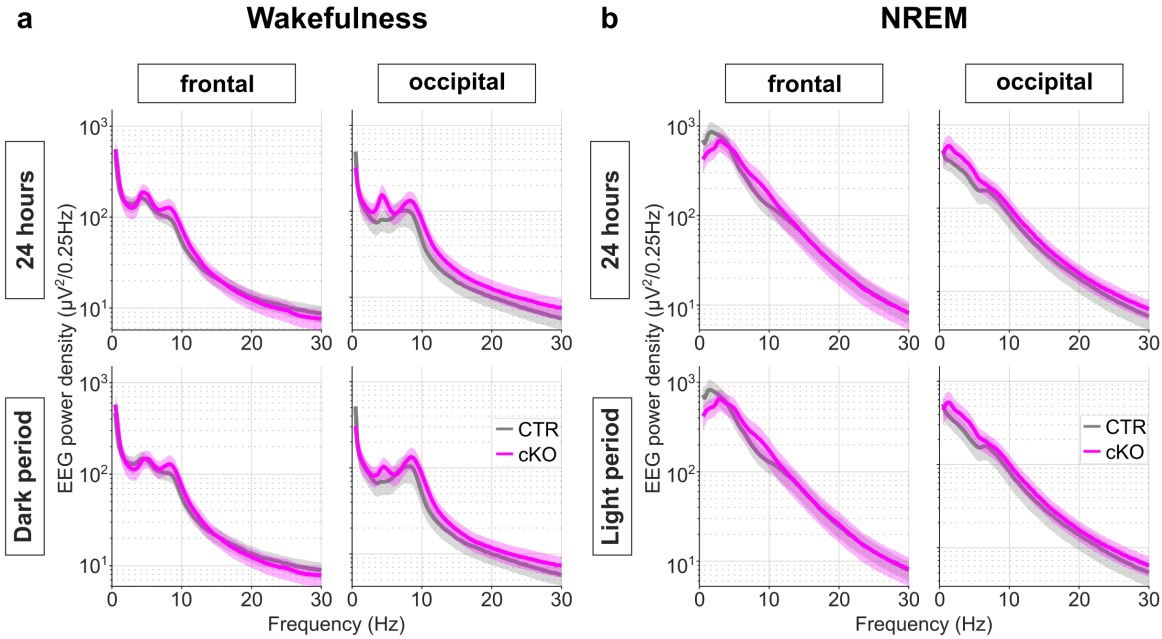



**Figure 41: EEG power spectra from the frontal and occipital derivations during waking and NREM sleep at baseline show no differences between genotypes.**

a) Wake EEG power spectra over 24h and during the dark period, when mice are mostly awake. b) NREM EEG power spectra over 24h and during the light period, when mice are mostly asleep. No significant genotype differences in either derivation or condition were found. Number of animals: n=5 CTR and n=8 cKO for EEG spectral analysis. Statistical methods and results provided in Suppl. Table 1. cKO: conditional knockout animals. CTR: control animals. EEG: Electroencephalogram. NREM: Non-rapid eye movement sleep.

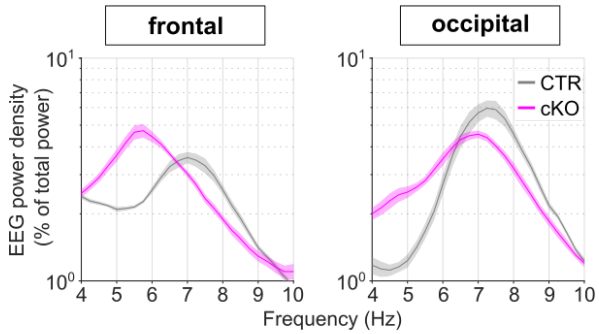



**Figure 42: The EEG theta peak during REM sleep is shifted towards lower frequencies in cortical SNAP25-ablated mice.**

EEG spectral power in the frequency range between 4 and 10 Hz normalised to the mean spectral power over the entire EEG spectrum (0.5 – 30 Hz) during REM sleep on the baseline day. Note that the peak of theta activity is shifted towards lower frequencies in cKOs compared to CTRs in both the frontal and occipital EEG derivations. Number of animals: n=5 CTR and n=8 cKO for EEG spectral analysis. Statistical methods and results provided in Suppl. Table 1. cKO: conditional knockout animals. CTR: control animals. EEG: Electroencephalogram. REM: Rapid eye movement sleep.

However, the NREM sleep spectrogram is strongly influenced by sleep-wake history and typically the level of EEG SWA during NREM sleep increases proportionally to the duration of preceding wakefulness. This makes NREM SWA the gold standard readout of sleep homeostasis (Achermann et al. 1993; Dijk, Beersma, and Daan 1987). I observed that even after extended wake episodes, which are characteristic for cKO mice (Figure 39a, Figure 43b), SWA during subsequent NREM sleep was only moderately elevated compared to the SWA levels prior to the respective wake episodes (Figure 43a). Therefore, I addressed the relationship between the change in NREM sleep SWA and the duration of spontaneous wake episodes. Both genotypes showed, as expected, a positive correlation whereby longer spontaneous wake episodes were followed by proportionally higher levels of SWA during NREM sleep. However, compared to CTR mice, cKO mice presented a smaller increase of SWA relative to the duration of wake episodes (main effect of genotype on SWA ratio, $F(1,57.37) = 6.44$, $p = 0.014$, general liner model, Figure 43), indicating that the relationship between sleep-wake history and the levels of SWA might be altered in cortical SNAP25-ablated animals.

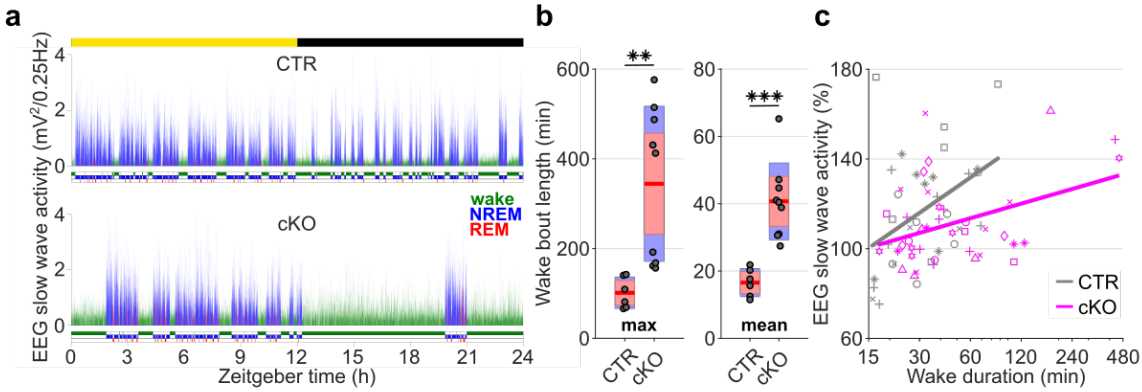



**Figure 43: Sleep architectural and electrophysiological measures during baseline recordings indicate reduced homeostatic sleep drive**

a) Hypnogram and EEG slow wave activity (0.5- 4.0Hz, 4s epochs) of one representative animal from each genotype in undisturbed 24h baseline recordings. Vigilance states colour coded: wake=green, NREM=blue, REM=red. b) Maximum and mean duration of all spontaneous wake episodes over the 2-day recording period, excluding the 6 h sleep deprivation. f) Relationship between wake duration and relative SWA in the frontal EEG derivation during NREM epochs on baseline day. Individual animals are represented with different symbols. Number of animals: n=6 CTR and n=9 cKO for vigilance state analysis (panel b), n=5 CTR and n=8 cKO for EEG spectral analysis (panel c). Black asterisks indicate post-hoc contrasts with significant differences (*P < 0.05, **P < 0.01, ***P < 0.001). Yellow and black bars above panel a indicate light and dark periods, respectively. Panels b represents grouped data including group mean (red line), 95% confidence interval (pink box), and one standard deviation (blue box) with individual data points overlaid. cKO: conditional knockout animals. CTR: control animals. EEG: electroencephalogram. NREM: non-rapid eye movement sleep. REM: rapid eye movement sleep.

### 5.3.4 Response to sleep deprivation in cortical SNAP25-ablated mice

To assess the homeostatic regulation of sleep, I performed six hours of sleep deprivation at light onset. Both genotypes showed a marked elevation of EEG SWA during subsequent NREM sleep. However, the level of SWA in the frontal derivation, which is conventionally used to quantify ‘sleep intensity’, was significantly lower in cKO compared to CTR mice (genotype x time interaction $F(11,121) = 7.561$, $p < 0.001$, mixed ANOVA; relative SWA for the first 30 min after sleep deprivation, cKO: 136.77±3.98 %, CTR: 180.57±5.13 %, $t(11)=6.78$, p<0.001, d=-3.87, t-test for independent samples, Figure 44). Spectral analysis confirmed that the diminished increase in SWA was restricted to the slow frequency range (Figure 44c), as expected (Borbély et al. 1981; Borbély, Tobler, and Hanagasioglu 1984).

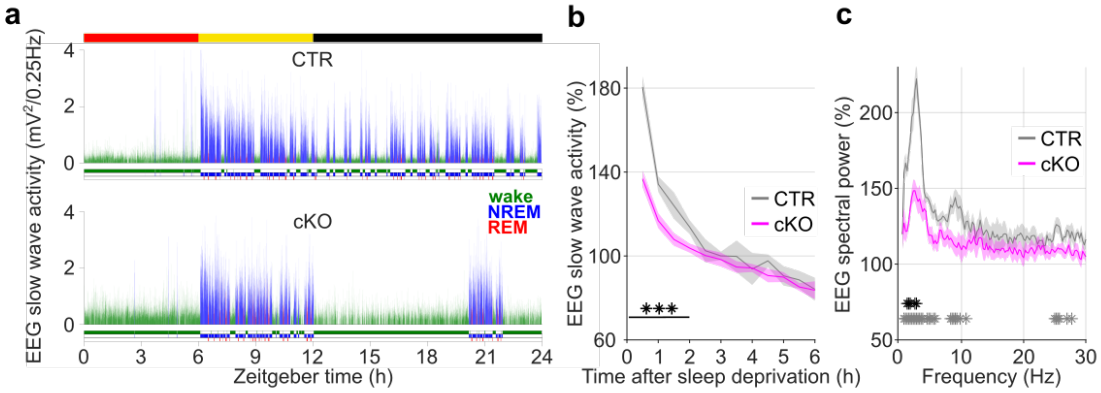



**Figure 44: Diminished electrophysiological response to sleep deprivation in cortical SNAP25-ablated mice**

Homeostatic response to 6h sleep deprivation at light onset based on EEG spectral analysis. a) Hypnogram and EEG slow wave activity (0.5- 4.0Hz, 4s epochs) of one representative animal from each genotype in 24h recordings with 6h sleep deprivation (red, yellow and black bars indicate sleep deprivation, light and dark periods, respectively). b) Time course of frontal EEG slow wave activity during NREM sleep after sleep deprivation relative to baseline average. Note that during the first 2 hours after sleep deprivation cortical Snap25-ablated (cKO) animals show lower levels of SWA compared to Cre-negative controls (CTR). c) Spectral power in the frontal EEG of NREM sleep during the first 30 minutes after sleep deprivation relative to baseline NREM average. Individual asterisks indicate frequency bins with significant differences in post-hoc comparison before (grey) and after (black) Bonferroni adjustment of α. Number of animals: n=5 CTR and n=8 cKO for EEG spectral analysis (panel b,c). Black asterisks indicate post-hoc contrasts with significant differences (*p < 0.05, **p < 0.01, ***p < 0.001). cKO: conditional knockout animals. CTR: control animals. EEG: electroencephalogram. NREM: Non-rapid eye movement sleep. REM: rapid eye movement sleep. SWA: Slow wave activity (0.5- 4.0Hz).

The deficit in the elevation of SWA after sleep deprivation was also found in layers 2/3 and 5 of the LFP recordings from primary motor cortex (genotype x time interactions: $F(2,16) = 8.699$, $p = 0.003$ for layer 2/3 and $F(2,16) = 9.022$, $p = 0.002$ for layer 5, mixed ANOVAS, Figure 45a). However, in line with the notion of a frontal predominance of the homeostatic response to sleep deprivation (Huber, Deboer, and Tobler 2000b), the elevation of slow wave activity in the occipital derivation of CTR mice was comparably smaller than in the frontal derivation and there were no genotype differences (genotype x time interaction for occipital derivation: Greenhouse-Geisser $F(1.234,13.574) = 0.078$, $p = 0.835$).

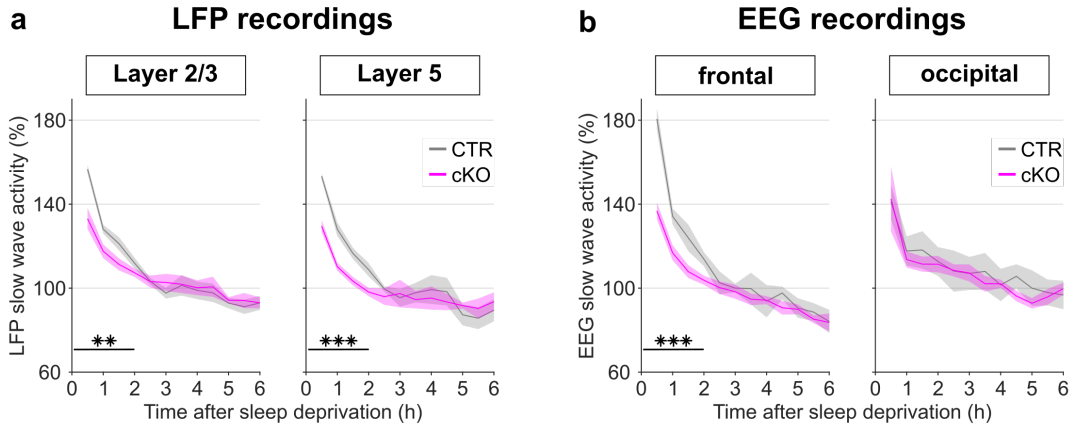



**Figure 45: Laminar and regional aspects of sleep homeostasis**

Time course of NREM slow wave activity (SWA) after sleep deprivation (a) in the LFPs from layers 2/3 and 5 in primary motor cortex and (b) in the frontal and occipital EEG derivation. Note that cortical SNAP25-ablated animals (cKO) compared to controls (CTR) show a lower level of initial slow wave activity after sleep deprivation in the frontal cortex in the EEG and in LFPs from different cortical depths but not in the occipital EEG. Black asterisks indicate post-hoc contrasts with significant differences (*$p < 0.05$, **$p < 0.01$, ***$p < 0.001$). Number of animals: n=5 CTR and n=5 cKO for laminar analysis, n=5 CTR and n=8 cKO for EEG spectral analysis. cKO: conditional knockout animals. CTR: control animals.

The genotype differences in ‘sleep intensity’ as measured by of frontal EEG SWA during NREM sleep, raises the question whether other metrics of sleep homeostasis such as ‘wake intensity’ or sleep duration also differ between genotypes. Interestingly, the typically observed elevation of EEG theta activity in the wake spectrogram during sleep deprivation was nearly abolished in cKO mice resulting in significant genotype differences (Figure 46).

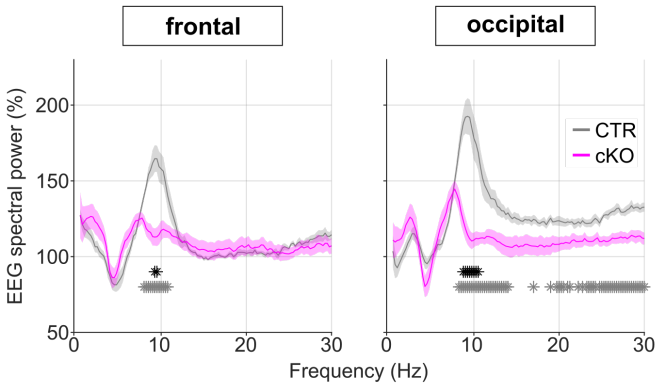



**Figure 46: Relative EEG power spectra during sleep deprivation show attenuation of theta increase in cortical SNAP25-ablated animals.**

Wake EEG spectral power during the 6-hour sleep deprivation shown as a frequency bin-wise percentage of 24h baseline values. Note that the expected increase in the theta-power during sleep deprivation, which is visible in CTR mice, is severely diminished in cKOs. Individual asterisks indicate spectral bins with significant differences in post-hoc comparison before (grey) and after (black) Bonferroni adjustment of α. Number of animals: n=5 CTR and n=8 cKO for EEG spectral analysis. cKO: conditional knockout animals. CTR: control animals. EEG: electroencephalogram.

Sleep deprivation affected sleep architecture in both genotypes (Figure 47). Despite the sleep deprivation procedure, cKO mice typically still engaged in the long wake episodes during the dark period as observed during baseline conditions (Figure 44a) and spent more time awake compared to CTRs (Figure 47a,b). However, the relative increase in NREM sleep time during the light and dark period following sleep deprivation and the duration of individual NREM sleep episodes compared to their own baseline values was not significantly different between genotypes (Figure 47c,d).

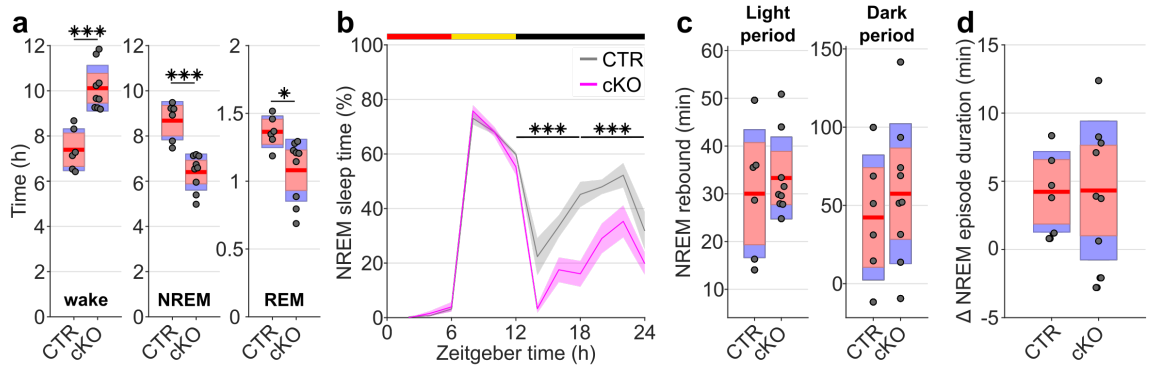



**Figure 47: Sleep amount and architecture following sleep deprivation between ZT 0-6**

a) Time spent in vigilance states (wake, NREM, and REM) during the 18 h recovery time following sleep deprivation. Note that overall cortical SNAP25-ablated animals (cKO) spent more time awake and less time in NREM and REM sleep compared to controls (CTR). b) Time course of NREM sleep on a sleep deprivation day compared between genotypes. Note that cKOs and CTRs do not differ in the time spent in NREM sleep during sleep deprivation (red bar above graph) or during the subsequent 6-h interval, but cKOs sleep less during the entire 12 h dark period following sleep deprivation. c) Rebound of NREM sleep time following sleep deprivation relative to individual baseline values. Note that both genotypes show a modest increase in the amount of NREM sleep relative to baseline after sleep deprivation during both the light and dark period with no differences between genotypes. d) Change in duration of NREM episodes during the first hour after sleep deprivation (ZT6-7 of SD day) relative to the same time window on BL day. Note that there is no difference in the initial increase of NREM episode duration between genotypes. Black asterisks indicate post-hoc contrasts with significant differences (*p < 0.05, **p < 0.01, ***p < 0.001). Data in panels a,c,d is presented as group mean (red line), 95% confidence interval (pink box), and one standard deviation (blue box) with individual data points overlaid. Number of animals: n=6 CTR and n=9 cKO for vigilance state analysis. BL: baseline. cKO: conditional knockout animals. CTR: control animals. NREM: Non-rapid eye movement sleep. REM: Rapid eye movement sleep. SD: sleep deprivation. ZT: zeitgeber time.

### 5.3.5 Circadian assessment of cortical SNAP25-ablated mice

Not only the homeostatic process, but also the the circadian clock is essential for the regulation of sleep (Borbély 1982), as discussed in more detail in the introduction (subchapter 1.4: Circadian and homeostatic regulation of sleep). Following a thorough analysis of the homeostatic process, I performed a comprehensive circadian screen in a new batch of cortical SNAP25-ablated mice. While it has been established that the suprachiasmatic nucleus of the hypothalamus represents the master clock in the mammalian brain (Ralph et al. 1990; Dibner,

Schibler, and Albrecht 2010; Morin 2013), the two processes dynamically influence each other (Deboer et al. 2003; Borbély et al. 2016; Deboer 2018).

For the circadian analysis, I recorded locomotor activity patterns using a PIR activity monitoring system as described in the general methods section. As illustrated in the representative actograms in Figure 48, mice were initially housed and recorded in a 12:12h light:dark cycle followed by release in constant darkness to measure free running circadian period. Subsequently, these same mice received a phase-delaying 2h light pulse in their early subjective night (Circadian Time ~13.5). With this approach I could acquire a range of established measures that have been widely used in characterizing the circadian phenotype of rodent models (Albrecht and Foster 2002; Jud et al. 2005; Brown et al. 2019).

To comprehensively characterise circadian regulation in our cortical SNAP25-ablated mouse model, I looked at the following parameters:

(1) Endogenous circadian free-running period

(2) Periodogram power

(3) Phase shift in response to a delaying light pulse

(4) Light phase activity under 12:12h light:dark conditions

(5) Amount and time course of wakefulness in constant darkness

In addition, this sleep screen based on locomotor activity allowed me to validate some key features of the sleep phenotype detected in the EEG study.

Visual inspection of individual actograms revealed that both genotypes are entrained to the ‘normal’ phase of the LD cycle, start free running in constant darkness, and respond with a

phase delay to a light pulse during their early active phase (see representative actograms in Figure 48a).

Chi-Square periodogram analysis of activity in constant darkness showed no difference in the mean free running period (cortical SNAP25-ablated: 23.86±0.04 h, controls: 23.80±0.07 h, $F(1,15)=0.695$, $p=0.42$, $d=0.39$, one-way ANOVA), the measure of the length of the intrinsic circadian cycle, which was slightly shorter than 24 hours in both genotypes as typically observed in wild type mice (Jud et al. 2005) (Figure 48b). Furthermore, there was no difference in the periodogram power ($F(1,15) = 0.304$, $p = 0.59$, one-way ANOVA), indicating the strength of the intrinsic circadian rhythm (Figure 48b). Comparable results were obtained using the Lomb-Scargle method (Schmid, Helfrich-Förster, and Yoshii 2011). A light pulse during the early activity phase (early subjective night) in the constant dark condition induces a delay the activity onset on subsequent days (Comas et al. 2006). I performed a 2-h light exposure centred over the time point CT13.5 across animals in the constant dark condition. This light pulse resulted in a phase delay with no indication for a difference between genotypes ($F(1,15) = 0.399$, $p = 0.54$, one-way ANOVA, see representative examples in Figure 48a and group data in Figure 48b).

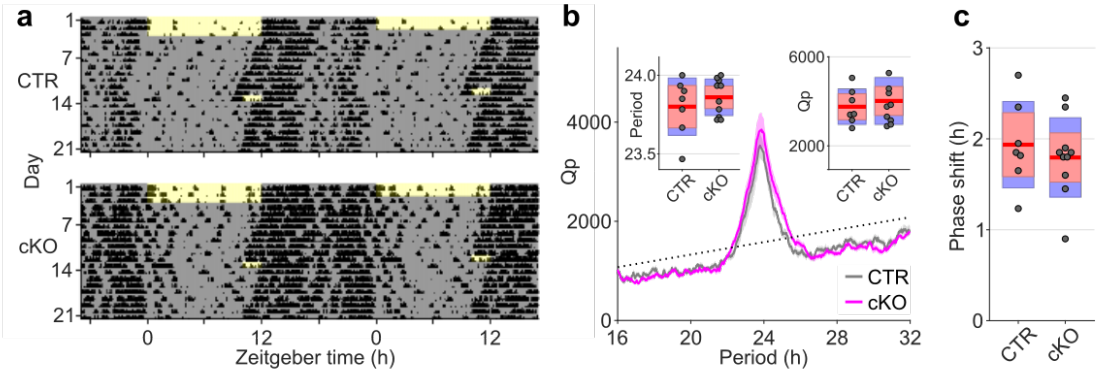



**Figure 48: Circadian characterisation of cortical SNAP25-ablated mice**

Circadian phenotyping based on passive infrared recordings (PIR). a) Representative actograms of one CTR and one cKO mouse. Day 1-3: 12:12h LD cycle. From day 4: constant darkness protocol. Day 13: a phase-delaying 2h light pulse is provided. b) Average Chi-square periodogram. Insets: period (h) and periodogram power (Qp). c) Phase shift in activity onset on the day after the light pulse. No significant differences were observed in any of the assessed circadian characteristics. Number of animals: n=7 CTR and n=10 cKO for PIR analysis. Panels b and c represent grouped data including group mean (red line), 95% confidence interval (pink box), and one standard deviation (blue box) with individual data points overlaid. cKO: conditional knockout animals. CTR: control animals. LD: light:dark. PIR: passive infrared recordings.

The PIR recordings fully replicated the genotype differences in the amounts of sleep and wakefulness under 12:12h LD condition observed in the cohort of mice, which had been recorded with EEG (Figure 49). The behaviourally-defined wake time in the PIR system over 24 hours differed between genotypes by nearly three hours (controls: 9.10±0.51 h; SNAP25-ablated: 11.79±0.29 h, $t(15)=-4.957$, $p<0.001$, $d=-2.35$, t-test for independent samples) replicating the strong genotype differences observed in the EEG-recorded cohort. It should be noted that the absolute wake time measured by the PIR system was slightly lower for both genotypes (14% in CTR, 15% in cKOs) compared to the wake time reported in the EEG recordings because episodes of resting wakefulness of 1 minute or longer are inevitably misclassified as sleep. Further confirming the sleep-wake profile previously revealed by EEG, the difference in the amount of wakefulness and sleep between genotypes was present both in the light and in the dark period under LD conditions, but again more pronounced in the dark period (Figure 49a,b). Light Phase Activity did not differ between genotypes, indicating that

there is no evidence for an altered distribution of activity between the light and the dark period (Figure 49c).

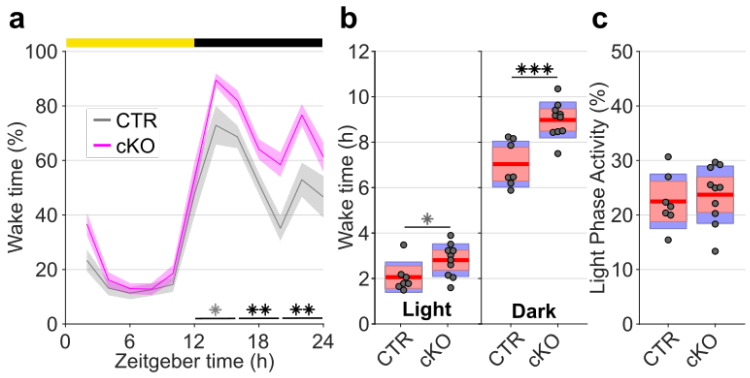



**Figure 49: Sleep assessment of cortical SNAP25-ablated mice based on PIR recordings replicates sleep phenotype detected in EEG recordings**

a) Time course of wakefulness averaged over the last 3 days of PIR recordings under 12:12 light-dark (LD) conditions. b) Estimated wake time during the light and dark period. Note that the time course of wakefulness based on PIR data closely resembles the time course of wakefulness based on electroencephalogram (EEG) recordings in a separate batch of animals. As previously observed, the absolute differences in wake time between genotypes are more pronounced during the dark phase. c) Light Phase Activity (percentage of total wake time spent during the light phase) for both genotypes. Note that there's no indication for a genotype difference in the relative distribution of wake time over the light and dark phase. Black asterisks indicate post-hoc contrasts with significant differences (*$p < 0.05$, **$p < 0.01$, ***$p < 0.001$), grey asterisks indicate post-hoc comparisons with $P < 0.05$, which do not reach significance after Bonferroni correction for multiple comparisons. Data in panels b and c is presented as group mean (red line), 95% confidence interval (pink box), and one standard deviation (blue box) with individual data points overlaid. Number of animals: n=7 CTR and n=10 for PIR recordings. cKO: conditional knockout animals. CTR: control animals. LD: light:dark. PIR: passive infrared recordings.

The sleep phenotype of the cortical SNAP25-ablated mice persisted in constant darkness (Figure 50), with a genotype difference in the amount of wakefulness of approximately three hours. There was also no indication that the constant dark condition would affect the distribution of wakefulness over the 24h day (Figure 50a).

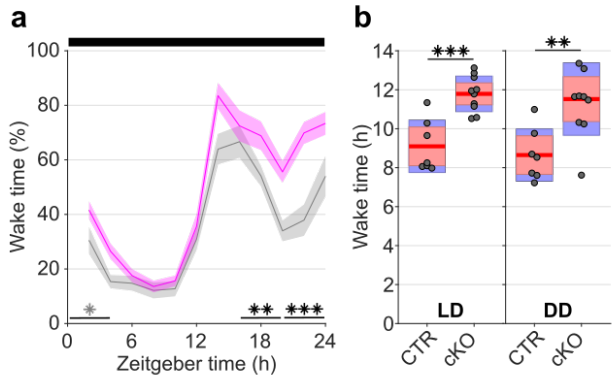



**Figure 50: Sleep-wake profile of cortical SNAP25-ablated mice remains stable in constant darkness**

a) Time course of wakefulness averaged over the first 3 days of PIR recordings in constant darkness (DD). b) Wake time estimates averaged over the last 3 days of PIR recordings under 12:12 light-dark (LD) conditions and over the first 3 days of constant darkness (DD). Note that the PIR data replicates the genotype differences in wake amount observed in the EEG study and that the genotype differences in the daily amount of wakefulness persist in the absence of light. Black asterisks indicate post-hoc contrasts with significant differences (*p < 0.05, **p < 0.01, ***p < 0.001), grey asterisks indicate post-hoc comparisons with P < 0.05, which do not reach significance after Bonferroni correction for multiple comparisons. Data in panel b is presented as group mean (red line), 95% confidence interval (pink box), and one standard deviation (blue box) with individual data points overlaid. Number of animals: n=7 CTR and n=10 for PIR recordings. cKO: conditional knockout animals. CTR: control animals. DD: constant darkness. LD: light-dark conditions. PIR: passive infrared recordings.

Finally, I wanted to use the PIR system to clarify the ambiguous results from the EEG study whether the two genotypes differ in their amount of sleep after sleep deprivation. This question could not be resolved from the EEG data alone, because sleep deprivation had been performed during the first half of the light period, which meant that many of the cKO mice had already been spontaneously awake when sleep deprivation started (Figure 51a). Sleep deprivation at this time point did not prevent the cKO animals from spending a significantly larger part of the recovery time awake compared to controls (Figure 47a,b). However, it had not resulted in significant genotype difference in the relative increase of NREM sleep time or NREM episode duration (Figure 47c,d) nor in the relative sleep amount on the sleep deprivation day compared to baseline day (Figure 51a). To assess whether a difference in the relative amount of rebound

sleep could be revealed at a different circadian time point, I performed sleep deprivation in the PIR system between zeitgeber time (ZT) 6-12. Because animals from both genotypes are typically asleep during the first hours of the light period (ZT 0-6), this shift of the sleep deprivation time window ensured that the effective wake duration as a result of sleep deprivation was close to 360 minutes (6 hours) and very similar between genotypes. Interestingly, as a result the relative amount of sleep for the 24h period starting with the onset of sleep deprivation was significantly reduced in cKO mice (Figure 51b).

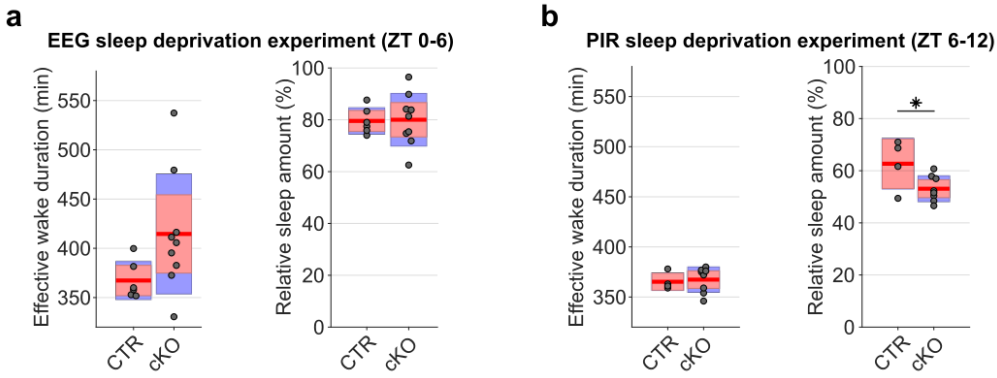



**Figure 51: The effects of sleep deprivation on sleep amount depend on circadian timing**

a) Electroencephalography (EEG) experiment with sleep deprivation at zeitgeber time (ZT) 0-6: effective wake duration (wake time during sleep deprivation plus wake bound duration preceding sleep deprivation) before termination of the sleep deprivation at ZT6 (left panel) and relative sleep amount for the 24-h interval starting with the onset of sleep deprivation (i.e. sleep deprivation day) relative to the preceding 24-h interval (i.e. baseline day). Note that many of the conditional knockout (cKO) mice had been awake when sleep deprivation started and the relative amount of sleep following sleep deprivation does not differ between genotypes. b) Passive infrared recording (PIR) experiment with sleep deprivation at zeitgeber time (ZT) 6-12: Note that sleep deprivation during the second half of the light period (ZT6-12) results in a significant difference in the amount of sleep in the 24-h interval starting at the beginning of sleep deprivation compared to the preceding 24-h interval, which could not be observed in the EEG experiment when sleep deprivation was performed during the first half of the light period (ZT 0-6). cKO: conditional knockout animals. CTR: control animals. EEG: electroencephalogram. PIR: passive infrared recordings. ZT: zeitgeber time.

## 5.4 Discussion

### 5.4.1 Summary of results

In this chapter, I presented neuroanatomical work, laminar recordings from primary motor cortex, EEG-based sleep analysis, and PIR-based circadian phenotyping of the cortical SNAP25-ablated mouse model.

The neuroanatomical work confirmed the previously described Cre-expression pattern in the Rbp4-Cre driver line used to generate cortical SNAP25-ablated mice. Epifluorescence and laser scanning confocal imaging validated the transgene expression in neocortical layer 5 and archicortical dentate gyrus granule cells. The histological assessment of established sleep-control centres in hypothalamus demonstrated the sparseness of tdTomato+ cells in the lateral hypothalamus (~1%) and showed that the few and scattered tdTomato+ cells in this region do no overlap with sleep-regulatory MCH+ or orexin+ cell populations. Interestingly, the lateral hypothalamus was enriched in tdTomato+ axonal projections, which might represent the terminal field of projections from prefrontal layer 5 pyramidal neurons that was recently described in a tracing study of the Rbp4-Cre line (Prasad, Carroll, and Sherman 2020). The suprachiasmatic nucleus appeared not only free of tdTomato+ cells but also void of fine tdTomato+ fibres, which one would expect to find if this region was a target of corticofugal projections of Rbp4-Cre expressing layer 5 pyramidal neurons.

Laminar recordings of MUA indicated that the surge of neuronal activity in layer 5 during OFF-ON transitions is reduced in cortical SNAP25-ablated mice. The laminar LFP recordings showed that in cortical SNAP25-ablated mice slow wave amplitudes and SWA in layer 5 are reduced, while the same measures are increased in layer 2/3 leading to a collapse of the gap in

slow wave amplitude and activity, which I had observed between the supragranular and infragranular level in both wild type C57BL/6J and CTR mice.

Sleep analysis based on EEG recordings indicated an increase in wake time of approximately three hours, which particularly manifested in extended wake episodes during the dark period. The increase of NREM sleep SWA relative to the duration of spontaneous wake episodes, a measure which typically reflects the build-up of homeostatic sleep pressure during wakefulness, was reduced in cortical SNAP25-ablated mice. While EEG power spectra during baseline NREM sleep showed no genotype differences, most likely due to the differential regulation of SWA in layers 2/3 and 5, the elevation of NREM sleep SWA in the frontal cortex following six hours of sleep deprivation was smaller compared to controls. In addition, the cortical SNAP25-ablated mice showed a lack of 'wake intensity' during sleep deprivation as manifested by the near absence of the expected theta-increase in sleep-deprived animals.

Circadian phenotyping provided no indication for genotype differences in the mice' clock function or phase-shifting response to light. The free running period and periodogram power were indistinguishable between cortical SNAP25-ablated and control mice. Both genotypes showed a nearly identical shift in their locomotor activity rhythm in response to a phase-delaying light pulse. The PIR recordings, performed primarily to characterise the circadian function in our mouse model, also allowed to measure sleep based on locomotor activity. These analyses replicated the genotype differences in sleep amount and sleep profile described in the EEG-recorded mouse cohort and showed that the sleep phenotype remains stable in constant darkness.

In summary, these results indicate that the cortical SNAP25-ablated (*Rbp4-Cre;Ai14,Snap25*$^{fl/fl}$) mouse is a suitable model to probe an involvement of the cortex in sleep-wake regulation. The cross of the pan layer 5 driver Rbp4-Cre and the *Snap25*$^{fl/fl}$ reporter,

provides an elegant way to functionally silence a considerable sub-population of cortical neurons without the need for invasive procedures, which could directly affect the main electrophysiological read-out of sleep – cortical oscillations. Laminar recordings, EEG-based sleep assessment, and circadian phenotyping provide a consistent picture that chronic silencing of cortical neurons can not only elicit profound changes in neocortical dynamics during NREM sleep but also evoke a sleep phenotype characterized by a strong homeostatic dysregulation without obvious effects on the circadian process.

### 5.4.2 Implications

It was previously thought that sleep and wakefulness are governed by an intricate interplay of subcortical nuclei. However, only very few mouse models with manipulations of these subcortical sleep-wake centres present such a strong sleep phenotype as the cortical SNAP25-ablated mouse (Yu et al. 2019; Ma et al. 2019; Honda et al. 2020; Oikonomou et al. 2019). In addition, to my knowledge, in none of the mouse models, where specific subcortical brain areas were inactivated using transgenic, pharmacological or ablation approaches, such a comprehensive and consistent sleep homeostasis phenotype, crucially including sleep architecture, sleep oscillations, and the response to sleep deprivation has been described. The absence of a detectable circadian phenotype renders the cortical SNAP25-ablated mouse a unique model to study the effects of altered homeostatic regulation in isolation.

### 5.4.3 Limitations

The cortical SNAP25-ablated mouse provided suitable model to address the question whether cortical manipulations could affect sleep oscillations and the control of vigilance states. However, a number of limitations, regarding Cre-mouse lines in general and this model in particular, should be highlighted.

While normal cortical development has been reported in this mouse model, the mice show early signs of axonal degeneration in young adulthood and start to present behavioural signs of upper motor neuron dysfunction from around 4-5 months of age as well as clear signs of degeneration of the silenced neurons at around 8 months (Hoerder-Suabedissen et al. 2019). Because the previous neuroanatomical description does not assess animals in the age group between 7 weeks and 8 months (Hoerder-Suabedissen et al. 2019), it cannot be fully excluded that our young adult mice were undergoing early stages of neurodegeneration, which did not manifest in any obvious phenotypical abnormalities. This possibility could be addressed by combining more detailed anatomical work with systematic behavioural testing of the animals.

It should also be considered that chronic neuronal silencing through ablation of SNAP25 might lead to long-term adaptations in cortex. Glial reactions, remodelling of synaptic connections, and changes in myelination are just a few of the conceivable consequences of this chronic manipulation. Ongoing neuroanatomical work in the Molnár lab currently investigates such secondary effects of layer 5 silencing on neocortical microstructure. However, to further clarify the role of cortex in sleep regulation it would be of uttermost importance to try to replicate the sleep phenotype in the cortical SNAP25-ablated mouse with acute manipulations of the same cell population, e.g. using refined DREADD approaches.

While we made great efforts to describe the Cre-expression under the Rbp4-Cre promotor in large detail, and excluded accidental silencing of hypothalamic sleep-wake and circadian control centres with high certainty, no Cre-driver line is without ectopic expression (J. A. Harris et al. 2014). It appears unlikely that a small set of ectopic Cre-expressing cells could create such a comprehensive phenotype including layer-specific changes of sleep oscillations, strong differences in the sleep amount, and considerable homeostatic deficits. However, this possibility cannot be fully excluded. The use of alternative Cre-driver lines, which target

layer 5 pyramidal neurons but have a different ectopic expression profile compared to Rbp4-Cre driver line, would be ideal to validate the sleep phenotype in the cortical SNAP25-ablated mouse model.

Despite the comprehensive circadian characterisation of this mouse model, the origin of the dark-pronounced phenotype remains elusive. It is striking that many mouse models with sleep phenotypes show larger effects in the dark than in the light phase (Funato et al. 2016; Peng et al. 2020; Yu et al. 2019) and more consideration should be given to the cause of this phenomenon.

### 5.4.4 Conclusions

For more than 40 years it is known that cortical SWA increases as a function of wake time (Borbély and Neuhaus 1979; Borbély et al. 1981; Borbély, Tobler, and Hanagasioglu 1984) and reflects the homeostatic sleep drive (Borbély 1982; Dijk, Beersma, and Daan 1987; Achermann et al. 1993; Guillaumin et al. 2018). In fact, the two process model of sleep regulation was developed based on the observation that the elevation of SWA reflects the accumulated sleep drive independent of the circadian time (Borbély 1982). It is now well established that the length and frequency of population ON and OFF periods underlying slow waves during NREM sleep as well as neocortical firing rates also reflect the homeostatic process (Vyazovskiy et al. 2009; Thomas et al. 2020). Therefore, it is surprising that it has not been tested previously whether manipulations of cortical layer 5 pyramidal neurons, which had long been suspected to drive the above-mentioned cortical population dynamics, impact NREM sleep slow waves and the homeostatic regulation of sleep.

The results from the cortical SNAP25-ablated mouse model indicate that chronic silencing of those cells in cortex, which are thought to drive the bistable pattern during NREM sleep, results in a profound change in sleep, most importantly sleep time and sleep homeostasis. While

further experiments must be conducted to validate this finding with alternative methodological approaches, the cortical SNAP25-ablated mouse model provides compelling evidence for an involvement of the cortex in the regulation of sleep.

One could hypothesise that the very same cells, which mirror homeostatic sleep drive in their firing patterns and which generate slow waves, also sense sleep need in cortex. From this hypothesis, the immediate question arises, what constitutes the molecular substrate of sleep need, how it is sensed and integrated, and through which circuit the cortical level of sleep homeostasis are broadcasted to established sleep-wake control centres that can trigger vigilance state transitions.

Due to their very large soma, high energy metabolism, their wide dendritic branching, and their long axonal projections to subcortical nuclei, one could imagine that layer 5 pyramidal neurons might act as the sensor, integrator, and broadcaster. An intra- or extracellular molecular process might drive some layer 5 pyramidal neurons into biostability, which is then coordinated across neocortex, and also propagated to subcortical centres of sleep-wake control. In the general discussion chapter, I will outline a set of experiments, which would allow to test this hypothesis.

However, it should be mentioned that a putative contribution of the silenced archicortical dentate gyrus granule cells to the sleep phenotype of the cortical SNAP25-ablated mouse line should by no means be excluded. Some features of our mouse model, in particular the leftward shift of the theta peak during REM sleep, might originate from silenced dentate gyrus granule cells. Their contribution to sleep regulation has never been studied, but the crucial position of the hippocampus in the integration of time and memory (Eichenbaum 2017) as well as the putative interactions of primarily hippocampal and neocortical rhythms during sleep (Y. Hayashi et al. 2015; Levenstein, Buzsáki, and Rinzel 2019) provide some grounds to speculate

that hippocampus may track wake time and contribute to sleep homeostasis. Localised manipulations of hippocampus could be used to test this hypothesis.

In summary, the sleep phenotype of the cortical SNAP25-ablated mice line clearly speaks for an involvement of cortex in sleep regulation. While technical limitations related to the Cre-driver line and the SNAP25-dependent silencing approach call for caution in reaching a final conclusion, the findings presented here provide a solid basis for further experimental interrogation of the cortical role in sleep regulation.

# Chapter 6: General discussion and future directions

Since Constantin von Economo's attempts to investigate 'sleep as a problem of localization', the centres for vigilance state control have been sought in subcortical regions (Economo 1930; Nauta 1946). The identification of an 'ascending arousal system' in the brainstem (Moruzzi and Magoun 1949) and the influential model of a hypothalamic 'sleep switch' (Saper, Chou, and Scammell 2001) have fuelled the successful search for ever more subcortical centres of sleep-wake control (Saper and Fuller 2017). However, despite the rapid identification of numerous subcortical sleep- or wake-promoting nuclei in recent years (Weber and Dan 2016), the essential question of which system in the mammalian brain titrates the exact amount and intensity of sleep to readily compensate for lost or surplus sleep remains unanswered: *What triggers the sleep switch?*

The search for the neurobiological implementation of sleep homeostasis is founded on the notion that sleep is regulated by the interaction of two oscillators: the circadian clock, a harmonic oscillator, and the sleep homeostat, a relaxation oscillator. The two process model of sleep regulation provides a simple, reliable, and mathematically well-defined concept of how sleep duration and intensity are governed by the interaction of the circadian and the homeostatic process (Borbély 1982; Daan, Beersma, and Borbély 1984; Achermann et al. 1993; Guillaumin et al. 2018). The circadian process, which generates an internal near 24-h rhythm of wake propensity and aligns our metabolism, endocrine rhythms, and regular bed time with the external day-night cycle, is extremely well understood at a molecular (Takahashi 2016) and circuit level (Dibner, Schibler, and Albrecht 2010; Morin 2013). In contrast, the physical correlates of the homeostatic process, which measures the accumulation of sleep debt during wakefulness and ensures its dissipation during sleep, are still largely elusive. Understanding the physiological implementation of sleep homeostasis will allow us to delineate how the sleep

switch is operated. It has been suggested that some of the subcortical centres, which generate vigilance state transitions also regulate sleep homeostasis (Gvilia et al. 2006). However, there are surprisingly few examples of subcortical manipulations that affect sleep homeostasis. Recent studies suggest that preoptic galanin neurons (Ma et al. 2019), GABAergic neurons in the ventral medial midbrain/pons region (VMP)(Honda et al. 2020), in particular in the ventral tegmental area (VTA)(Yu et al. 2020), as well as serotoninergic neurons in the raphe nuclei (Oikonomou et al. 2019) contribute to the homeostatic regulation of sleep. However, most of these models show a mixed phenotype, for example with altered temperature regulation (Ma et al. 2019) or mania-like behaviours (Yu et al. 2020; Honda et al. 2020).

Most sleep studies in rodents and humans use EEG SWA during NREM sleep as the read out of the homeostatic process. Neocortex can locally regulate the level of SWA (Kattler, Dijk, and Borbély 1994; Vyazovskiy, Borbély, and Tobler 2000; Huber et al. 2004; 2006) and local slow waves during wakefulness appear under conditions of elevated sleep pressure (Borbély, Tobler, and Hanagasioglu 1984; Vyazovskiy et al. 2011) and foreshadow sleep (Vyazovskiy et al. 2011). In addition, it has been shown that SWA in cortex can be triggered by molecules that are known to induce sleep (Clinton et al. 2011). It therefore seemed timely to address the question: *Does cortex regulate sleep?*

In this general discussion chapter, I will briefly summarise the key findings of the three projects presented above and explain how, in my view, they support the hypothesis that cortex contributes to the regulation of sleep. I will then set these findings into the context of previous literature, and discuss the current evidence for homeostatic regulation of sleep by subcortical structures and cortex, respectively. Subsequently, I will briefly reflect on common problems in the investigation of sleep homeostasis and present criteria, which could be implemented in the design of future studies on sleep homeostasis in mammals. Towards the end of this chapter, I

will speculate on putative neural circuits and molecular mechanisms underlying cortical sleep regulation. This will include a brief outlook on future experiments, which are needed to validate and clarify the role of the cortex in sleep-regulation. Finally, I will outline some possible clinical implications, which might arise as a result of future investigations into the cortical regulation of sleep.

## 6.1 Summary of key findings

In the first results chapter of this thesis, I showed in C57BL/6J wild type mice that layer 5 leads the surge of population activity at OFF-ON transitions during NREM sleep. I also showed that slow waves have greater amplitude and SWA is larger in layer 5 compared to layer 2/3. Layer 2/3 presented a stronger increase in spectral power after sleep deprivation than layer 5. Thus, neocortical dynamics during NREM sleep are rich and these results suggest an intrinsic cortical regulation of sleep oscillations.

I then described my attempts to chemogenetically manipulate neocortical layer 5 pyramidal cells using the Rbp4-Cre driver line, which also expresses Cre-recombinase in archicortical dentate gyrus granule cells. Using a cross with a hM4Di-DREADD reporter line, which enables Cre-dependent expression of an inhibitory DREADD, I found a temporary suppression of SWA in one pilot animal when the inhibitory DREADD was stimulated through CNO injections. However, the sleep architectural pattern, which was reminiscent of sleep effects associated with clozapine, encouraged me to perform CNO injections in wild type mice. The main finding of this chapter was that, unexpectedly, the two most commonly used DREADD actuators, CNO and Cmpd21, influence sleep architecture and electrophysiology even in wild type C57BL/6J mice. The raises important considerations when using existing chemogenetic technologies in the investigation of sleep homeostasis.

Finally, I presented extensive work on a cortical SNAP25-ablated mouse model (*Rbp4-Cre;Ai14,Snap25*$^{fl/fl}$) including neocortical laminar recordings, EEG-based sleep assessment, and PIR actigraphy. This conditional knockout mouse primarily served as a model for chronic silencing of layer 5 pyramidal neurons in neocortex, but also contains a considerable population of silenced archicortical dentate gyrus granule cells. Conditional knockout mice showed a loss of the previously described layer differences in slow wave amplitudes and SWA. Sleep time was reduced by approximately 3 hours, and the homeostatic response to extended wakefulness appeared diminished while circadian rhythms remained intact.

Several methodological limitations, discussed at the end of each chapter, warrant caution in the interpretation of the findings presented in this thesis. However, overall, my work provides strong evidence in support of the hypothesis that cortex actively regulates slow waves and SWA during NREM sleep and contributes to the global control of vigilance states and, in particular, the homeostatic regulation of sleep.

## 6.2 Subcortical vs. cortical regulation of sleep homeostasis

While the findings from the cortical SNAP25-ablated mouse line suggest that cortex actively contributes to the homeostatic process of sleep regulation, the evidence for a subcortical contribution should not be overlooked. Here, I will briefly summarise literature suggesting subcortical or cortical regulation of sleep homeostasis with the aim to provide the reader with an unbiased overview of the evidence for both concepts. It should be emphasised that homeostatic regulation of sleep is most likely a distributed process, that could be considered a fundamental feature of neuronal assemblies (Krueger et al. 2008). While some brain areas might be more involved than others, it appears likely that there is no single anatomically defined master-regulator of the homeostatic process. Avoiding insufficient or excess sleep appears to be such an essential requirement for a functional nervous system, that most likely a

redundant biological mechanism ensures that this process is maintained to some extent, even if parts of the brain are damaged (Krueger and Tononi 2011). In light of this 'local sleep' concept, my discussion of subcortical vs. cortical regulation of sleep homeostasis should not be understood as the search for an answer to a binary question, but rather as an attempt to lay out evidence for the involvement of two evolutionarily, anatomically, and functionally very distinct brain structures in the homeostatic regulation of sleep.

### 6.2.1 Subcortical regulation of sleep homeostasis

The preoptic area (PO) of the hypothalamus has been the main focus in the search for a subcortical centre that regulates sleep homeostasis. Expression of the immediate-early gene cFOS in the ventrolateral preoptic (VLPO) nucleus is higher in rat brains when the animals are killed during sleep rather than during wakefulness, suggesting that many neurons in VLPO are sleep active (Sherin et al. 1996). In addition, the average number of cFOS-expressing cells correlates with the amount of total sleep during the hour before death (Sherin et al. 1996). It was later found that the discharge of different VLPO neuron populations reflects to some extent the depth of sleep. Wake-active cells reduce their firing at the transition from wakefulness into sleep and become even less active in early and late NREM sleep. Other sleep-active cells in the same region increase their firing when sleep deepens (Szymusiak et al. 1998). Hypothalamic cells with increased cFOS expression during sleep are GABAergic neurons in the VLPO and the adjacent median preoptic nucleus (MnPO) (H. Gong et al. 2004). The cFOS expression of those neurons is further elevated during recovery sleep period following a 24-h sleep deprivation compared to normal sleep (H. Gong et al. 2004). In addition to these initial findings, which suggested that VLPO activity reflects the depth of sleep, it was later shown via extracellular recordings that both VLPO and MnPO sleep-active neurons increase their firing rates towards the end of a 2-h sleep deprivation, show highest firing rates during early NREM

sleep, and then gradually return to baseline rates – a pattern which reflects the time course of the homeostatic process (Alam et al. 2013). Whether the VLPO and MnPO actively contribute to sleep homeostasis is, however, less clear. Lesions of the VLPO using microinjections of ibotenic acid cause a profound decrease in delta power and NREM sleep for approximately three weeks and the degree of the change from baseline inversely correlates with the number of remaining cFOS+ neurons in the region (Lu et al. 2000). However, the homeostatic regulation of sleep, in particular the response to sleep deprivation, was not tested in this study (Lu et al. 2000). More recent work shows that ablation of galanin/GABA cells in the preoptic area, a manipulation that is known to induce NREM sleep and concomitant body cooling (Kroeger et al. 2018), also reduces the rebound of sleep and delta activity following sleep deprivation (Ma et al. 2019). Sleep in undisturbed baseline conditions was fragmented but overall increased during the dark period, which is somewhat surprising in the light of previous lesion experiments and considering that chemogenetic stimulation of the same cell population in this study (Ma et al. 2019) and optogenetic stimulation in a previous study elicited sleep promoting effects (Kroeger et al. 2018). The lack of a sleep deficit after ablation of VLPO galanin/GABA neurons, which also resulted in chronically elevated body temperature in these mice, might be explained in part by hyperthermia-induced sleep counteracting the reduced homeostatic sleep drive (Ma et al. 2019). In my view, the lack of a sleep deficit at baseline despite the strong deficit of a homeostatic rebound following sleep deprivation could also be explained by a hierarchical model of sleep homeostasis: The VLPO as an evolutionarily 'older' region, might have an intrinsic ability to perform sleep homeostasis, yet the level to which sleep debt must accumulate to trigger a homeostatic response could be higher than in other, evolutionarily 'younger' brain regions. Hence, one could speculate that in the mammalian brain the VLPO acts as an 'emergency break' if sleep debt accumulates beyond a certain threshold,

but under undisturbed conditions, other brain regions react first to the gradual increase in sleep debt.

### 6.2.2 Cortical interneurons

One neocortical GABAergic interneuron population, which co-expresses neuronal nitric oxide synthetase (nNOS) and the neurokinin 1 receptor (NK1), has been linked to the homeostatic regulation of SWA (Morairty et al. 2013). The initial discovery of nNOS sleep-active interneurons in the cortex of mice, rats, and hamsters and the finding that changes in cFOS expression of NOS+ interneurons parallel the elevated levels and gradual decay of NREM sleep SWA after sleep deprivation, triggered the quest to investigate their involvement in the regulation of SWA and sleep homeostasis (Gerashchenko et al. 2008). It was later found that cFOS expression in nNOS/NK1 interneurons correlates with NREM sleep time, $\delta$-activity (here 0.5 – 4.5 Hz), and sleep architectural indicators of the homeostatic rebound following sleep deprivation in rats (Morairty et al. 2013). Interestingly, a neuronal (although not cortical specific) mouse knockout of nNOS exhibits reduced NREM sleep time and a dysregulation of $\delta$-activity during wakefulness and sleep, with elevated $\delta$-power during wakefulness and reduced $\delta$-power during sleep (Morairty et al. 2013). Somewhat surprisingly, the amount of NREM sleep during nap opportunities in the murine multiple sleep latency test (MSLT) was increased and the latency to NREM sleep reduced in nNOS knockout mice (Morairty et al. 2013). This indicates a dissociation of behavioural and electrophysiological markers of sleep homeostasis in the nNOS knockout mouse. In addition, sleep deprivation still increased cFOS expression in NK1 neurons to a similar extent as observed in wild type mice (Morairty et al. 2013), which suggests that increased activity in cortical NK1/nNOS neurons might not be sufficient to generate SWA. Later experiments, which used the hypnotics zolpidem and almorexant to equalise the amount of NREM sleep in a low sleep pressure and high sleep

pressure condition, clarified that the increase in cFOS expression of NK1/nNOS is indeed related to homeostatic sleep pressure and not the amount of NREM sleep itself (Dittrich et al. 2015). It has further been shown that cortical NK1/nNOS neurons are under the influence of cholinergic basal forebrain neurons (R. H. Williams et al. 2018) and also respond to orexin (R. H. Williams et al. 2019). Importantly, cortical nNOS neurons only represent ~0.1 to 0.15 % of all cortical neurons and only 1 in 10 of those nNOS neurons are of the Type I category, which is sleep active and found in deep layers (Wisor, Gerashchenko, and Kilduff 2011). The proportion of sleep active nNOS neurons in cortex is therefore extremely small and it remains unclear whether changes in sleep regulation in the nNOS knockout are mediated by the cortical nNOS neurons, or other nNOS neurons elsewhere in the brain or in the organism (L. Chen, Majde, and Krueger 2003; Rivera et al. 2011). There is mixed evidence for the effects of NO on sleep, and some biochemical and electrophysiological work rather favours a view of wake promoting rather than sleep-promoting effects of nNOS (Wisor, Gerashchenko, and Kilduff 2011). Until further evidence from targeted manipulations of cortical nNOS neurons emerges, it remains unclear whether activation of cortical nNOS/NK1 neurons during sleep, which correlates with the level of SWA, is *sleep-induced* or *sleep- and SWA-inducing* (Wisor, Gerashchenko, and Kilduff 2011). Whether this interneuron population is involved in the regulation of sleep and SWA can only be clarified once a suitable Cre-driver line has been developed (Wisor, Gerashchenko, and Kilduff 2011).

Most of the nNOS-expressing interneurons co-express neuropeptide Y (NPY, 80%), but not somatostatin (SOM, 13%)(Karagiannis et al. 2009). However, SOM+ interneurons have recently been suggested to contribute to the homeostatic regulation of SWA (Funk et al. 2017) and the initiation of sleep and sleep-preparatory behaviours in response to sleep deprivation (Tossell et al. 2020). A first study by Funk et al., aimed at manipulating a subset of SOM+ neurons, so called Martinotti cells. Martinotti cells target presynaptic glutamatergic terminals

and apical dendrites in neocortical layer 1. However, no specific Cre-driver line for Martinotti cells is available and hence a SOM-Cre driver line was used. Optogenetic and chemogenetic constructs were delivered through bilateral frontal and parietal injections of AAV-vectors. SOM+ interneurons fire immediately before slow waves (Niethard et al. 2018) and Funk et al. found that their optogenetic activation can trigger OFF periods (Funk et al. 2017). The study further reported that chemogenetic activation of SOM+ cells elevates SWA and increases the slope of individual slow waves, while chemogenetic inactivation decreases SWA and slow wave incidence (Funk et al. 2017). NREM sleep time was increased after chemogenetic activation of SOM+ cells, but unaltered after chemogenetic inhibition (Funk et al. 2017). While the bidirectional modulation of SWA indicates a genuine DREADD effect, the modulation of NREM sleep time should be evaluated with some caution in light of the direct CNO effects on sleep presented earlier in chapter 4 of this thesis and observed in the CNO-injected control group of the SOM-DREADD animals. Medium and high CNO doses (5 mg/kg CNO for excitatory DREADD and 10 mg/kg for inhibitory DREADD) were used for the chemogenetic manipulation of SOM+ neurons (Funk et al. 2017). In addition, the two conditions were also performed at different times of the day. Chemogenetic inhibition of SOM+ neurons was performed at light onset, when the homeostatic sleep drive is typically high, whereas excitation was performed midway through the light period, when the homeostatic sleep pressure is typically low. It could be speculated that a sedative effect of the high (10 mg/kg) CNO dose at a circadian time when sleep pressure is already high might have prevented a significant suppression of NREM sleep in the inhibitory DREADD experiment. One would have expected that DREADD-inhibition of SOM+ cells that are putatively sleep- and SWA-promoting reduces both sleep and SWA. In a control experiment, chemogenetic activation of PV+ interneurons midway through the light period resulted in a reduction of SWA but increase of NREM sleep (Funk et al. 2017), which further complicates the picture of the role of different

cortical interneuron types in the regulation of SWA and sleep. While the bidirectional regulation of SWA after excitatory and inhibitory DREADD stimulation of SOM+ neurons suggests a SWA-modulating effect of SOM+ neurons, the somewhat inconsistent effects of these chemogenetic manipulations on NREM sleep requires further clarification with a different methodological approach (Funk et al. 2017).

A more comprehensive characterisation of the contribution of prefrontal cortex SOM+/GABA+ interneurons to sleep regulation, was presented in a recent preprint (Tossell et al. 2020). Using cFOS activity-tagging of different prefrontal interneuron populations during sleep deprivation and recovery sleep, the authors expressed excitatory optogenetic and chemogenetic constructs in VGAT+, SOM+, and NOS+ neurons. They found that 20% of the VGAT+ activity-tagged neurons were SOM+/NOS+ co-expressing, suggesting that the interneuron population investigated here only partially overlapped with the previously mentioned sleep-active nNOS+ neurons. Optogenetic stimulation of VGAT+ neurons provoked induction of nesting behaviour and NREM sleep in mice. In addition, chemogenetic activation of all three mouse lines (prefrontal activity-tagged VGAT+, SOM+, and NOS+ neurons) induced NREM sleep without affecting REM sleep. The activation of prefrontal VGAT+ and SOM+ neurons, but not NOS+ neurons, also induced nesting. The authors then confirmed that also optogenetic activation of PFC SOM+ neurons induces nesting and NREM sleep and went on to stimulate only the terminals of these neurons in the lateral preoptic area (LPO) of the hypothalamus and the lateral hypothalamus (LH). Optogenetic stimulation of terminals of long-ranging SOM+ neurons in LPO induced nesting and a mild increase in NREM sleep, while stimulation of terminals in LH induced a strong increase in NREM sleep but only mildly affected nesting behaviour (Tossell et al. 2020). Together, these findings suggest that GABAergic neurons in prefrontal cortex, especially a SOM+ subpopulation with long-ranging projections, respond to homeostatic sleep pressure and promote nesting and

NREM sleep through projections to sleep control centres in the hypothalamus. It would be interesting to know whether the activation of SOM+ neurons also promotes SWA as reported by Funk et al. and whether their acute or chronic silencing would reduce the electrophysiological and/or behavioural response to sleep deprivation.

Interestingly, SOM+ interneurons strongly inhibit excitatory signalling between (layer 2/3) pyramidal cells through $GABA_B$ receptors in layer 1 (Urban-Ciecko, Fanselow, and Barth 2015). In turn, activation of cortical SOM+ interneurons occurs when neocortical pyramidal neurons engage in strong and synchronous firing (Kapfer et al. 2007; Fanselow, Richardson, and Connors 2008; Silberberg and Markram 2007). One could hypothesise that the dendritic inhibition of pyramidal neurons might protect their intrinsic oscillatory activity from interruptions through afferent signals, while the burst firing in pyramidal neurons could in turn initiate NREM sleep through activation of long-ranging SOM+ neurons.

### 6.2.3 Cortical astrocytes

Since an initial report that astrocytes contribute to the homeostatic regulation of sleep through their involvement in adenosine signalling (Halassa et al. 2009), it has been established that glial regulation of adenosine levels and neuronal adenosine sensing contribute to the molecular regulation of sleep homeostasis (Bjorness et al. 2016). However, due to the previous lack of suitable tools to image and manipulate astrocytes, it was only recently found that $Ca^{2+}$ dynamics in neocortical astrocytes reflect the homeostatic sleep drive (Bojarskaite et al. 2020; Ingiosi et al. 2020). Neocortical astrocytic $Ca^{2+}$ signals are highest during waking and lowest during sleep and calcium signals during NREM sleep reflect the level of the homeostatic process (Ingiosi et al. 2020). Interestingly both studies also used conditional knockout mouse models to alter astrocytic calcium signalling and found changes in global sleep parameters, yet none of the manipulations was restricted to cortex (Bojarskaite et al. 2020; Ingiosi et al. 2020). A recent

study aimed to clarify specifically the role of neocortical astrocytes in the regulation of sleep (Vaidyanathan et al. 2021). Vaidyanathan et al. used simultaneous $Ca^{2+}$ imaging of cortical astrocytes and electrophysiological recordings of vigilance states to investigate the relationship between astrocyte activity in cortex, slow wave activity, and sleep architecture parameters. Astrocytic $Ca^{2+}$ event rates were found to be inversely correlated with SWA (Vaidyanathan et al. 2021). Chemogenetic manipulation of astrocytes using hM4Di-DREADDs increased $Ca^{2+}$ events but also SWA. Chemogenetic manipulation of astrocytes using hM3Dq-DREADDs temporarily increased and then abolished $Ca^{2+}$ events and led to an increase in NREM sleep, a reduction of wake time and fewer state transitions, but did not affect SWA. The authors suggest that the hM4Di-mediated increase in $Ca^{2+}$ and SWA might be consistent with an involvement of astrocytic $Ca^{2+}$ signalling SWA homeostasis. However, it needs to be emphasised that DREADD modulation of astrocytes is far less established than that of neurons. The observed $Ca^{2+}$ dynamics, especially the elevated $Ca^{2+}$ level after hM4Di stimulation and the initially elevated then abolished $Ca^{2+}$ signal after hM3Dq stimulation, are somewhat surprising and might be due to depletion of intracellular calcium stores as discussed by the authors (Vaidyanathan et al. 2021). Similarly, it is puzzling that astrocytic hM4Di stimulation elevates SWA without affecting sleep time or architecture, while hM3Dq stimulation of the same cell type increases NREM sleep time and alters sleep architecture but has no effect on SWA. One might have assumed that a bidirectional modulation would evoke opposing effects on the same parameters, yet the pattern of results found here for each of the two DREADDs is highly complex (Vaidyanathan et al. 2021). Sleep homeostasis was not directly assessed in this study either using sleep deprivation or sleep architectural or behavioural measures, and it remains unclear whether the interesting dichotomy between SWA elevation after hM4Di stimulation and NREM sleep increase after hM3Dq stimulation is related to the homeostatic process or to previously described pharmacological and neurophysiological mechanisms, which can change

SWA independent of sleep-wake history (Davis et al. 2011). However, the observed effects on sleep time and architecture in the hM3Dq condition are unlikely induced by CNO considering the thorough controls presented in this paper. Therefore, this study can be considered first evidence that cortical astrocytes contribute to the regulation of sleep yet the mechanisms involved require further clarification (Vaidyanathan et al. 2021). Although some evidence points towards a role of astrocytes in adenosine-mediated neuro-glial regulation of sleep homeostasis (Greene, Bjorness, and Suzuki 2017; Bjorness et al. 2016), the concept of gliotransmission has also been criticised (Sloan and Barres 2014; Fiacco and McCarthy 2018). Interestingly, it was found that the dnSNARE-based mechanism of astrocytic silencing, which produced a sleep phenotype similar to that observed in our cortical SNAP25-ablated mouse (Halassa et al. 2009), is not specific for astrocytes and is also expressed in cortical neurons, reducing their activity and lowering EEG power (Fujita et al. 2014). In conclusion, more work is needed to clarify the role of cortical astrocytes in (homeostatic) sleep regulation. While their calcium dynamics appear to reflect the homeostatic process, targeted manipulations are methodologically challenging and have so far produced inconsistent results.

### 6.2.4 Thalamocortical neurons

Another brain region of potential relevance for a cortical regulation of vigilance states and sleep homeostasis is the thalamus. Although anatomically distinct from the cortex, the thalamus represents a functional unit with the cortex as most sensory modalities are relayed through the thalamus and thalamocortical loops are essential for information processing (Sherman and Usrey 2021). During NREM sleep, sleep spindles and slow waves during are generated in a corticothalamic interplay (Steriade 2003; Franks 2008). Interestingly, the centromedial thalamus (CMT) appears to play a dual role in the regulation of sleep-wake transitions and delta-activity during sleep (Gent et al. 2018). More specifically, tonic optogenetic activation of

CMT leads to awakening while burst firing induces slow waves and accelerates the decline of cortical SWA during recovery sleep after sleep deprivation. These effects are relayed by anterodorsal thalamus (AD) and cingulate cortex (CING). Silencing of CMT or CING delays the return of SWA to baseline (Gent et al. 2018). While the authors interpret these differences in the decay of SWA as an indication for an accelerated or delayed 'recovery process' from sleep deprivation, it is not clear whether the demonstrated circuit mechanism is only relevant for the electrophysiological rebound of SWA or also for the homeostatic regulation of sleep. Subacute or chronic manipulations of this cell population could address this question.

In summary, sets of subcortical and cortical cell populations have been identified, which reflect the homeostatic process in their activity profile. Targeted manipulations of sleep-active hypothalamic VLPO GABA/galanin and prefrontal cortex GABAergic SOM+ interneurons suggest a putative role of these neuron populations in the homeostatic process. For cortical nNOS neurons and astrocytes, selected manipulations appear more difficult and results are less consistent. It remains to be tested whether the activity of cortical nNOS neurons or the $Ca^{2+}$ signals in cortical astrocytes merely reflect the level of the homeostatic process, or actively contribute to sleep homeostasis. Thalamocortical interactions appear important for the homeostatic regulation of SWA, but whether their ability to accelerate or delay the return of elevated SWA to baseline is linked to the dissipation of sleep debt is so far unclear.

## 6.3 How to study sleep homeostasis?

The notion that SWA during physiological NREM sleep is a reliable marker of the homeostatic process has led to its widespread use in the study of sleep homeostasis. However, it is problematic that the SWA rebound after sleep deprivation and its decay during recovery sleep is often used as the only measure of sleep homeostasis. Sleep deprivation usually elevates the activity of the hypothalamic-pituitary-adrenal (HPA) axis and the reciprocal relationships of

sleep deprivation and stress provides a conceptual challenge when studying sleep homeostasis (Nollet, Wisden, and Franks 2020). In addition, there are many examples that demonstrate EEG power across slow frequencies can be modulated independently of sleep-wake history (Davis et al. 2011). It has been suggested that SWA is the default mode of the cerebral cortex (Sanchez-Vives and Mattia 2014). Slow waves are consistently found in isolated, severed, or damaged cortical areas (Sanchez-Vives and McCormick 2000b; Timofeev et al. 2000; Sheroziya and Timofeev 2014; Krone and Vyazovskiy 2020; Sarasso et al. 2021) and even cortical cell cultures (Hinard et al. 2012). Local changes in SWA can also be readily induced by local action of inflammatory markers (Krueger 2008). Therefore, it is of uttermost importance to reflect on the question: *How to study sleep homeostasis?*

While this matter deserves thorough discussion in the sleep research community, here I attempt to outline a few key criteria, which should be fulfilled to claim that a specific cell population actively contributes to sleep homeostasis:

**Observational evidence:** One or more cellular properties should reflect the homeostatic process. This indicator should increase during wakefulness, dissipate during sleep, and be elevated after sleep deprivation. Examples of such cellular markers are: neuronal firing rates or firing patterns (Vyazovskiy et al. 2009; Alam et al. 2013; Thomas et al. 2020), expression of immediate early genes such as cFOS (H. Gong et al. 2004; Gerashchenko et al. 2008), astrocytic intracellular $Ca^{2+}$ signals (Bojarskaite et al. 2020; Ingiosi et al. 2020), protein phosphorylation (Brüning et al. 2019), markers of oxidative stress (Kempf et al. 2019) or of the unfolded protein response (Naidoo et al. 2005), or generation of sleep-regulatory substances such as adenosine (Porkka-Heiskanen, Strecker, and McCarley 2000; Kalinchuk et al. 2011).

**Perturbational evidence:** When observational evidence suggests the involvement of a cell population in the homeostatic regulation of sleep, these candidate cells should be targeted in

the most selective manner, e.g. using cell-type or site-specific recombinant technology. Bidirectional manipulations of the candidate cell population should elicit opposite effects on electrophysiological and behavioural markers of sleep homeostasis, but not affect circadian rhythms.

Targeted manipulations should evoke altered electrophysiological responses to sleep deprivation, for example in the level of SWA in the NREM spectrogram after sleep deprivation (Borbély et al. 1981; Tobler and Borbély 1986), theta activity in the wake spectrogram during sleep deprivation (Finelli et al. 2000; Vassalli and Franken 2017), or the number and duration of OFF-periods after sleep deprivation (Vyazovskiy et al. 2009).

As a result of targeted manipulations, one would also expect altered behavioural responses to sleep deprivation, for example in the amount of rebound sleep (Franken et al. 1991), NREM episode duration (Vyazovskiy and Tobler 2012), number of brief awakenings (Huber, Deboer, and Tobler 2000a; Franken et al. 1991), or arousal threshold to sensory stimuli (Neckelmann and Ursin 1993; Rechtschaffen, Hauri, and Zeitlin 1966).

Targeted manipulations of candidate cells should also modulate homeostatic measures during baseline sleep, e.g. the relationship between wake duration and change in NREM SWA (Huber, Deboer, and Tobler 2000a) as well as wake time, wake episode duration, or brief awakenings from sleep (Franken et al. 1991).

Finally, one would expect to observe intact circadian regulation of sleep. Suitable markers for a circadian screen based on non-invasive actimetry are for example the free running period and periodogram power, or the phase-shifting response to a light pulse delivered at specific circadian times in constant darkness (Brown et al. 2019). However, it should be mentioned again that the homeostatic and circadian regulation of sleep are intertwined and manipulating one of the two processes might affect the other (Deboer 2018; 2009; Challet et al. 2001).

In summary, the assessment of sleep homeostasis should never be based on one individual marker such as the time course of SWA after sleep deprivation. Other commonly used markers, such as the amount of rebound sleep, are also inadequate as single readout of sleep homeostasis. For example, sleep time and behavioural measures of sleep debt such as sleep latency are strongly affected by circadian timing, arousal and motivation (Borbély 1982; Suzuki et al. 2013). Instead, the assessment of sleep homeostasis should ideally be based on a combination of electrophysiological and behavioural measures acquired during baseline sleep and after sleep deprivation, and optimally include a basic circadian screen.

## 6.4 Neural circuits linking cortex with subcortical sleep-control centres

Cortical regulation of sleep is an emerging concept, which must be reconciled with the well-established circuit models of subcortical sleep-wake control (Saper and Fuller 2017). The cortical SNAP25-ablated mouse model suggests that either layer 5 pyramidal neurons or hippocampal dentate gyrus cells or both cell populations contribute to the global regulation of vigilance states. Here, I will present a few considerations on possible circuits through which these neurons could interact with subcortical sleep-wake centres.

### 6.4.1 Putative circuits of cortical sleep regulation

One possibility is that layer 5 pyramidal neurons signal to sleep-wake centres in the lateral hypothalamus. This hypothesis is supported by the finding that in the Rbp4-Cre mouse line, which was used as driver line in our ‘cortical SNAP25-ablated’ mouse model, prefrontal layer 5 pyramidal neurons project to the lateral hypothalamus and create a terminal field there (Prasad, Carroll, and Sherman 2020). The prefrontal origin is especially interesting because previous research suggests that the prefrontal cortex might be most sensitive to homeostatic sleep pressure (Marzano et al. 2013; Massimini et al. 2004; Werth, Achermann, and Borbély

1997; Huber, Deboer, and Tobler 2000b; Cajochen, Foy, and Dijk 1999). One could imagine a model, in which prefrontal cortex accrues sleep debt and its layer 5 pyramidal neurons mediate the activation of sleep-promoting MCH neurons or a bisynaptic inhibition of wake-promoting ORX+ neurons in the lateral hypothalamus.

Alternatively, layer 5 pyramidal neurons might interact with cortical SOM+ interneurons. As briefly mentioned above, long-range interneurons also project into the hypothalamus (LH and LPO) and initiate sleep preparatory behaviours and sleep initiation through these pathways (Tossell et al. 2020). It could be speculated that layer 5 pyramidal neurons increasingly engage in burst firing with accumulating sleep pressure and thereby activate subcortically-projecting SOM+ cells, which trigger the subcortical sleep switch.

A third possibility arises from connections of layer 5 pyramidal neurons to the thalamus. Given that bistable firing of layer 5 pyramidal neurons foreshadows sleep onset (Vyazovskiy et al. 2011), it could be hypothesised that an intracellular or extracellular process triggers the bistability, which is then conveyed to thalamic centres. This process might contribute to the entrainment of slow oscillations in thalamocortical loops and the decay of delta-activity over the course of NREM sleep (Gent et al. 2018). After sufficient discharge of sleep debt, this corticothalamic interplay could lose momentum allowing pyramidal neurons to switch back into their tonic firing mode and to promote the wake state. Interestingly, an acceleration of the power decay in slow frequencies during NREM sleep as observed after optogenetic burst stimulation of centromedial thalamus in mice (Gent et al. 2018), has also been described after transcranial electric stimulation at 0.75 Hz frequency over frontal cortical areas (Reato et al. 2013). Although it should be mentioned that the ‘slow wave oscillations’ in this study were defined as 0.5-1 Hz (Reato et al. 2013). Based on these and other findings, which suggest that non-invasive brain stimulation methods might affect both corticothalamic oscillations and

sleep time (Marshall et al. 2006; Frase et al. 2016; Marshall et al. 2004; Mensen et al. 2014), I previously postulated that cortex could affect global sleep regulation through corticothalamic interactions (Krone et al. 2016). Considering that layer 5 pyramidal neurons with projections to thalamus as well as their specific terminals can be selectively targeted in transgenic mouse models, it would be exciting to now test this hypothesis in a mouse model.

Finally, a contribution of hippocampal dentate gyrus granule cells should not be dismissed. Considering their role in time keeping they might play a so far unrecognised role (Eichenbaum 2017). A recent clinical study reported reduced slow wave sleep and SWA in four memory-impaired patients with bilateral hippocampal damage following antibody-mediated limbic encephalitis (Spanò et al. 2020). However, to my knowledge, a hippocampal contribution to the regulation of slow waves or vigilance states remains to be tested in animal models (Levenstein, Buzsáki, and Rinzel 2019).

### 6.4.2 Experimental strategies to probe neural circuits of cortical sleep regulation

Several experimental strategies would allow to narrow down whether intracortically projecting or subcortically projecting layer 5 pyramidal neurons, or both, caused the effects on global sleep-wake regulation in the cortical SNAP25-ablated mouse model. A simple first step would be to use different driver lines for subsets of layer 5 pyramidal neurons, e.g. the Tlx3-Cre line, which exclusively labels cortico-cortical and striatal projections, or the Efr3a-Cre line, which labels exclusively cortico-cortical projections and the Glt25d2-Cre line, which labels subcortically projecting layer 5 pyramidal neurons (Kim et al. 2015). If crossed to the $SNAP25^{fl/fl}$ line, one could create three new mouse models, in which only the projections to specific postsynaptic partners of layer 5 pyramidal neurons are silenced. This approach would also help to probe whether the hippocampus contributed to the observed sleep phenotype in the cortical SNAP25-ablated mouse line.

Acute manipulations could further help to clarify whether the suggested circuits are involved in the modulation of sleep and/or SWA. One possibility would be to express an excitatory opsin in prefrontal cortex layer 5 pyramidal cells using prefrontal injections of a viral vector. Optogenetic stimulation of layer 5 pyramidal neuron terminals, for example in LH, could then be used to test if cortico-subcortical projections to established centres of sleep-wake control modulate the vigilance state transitions. Optogenetic stimulation of layer 5 pyramidal neuron terminals could further be performed in centromedial thalamus to probe the involvement of cortico-thalamic circuits in sleep-wake control. Based on previous experiments, which suggested that tonic and burst firing of the centromedial thalamus promotes sleep or accelerates the rebound of SWA, respectively, it would be worthwhile to test whether different activation patterns of layer 5 pyramidal neuron terminals can switch the thalamic mode of action (Gent et al. 2018).

One could also reconsider the use of DREADD technologies, including appropriate controls and administering only low doses of CNO or very low doses of clozapine to activate the designer receptors (Gomez et al. 2017). As discussed earlier, one major challenge in probing the role of the cortex in sleep regulation is to target only a selected cell population but over a sizable area. This is particularly true for neocortex, where viral injections cover small areas and where the invasiveness of the injection procedure might affect cortical oscillations, which are the main readout of sleep. Very recent advances in the design of intravenously delivered AAVs, which cross the blood-brain barrier and transduce specific cell types in the adult mouse brain, might make it possible to circumvent this problem (Ravindra Kumar et al. 2020). It could soon become possible to perform an experiment in which neocortical (layer 5) pyramidal neurons are selectively, and non-invasively, targeted to express a DREADD construct. Another cell population, e.g. dentate gyrus granule cells, targeted in a separate group of mice with the same construct, could then serve as a comparison for sleep analysis in CNO-injected animals.

Such subacute manipulations of cortical neurons might allow for a bidirectional manipulation of homeostatic sleep pressure, not only in terms of SWA as observed in one pilot animal from the *Rbp4-Cre:hM4Di* cross but also in terms of behavioural measures of sleep homeostasis.

## 6.5 Putative molecular mechanisms of cortical sleep regulation

Parallel to the investigation of the circuits underlying cortical sleep regulation, efforts should be put into delineating the molecular mechanisms. Several candidate mechanisms have been discovered in rodent sleep research in previous years and recent work in fruit flies has broadened the range mechanistic principles, which could govern the homeostatic regulation of sleep (Allada, Cirelli, and Sehgal 2017). Much of this work suggests that the primary function of sleep might be to allow individual cells to perform prophylactic cellular maintenance (Vyazovskiy and Harris 2013). The molecular counterpart of sleep homeostasis should therefore be sought in those cells, which actively contribute to sleep homeostasis. As a next step, one could therefore start to manipulate intracellular processes, which have been proposed to underlie the homeostatic regulation of sleep, specifically in Rbp4-Cre expressing layer 5 pyramidal neurons or dentate gyrus granule cells.

Intracellular processes, which change in a wake- and sleep-dependent pattern, and are conserved both in mammalian and non-mammalian organisms, are for example phosphorylation changes at synaptic proteins (Brüning et al. 2019; Ode and Ueda 2020), endoplasmic reticulum stress (J. A. Williams and Naidoo 2020), or redox homeostasis (Kempf et al. 2019). In turn, extracellular signals of sleep homeostasis could be represented in inflammatory and neurotrophic molecules (Krueger et al. 2019), extracellular adenosine levels (Greene, Bjorness, and Suzuki 2017), and possibly other metabolites that accumulate during wakefulness and undergo glymphatic clearance during sleep (Xie et al. 2013). If layer 5 pyramidal neurons are in fact actively driving the homeostatic process, one would expect that

manipulating these intracellular processes or the sensing of extracellular molecules specifically in layer 5 pyramidal neurons would affect the homeostatic process. This could provide the molecular groundwork for pharmacological manipulations of sleep homeostasis.

In addition, one should not forget that the t-SNARE-based silencing mechanism used here is related to synaptic function (Washbourne et al. 2002) and inevitably affects activity-dependent synaptic modelling. Considering that synaptic down-selection might be one of the core functions of sleep in order to avoid runaway potentiation (Tononi and Cirelli 2020) and that in our mouse model the activity-dependent growth of synapses after the initial formation is impaired (S. Hayashi et al. 2021), it could be hypothesised that the apparent lack of homeostatic sleep drive in the cortical SNAP25-ablated mouse model may be due to a reduced demand for synaptic scaling. Given that other mouse models with genetic modifications of synaptic proteins have presented strong sleep phenotypes (Banks et al. 2020), it could be worthwhile to test whether other tools for synaptic silencing in cortex could affect sleep homeostasis. One possible approach would be Cre-dependent expression of the tetanus toxin light chain in a selected area (Zhou et al. 2018), although it would need to be clarified whether the induced synaptobrevin cleavage would also be suited to impair synaptic function of excitatory neurons.

In conclusion, this work suggests that the investigation of neural circuits and molecular mechanisms underlying sleep homeostasis should include the cortex as a new focus. It is important to mention that species that lack a cortex also exhibit sleep homeostasis (Tobler 1983; Nath et al. 2017; Anafi, Kayser, and Raizen 2019). However, it remains unclear whether there is an electrophysiological intensity domain of sleep homeostasis in those organisms. From an evolutionary perspective, cortex can be viewed as an ‘add on’ to an already functional nervous system, allowing for the refinement of pre-existing functions (Sherman and Usrey 2021). It could be speculated that the role of the cortex, which represents 80% of the brain mass

in humans, is to optimise sleep homeostasis by pre-emptively sensing sleep need and ensuring accelerated recovery of the homeostatic process through the regulation of sleep intensity. One could picture the cortex as the 'canary in the coal mine', which first senses when homeostatic sleep pressure rises and initiates the brain's transition into sleep before the risks of neuronal exertion or synaptic overload become relevant. Interestingly, molecular and microstructural changes that reflect the homeostatic process of sleep regulation have mostly been observed in neocortex (Naidoo et al. 2005; De Vivo et al. 2017; Diering et al. 2017). However, no brain lesion has so far abolished sleep and one would not expect that decortication leads to a complete absence of sleep homeostasis, given the putative distributed nature of sleep regulation (Krueger and Tononi 2011). Although one could speculate that in a decorticate organism, the primary element of a hierarchically organised sleep homeostat is removed and therefore sleep becomes mostly driven by the circadian process and the essential physiological stimuli integrated in the hypothalamus. Interestingly, 'diencephalic cats', in which the telencephalon has been removed *"display only atypical NREM sleep"* and *"are hyperactive and show a pronounced, permanent insomnia; however, a low dose of barbiturate triggers a dramatic REMS/atypical NREMS rebound."* (Villablanca 2004). Although such large-scale lesions are extremely unspecific, this finding might be interpreted as an indication of altered sleep homeostasis but intact hypothalamic and brainstem regulation of sleep when cortex is removed.

Sleep remains one of the biggest mysteries of biology and at the heart of this enigma is the physical interpretation of sleep homeostasis. One can hope that the identification of cortex as a putatively active player in the homeostatic process will contribute to solving this mystery. The identification of molecular and circuit mechanisms will further allow manipulation of sleep homeostasis using perturbational methods. The final paragraph dedicated to a rather speculative outlook on the clinical perspective of manipulating sleep homeostasis through targeting cortex.

## 6.6 Clinical implications of cortical sleep regulation

In a clinical context, for the majority of patients presenting with disturbed sleep, no pathophysiological cause can be established. The view that cortex is actively involved in the homeostatic regulation of sleep might change our diagnostic perspective and therapeutic options. For example stroke patients commonly report sleep disturbances (Gottlieb et al. 2019). However, it was only recently found that perilesional cortex can engage in local sleep-like activity during wakefulness (Sarasso et al. 2021). While it has been established that the size of cortical lesions correlates with the degree of sleep disruption, it has not been considered that local sleep like activity, which is thought to convey behavioural impairment (Vyazovskiy et al. 2011), might be contributing to the global sleep disruption observed in stroke patients (Krone and Vyazovskiy 2020). One could imagine that cortical pathology might further contribute to so far unexplained sleep changes in neurodegenerative and neuroinflammatory disorders.

As the most superficial structure of the mammalian brain, neocortex provides the primary target for non-invasive brain stimulation (Krone et al. 2016). Interestingly, due to their neuroanatomical features, layer 5 pyramidal neurons are strongly modulated by transcranial electric and magnetic stimulation methods (Di Lazzaro, Rothwell, and Capogna 2018; S. C. Murphy et al. 2016). Sleep oscillations can be effectively modulated with non-invasive brain stimulation with functional consequences for sleep-related memory consolidation and neuroplasticity (Fattinger et al. 2017; Ngo et al. 2013; Marshall et al. 2006). Previous work, I was involved with as a medical student at the University of Freiburg, Germany, also suggests that total sleep time can be modulated by transcranial direct current stimulation (Frase et al. 2016), a method that changes cortical excitability (Nitsche and Paulus 2000) and cortical neurotransmitter levels (Stagg et al. 2009), with widespread network effects (Stagg et al. 2013). Considering that the prefrontal cortex might be most sensitive to homeostatic sleep debt and

might signal the need for sleep to subcortical centres of sleep-wake control, it appears conceivable that non-invasive modulation of neocortex could become a therapeutic approach to modulate sleep.

Most of the substances currently marketed as sleep medication are in principle sedatives (Riemann and Nissen 2012). Due to the range of side effects and the addictive potential of benzodiazepine receptor agonists, these substances are not recommended for long term use in patients with insomnia (Wilson et al. 2019; Riemann et al. 2019) and we have recently shown that benzodiazepines profoundly disturb physiological cortical firing patterns during sleep (McKillop et al. 2021). One would hope that targeting the intrinsic cortical mechanisms of sleep homeostasis could induce sleep through manipulation of the core mechanisms underlying sleep initiation rather than pushing one side of the sleep switch. This might allow rapid state reversibility, reduce the memory impact of sedating sleep drugs, and circumvent the problem of addiction. Overall, cortex provides a novel and unexplored target both for the neurobiological investigation of sleep homeostasis and for its manipulation in the clinical context.

*"Imagine we once had an effective method of influencing deep lying centers, in this case the exact knowledge of the localization of the center for sleep regulation, which I have attempted to give you, would make it possible to treat insomnia and other sleep disturbances in a better and more active way than by drugs or by the roundabout way of hydrotherapy and psychotherapy."*

Constantin von Economo

# Bibliography

Achermann, Peter, and Alexander A. Borbély. 1998. “Coherence Analysis of the Human Sleep Electroencephalogram.” *Neuroscience* 85 (4): 1195–1208. https://doi.org/10.1016/s0306-4522(97)00692-1.

———. 2003. “Mathematical Models of Sleep Regulation.” *Frontiers in Bioscience : A Journal and Virtual Library* 8 (6): s683-93. https://doi.org/10.2741/1064.

Achermann, Peter, Derk-Jan Dijk, Daniel P. Brunner, and Alexander A. Borbély. 1993. “A Model of Human Sleep Homeostasis Based on EEG Slow-Wave Activity: Quantitative Comparison of Data and Simulations.” *Brain Research Bulletin* 31 (1–2): 97–113. https://doi.org/10.1016/0361-9230(93)90016-5.

Adamantidis, Antoine, Carolina Gutierrez Herrera, and Thomas C Gent. 2019. “Oscillating Circuitries in the Sleeping Brain.” *Nature Reviews Neuroscience* 20 (12): 746–62. https://doi.org/10.1038/s41583-019-0223-4.

Adamantidis, Antoine, Feng Zhang, Alexander M Aravanis, Karl Deisseroth, Luis De Lecea, and Luis de Lecea. 2007. “Neural Substrates of Awakening Probed with Optogenetic Control of Hypocretin Neurons.” *Nature* 450 (7168): 420–24. https://doi.org/10.1038/nature06310.

Aerde, Karlijn I van, Guanxiao Qi, and Dirk Feldmeyer. 2015. “Cell Type-Specific Effects of Adenosine on Cortical Neurons.” *Cerebral Cortex* 25 (3): 772–87. https://doi.org/10.1093/cercor/bht274.

Akert, K, W P Koella, and R Jr Hess. 1952. “Sleep Produced by Electrical Stimulation of the Thalamus.” *The American Journal of Physiology* 168 (1): 260–67. https://doi.org/10.1152/ajplegacy.1951.168.1.260.

Alam, Md. Aftab, Sunil Kumar, Dennis McGinty, Md. Noor Alam, and Ronald Szymusiak. 2013. “Neuronal Activity in the Preoptic Hypothalamus during Sleep Deprivation and Recovery Sleep.” *Journal of Neurophysiology* 111 (2): 287–99. https://doi.org/10.1152/jn.00504.2013.

Albrecht, Urs, and Russell G. Foster. 2002. “Placing Ocular Mutants into a Functional Context: A Chronobiological Approach.” *Methods* 28 (4): 465–77. https://doi.org/10.1016/S1046-2023(02)00266-9.

Alexander, Georgia M, Sarah C Rogan, Atheir I Abbas, Blaine N Armbruster, Ying Pei, John A Allen, Randal J Nonneman, et al. 2009. “Remote Control of Neuronal Activity in Transgenic Mice Expressing Evolved G Protein-Coupled Receptors.” *Neuron* 63 (1): 27–39. https://doi.org/10.1016/j.neuron.2009.06.014.

Allada, Ravi, Chiara Cirelli, and Amita Sehgal. 2017. “Molecular Mechanisms of Sleep Homeostasis in Flies and Mammals.” *Cold Spring Harbor Perspectives in Biology* 9 (8): a027730. https://doi.org/10.1101/cshperspect.a027730.

Allen, Daicia C, Timothy L. Carlson, Yan Xiong, Jian Jin, Kathleen A Grant, and Verginia C. Cuzon Carlson. 2019. “A Comparative Study of the Pharmacokinetics of Clozapine N -Oxide and Clozapine N -Oxide Hydrochloride Salt in Rhesus Macaques.” *Journal of Pharmacology and Experimental Therapeutics* 368 (2): 199–207. https://doi.org/10.1124/jpet.118.252031.

Allen, S R, and I Oswald. 1973. “The Effects of Perlapine on Sleep.” *Psychopharmacologia* 32 (1): 1–9. https://doi.org/10.1007/BF00421703.

Anaclet, Christelle, Nigel P Pedersen, Loris L Ferrari, Anne Venner, Caroline E Bass, Elda Arrigoni, and Patrick M Fuller. 2015. “Basal Forebrain Control of Wakefulness and Cortical Rhythms.” *Nature Communications* 6 (1): 8744. https://doi.org/10.1038/ncomms9744.

Anafi, Ron C, Matthew S Kayser, and David M Raizen. 2019. “Exploring Phylogeny to Find the Function of Sleep.” *Nature Reviews Neuroscience* 20 (2): 109–16. https://doi.org/10.1038/s41583-018-0098-9.

Ando, Susumu, Masaaki Ishido, Yoshio Hayano, Tadanori Seino, Yoichiro Orihashi, Kenzo Katoh, Tetsuya Suzuki, Satoru Kutzkake, and Michinobu Haga. 1970. “A Comparative Study of the New Hypnotics Perlapine and Nitrazepam.” *Rinsho Yakuri/Japanese Journal of Clinical Pharmacology and Therapeutics* 1 (3–4): 172–80. https://doi.org/10.3999/jscpt.1.172.

Andrillon, Thomas, Angus Burns, Teigane Mackay, Jennifer Windt, and Naotsugu Tsuchiya. 2021. “Predicting Lapses of Attention with Sleep-like Slow Waves.” *Nature Communications* 12 (1): 3657. https://doi.org/10.1038/s41467-021-23890-7.

Armbruster, Blaine N, Xiang Li, Mark H Pausch, Stefan Herlitze, and Bryan L Roth. 2007. “Evolving the Lock to Fit the Key to Create a Family of G Protein-Coupled Receptors Potently Activated by an Inert Ligand.” *Proceedings of the National Academy of Sciences* 104 (12): 5163 LP – 5168. https://doi.org/10.1073/pnas.0700293104.

Aschoff, Jürgen. 1965. “Circadian Rhythms in Man.” *Science* 148 (3676): 1427–32.

Baker, Arielle, Brian Kalmbach, Mieko Morishima, Juhyun Kim, Ashley Juavinett, Nuo Li, and Nikolai Dembrow. 2018. “Specialized Subpopulations of Deep-Layer Pyramidal Neurons in the Neocortex: Bridging Cellular Properties to Functional Consequences.” *The Journal of Neuroscience* 38 (24): 5441 LP – 5455. https://doi.org/10.1523/JNEUROSCI.0150-18.2018.

Balaram, Pooja, Nicole A Young, and Jon H Kaas. 2014. “Histological Features of Layers and Sublayers in Cortical Visual Areas V1 and V2 of Chimpanzees, Macaque Monkeys, and Humans.” *Eye and Brain* 2014 (6 Suppl 1): 5–18. https://doi.org/10.2147/EB.S51814.

Banks, Gareth T, Mathilde C C Guillaumin, Ines Heise, Petrina Lau, Minghui Yin, Nora Bourbia, Carlos Aguilar, et al. 2020. “Forward Genetics Identifies a Novel Sleep Mutant with Sleep State Inertia and REM Sleep Deficits.” *Science Advances* 6 (33): eabb3567–eabb3567. https://doi.org/10.1126/sciadv.abb3567.

Bassetti, Claudio L A, Antoine Adamantidis, Denis Burdakov, Fang Han, Steffen Gay, Ulf Kallweit, Ramin Khatami, et al. 2019. “Narcolepsy — Clinical Spectrum, Aetiopathophysiology, Diagnosis and Treatment.” *Nature Reviews Neurology* 15 (9): 519–39. https://doi.org/10.1038/s41582-019-0226-9.

Beltramo, Riccardo, Giulia D’Urso, Marco Dal Maschio, Pasqualina Farisello, Serena Bovetti, Yoanne Clovis, Glenda Lassi, Valter Tucci, Davide De Pietri Tonelli, and Tommaso Fellin. 2013. “Layer-Specific Excitatory Circuits Differentially Control Recurrent Network Dynamics in the Neocortex.” *Nature Neuroscience* 16 (2): 227–34. https://doi.org/10.1038/nn.3306.

Berger, Hans. 1929. “Über Das Elektrenkephalogramm Des Menschen.” *Archiv Für Psychiatrie Und Nervenkrankheiten* 87 (1): 527–70. https://doi.org/10.1007/BF01797193.

Bjorness, Theresa E, Nicholas Dale, Gabriel Mettlach, Alex Sonneborn, Bogachan Sahin, Allen A Fienberg, Masashi Yanagisawa, James A Bibb, and Robert W Greene. 2016. “An Adenosine-Mediated Glial-Neuronal Circuit for Homeostatic Sleep.” *The Journal of Neuroscience* 36 (13): 3709 LP – 3721. http://www.jneurosci.org/content/36/13/3709.abstract.

Blake, H, and R. W. Gerard. 1937. “Brain Potentials during Sleep.” *American Journal of Physiology--Legacy Content* 119 (4): 692–703.

Blakey, Daniel, Michael C Wilson, and Zoltán Molnár. 2012. “Termination and Initial Branch Formation of SNAP-25-Deficient Thalamocortical Fibres in Heterochronic Organotypic Co-Cultures.” *The European Journal of Neuroscience* 35 (10): 1586–94. https://doi.org/10.1111/j.1460-9568.2012.08120.x.

Boender, Arjen J, Leonardo Bontempi, Luca Nava, Yann Pelloux, and Raffaella Tonini. 2021. “Striatal Astrocytes Shape Behavioral Flexibility via Regulation of the Glutamate Transporter EAAT2.” *Biological Psychiatry* 89 (11): 1045–57. https://doi.org/10.1016/j.biopsych.2020.11.015.

Bojarskaite, Laura, Daniel M Bjørnstad, Klas H Pettersen, Céline Cunen, Gudmund Horn Hermansen, Knut Sindre Åbjørsbråten, Anna R Chambers, et al. 2020. “Astrocytic Ca(2+) Signaling Is Reduced during Sleep and Is Involved in the Regulation of Slow Wave Sleep.” *Nature Communications* 11 (1): 3240. https://doi.org/10.1038/s41467-020-17062-2.

Bon-Jego, Morgane Le, and Rafael Yuste. 2007. “Persistently Active, Pacemaker-like Neurons in Neocortex.” *Frontiers in Neuroscience* 1 (1): 123–29. https://doi.org/10.3389/neuro.01.1.1.009.2007.

Borbély, Alexander A. 1982. “A Two Process Model of Sleep Regulation.” *Human Neurobiology* 1 (3): 195–204.

Borbély, Alexander A., Peter Achermann, L Trachsel, and Irene Tobler. 1989. “Sleep Initiation and Initial Sleep Intensity: Interactions of Homeostatic and Circadian Mechanisms.” *Journal of Biological Rhythms* 4 (2): 149–60.

Borbély, Alexander A., Fritz Baumann, Daniel Brandeis, Inge Strauch, and Dietrich Lehmann. 1981. “Sleep Deprivation: Effect on Sleep Stages and EEG Power Density in Man.” *Electroencephalography and Clinical Neurophysiology* 51 (5): 483–93. https://doi.org/https://doi.org/10.1016/0013-4694(81)90225-X.

Borbély, Alexander A., Serge Daan, Anna Wirz-Justice, and Tom Deboer. 2016. “The Two-Process Model of Sleep Regulation: A Reappraisal.” *Journal of Sleep Research* 25 (2): 131–43. https://doi.org/10.1111/jsr.12371.

Borbély, Alexander A., and Hans Ulrich Neuhaus. 1979. “Sleep-Deprivation: Effects on Sleep and EEG in the Rat.” *Journal of Comparative Physiology A* 133 (1): 71–87. https://doi.org/10.1007/BF00663111.

Borbély, Alexander A., Irene Tobler, and Mehmet Hanagasioglu. 1984. “Effect of Sleep Deprivation on Sleep and EEG Power Spectra in the Rat.” *Behavioural Brain Research* 14 (3): 171–82. https://doi.org/https://doi.org/10.1016/0166-4328(84)90186-4.

Bronk, Peter, Ferenc Deák, Michael C Wilson, Xinran Liu, Thomas C Südhof, and Ege T Kavalali. 2007. "Differential Effects of SNAP-25 Deletion on Ca2+-Dependent and Ca2+-Independent Neurotransmission." *Journal of Neurophysiology* 98 (2): 794–806. https://doi.org/10.1152/jn.00226.2007.

Brown, Laurence, Angus Fisk, Carina Pothecary, and Stuart Peirson. 2019. "Telling the Time with a Broken Clock: Quantifying Circadian Disruption in Animal Models." *Biology* 8 (1): 18. https://doi.org/10.3390/biology8010018.

Brown, Laurence, Sibah Hasan, Russell G. Foster, and Stuart N Peirson. 2016. "COMPASS: Continuous Open Mouse Phenotyping of Activity and Sleep Status." *Wellcome Open Research* 1: 2. https://doi.org/10.12688/wellcomeopenres.9892.2.

Brüning, Franziska, Sara B Noya, Tanja Bange, Stella Koutsouli, Jan D Rudolph, Shiva K Tyagarajan, Jürgen Cox, Matthias Mann, Steven A Brown, and Maria S Robles. 2019. "Sleep-Wake Cycles Drive Daily Dynamics of Synaptic Phosphorylation." *Science* 366 (6462): eaav3617. https://doi.org/10.1126/science.aav3617.

Buzsáki, György, Costas A. Anastassiou, and Christof Koch. 2012. "The Origin of Extracellular Fields and Currents — EEG, ECoG, LFP and Spikes." *Nature Reviews Neuroscience* 13 (6): 407–20. https://doi.org/10.1038/nrn3241.

Buzsáki, György, Eran Stark, Antal Berényi, Dion Khodagholy, Daryl R. Kipke, Euisik Yoon, and Kensall D. Wise. 2015. "Tools for Probing Local Circuits: High-Density Silicon Probes Combined with Optogenetics." *Neuron* 86 (1): 92–105. https://doi.org/10.1016/j.neuron.2015.01.028.

Cajochen, C, D P Brunner, K Krauchi, P Graw, and a Wirz-Justice. 1995. "Power Density in Theta/Alpha Frequencies of the Waking EEG Progressively Increases during Sustained Wakefulness." *Sleep* 18 (10): 890–94. https://doi.org/Cited By (since 1996) 113\nExport Date 14 February 2012.

Cajochen, C, R Foy, and Derk-Jan Dijk. 1999. "Frontal Predominance of a Relative Increase in Sleep Delta and Theta EEG Activity after Sleep Loss in Humans." *Sleep Research Online : SRO* 2 (3): 65–69. https://doi.org/10.1016/j.neuroimage.2008.04.236.

Campbell, Erin J, and Nathan J Marchant. 2018. "The Use of Chemogenetics in Behavioural Neuroscience: Receptor Variants, Targeting Approaches and Caveats." *British Journal of Pharmacology* 175 (7): 994–1003. https://doi.org/10.1111/bph.14146.

Campbell, Scott S., and Irene Tobler. 1984. "Animal Sleep: A Review of Sleep Duration across Phylogeny." *Neuroscience and Biobehavioral Reviews* 8 (3): 269–300. https://doi.org/10.1016/0149-7634(84)90054-X.

Carter, Matthew E, Ofer Yizhar, Sachiko Chikahisa, Hieu Nguyen, Antoine Adamantidis, Seiji Nishino, Karl Deisseroth, and Luis de Lecea. 2010. "Tuning Arousal with Optogenetic Modulation of Locus Coeruleus Neurons." *Nature Neuroscience* 13 (12): 1526–33. https://doi.org/10.1038/nn.2682.

Challet, Etienne, Fred W Turek, Marie-Aline Laute, and Olivier Van Reeth. 2001. "Sleep Deprivation Decreases Phase-Shift Responses of Circadian Rhythms to Light in the Mouse: Role of Serotonergic and Metabolic Signals." *Brain Research* 909 (1): 81–91. https://doi.org/https://doi.org/10.1016/S0006-8993(01)02625-7.

Chang, Chih-Hua, and Po-Wu Gean. 2019. "The Ventral Hippocampus Controls Stress-Provoked Impulsive Aggression through the Ventromedial Hypothalamus in Post-Weaning Social Isolation Mice." *Cell Reports* 28 (5): 1195-1205.e3. https://doi.org/10.1016/j.celrep.2019.07.005.

Chauvette, Sylvain, Maxim Volgushev, and Igor Timofeev. 2010. "Origin of Active States in Local Neocortical Networks during Slow Sleep Oscillation." *Cerebral Cortex* 20 (11): 2660–74. https://doi.org/10.1093/cercor/bhq009.

Chemelli, R M, J T Willie, C M Sinton, J K Elmquist, T Scammell, C Lee, J A Richardson, et al. 1999. "Narcolepsy in Orexin Knockout Mice: Molecular Genetics of Sleep Regulation." *Cell* 98 (4): 437–51. https://doi.org/10.1016/S0092-8674(00)81973-X.

Chen, Lichao, Jeannine A Majde, and James M Krueger. 2003. "Spontaneous Sleep in Mice with Targeted Disruptions of Neuronal or Inducible Nitric Oxide Synthase Genes." *Brain Research* 973 (2): 214–22. https://doi.org/https://doi.org/10.1016/S0006-8993(03)02484-3.

Chen, Xin, Hyunah Choo, Xi-Ping Huang, Xiaobao Yang, Orrin Stone, Bryan L Roth, and Jian Jin. 2015. "The First Structure-Activity Relationship Studies for Designer Receptors Exclusively Activated by Designer Drugs." *ACS Chemical Neuroscience* 6 (3): 476–84. https://doi.org/10.1021/cn500325v.

Chou, Thomas C, Thomas E Scammell, Joshua J Gooley, Stephanie E Gaus, Clifford B Saper, and Jun Lu. 2003. "Critical Role of Dorsomedial Hypothalamic Nucleus in a Wide Range of Behavioral Circadian Rhythms." *Journal of Neuroscience* 23 (33): 10691–702.

Chung, Shinjae, Franz Weber, Peng Zhong, Chan Lek Tan, Thuc Nghi Nguyen, Kevin T Beier, Nikolai Hörmann, et al. 2017. "Identification of Preoptic Sleep Neurons Using Retrograde Labelling and Gene Profiling." *Nature* 545 (7655): 477–81. https://doi.org/10.1038/nature22350.

Cirelli, Chiara, and Giulio Tononi. 2008. "Is Sleep Essential?" *PLoS Biology* 6 (8): 1605–11. https://doi.org/10.1371/journal.pbio.0060216.

Clinton, James M., Christopher J. Davis, Mark R. Zielinski, Kathryn A. Jewett, and James Krueger. 2011. "Biochemical Regulation of Sleep and Sleep Biomarkers." *Journal of Clinical Sleep Medicine* 7 (5). https://doi.org/10.5664/JCSM.1360.

Comas, M, D G M Beersma, K Spoelstra, and S Daan. 2006. "Phase and Period Responses of the Circadian System of Mice (Mus Musculus) to Light Stimuli of Different Duration." *Journal of Biological Rhythms* 21 (5): 362–72. https://doi.org/10.1177/0748730406292446.

Contreras, D, and Mircea Steriade. 1995. "Cellular Basis of EEG Slow Rhythms: A Study of Dynamic Corticothalamic Relationships." *The Journal of Neuroscience : The Official Journal of the Society for Neuroscience* 15 (1 Pt 2): 604–22. https://doi.org/10.1523/JNEUROSCI.15-01-00604.1995.

Crunelli, Vincenzo, and Stuart W Hughes. 2010. "The Slow (<1 Hz) Rhythm of Non-REM Sleep: A Dialogue between Three Cardinal Oscillators." *Nature Neuroscience* 13 (1): 9–17. https://doi.org/10.1038/nn.2445.

Cui, Yilong, Yosky Kataoka, Takashi Inui, Takatoshi Mochizuki, Hirotaka Onoe, Kiyoshi Matsumura, Yoshihiro Urade, Hisao Yamada, and Yasuyoshi Watanabe. 2008. "Up-Regulated Neuronal COX-2 Expression after Cortical Spreading Depression Is Involved in Non-REM Sleep Induction in Rats." *Journal of Neuroscience Research* 86 (4): 929–36. https://doi.org/10.1002/jnr.21531.

Daan, Serge, Domien G. M. Beersma, and Alexander A. Borbély. 1984. "Timing of Human Sleep: Recovery Process Gated by a Circadian Pacemaker." *The American Journal of Physiology* 246 (2 Pt 2): R161-83. http://www.ncbi.nlm.nih.gov/pubmed/6696142.

David, François, Joscha T Schmiedt, Hannah L Taylor, Gergely Orban, Giuseppe Di Giovanni, Victor N Uebele, John J Renger, Régis C Lambert, Nathalie Leresche, and Vincenzo Crunelli. 2013. "Essential Thalamic Contribution to Slow Waves of Natural Sleep." *Journal of Neuroscience* 33 (50): 19599–610. https://doi.org/10.1523/JNEUROSCI.3169-13.2013.

Davis, C J, J M Clinton, K A Jewett, M R Zielinski, and James Krueger. 2011. "Delta Wave Power: An Independent Sleep Phenotype or Epiphenomenon?" *Journal of Clinical Sleep Medicine* 7 (5): S16–18. https://doi.org/10.5664/JCSM.1346.

Deboer, Tom. 2009. "Sleep and Sleep Homeostasis in Constant Darkness in the Rat." *Journal of Sleep Research* 18 (3): 357–64. https://doi.org/10.1111/j.1365-2869.2008.00728.x.

———. 2018. "Sleep Homeostasis and the Circadian Clock: Do the Circadian Pacemaker and the Sleep Homeostat Influence Each Other's Functioning?" *Neurobiology of Sleep and Circadian Rhythms* 5: 68–77. https://doi.org/https://doi.org/10.1016/j.nbscr.2018.02.003.

Deboer, Tom, Mariska J Vansteensel, László Détári, and Johanna H Meijer. 2003. "Sleep States Alter Activity of Suprachiasmatic Nucleus Neurons." *Nature Neuroscience* 6 (10): 1086–90. https://doi.org/10.1038/nn1122.

Dibner, Charna, Ueli Schibler, and Urs Albrecht. 2010. "The Mammalian Circadian Timing System: Organization and Coordination of Central and Peripheral Clocks." *Annual Review of Physiology* 72 (1): 517–49. https://doi.org/10.1146/annurev-physiol-021909-135821.

Diering, Graham H, Raja S Nirujogi, Richard H Roth, Paul F Worley, Akhilesh Pandey, and Richard L Huganir. 2017. "Homer1a Drives Homeostatic Scaling-down of Excitatory Synapses during Sleep." *Science* 355 (6324): 511–15.

Dijk, Derk-Jan. 1995. "EEG Slow Waves and Sleep Spindles: Windows on the Sleeping Brain." *Behavioural Brain Research* 69 (1–2): 109–16. https://doi.org/10.1016/0166-4328(95)00007-G.

Dijk, Derk-Jan, D G Beersma, and Serge Daan. 1987. "EEG Power Density during Nap Sleep: Reflection of an Hourglass Measuring the Duration of Prior Wakefulness." *Journal of Biological Rhythms* 2 (3): 207–19. https://doi.org/10.1177/074873048700200304.

Dijk, Derk-Jan, and CA Czeisler. 1995. "Contribution of the Circadian Pacemaker and the Sleep Homeostat to Sleep Propensity, Sleep Structure, Electroencephalographic Slow Waves, and Sleep Spindle Activity in Humans." *The Journal of Neuroscience* 15 (5): 3526–38. https://doi.org/10.1523/JNEUROSCI.15-05-03526.1995.

Dittrich, Lars, Stephen R Morairty, Deepti R Warrier, and Thomas S Kilduff. 2015. "Homeostatic Sleep Pressure Is the Primary Factor for Activation of Cortical NNOS/NK1 Neurons." *Neuropsychopharmacology : Official Publication of the American College of Neuropsychopharmacology* 40 (3): 632–39. https://doi.org/10.1038/npp.2014.212.

Dongen, Hans P A Van, Gregory Belenky, and James M Krueger. 2011. "A Local, Bottom-up Perspective on Sleep Deprivation and Neurobehavioral Performance." *Current Topics in Medicinal Chemistry* 11 (19): 2414–22. https://doi.org/10.2174/156802611797470286.

Dort, C J Van, H A Baghdoyan, and R Lydic. 2009. "Adenosine A1 and A2A Receptors in Mouse Prefrontal Cortex Modulate Acetylcholine Release and Behavioral Arousal." *Journal of Neuroscience* 29 (3): 871–81. https://doi.org/10.1523/JNEUROSCI.4111-08.2009.

Eban-Rothschild, Ada, Gideon Rothschild, William J Giardino, Jeff R Jones, and Luis de Lecea. 2016. "VTA Dopaminergic Neurons Regulate Ethologically Relevant Sleep–Wake Behaviors." *Nature Neuroscience* 19 (10): 1356–66. https://doi.org/10.1038/nn.4377.

Economo, C V. 1930. "Sleep as a Problem of Localization." *The Journal of Nervous and Mental Disease* 71 (3): 249–59.

Eichenbaum, Howard. 2017. "On the Integration of Space, Time, and Memory." *Neuron* 95 (5): 1007–18. https://doi.org/https://doi.org/10.1016/j.neuron.2017.06.036.

Erickson, Evelyn T M, Loris L Ferrari, Heinrich S Gompf, and Christelle Anaclet. 2019. "Differential Role of Pontomedullary Glutamatergic Neuronal Populations in Sleep-Wake Control." *Frontiers in Neuroscience*. https://www.frontiersin.org/article/10.3389/fnins.2019.00755.

Fanselow, Erika E, Kristen A Richardson, and Barry W Connors. 2008. "Selective, State-Dependent Activation of Somatostatin-Expressing Inhibitory Interneurons in Mouse Neocortex." *Journal of Neurophysiology* 100 (5): 2640–52. https://doi.org/10.1152/jn.90691.2008.

Faraguna, Ugo, Aaron Nelson, Vladyslav V. Vyazovskiy, Chiara Cirelli, and Giulio Tononi. 2010. "Unilateral Cortical Spreading Depression Affects Sleep Need and Induces Molecular and Electrophysiological Signs of Synaptic Potentiation In Vivo." *Cerebral Cortex* 20 (12): 2939–47. https://doi.org/10.1093/cercor/bhq041.

Fattinger, Sara, Toon T de Beukelaar, Kathy L Ruddy, Carina Volk, Natalie C Heyse, Joshua A Herbst, Richard H R Hahnloser, Nicole Wenderoth, and Reto Huber. 2017. "Deep Sleep Maintains Learning Efficiency of the Human Brain." *Nature Communications* 8 (May): 15405. https://doi.org/10.1038/ncomms15405.

Faul, Franz, Edgar Erdfelder, Albert-Georg Lang, and Axel Buchner. 2007. "G*Power 3: A Flexible Statistical Power Analysis Program for the Social, Behavioral, and Biomedical Sciences." *Behavior Research Methods* 39 (2): 175–91. https://doi.org/10.3758/bf03193146.

Fernandez, Laura M J, and Anita Lüthi. 2019. "Sleep Spindles: Mechanisms and Functions." *Physiological Reviews* 100 (2): 805–68. https://doi.org/10.1152/physrev.00042.2018.

Fernandez, Laura M J, Gil Vantomme, Alejandro Osorio-Forero, Romain Cardis, Elidie Béard, and Anita Lüthi. 2018. "Thalamic Reticular Control of Local Sleep in Mouse Sensory Cortex." Edited by John Huguenard and Andrew J King. *ELife* 7: e39111. https://doi.org/10.7554/eLife.39111.

Fiacco, Todd A, and Ken D McCarthy. 2018. "Multiple Lines of Evidence Indicate That Gliotransmission Does Not Occur under Physiological Conditions." *The Journal of Neuroscience* 38 (1): 3 LP – 13. https://doi.org/10.1523/JNEUROSCI.0016-17.2017.

Finelli, L. A., H. Baumann, Alexander A. Borbély, and Peter Achermann. 2000. "Dual Electroencephalogram Markers of Human Sleep Homeostasis: Correlation between Theta Activity in Waking and Slow-Wave Activity in Sleep." *Neuroscience* 101 (3): 523–29. https://doi.org/10.1016/S0306-4522(00)00409-7.

Fleury Curado, Thomaz A, Huy Pho, Olga Dergacheva, Slava Berger, Rachel Lee, Carla Freire, Aya Asherov, et al. 2018. "Silencing of Hypoglossal Motoneurons Leads to Sleep Disordered Breathing in Lean Mice." *Frontiers in Neurology*. https://www.frontiersin.org/article/10.3389/fneur.2018.00962.

Frank, M G, and H C Heller. 2019. "The Function(s) of Sleep." *Handbook of Experimental Pharmacology*. Department of Biomedical Sciences, Elson S. Floyd College of Medicine, Washington State University Spokane, Spokane, WA, United States: Springer New York LLC. https://doi.org/10.1007/164_2018_140.

Franken, P, Derk-Jan Dijk, Irene Tobler, and Alexander A. Borbély. 1991. "Sleep Deprivation in Rats: Effects on EEG Power Spectra, Vigilance States, and Cortical Temperature." *American Journal of Physiology-Regulatory, Integrative and Comparative Physiology* 261 (1): R198–208. https://doi.org/10.1152/ajpregu.1991.261.1.R198.

Franken, P, A Malafosse, and M Tafti. 1999. "Genetic Determinants of Sleep Regulation in Inbred Mice." *Sleep* 22 (2): 155–69. https://www.scopus.com/inward/record.uri?eid=2-s2.0-0033559893&partnerID=40&md5=d97d8c0915f7e84511a76874fcfab91b.

Franks, Nicholas P. 2008. "General Anaesthesia: From Molecular Targets to Neuronal Pathways of Sleep and Arousal." *Nature Reviews Neuroscience* 9 (5): 370–86. https://doi.org/10.1038/nrn2372.

Frase, Lukas, Hannah Piosczyk, Sulamith Zittel, Friederike Jahn, Peter Selhausen, Lukas B Krone, Bernd Feige, et al. 2016. "Modulation of Total Sleep Time by Transcranial Direct Current Stimulation (TDCS)." *Neuropsychopharmacology* 41 (10): 2577–86. https://doi.org/10.1038/npp.2016.65.

Fujita, Takumi, Michael J Chen, Baoman Li, Nathan A Smith, Weiguo Peng, Wei Sun, Michael J Toner, et al. 2014. "Neuronal Transgene Expression in Dominant-Negative SNARE Mice." *The Journal of Neuroscience* 34 (50): 16594 LP – 16604. https://doi.org/10.1523/JNEUROSCI.2585-14.2014.

Funato, Hiromasa, Chika Miyoshi, Tomoyuki Fujiyama, Takeshi Kanda, Makito Sato, Zhiqiang Wang, Jing Ma, et al. 2016. "Forward-Genetics Analysis of Sleep in Randomly Mutagenized Mice." *Nature* 539 (7629): 378–83. https://doi.org/10.1038/nature20142.

Funk, Chadd M., Sakiko Honjoh, Alexander V. Rodriguez, Chiara Cirelli, and Giulio Tononi. 2016. "Local Slow Waves in Superficial Layers of Primary Cortical Areas during REM Sleep." *Current Biology* 26 (3): 396–403. https://doi.org/10.1016/j.cub.2015.11.062.

Funk, Chadd M., Kayla Peelman, Michele Bellesi, William Marshall, Chiara Cirelli, and Giulio Tononi. 2017. "Role of Somatostatin-Positive Cortical Interneurons in the Generation of Sleep Slow Waves." *The Journal of Neuroscience* 37 (38): 9132–48. https://doi.org/10.1523/JNEUROSCI.1303-17.2017.

Gent, Thomas C, Mojtaba Bandarabadi, Carolina Gutierrez Herrera, and Antoine Adamantidis. 2018. "Thalamic Dual Control of Sleep and Wakefulness." *Nature Neuroscience* 21 (7): 974–84. https://doi.org/10.1038/s41593-018-0164-7.

Gerashchenko, Dmitry, Jonathan P Wisor, Deirdre Burns, Rebecca K Reh, Priyattam J Shiromani, Takeshi Sakurai, Horacio O de la Iglesia, and Thomas S Kilduff. 2008. "Identification of a Population of Sleep-Active Cerebral Cortex Neurons." *Proceedings of the National Academy of Sciences of the United States of America* 105 (29): 10227–32. https://doi.org/10.1073/pnas.0803125105.

Gerfen, Charles R., Ronald Paletzki, and Nathaniel Heintz. 2013. "GENSAT BAC Cre-Recombinase Driver Lines to Study the Functional Organization of Cerebral Cortical and Basal Ganglia Circuits." *Neuron* 80 (6): 1368–83. https://doi.org/10.1016/j.neuron.2013.10.016.

Gomez, Juan L, Jordi Bonaventura, Wojciech Lesniak, William B Mathews, Polina Sysa-Shah, Lionel A Rodriguez, Randall J Ellis, et al. 2017. "Chemogenetics Revealed: DREADD Occupancy and Activation via Converted Clozapine." *Science* 357 (6350): 503–7. https://doi.org/10.1126/science.aan2475.

Gong, Hui, Dennis McGinty, Ruben Guzman-Marin, Keng-Tee Chew, Darya Stewart, and Ronald Szymusiak. 2004. "Activation of C-Fos in GABAergic Neurones in the Preoptic Area during Sleep and in Response to Sleep Deprivation." *The Journal of Physiology* 556 (3): 935–46. https://doi.org/https://doi.org/10.1113/jphysiol.2003.056622.

Gong, Shiaoching, Martin Doughty, Carroll R Harbaugh, Alexander Cummins, Mary E Hatten, Nathaniel Heintz, and Charles R Gerfen. 2007. "Targeting Cre Recombinase to Specific Neuron Populations with Bacterial Artificial Chromosome Constructs." *Journal of Neuroscience* 27 (37): 9817–23. https://doi.org/10.1523/JNEUROSCI.2707-07.2007.

González-Rueda, Ana, Victor Pedrosa, Rachael C. Feord, Claudia Clopath, and Ole Paulsen. 2018. "Activity-Dependent Downscaling of Subthreshold Synaptic Inputs during Slow-Wave-Sleep-like Activity In Vivo." *Neuron* 97 (6): 1244-1252.e5. https://doi.org/10.1016/j.neuron.2018.01.047.

Gottlieb, Elie, Elizabeth Landau, Helen Baxter, Emilio Werden, Mark E Howard, and Amy Brodtmann. 2019. "The Bidirectional Impact of Sleep and Circadian Rhythm Dysfunction in Human Ischaemic Stroke: A Systematic Review." *Sleep Medicine Reviews* 45: 54–69. https://doi.org/https://doi.org/10.1016/j.smrv.2019.03.003.

Goutaudier, Raphaël, Véronique Coizet, Carole Carcenac, and Sebastien Carnicella. 2020. "Compound 21, a Two-Edged Sword with Both DREADD-Selective and off-Target Outcomes in Rats." *PloS One* 15 (9): e0238156. https://doi.org/10.1371/journal.pone.0238156.

Grant, Eleanor, Anna Hoerder-Suabedissen, and Zoltán Molnár. 2016. "The Regulation of Corticofugal Fiber Targeting by Retinal Inputs." *Cerebral Cortex* 26 (3): 1336–48. https://doi.org/10.1093/cercor/bhv315.

Greene, Robert W., Theresa E. Bjorness, and Ayako Suzuki. 2017. "The Adenosine-Mediated, Neuronal-Glial, Homeostatic Sleep Response." *Current Opinion in Neurobiology* 44: 236–42. https://doi.org/10.1016/j.conb.2017.05.015.

Grønli, Janne, William C Clegern, Michelle A Schmidt, Rahmi S Nemri, Michael J Rempe, Amelia L Gallitano, and Jonathan P Wisor. 2016. "Sleep Homeostatic and Waking Behavioral Phenotypes in Egr3-Deficient Mice Associated with Serotonin Receptor 5-HT(2) Deficits." *Sleep* 39 (12): 2189–99. https://doi.org/10.5665/sleep.6324.

Guettier, Jean-Marc, Dinesh Gautam, Marco Scarselli, Inigo Ruiz de Azua, Jian Hua Li, Erica Rosemond, Xiaochao Ma, et al. 2009. “A Chemical-Genetic Approach to Study G Protein Regulation of β Cell Function in Vivo.” *Proceedings of the National Academy of Sciences* 106 (45): 19197 LP – 19202. https://doi.org/10.1073/pnas.0906593106.

Guillaumin, Mathilde C C, Laura E McKillop, Nanyi Cui, Simon P Fisher, Russell G. Foster, Maarten de Vos, Stuart N Peirson, Peter Achermann, and Vladyslav V. Vyazovskiy. 2018. “Cortical Region–Specific Sleep Homeostasis in Mice: Effects of Time of Day and Waking Experience.” *Sleep* 41 (7): 31. https://doi.org/10.1093/sleep/zsy079.

Gvilia, Irma, Feng Xu, Dennis McGinty, and Ronald Szymusiak. 2006. “Homeostatic Regulation of Sleep: A Role for Preoptic Area Neurons.” *The Journal of Neuroscience : The Official Journal of the Society for Neuroscience* 26 (37): 9426–33. https://doi.org/10.1523/JNEUROSCI.2012-06.2006.

Halassa, Michael M., Cedrick Florian, Tommaso Fellin, James R Munoz, So-young Lee, Ted Abel, Philip G Haydon, and Marcos G Frank. 2009. “Astrocytic Modulation of Sleep Homeostasis and Cognitive Consequences of Sleep Loss.” *Neuron* 61 (2): 213–19. https://doi.org/10.1016/j.neuron.2008.11.024.

Hanlon, Erin C, Ugo Faraguna, Vladyslav V. Vyazovskiy, Giulio Tononi, and Chiara Cirelli. 2009. “Effects of Skilled Training on Sleep Slow Wave Activity and Cortical Gene Expression in the Rat.” *Sleep* 32 (6): 719–29. http://www.pubmedcentral.nih.gov/articlerender.fcgi?artid=2690558&tool=pmcentrez&rendertype=abstract.

Hara, J, C T Beuckmann, T Nambu, J T Willie, R M Chemelli, C M Sinton, F Sugiyama, et al. 2001. “Genetic Ablation of Orexin Neurons in Mice Results in Narcolepsy, Hypophagia, and Obesity.” *Neuron* 30 (2): 345–54. https://doi.org/10.1016/s0896-6273(01)00293-8.

Harding, Edward C, Xiao Yu, Andawei Miao, Nathanael Andrews, Ying Ma, Zhiwen Ye, Leda Lignos, et al. 2018. “A Neuronal Hub Binding Sleep Initiation and Body Cooling in Response to a Warm External Stimulus.” *Current Biology* 28 (14): 2263-2273.e4. https://doi.org/https://doi.org/10.1016/j.cub.2018.05.054.

Harris, Julie A, Karla E Hirokawa, Staci A Sorensen, Hong Gu, Maya Mills, Lydia L Ng, Phillip Bohn, et al. 2014. “Anatomical Characterization of Cre Driver Mice for Neural Circuit Mapping and Manipulation.” *Frontiers in Neural Circuits*. https://www.frontiersin.org/article/10.3389/fncir.2014.00076.

Harris, Kenneth D., and Gordon M G Shepherd. 2015. “The Neocortical Circuit: Themes and Variations.” *Nature Neuroscience* 18 (2): 170–81. https://doi.org/10.1038/nn.3917.

Hay, Y Audrey, Nicolas Deperrois, Tanja Fuchsberger, Thomas Matthew Quarrell, Anna-Lucia Koerling, and Ole Paulsen. 2021. “Thalamus Mediates Neocortical Down State Transition via GABAB-Receptor-Targeting Interneurons.” *Neuron*. https://doi.org/https://doi.org/10.1016/j.neuron.2021.06.030.

Hayashi, Shuichi, Anna Hoerder-Suabedissen, Emi Kiyokage, Catherine Maclachlan, Kazunori Toida, Graham Knott, and Zoltán Molnár. 2021. “Maturation of Complex Synaptic Connections of Layer 5 Cortical Axons in the Posterior Thalamic Nucleus Requires SNAP25.” *Cerebral Cortex* 31 (5): 2625–38. https://doi.org/10.1093/cercor/bhaa379.

Hayashi, Yu, Mitsuaki Kashiwagi, Kosuke Yasuda, Reiko Ando, Mika Kanuka, Kazuya Sakai, and Shigeyoshi Itohara. 2015. "Cells of a Common Developmental Origin Regulate REM/Non-REM Sleep and Wakefulness in Mice." *Science* 350 (6263): 957 LP – 961. http://science.sciencemag.org/content/350/6263/957.abstract.

Hendricks, Joan C, Stefanie M Finn, Karen A Panckeri, Jessica Chavkin, Julie A Williams, Amita Sehgal, and Allan I Pack. 2000. "Rest in Drosophila Is a Sleep-like State." *Neuron* 25 (1): 129–38. https://doi.org/10.1016/S0896-6273(00)80877-6.

Herrera, Carolina Gutierrez, Marta Carus Cadavieco, Sonia Jego, Alexey Ponomarenko, Tatiana Korotkova, and Antoine Adamantidis. 2016. "Hypothalamic Feedforward Inhibition of Thalamocortical Network Controls Arousal and Consciousness." *Nature Neuroscience* 19 (2): 290–98. https://doi.org/10.1038/nn.4209.

Hinard, Valérie, Cyril Mikhail, Sylvain Pradervand, Thomas Curie, Riekelt H Houtkooper, Johan Auwerx, Paul Franken, and Mehdi Tafti. 2012. "Key Electrophysiological, Molecular, and Metabolic Signatures of Sleep and Wakefulness Revealed in Primary Cortical Cultures." *The Journal of Neuroscience* 32 (36): 12506 LP – 12517. http://www.jneurosci.org/content/32/36/12506.abstract.

Hinze-Selch, Dunja, Janet Mullington, Armin Orth, Christoph J Lauer, and Thomas Pollmächer. 1997. "Effects of Clozapine on Sleep: A Longitudinal Study." *Biological Psychiatry* 42 (4): 260–66. https://doi.org/https://doi.org/10.1016/S0006-3223(96)00347-2.

Hoerder-Suabedissen, Anna, Kim V Korrell, Shuichi Hayashi, Alexander Jeans, Denise M O Ramirez, Eleanor Grant, Helen C Christian, Ege T Kavalali, Michael C Wilson, and Zoltán Molnár. 2019. "Cell-Specific Loss of SNAP25 from Cortical Projection Neurons Allows Normal Development but Causes Subsequent Neurodegeneration." *Cerebral Cortex* 29 (5): 2148–59. https://doi.org/10.1093/cercor/bhy127.

Hoerder-Suabedissen, Anna, and Zoltán Molnár. 2015. "Development, Evolution and Pathology of Neocortical Subplate Neurons." *Nature Reviews Neuroscience* 16 (3): 133–46. https://doi.org/10.1038/nrn3915.

Honda, Takato, Yohko Takata, Yoan Cherasse, Seiya Mizuno, Fumihiro Sugiyama, Satoru Takahashi, Hiromasa Funato, Masashi Yanagisawa, Michael Lazarus, and Yo Oishi. 2020. "Ablation of Ventral Midbrain/Pons GABA Neurons Induces Mania-like Behaviors with Altered Sleep Homeostasis and Dopamine D2R-Mediated Sleep Reduction." *IScience* 23 (6): 101240. https://doi.org/https://doi.org/10.1016/j.isci.2020.101240.

Howell, David C. 2012. *Statistical Methods for Psychology*. Cengage Learning.

Howell, Glen T, and Guy L Lacroix. 2012. "Decomposing Interactions Using GLM in Combination with the COMPARE, LMATRIX and MMATRIX Subcommands in SPSS." *Tutorials in Quantitative Methods for Psychology* 8 (1): 1–22. https://doi.org/10.20982/tqmp.08.1.p001.

Huang, Zhi-Li, Takatoshi Mochizuki, Wei-Min Qu, Zong-Yuan Hong, Takeshi Watanabe, Yoshihiro Urade, and Osamu Hayaishi. 2006. "Altered Sleep-Wake Characteristics and Lack of Arousal Response to H3 Receptor Antagonist in Histamine H1 Receptor Knockout Mice." *Proceedings of the National Academy of Sciences of the United States of America* 103 (12): 4687–92. https://doi.org/10.1073/pnas.0600451103.

Huber, Reto, Tom Deboer, and Irene Tobler. 1999. “Prion Protein: A Role in Sleep Regulation?” *Journal of Sleep Research* 8 (SUPPL. 1): 30–36. https://doi.org/10.1046/j.1365-2869.1999.00006.x.

———. 2000a. “Effects of Sleep Deprivation on Sleep and Sleep EEG in Three Mouse Strains: Empirical Data and Simulations.” *Brain Research* 857 (1–2): 8–19. https://doi.org/10.1016/S0006-8993(99)02248-9.

———. 2000b. “Topography of EEG Dynamics After Sleep Deprivation in Mice.” *Journal of Neurophysiology* 84 (4): 1888–93. https://doi.org/10.1152/jn.2000.84.4.1888.

Huber, Reto, Steve K. Esser, Fabio Ferrarelli, Marcello Massimini, Michael J. Peterson, and Giulio Tononi. 2007. “TMS-Induced Cortical Potentiation during Wakefulness Locally Increases Slow Wave Activity during Sleep.” *PLoS ONE* 2 (3): 1–7. https://doi.org/10.1371/journal.pone.0000276.

Huber, Reto, M Felice Ghilardi, Marcello Massimini, and Giulio Tononi. 2004. “Local Sleep and Learning.” *Nature* 430 (6995): 78–81. https://doi.org/10.1038/nature02663.

Huber, Reto, M Felice Ghilardi, Marcello Massimini, Fabio Ferrarelli, Brady A Riedner, Michael J Peterson, and Giulio Tononi. 2006. “Arm Immobilization Causes Cortical Plastic Changes and Locally Decreases Sleep Slow Wave Activity.” *Nature Neuroscience* 9 (9): 1169–76. https://doi.org/10.1038/nn1758.

Huber, Reto, Giulio Tononi, and Chiara Cirelli. 2007. “Exploratory Behavior, Cortical BDNF Expression, and Sleep Homeostasis.” *Sleep* 30 (2): 129–39. http://www.ncbi.nlm.nih.gov/pubmed/17326538.

Ikeda-Sagara, Masami, Tomoya Ozaki, Mohammad Shahid, Eri Morioka, Kazuma Wada, Kazuki Honda, Ayana Hori, Yuji Matsuya, Naoki Toyooka, and Masayuki Ikeda. 2012. “Induction of Prolonged, Continuous Slow-Wave Sleep by Blocking Cerebral H1 Histamine Receptors in Rats.” *British Journal of Pharmacology* 165 (1): 167–82. https://doi.org/10.1111/j.1476-5381.2011.01547.x.

Ilg, Ann-Kathrin, Thomas Enkel, Dusan Bartsch, and Florian Bähner. 2018. “Behavioral Effects of Acute Systemic Low-Dose Clozapine in Wild-Type Rats: Implications for the Use of DREADDs in Behavioral Neuroscience.” *Frontiers in Behavioral Neuroscience*. https://www.frontiersin.org/article/10.3389/fnbeh.2018.00173.

Ingiosi, Ashley M, Christopher R Hayworth, Daniel O Harvey, Kristan G Singletary, Michael J Rempe, Jonathan P Wisor, and Marcos G Frank. 2020. “A Role for Astroglial Calcium in Mammalian Sleep and Sleep Regulation.” *Current Biology* 30 (22): 4373-4383.e7. https://doi.org/https://doi.org/10.1016/j.cub.2020.08.052.

Iqbal, Ehtesham, Risha Govind, Alvin Romero, Olubanke Dzahini, Matthew Broadbent, Robert Stewart, Tanya Smith, et al. 2020. “The Side Effect Profile of Clozapine in Real World Data of Three Large Mental Health Hospitals.” *PloS One* 15 (12): e0243437. https://doi.org/10.1371/journal.pone.0243437.

Jego, Sonia, Stephen D Glasgow, Carolina Gutierrez Herrera, Mats Ekstrand, Sean J Reed, Richard Boyce, Jeffrey Friedman, Denis Burdakov, and Antoine Adamantidis. 2013. “Optogenetic Identification of a Rapid Eye Movement Sleep Modulatory Circuit in the Hypothalamus.” *Nature Neuroscience* 16 (11): 1637–43. https://doi.org/10.1038/nn.3522.

Jendryka, Martin, Monika Palchaudhuri, Daniel Ursu, Bastiaan van der Veen, Birgit Liss, Dennis Kätzel, Wiebke Nissen, and Anton Pekcec. 2019. "Pharmacokinetic and Pharmacodynamic Actions of Clozapine-N-Oxide, Clozapine, and Compound 21 in DREADD-Based Chemogenetics in Mice." *Scientific Reports* 9 (1): 4522. https://doi.org/10.1038/s41598-019-41088-2.

Jouvet, M. 1967. "Neurophysiology of the States of Sleep." *Physiological Reviews* 47 (2): 117–77. https://doi.org/10.1152/physrev.1967.47.2.117.

Jud, Corinne, Isabelle Schmutz, Gabriele Hampp, Henrik Oster, and Urs Albrecht. 2005. "A Guideline for Analyzing Circadian Wheel-Running Behavior in Rodents under Different Lighting Conditions." *Biological Procedures Online* 7: 101–16. https://doi.org/10.1251/bpo109.

Jun, James J, Nicholas A Steinmetz, Joshua H Siegle, Daniel J Denman, Marius Bauza, Brian Barbarits, Albert K Lee, et al. 2017. "Fully Integrated Silicon Probes for High-Density Recording of Neural Activity." *Nature* 551 (7679): 232–36. https://doi.org/10.1038/nature24636.

Kahle, Kristopher T, and Kevin J Staley. 2008. "The Bumetanide-Sensitive Na-K-2Cl Cotransporter NKCC1 as a Potential Target of a Novel Mechanism-Based Treatment Strategy for Neonatal Seizures." *Neurosurgical Focus* 25 (3): E22. https://doi.org/10.3171/FOC/2008/25/9/E22.

Kalinchuk, Anna V, Robert W McCarley, Tarja Porkka-Heiskanen, and Radhika Basheer. 2011. "The Time Course of Adenosine, Nitric Oxide (NO) and Inducible NO Synthase Changes in the Brain with Sleep Loss and Their Role in the Non-Rapid Eye Movement Sleep Homeostatic Cascade." *Journal of Neurochemistry* 116 (2): 260–72. https://doi.org/10.1111/j.1471-4159.2010.07100.x.

Kapfer, Christoph, Lindsey L Glickfeld, Bassam V Atallah, and Massimo Scanziani. 2007. "Supralinear Increase of Recurrent Inhibition during Sparse Activity in the Somatosensory Cortex." *Nature Neuroscience* 10 (6): 743–53. https://doi.org/10.1038/nn1909.

Karagiannis, Anastassios, Thierry Gallopin, Csaba Dávid, Demian Battaglia, Hélène Geoffroy, Jean Rossier, Elizabeth M C Hillman, Jochen F Staiger, and Bruno Cauli. 2009. "Classification of NPY-Expressing Neocortical Interneurons." *The Journal of Neuroscience* 29 (11): 3642 LP – 3659. https://doi.org/10.1523/JNEUROSCI.0058-09.2009.

Kattler, Herbert, Derk-Jan Dijk, and Alexander A. Borbély. 1994. "Effect of Unilateral Somatosensory Stimulation Prior to Sleep on the Sleep EEG in Humans." *Journal of Sleep Research* 3 (3): 159–64. https://doi.org/10.1111/j.1365-2869.1994.tb00123.x.

Kempf, Anissa, Seoho M Song, Clifford B Talbot, and Gero Miesenböck. 2019. "A Potassium Channel β-Subunit Couples Mitochondrial Electron Transport to Sleep." *Nature* 568 (7751): 230–34. https://doi.org/10.1038/s41586-019-1034-5.

Kim, Euiseok J., Ashley L. Juavinett, Espoir M. Kyubwa, Matthew W. Jacobs, and Edward M. Callaway. 2015. "Three Types of Cortical Layer 5 Neurons That Differ in Brain-Wide Connectivity and Function." *Neuron* 88 (6): 1253–67. https://doi.org/https://doi.org/10.1016/j.neuron.2015.11.002.

Kita, Takako, and Hitoshi Kita. 2012. “The Subthalamic Nucleus Is One of Multiple Innervation Sites for Long-Range Corticofugal Axons: A Single-Axon Tracing Study in the Rat.” *The Journal of Neuroscience* 32 (17): 5990 LP – 5999. https://doi.org/10.1523/JNEUROSCI.5717-11.2012.

Konadhode, Roda Rani, Dheeraj Pelluru, Carlos Blanco-Centurion, Andrew Zayachkivsky, Meng Liu, Thomas Uhde, W Bailey Glen, Anthony N van den Pol, Patrick J Mulholland, and Priyattam J Shiromani. 2013. “Optogenetic Stimulation of MCH Neurons Increases Sleep.” *The Journal of Neuroscience* 33 (25): 10257 LP – 10263. https://doi.org/10.1523/JNEUROSCI.1225-13.2013.

Krause, Adam J, Eti Ben Simon, Bryce A Mander, Stephanie M Greer, Jared M Saletin, Andrea N Goldstein-Piekarski, and Matthew P Walker. 2017. “The Sleep-Deprived Human Brain.” *Nature Reviews Neuroscience* 18 (7): 404–18. https://doi.org/10.1038/nrn.2017.55.

Kroeger, Daniel, Gianna Absi, Celia Gagliardi, Sathyajit S Bandaru, Joseph C Madara, Loris L Ferrari, Elda Arrigoni, et al. 2018. “Galanin Neurons in the Ventrolateral Preoptic Area Promote Sleep and Heat Loss in Mice.” *Nature Communications* 9 (1): 4129. https://doi.org/10.1038/s41467-018-06590-7.

Krone, Lukas B, Lukas Frase, Hannah Piosczyk, Peter Selhausen, Sulamith Zittel, Friederike Jahn, Marion Kuhn, et al. 2016. “Top-down Control of Arousal and Sleep: Fundamentals and Clinical Implications.” *Sleep Medicine Reviews*, January. https://doi.org/10.1016/j.smrv.2015.12.005.

Krone, Lukas B, and Vladyslav V. Vyazovskiy. 2019. “The Function of Sleep.” In *Dreams: Understanding Biology, Psychology, and Culture (Vol 1)*, edited by Katja Valli, Robert Hoss, and Robert Gongloff, 42–54. Santa Barbara, CA: Greenwood, an Imprint of ABC-CLIO, LLC.

———. 2020. “Unresponsive or Just Asleep? Do Local Slow Waves in the Perilesional Cortex Have a Function?” *Brain* 143 (12): 3513–15. https://doi.org/10.1093/brain/awaa396.

Krone, Lukas B, Tomoko Yamagata, Cristina Blanco-Duque, Mathilde C C Guillaumin, Martin C Kahn, Vincent van der Vinne, Laura E McKillop, et al. 2021. “A Role for the Cortex in Sleep–Wake Regulation.” *Nature Neuroscience* 24 (9): 1210–15. https://doi.org/10.1038/s41593-021-00894-6.

Krueger, James. 2008. “The Role of Cytokines in Sleep Regulation.” *Current Pharmaceutical Design* 14 (32): 3408–16. https://doi.org/10.2174/138161208786549281.

Krueger, James, Joseph T Nguyen, Cheryl J Dykstra-Aiello, and Ping Taishi. 2019. “Local Sleep.” *Sleep Medicine Reviews* 43: 14–21. https://doi.org/https://doi.org/10.1016/j.smrv.2018.10.001.

Krueger, James, and Ferenc Obál. 1993. “A Neuronal Group Theory of Sleep Function.” *Journal of Sleep Research* 2 (2): 63–69.

Krueger, James, David M. Rector, Sandip Roy, Hans P. A. Van Dongen, Gregory Belenky, and Jaak Panksepp. 2008. “Sleep as a Fundamental Property of Neuronal Assemblies.” *Nature Reviews Neuroscience* 9 (12): 910–19. https://doi.org/10.1038/nrn2521.

Krueger, James, and Giulio Tononi. 2011. “Local Use-Dependent Sleep; Synthesis of the New Paradigm.” *Current Topics in Medicinal Chemistry* 11 (19): 2490–92. https://doi.org/10.2174/156802611797470330.

Landolt, Hans-Peter, Julia V Rétey, Karin Tönz, Julie M Gottselig, Ramin Khatami, Isabelle Buckelmüller, and Peter Achermann. 2004. "Caffeine Attenuates Waking and Sleep Electroencephalographic Markers of Sleep Homeostasis in Humans." *Neuropsychopharmacology* 29 (10): 1933.

Lazarus, Michael, Yo Oishi, Theresa Bjorness, and Robert Greene. 2019. "Gating and the Need for Sleep: Dissociable Effects of Adenosine A1 and A2A Receptors." *Frontiers in Neuroscience* 13: 740.

Lazzaro, Vincenzo Di, John Rothwell, and Marco Capogna. 2018. "Noninvasive Stimulation of the Human Brain: Activation of Multiple Cortical Circuits." *The Neuroscientist* 24 (3): 246–60. https://doi.org/10.1177/1073858417717660.

Lefort, Sandrine, Christian Tomm, J.-C. Floyd Sarria, and Carl C H Petersen. 2009. "The Excitatory Neuronal Network of the C2 Barrel Column in Mouse Primary Somatosensory Cortex." *Neuron* 61 (2): 301–16. https://doi.org/https://doi.org/10.1016/j.neuron.2008.12.020.

Lemieux, Maxime, Jen-Yung Chen, Peter Lonjers, Maxim Bazhenov, and Igor Timofeev. 2014. "The Impact of Cortical Deafferentation on the Neocortical Slow Oscillation." *The Journal of Neuroscience* 34 (16): 5689 LP – 5703. https://doi.org/10.1523/JNEUROSCI.1156-13.2014.

Leone, Dino P, Whitney E Heavner, Emily A Ferenczi, Gergana Dobreva, John R Huguenard, Rudolf Grosschedl, and Susan K McConnell. 2014. "Satb2 Regulates the Differentiation of Both Callosal and Subcerebral Projection Neurons in the Developing Cerebral Cortex." *Cerebral Cortex* 25 (10): 3406–19. https://doi.org/10.1093/cercor/bhu156.

Levenstein, Daniel, György Buzsáki, and John Rinzel. 2019. "NREM Sleep in the Rodent Neocortex and Hippocampus Reflects Excitable Dynamics." *Nature Communications* 10 (1): 2478. https://doi.org/10.1038/s41467-019-10327-5.

Lima, Susana Q., and Gero Miesenböck. 2005. "Remote Control of Behavior through Genetically Targeted Photostimulation of Neurons." *Cell* 121 (1): 141–52. https://doi.org/10.1016/j.cell.2005.02.004.

Liu, Danqian, and Yang Dan. 2019. "A Motor Theory of Sleep-Wake Control: Arousal-Action Circuit." *Annual Review of Neuroscience* 42 (1): 27–46. https://doi.org/10.1146/annurev-neuro-080317-061813.

Liu, Danqian, Weifu Li, Chenyan Ma, Weitong Zheng, Yuanyuan Yao, Chak Foon Tso, Peng Zhong, et al. 2020. "A Common Hub for Sleep and Motor Control in the Substantia Nigra." *Science* 367 (6476): 440 LP – 445. https://doi.org/10.1126/science.aaz0956.

Lőrincz, Magor L, David Gunner, Ying Bao, William M. Connelly, John T. R. Isaac, Stuart W. Hughes, and Vincenzo Crunelli. 2015. "A Distinct Class of Slow (~0.2-2 Hz) Intrinsically Bursting Layer 5 Pyramidal Neurons Determines UP/DOWN State Dynamics in the Neocortex." *The Journal of Neuroscience* 35 (14): 5442–58. https://doi.org/10.1523/JNEUROSCI.3603-14.2015.

Lu, Jun, M a Greco, P Shiromani, and C B Saper. 2000. "Effect of Lesions of the Ventrolateral Preoptic Nucleus on NREM and REM Sleep." *The Journal of Neuroscience* 20 (10): 3830–42. https://doi.org/20/10/3830 [pii] ET - 2000/05/11.

Lu, Jun, David Sherman, Marshall Devor, and Clifford B Saper. 2006. "A Putative Flip–Flop Switch for Control of REM Sleep." *Nature* 441 (7093): 589–94. https://doi.org/10.1038/nature04767.

Luczak, Artur, Peter Barthó, Stephan L Marguet, György Buzsáki, and Kenneth D. Harris. 2007. "Sequential Structure of Neocortical Spontaneous Activity in Vivo." *Proceedings of the National Academy of Sciences of the United States of America* 104 (1): 347–52. https://doi.org/10.1073/pnas.0605643104.

Ma, Ying, Giulia Miracca, Xiao Yu, Edward C Harding, Andawei Miao, Raquel Yustos, Alexei L Vyssotski, Nicholas P Franks, and William Wisden. 2019. "Galanin Neurons Unite Sleep Homeostasis and A2-Adrenergic Sedation." *Current Biology* 29 (19): 3315-3322.e3. https://doi.org/https://doi.org/10.1016/j.cub.2019.07.087.

MacLaren, Duncan A A, Richard W Browne, Jessica K Shaw, Sandhya Krishnan Radhakrishnan, Prachi Khare, Rodrigo A España, and Stewart D Clark. 2016. "Clozapine N-Oxide Administration Produces Behavioral Effects in Long-Evans Rats: Implications for Designing DREADD Experiments." *ENeuro* 3 (5). https://doi.org/10.1523/ENEURO.0219-16.2016.

Magill, Peter J, Alek Pogosyan, Andrew Sharott, Jozsef Csicsvari, J Paul Bolam, and Peter Brown. 2006. "Changes in Functional Connectivity within the Rat Striatopallidal Axis during Global Brain Activation In Vivo." *Journal of Neuroscience* 26 (23): 6318–29. https://doi.org/10.1523/JNEUROSCI.0620-06.2006.

Magnus, Christopher J, Peter H Lee, Jordi Bonaventura, Roland Zemla, Juan L Gomez, Melissa H Ramirez, Xing Hu, et al. 2019. "Ultrapotent Chemogenetics for Research and Potential Clinical Applications." *Science* 364 (6436): eaav5282. https://doi.org/10.1126/science.aav5282.

Mahler, Stephen V, and Gary Aston-Jones. 2018. "CNO Evil? Considerations for the Use of DREADDs in Behavioral Neuroscience." *Neuropsychopharmacology* 43 (5): 934–36. https://doi.org/10.1038/npp.2017.299.

Manvich, Daniel F, Kevin A Webster, Stephanie L Foster, Martilias S Farrell, James C Ritchie, Joseph H Porter, and David Weinshenker. 2018. "The DREADD Agonist Clozapine N-Oxide (CNO) Is Reverse-Metabolized to Clozapine and Produces Clozapine-like Interoceptive Stimulus Effects in Rats and Mice." *Scientific Reports* 8 (1): 3840. https://doi.org/10.1038/s41598-018-22116-z.

Markram, H, J Lübke, M Frotscher, A Roth, and B Sakmann. 1997. "Physiology and Anatomy of Synaptic Connections between Thick Tufted Pyramidal Neurones in the Developing Rat Neocortex." *The Journal of Physiology* 500 (2): 409–40. https://doi.org/10.1113/jphysiol.1997.sp022031.

Marques-Smith, Andre, Daniel Lyngholm, Anna-Kristin Kaufmann, Jacqueline A. Stacey, Anna Hoerder-Suabedissen, Esther B.E. Becker, Michael C. Wilson, Zoltán Molnár, and Simon J.B. Butt. 2016. "A Transient Translaminar GABAergic Interneuron Circuit Connects Thalamocortical Recipient Layers in Neonatal Somatosensory Cortex." *Neuron* 89 (3): 536–49. https://doi.org/10.1016/j.neuron.2016.01.015.

Marshall, Lisa, Halla Helgadóttir, Matthias Mölle, and Jan Born. 2006. "Boosting Slow Oscillations during Sleep Potentiates Memory." *Nature* 444 (7119): 610–13. https://doi.org/10.1038/nature05278.

Marshall, Lisa, Matthias Mölle, Manfred Hallschmid, and Jan Born. 2004. "Transcranial Direct Current Stimulation during Sleep Improves Declarative Memory." *The Journal of Neuroscience : The Official Journal of the Society for Neuroscience* 24 (44): 9985–92. https://doi.org/10.1523/JNEUROSCI.2725-04.2004.

Marzano, Cristina, Fabio Moroni, Maurizio Gorgoni, Lino Nobili, Michele Ferrara, and Luigi De Gennaro. 2013. "How We Fall Asleep: Regional and Temporal Differences in Electroencephalographic Synchronization at Sleep Onset." *Sleep Medicine* 14 (11): 1112–22. https://doi.org/10.1016/j.sleep.2013.05.021.

Massimini, Marcello, Reto Huber, Fabio Ferrarelli, Sean Hill, and Giulio Tononi. 2004. "The Sleep Slow Oscillation as a Traveling Wave." *The Journal of Neuroscience : The Official Journal of the Society for Neuroscience* 24 (31): 6862–70. https://doi.org/10.1523/JNEUROSCI.1318-04.2004.

McKillop, Laura E, Simon P Fisher, Nanyi Cui, Stuart N Peirson, Russell G. Foster, Keith A Wafford, and Vladyslav V. Vyazovskiy. 2018. "Effects of Aging on Cortical Neural Dynamics and Local Sleep Homeostasis in Mice." *The Journal of Neuroscience* 38 (16): 3911 LP – 3928. https://doi.org/10.1523/JNEUROSCI.2513-17.2018.

McKillop, Laura E, Simon P Fisher, Linus Milinski, Lukas B Krone, and Vladyslav V. Vyazovskiy. 2021. "Diazepam Effects on Local Cortical Neural Activity during Sleep in Mice." *Biochemical Pharmacology*, March, 114515. https://doi.org/10.1016/j.bcp.2021.114515.

McOmish, Caitlin E, Alena Lira, James B Hanks, and Jay A Gingrich. 2012. "Clozapine-Induced Locomotor Suppression Is Mediated by 5-HT2A Receptors in the Forebrain." *Neuropsychopharmacology* 37 (13): 2747–55. https://doi.org/10.1038/npp.2012.139.

Melzer, Sarah, and Hannah Monyer. 2020. "Diversity and Function of Corticopetal and Corticofugal GABAergic Projection Neurons." *Nature Reviews Neuroscience* 21 (9): 499–515. https://doi.org/10.1038/s41583-020-0344-9.

Mensen, Armand, Corina Gorban, Marcel Niklaus, Eva Kuske, and Ramin Khatami. 2014. "The Effects of Theta-Burst Stimulation on Sleep and Vigilance in Humans." *Frontiers in Human Neuroscience* 8 (June): 1–10. https://doi.org/10.3389/fnhum.2014.00420.

Miesenböck, Gero. 2009. "The Optogenetic Catechism." *Science* 326 (5951): 395–99. https://doi.org/10.1126/science.1174520.

———. 2011. "Optogenetic Control of Cells and Circuits." *Annual Review of Cell and Developmental Biology* 27 (1): 731–58. https://doi.org/10.1146/annurev-cellbio-100109-104051.

Milinski, Linus, Simon P Fisher, Nanyi Cui, Laura E McKillop, Cristina Blanco-Duque, Gauri Ang, Tomoko Yamagata, David M. Bannerman, and Vladyslav V. Vyazovskiy. 2021. "Waking Experience Modulates Sleep Need in Mice." *BMC Biology* 19 (1): 65. https://doi.org/10.1186/s12915-021-00982-w.

Mistlberger, Ralph E. 2005. "Circadian Regulation of Sleep in Mammals: Role of the Suprachiasmatic Nucleus." *Brain Research Reviews* 49 (3): 429–54. https://doi.org/https://doi.org/10.1016/j.brainresrev.2005.01.005.

Molnár, Zoltán, Guillermina López-Bendito, Juan Small, L Donald Partridge, Colin Blakemore, and Michael C Wilson. 2002. "Normal Development of Embryonic Thalamocortical Connectivity in the Absence of Evoked Synaptic Activity." *The Journal of Neuroscience* 22 (23): 10313 LP – 10323. https://doi.org/10.1523/JNEUROSCI.22-23-10313.2002.

Mondino, Alejandra, Viviane S Hambrecht-Wiedbusch, Duan Li, A Kane York, Dinesh Pal, Joaquin González, Pablo Torterolo, George A Mashour, and Giancarlo Vanini. 2021. "Glutamatergic Neurons in the Preoptic Hypothalamus Promote Wakefulness, Destabilize NREM Sleep, Suppress REM Sleep, and Regulate Cortical Dynamics." *The Journal of Neuroscience* 41 (15): 3462 LP – 3478. https://doi.org/10.1523/JNEUROSCI.2718-20.2021.

Monti, Jaime M, Pablo Torterolo, and Seithikurippu R Pandi Perumal. 2017. "The Effects of Second Generation Antipsychotic Drugs on Sleep Variables in Healthy Subjects and Patients with Schizophrenia." *Sleep Medicine Reviews* 33: 51–57. https://doi.org/https://doi.org/10.1016/j.smrv.2016.05.002.

Morairty, S R, L Dittrich, R K Pasumarthi, D Valladao, J E Heiss, D Gerashchenko, and T S Kilduff. 2013. "A Role for Cortical NNOS/NK1 Neurons in Coupling Homeostatic Sleep Drive to EEG Slow Wave Activity." *Proc Natl Acad Sci U S A* 110 (50): 20272–77. https://doi.org/10.1073/pnas.1314762110.

Morin, Lawrence P. 2013. "Neuroanatomy of the Extended Circadian Rhythm System." *Experimental Neurology* 243 (May): 4–20. https://doi.org/10.1016/j.expneurol.2012.06.026.

Moruzzi, G., and H.W. Magoun. 1949. "Brain Stem Reticular Formation and Activation of the EEG." *Electroencephalography and Clinical Neurophysiology* 1 (1): 455–73. https://doi.org/10.1016/0013-4694(49)90219-9.

Murphy, Michael, Marie-Aurélie Bruno, Brady a Riedner, Pierre Boveroux, Quentin Noirhomme, Eric C Landsness, Jean-Francois Brichant, et al. 2011. "Propofol Anesthesia and Sleep: A High-Density EEG Study." *Sleep* 34 (3): 283-91A. http://www.ncbi.nlm.nih.gov/pubmed/21358845.

Murphy, Sean C, Lucy M Palmer, Thomas Nyffeler, René M Müri, and Matthew E Larkum. 2016. "Transcranial Magnetic Stimulation (TMS) Inhibits Cortical Dendrites." Edited by Marlene Bartos. *ELife* 5: e13598. https://doi.org/10.7554/eLife.13598.

Naganuma, Fumito, Sathyajit S Bandaru, Gianna Absi, Carrie E Mahoney, Thomas E Scammell, and Ramalingam Vetrivelan. 2018. "Melanin-Concentrating Hormone Neurons Contribute to Dysregulation of Rapid Eye Movement Sleep in Narcolepsy." *Neurobiology of Disease* 120: 12–20. https://doi.org/https://doi.org/10.1016/j.nbd.2018.08.012.

Naidoo, Nirinjini, William Giang, Raymond J Galante, and Allan I Pack. 2005. "Sleep Deprivation Induces the Unfolded Protein Response in Mouse Cerebral Cortex." *Journal of Neurochemistry* 92 (5): 1150–57. https://doi.org/https://doi.org/10.1111/j.1471-4159.2004.02952.x.

Nath, Ravi D, Claire N Bedbrook, Michael J Abrams, Ty Basinger, Justin S Bois, David A Prober, Paul W Sternberg, Viviana Gradinaru, and Lea Goentoro. 2017. "The Jellyfish Cassiopea Exhibits a Sleep-like State." *Current Biology* 27 (19): 2984-2990.e3. https://doi.org/10.1016/j.cub.2017.08.014.

Nauta, W J H. 1946. "Hypothalamic Regulation of Sleep in Rats; an Experimental Study." *Journal of Neurophysiology* 9 (4): 285–316. https://doi.org/10.1152/jn.1946.9.4.285.

Neckelmann, D, and R Ursin. 1993. "Sleep Stages and EEG Power Spectrum in Relation to Acoustical Stimulus Arousal Threshold in the Rat." *Sleep* 16 (5): 467–77. http://www.ncbi.nlm.nih.gov/pubmed/8378687.

Neske, Garrett T. 2016. “The Slow Oscillation in Cortical and Thalamic Networks: Mechanisms and Functions.” *Frontiers in Neural Circuits* 9 (January): 88. https://doi.org/10.3389/fncir.2015.00088.

Ngo, Hong-Viet V., Thomas Martinetz, Jan Born, and Matthias Mölle. 2013. “Auditory Closed-Loop Stimulation of the Sleep Slow Oscillation Enhances Memory.” *Neuron* 78 (3): 545–53. https://doi.org/10.1016/j.neuron.2013.03.006.

Ni Mhuircheartaigh, R., Catherine Warnaby, Richard Rogers, Saad Jbabdi, and Irene Tracey. 2013. “Slow-Wave Activity Saturation and Thalamocortical Isolation During Propofol Anesthesia in Humans.” *Science Translational Medicine* 5 (208): 208ra148-208ra148. https://doi.org/10.1126/scitranslmed.3006007.

Niethard, Niels, Hong-Viet V Ngo, Ingrid Ehrlich, and Jan Born. 2018. “Cortical Circuit Activity Underlying Sleep Slow Oscillations and Spindles.” *Proceedings of the National Academy of Sciences of the United States of America* 115 (39): E9220–29. https://doi.org/10.1073/pnas.1805517115.

Nir, Yuval, Thomas Andrillon, Amit Marmelshtein, Nanthia Suthana, Chiara Cirelli, Giulio Tononi, and Itzhak Fried. 2017. “Selective Neuronal Lapses Precede Human Cognitive Lapses Following Sleep Deprivation.” *Nature Medicine* 23 (12): 1474–80. https://doi.org/10.1038/nm.4433.

Nir, Yuval, and Giulio Tononi. 2010. “Dreaming and the Brain: From Phenomenology to Neurophysiology.” *Trends in Cognitive Sciences* 14 (2): 88–100.

Nitsche, Michael A, and W Paulus. 2000. “Excitability Changes Induced in the Human Motor Cortex by Weak Transcranial Direct Current Stimulation.” *The Journal of Physiology* 527 (3): 633–39. https://doi.org/10.1111/j.1469-7793.2000.t01-1-00633.x.

Noda, Hiroharu, and W Ross Adey. 1970. “Changes in Neuronal Activity in Association Cortex of the Cat in Relation to Sleep and Wakefulness.” *Brain Research* 19 (2): 263–75. https://doi.org/https://doi.org/10.1016/0006-8993(70)90439-7.

Nollet, Mathieu, William Wisden, and Nicholas P Franks. 2020. “Sleep Deprivation and Stress: A Reciprocal Relationship.” *Interface Focus* 10 (3): 20190092. https://doi.org/10.1098/rsfs.2019.0092.

Noya, Sara B, David Colameo, Franziska Brüning, Andrea Spinnler, Dennis Mircsof, Lennart Opitz, Matthias Mann, Shiva K Tyagarajan, Maria S Robles, and Steven A Brown. 2019. “The Forebrain Synaptic Transcriptome Is Organized by Clocks but Its Proteome Is Driven by Sleep.” *Science* 366 (6462): eaav2642. https://doi.org/10.1126/science.aav2642.

Ode, Koji L, and Hiroki R Ueda. 2020. “Phosphorylation Hypothesis of Sleep.” *Frontiers in Psychology*. https://www.frontiersin.org/article/10.3389/fpsyg.2020.575328.

Oikonomou, Grigorios, Michael Altermatt, Rong-Wei Zhang, Gerard M Coughlin, Christin Montz, Viviana Gradinaru, and David A Prober. 2019. “The Serotonergic Raphe Promote Sleep in Zebrafish and Mice.” *Neuron* 103 (4): 686-701.e8. https://doi.org/10.1016/j.neuron.2019.05.038.

Parikh, Hirak, Timothy C Marzullo, Azadeh Yazdan-Shahmorad, Gregory J Gage, and Daryl Kipke. 2007. “Laminar Characterization of Spiking Activity in the Rat Motor Cortex.” In *2007 29th Annual International Conference of the IEEE Engineering in Medicine and Biology Society*, 4735–38. IEEE. https://doi.org/10.1109/IEMBS.2007.4353397.

Partch, Cl, Cb Green, and Js Takahashi. 2014. “Molecular Architecture of the Mammalian Circadian Clock.” *Trends in Cell Biology* 24 (2): 90–99. https://doi.org/10.1016/j.tcb.2013.07.002.Molecular.

Paxinos, George, and Keith B J Franklin. 2019. *Paxinos and Franklin’s the Mouse Brain in Stereotaxic Coordinates*. 5th ed. San Diego: Elsevier Academic Press.

Peñaloza-Rojas, J H, M Elterman, and N Olmos. 1964. “Sleep Induced by Cortical Stimulation.” *Experimental Neurology* 10 (2): 140–47. https://doi.org/https://doi.org/10.1016/0014-4886(64)90091-3.

Peng, Wanling, Zhaofa Wu, Kun Song, Siyu Zhang, Yulong Li, and Min Xu. 2020. “Regulation of Sleep Homeostasis Mediator Adenosine by Basal Forebrain Glutamatergic Neurons.” *Science* 369 (6508): eabb0556. https://doi.org/10.1126/science.abb0556.

Piéron, H. 1913. “Le Problème Physiologique Du Sommeil.” Paris: Masson.

Pigarev, Ivan N., Hans Christoph Nothdurft, and Sabine Kastner. 1997. “Evidence for Asynchronous Development of Sleep in Cortical Areas.” *NeuroReport* 8 (11): 2557–60. https://doi.org/10.1097/00001756-199707280-00027.

Porkka-Heiskanen, Tarja, R E Strecker, and R W McCarley. 2000. “Brain Site-Specificity of Extracellular Adenosine Concentration Changes during Sleep Deprivation and Spontaneous Sleep: An in Vivo Microdialysis Study.” *Neuroscience* 99 (3): 507–17.

Prasad, Judy A, Briana J Carroll, and S.Murray Sherman. 2020. “Layer 5 Corticofugal Projections from Diverse Cortical Areas: Variations on a Pattern of Thalamic and Extrathalamic Targets.” *The Journal of Neuroscience* 40 (30): 5785 LP – 5796. https://doi.org/10.1523/JNEUROSCI.0529-20.2020.

Radnikow, Gabriele, and Dirk Feldmeyer. 2018. “Layer-and Cell Type-Specific Modulation of Excitatory Neuronal Activity in the Neocortex.” *Frontiers in Neuroanatomy* 12.

Ralph, M., Russell G. Foster, F. Davis, and Michael Menaker. 1990. “Transplanted Suprachiasmatic Nucleus Determines Circadian Period.” *Science* 247 (4945): 975–78. https://doi.org/10.1126/science.2305266.

Ravindra Kumar, Sripriya, Timothy F Miles, Xinhong Chen, David Brown, Tatyana Dobreva, Qin Huang, Xiaozhe Ding, et al. 2020. “Multiplexed Cre-Dependent Selection Yields Systemic AAVs for Targeting Distinct Brain Cell Types.” *Nature Methods* 17 (5): 541–50. https://doi.org/10.1038/s41592-020-0799-7.

Reato, Davide, Fernando Gasca, Abhishek Datta, Marom Bikson, Lisa Marshall, and Lucas C Parra. 2013. “Transcranial Electrical Stimulation Accelerates Human Sleep Homeostasis.” *PLOS Computational Biology* 9 (2): e1002898. https://doi.org/10.1371/journal.pcbi.1002898.

Rechtschaffen, A, M. Gilliland, B. Bergmann, and J. Winter. 1983. “Physiological Correlates of Prolonged Sleep Deprivation in Rats.” *Science* 221 (4606): 182–84. https://doi.org/10.1126/science.6857280.

Rechtschaffen, A, P Hauri, and M Zeitlin. 1966. “Auditory Awakening Thresholds in REM and NREM Sleep Stages.” *Perceptual and Motor Skills* 22 (3): 927–42. https://doi.org/10.2466/pms.1966.22.3.927.

Riemann, Dieter, Lukas B Krone, Katharina Wulff, and Christoph Nissen. 2019. “Sleep, Insomnia, and Depression.” *Neuropsychopharmacology*. https://doi.org/10.1038/s41386-019-0411-y.

Riemann, Dieter, and Christoph Nissen. 2012. *Sleep and Psychotropic Drugs*. Edited by Colin A. Espie and Charles M. Morin. *Oxford Handbook of Sleep and Sleep Disorders*. Oxford: Oxford University Press. https://doi.org/10.1093/oxfordhb/9780195376203.013.0011.

Rivera, L R, D P Poole, M Thacker, and J B Furness. 2011. "The Involvement of Nitric Oxide Synthase Neurons in Enteric Neuropathies." *Neurogastroenterology and Motility : The Official Journal of the European Gastrointestinal Motility Society* 23 (11): 980–88. https://doi.org/10.1111/j.1365-2982.2011.01780.x.

Roth, Bryan L. 2016. "DREADDs for Neuroscientists." *Neuron* 89 (4): 683–94. https://doi.org/10.1016/j.neuron.2016.01.040.

Russo, S, A Pigorini, E Mikulan, S Sarasso, A Rubino, F M Zauli, S Parmigiani, et al. 2021. "Focal Lesions Induce Large-Scale Percolation of Sleep-like Intracerebral Activity in Awake Humans." *NeuroImage*, 117964. https://doi.org/https://doi.org/10.1016/j.neuroimage.2021.117964.

Sakata, Shuzo, and Kenneth D. Harris. 2009. "Laminar Structure of Spontaneous and Sensory-Evoked Population Activity in Auditory Cortex." *Neuron* 64 (3): 404–18. https://doi.org/https://doi.org/10.1016/j.neuron.2009.09.020.

Sanchez-Vives, M V, and M Mattia. 2014. "Slow Wave Activity as the Default Mode of the Cerebral Cortex." *Arch Ital Biol* 152 (2–3): 147–55.

Sanchez-Vives, M V, and D A McCormick. 2000a. "Cellular and Network Mechanisms of Rhythmic Recurrent Activity in Neocortex." *Nature Neuroscience* 3 (10): 1027–34. https://doi.org/10.1038/79848.

Sanchez-Vives, and David A McCormick. 2000b. "Cellular and Network Mechanisms of Rhythmic Recurrent Activity in Neocortex." *Nature Neuroscience* 3 (10): 1027–34. https://doi.org/10.1038/79848.

Sanchez-Vives, David A McCormick, M V Sanchez-Vives, and David A McCormick. 2000. "Cellular and Network Mechanisms of Rhythmic Recurrent Activity in Neocortex." *Nature Neuroscience* 3 (10): 1027–34. https://doi.org/10.1038/79848.

Saper, Clifford B., Thomas C. Chou, and Thomas E. Scammell. 2001. "The Sleep Switch: Hypothalamic Control of Sleep and Wakefulness." *Trends in Neurosciences* 24 (12): 726–31. https://doi.org/10.1016/S0166-2236(00)02002-6.

Saper, Clifford B, and Patrick M Fuller. 2017. "Wake–Sleep Circuitry: An Overview." *Current Opinion in Neurobiology* 44 (June): 186–92. https://doi.org/10.1016/j.conb.2017.03.021.

Saper, Clifford B, Thomas E Scammell, and Jun Lu. 2005. "Hypothalamic Regulation of Sleep and Circadian Rhythms." *Nature* 437 (7063): 1257–63. https://doi.org/10.1038/nature04284.

Sarasso, Simone, Sasha D'Ambrosio, Matteo Fecchio, Silvia Casarotto, Alessandro Viganò, Cristina Landi, Giulia Mattavelli, et al. 2021. "Local Sleep-like Cortical Reactivity in the Awake Brain after Focal Injury." *Brain* 143 (12): 3672–84. https://doi.org/10.1093/brain/awaa338.

Sauer, B, and N Henderson. 1988. "Site-Specific DNA Recombination in Mammalian Cells by the Cre Recombinase of Bacteriophage P1." *Proceedings of the National Academy of Sciences* 85 (14): 5166–70. https://doi.org/10.1073/pnas.85.14.5166.

Schindelin, Johannes, Ignacio Arganda-Carreras, Erwin Frise, Verena Kaynig, Mark Longair, Tobias Pietzsch, Stephan Preibisch, et al. 2012. "Fiji: An Open Source Platform for Biological Image Analysis." *Nature Methods* 9 (7): 676–82. https://doi.org/10.1038/nmeth.2019.Fiji.

Schmid, Benjamin, Charlotte Helfrich-Förster, and Taishi Yoshii. 2011. "A New ImageJ Plug-in 'ActogramJ' for Chronobiological Analyses." *Journal of Biological Rhythms* 26 (5): 464–67. https://doi.org/10.1177/0748730411414264.

Shaw, Paul J., C Cirelli, R J Greenspan, and G Tononi. 2000. "Correlates of Sleep and Waking in Drosophila Melanogaster." *Science* 287 (5459): 1834–37. https://doi.org/10.1126/science.287.5459.1834.

Sherin, Jonathan E, Joel K Elmquist, Fernando Torrealba, and Clifford B Saper. 1998. "Innervation of Histaminergic Tuberomammillary Neurons by GABAergic and Galaninergic Neurons in the Ventrolateral Preoptic Nucleus of the Rat" 18 (12): 4705–21.

Sherin, Jonathan E, P J Shiromani, R W McCarley, and C B Saper. 1996. "Activation of Ventrolateral Preoptic Neurons During Sleep." *Science* 271 (5246): 216 LP – 219. https://doi.org/10.1126/science.271.5246.216.

Sherman, S.Murray, and W Martin Usrey. 2021. "Cortical Control of Behavior and Attention from an Evolutionary Perspective." *Neuron*, July. https://doi.org/10.1016/j.neuron.2021.06.021.

Sheroziya, Maxim, and Igor Timofeev. 2014. "Global Intracellular Slow-Wave Dynamics of the Thalamocortical System." *Journal of Neuroscience* 34 (26): 8875–93. https://doi.org/10.1523/JNEUROSCI.4460-13.2014.

Siclari, Francesca, Giulio Bernardi, Brady A Riedner, Joshua J LaRocque, Ruth M Benca, and Giulio Tononi. 2014. "Two Distinct Synchronization Processes in the Transition to Sleep: A High-Density Electroencephalographic Study." *Sleep* 37 (10): 1621–37. https://doi.org/10.5665/sleep.4070.

Silberberg, Gilad, and Henry Markram. 2007. "Disynaptic Inhibition between Neocortical Pyramidal Cells Mediated by Martinotti Cells." *Neuron* 53 (5): 735–46. https://doi.org/https://doi.org/10.1016/j.neuron.2007.02.012.

Sivakumaran, Sudhir, Ross A Cardarelli, Jamie Maguire, Matt R Kelley, Liliya Silayeva, Danielle H Morrow, Jayanta Mukherjee, et al. 2015. "Selective Inhibition of KCC2 Leads to Hyperexcitability and Epileptiform Discharges in Hippocampal Slices and In Vivo." *Journal of Neuroscience* 35 (21): 8291–96. https://doi.org/10.1523/JNEUROSCI.5205-14.2015.

Sjulson, Lucas, Daniela Cassataro, Shamik Dasgupta, and Gero Miesenböck. 2016. "Cell-Specific Targeting of Genetically Encoded Tools for Neuroscience." *Annual Review of Genetics* 50: 571–94. https://doi.org/10.1146/annurev-genet-120215-035011.

Sleigh, Jamie, Rebecca M Pullon, Phillip E Vlisides, and Catherine E Warnaby. 2019. "Electroencephalographic Slow Wave Dynamics and Loss of Behavioural Responsiveness Induced by Ketamine in Human Volunteers." *British Journal of Anaesthesia* 123 (5): 592–600. https://doi.org/10.1016/j.bja.2019.07.021.

Sloan, Steven A, and Ben A Barres. 2014. "Looks Can Be Deceiving: Reconsidering the Evidence for Gliotransmission." *Neuron* 84 (6): 1112–15. https://doi.org/10.1016/j.neuron.2014.12.003.

Sorge, Silke, Thomas Pollmächer, and Marike Lancel. 2004. “Clozapine Alters Sleep-Wake Behavior in Rats.” *Neuropsychopharmacology* 29 (8): 1462–69. https://doi.org/10.1038/sj.npp.1300445.

Spanò, Goffredina, Frederik D Weber, Gloria Pizzamiglio, Cornelia McCormick, Thomas D Miller, Clive R Rosenthal, Jamie O Edgin, and Eleanor A Maguire. 2020. “Sleeping with Hippocampal Damage.” *Current Biology* 30 (3): 523-529.e3. https://doi.org/10.1016/j.cub.2019.11.072.

Spierings, E L, M R Dzoljic, and M Godschalk. 1977. “Effect of Clozapine on the Sleep Pattern in the Rat.” *Pharmacology* 15 (6): 551–56. https://doi.org/10.1159/000136734.

Stagg, Charlotte Jane, J. G. Best, M. C. Stephenson, J. O’Shea, M. Wylezinska, Z. T. Kincses, P. G. Morris, P. M. Matthews, and H. Johansen-Berg. 2009. “Polarity-Sensitive Modulation of Cortical Neurotransmitters by Transcranial Stimulation.” *Journal of Neuroscience* 29 (16): 5202–6. https://doi.org/10.1523/JNEUROSCI.4432-08.2009.

Stagg, Charlotte Jane, Richard L Lin, Melvin Mezue, Andrew Segerdahl, Yazhuo Kong, Jingyi Xie, and Irene Tracey. 2013. “Widespread Modulation of Cerebral Perfusion Induced during and after Transcranial Direct Current Stimulation Applied to the Left Dorsolateral Prefrontal Cortex.” *The Journal of Neuroscience* 33 (28): 11425–31. https://doi.org/10.1523/JNEUROSCI.3887-12.2013.

Steinmetz, Nicholas A, Cagatay Aydin, Anna Lebedeva, Michael Okun, Marius Pachitariu, Marius Bauza, Maxime Beau, et al. 2021. “Neuropixels 2.0: A Miniaturized High-Density Probe for Stable, Long-Term Brain Recordings.” *Science* 372 (6539): eabf4588. https://doi.org/10.1126/science.abf4588.

Steriade, Mircea. 2003. “The Corticothalamic System in Sleep.” *Frontiers in Bioscience*, no. 4: 878–99.

Steriade, Mircea, D Contreras, R Curró Dossi, and A Nuñez. 1993. “The Slow (< 1 Hz) Oscillation in Reticular Thalamic and Thalamocortical Neurons: Scenario of Sleep Rhythm Generation in Interacting Thalamic and Neocortical Networks.” *The Journal of Neuroscience : The Official Journal of the Society for Neuroscience* 13 (8): 3284–99. http://www.ncbi.nlm.nih.gov/pubmed/8340808.

Steriade, Mircea, A Nunez, and F Amzica. 1993. “Intracellular Analysis of Relations between the Slow (< 1 Hz) Neocortical Oscillation and Other Sleep Rhythms of the Electroencephalogram.” *The Journal of Neuroscience* 13 (8): 3266–83. https://doi.org/10.1523/JNEUROSCI.13-08-03266.1993.

Steriade, Mircea, A Nuñez, and F Amzica. 1993. “A Novel Slow (< 1 Hz) Oscillation of Neocortical Neurons in Vivo: Depolarizing and Hyperpolarizing Components.” *The Journal of Neuroscience : The Official Journal of the Society for Neuroscience* 13 (8): 3252–65. http://www.ncbi.nlm.nih.gov/pubmed/8340806.

Steriade, Mircea, Igor Timofeev, and F Grenier. 2001. “Natural Waking and Sleep States: A View from inside Neocortical Neurons.” *Journal of Neurophysiology* 85 (5): 1969–85. https://doi.org/10.1152/jn.2001.85.5.1969.

Stille, G, A Sayers, H Lauener, and E Eichenberger. 1973. “6-(4-Methyl-1-Piperazinyl)Morphanthridine (Perlapine), a New Tricyclic Compound with Sedative and Sleep-Promoting Properties.” *Psychopharmacologia* 28 (4): 325–37. https://doi.org/10.1007/BF00422753.

Südhof, Thomas C, and Josep Rizo. 2011. “Synaptic Vesicle Exocytosis.” *Cold Spring Harbor Perspectives in Biology* 3 (12): a005637. https://doi.org/10.1101/cshperspect.a005637.

Suzuki, Ayako, Christopher M Sinton, Robert W Greene, and Masashi Yanagisawa. 2013. “Behavioral and Biochemical Dissociation of Arousal and Homeostatic Sleep Need Influenced by Prior Wakeful Experience in Mice.” *Proceedings of the National Academy of Sciences* 110 (25): 10288 LP – 10293. https://doi.org/10.1073/pnas.1308295110.

Szymusiak, Ronald, Noor Alam, Teresa L Steininger, and Dennis McGinty. 1998. “Sleep-Waking Discharge Patterns of Ventrolateral Preoptic/Anterior Hypothalamic Neurons in Rats.” *Brain Research* 803 (1–2): 178–88. https://doi.org/10.1016/S0006-8993(98)00631-3.

Tabachnick, B, and L Fidell. 2011. “Multivariate Analysis of Variance (MANOVA).” In *International Encyclopedia of Statistical Science*.

Takahashi, Joseph S. 2016. “Transcriptional Architecture of the Mammalian Circadian Clock.” *Nature Reviews Genetics* 18 (December): 164. https://doi.org/10.1038/nrg.2016.150.

Takata, Y, Y Oishi, X.-Z. Zhou, E Hasegawa, K Takahashi, Y Cherasse, T Sakurai, and M Lazarus. 2018. “Sleep and Wakefulness Are Controlled by Ventral Medial Midbrain/Pons GABAergic Neurons in Mice.” *Journal of Neuroscience* 38 (47): 10080–92. https://doi.org/10.1523/JNEUROSCI.0598-18.2018.

Tasic, Bosiljka, Zizhen Yao, Lucas T Graybuck, Kimberly A Smith, Thuc Nghi Nguyen, Darren Bertagnolli, Jeff Goldy, et al. 2018. “Shared and Distinct Transcriptomic Cell Types across Neocortical Areas.” *Nature* 563 (7729): 72–78. https://doi.org/10.1038/s41586-018-0654-5.

Taylor, Norman E, Christa J Van Dort, Jonathan D Kenny, JunZhu Pei, Jennifer A Guidera, Ksenia Y Vlasov, Justin T Lee, Edward S Boyden, Emery N Brown, and Ken Solt. 2016. “Optogenetic Activation of Dopamine Neurons in the Ventral Tegmental Area Induces Reanimation from General Anesthesia.” *Proceedings of the National Academy of Sciences of the United States of America* 113 (45): 12826–31. https://doi.org/10.1073/pnas.1614340113.

Thomas, Christopher W, Mathilde C C Guillaumin, Laura E McKillop, Peter Achermann, and Vladyslav V. Vyazovskiy. 2020. “Global Sleep Homeostasis Reflects Temporally and Spatially Integrated Local Cortical Neuronal Activity.” Edited by Inna Slutsky and Laura L Colgin. *ELife* 9: e54148. https://doi.org/10.7554/eLife.54148.

Thompson, Karen J, Elham Khajehali, Sophie J Bradley, Jovana S Navarrete, Xi Ping Huang, Samuel Slocum, Jian Jin, et al. 2018. “DREADD Agonist 21 Is an Effective Agonist for Muscarinic-Based DREADDs in Vitro and in Vivo.” *ACS Pharmacology & Translational Science* 1 (1): 61–72. https://doi.org/10.1021/acsptsci.8b00012.

Timofeev, Igor, and Sylvain Chauvette. 2018. “Sleep, Anesthesia, and Plasticity.” *Neuron* 97 (6): 1200–1202. https://doi.org/10.1016/j.neuron.2018.03.013.

Timofeev, Igor, F Grenier, M Bazhenov, T J Sejnowski, and Mircea Steriade. 2000. “Origin of Slow Cortical Oscillations in Deafferented Cortical Slabs.” *Cerebral Cortex* 10 (12): 1185–99. https://doi.org/10.1093/cercor/10.12.1185.

Tobler, Irene. 1983. “Effect of Forced Locomotion on the Rest-Activity Cycle of the Cockroach.” *Behavioural Brain Research* 8 (3): 351–60. https://doi.org/10.1016/0166-4328(83)90180-8.

Tobler, Irene, and Alexander A. Borbély. 1986. “Sleep EEG in the Rat as a Function of Prior Waking.” *Electroencephalography and Clinical Neurophysiology* 64 (1): 74–76. https://doi.org/10.1016/0013-4694(86)90044-1.

Tobler, Irene, and J Stalder. 1988. “Rest in the Scorpion—a Sleep-like State?” *Journal of Comparative Physiology A: Neuroethology*, 227–35. https://doi.org/10.1007/BF00612431.

Tononi, Giulio, and Chiara Cirelli. 2020. “Sleep and Synaptic Down-Selection.” *The European Journal of Neuroscience* 51 (1): 413–21. https://doi.org/10.1111/ejn.14335.

Torao-Angosto, Melody, Arnau Manasanch, Maurizio Mattia, and Maria V Sanchez-Vives. 2021. “Up and Down States During Slow Oscillations in Slow-Wave Sleep and Different Levels of Anesthesia.” *Frontiers in Systems Neuroscience*. https://www.frontiersin.org/article/10.3389/fnsys.2021.609645.

Tossell, Kyoko, Xiao Yu, Berta Anuncibay Soto, Mikal Vicente, Giulia Miracca, Panagiotis Giannos, Andawei Miao, et al. 2020. “Sleep Deprivation Triggers Somatostatin Neurons in Prefrontal Cortex to Initiate Nesting and Sleep via the Preoptic and Lateral Hypothalamus.” *BioRxiv*, January, 2020.07.01.179671. https://doi.org/10.1101/2020.07.01.179671.

Urban-Ciecko, Joanna, Erika E. Fanselow, and Alison L. Barth. 2015. “Neocortical Somatostatin Neurons Reversibly Silence Excitatory Transmission via GABAb Receptors.” *Current Biology* 25 (6): 722–31. https://doi.org/10.1016/j.cub.2015.01.035.

Urry, Emily, and Hans-Peter Landolt. 2015. “Adenosine, Caffeine, and Performance: From Cognitive Neuroscience of Sleep to Sleep Pharmacogenetics.” *Current Topics in Behavioral Neurosciences* 25: 331–66. https://doi.org/10.1007/7854_2014_274.

Uygun, David S, Zhiwen Ye, Anna Y Zecharia, Edward C Harding, Xiao Yu, Raquel Yustos, Alexei L Vyssotski, Stephen G Brickley, Nicholas P Franks, and William Wisden. 2016. “Bottom-Up versus Top-Down Induction of Sleep by Zolpidem Acting on Histaminergic and Neocortex Neurons.” *The Journal of Neuroscience : The Official Journal of the Society for Neuroscience* 36 (44): 11171–84. https://doi.org/10.1523/JNEUROSCI.3714-15.2016.

Vaidyanathan, Trisha V, Max Collard, Sae Yokoyama, Michael E Reitman, and Kira E Poskanzer. 2021. “Cortical Astrocytes Independently Regulate Sleep Depth and Duration via Separate GPCR Pathways.” Edited by Beth Stevens and Laura L Colgin. *ELife* 10: e63329. https://doi.org/10.7554/eLife.63329.

Varin, Christophe, and Patricia Bonnavion. 2019. “Pharmacosynthetic Deconstruction of Sleep-Wake Circuits in the Brain.” *Handbook of Experimental Pharmacology* 253: 153–206. https://doi.org/10.1007/164_2018_183.

Varin, Christophe, Pierre-Hervé Luppi, and Patrice Fort. 2018. “Melanin-Concentrating Hormone-Expressing Neurons Adjust Slow-Wave Sleep Dynamics to Catalyze Paradoxical (REM) Sleep.” *Sleep* 41 (6). https://doi.org/10.1093/sleep/zsy068.

Vassalli, Anne, and Paul Franken. 2017. “Hypocretin (Orexin) Is Critical in Sustaining Theta/Gamma-Rich Waking Behaviors That Drive Sleep Need.” *Proceedings of the National Academy of Sciences* 114 (27): E5464 LP-E5473. https://doi.org/10.1073/pnas.1700983114.

Vecchia, Dania, Riccardo Beltramo, Fabio Vallone, Ronan Chéreau, Angelo Forli, Manuel Molano-Mazón, Tanika Bawa, et al. 2020. "Temporal Sharpening of Sensory Responses by Layer V in the Mouse Primary Somatosensory Cortex." *Current Biology* 30 (9): 1589-1599.e10. https://doi.org/https://doi.org/10.1016/j.cub.2020.02.004.

Venner, Anne, Christelle Anaclet, Rebecca Y. Broadhurst, Clifford B. Saper, and Patrick M. Fuller. 2016. "A Novel Population of Wake-Promoting GABAergic Neurons in the Ventral Lateral Hypothalamus." *Current Biology* 26 (16): 2137–43. https://doi.org/https://doi.org/10.1016/j.cub.2016.05.078.

Verhage, Matthijs, Ascanio S Maia, Jaap J Plomp, Arjen B Brussaard, Joost H Heeroma, Hendrika Vermeer, Ruud F Toonen, et al. 2000. "Synaptic Assembly of the Brain in the Absence of Neurotransmitter Secretion." *Science* 287 (5454): 864 LP – 869. https://doi.org/10.1126/science.287.5454.864.

Villablanca, Jaime R. 2004. "Counterpointing the Functional Role of the Forebrain and of the Brainstem in the Control of the Sleep-Waking System." *Journal of Sleep Research* 13 (3): 179–208. https://doi.org/10.1111/j.1365-2869.2004.00412.x.

Vivo, Luisa De, Michele Bellesi, William Marshall, Eric A Bushong, Mark H Ellisman, Giulio Tononi, and Chiara Cirelli. 2017. "Ultrastructural Evidence for Synaptic Scaling Across the Wake/ Sleep Cycle." *Science* 355 (6324): 507–10. https://doi.org/10.1126/science.aah5982.

Vyazovskiy, Vladyslav V., Alexander A. Borbély, and Irene Tobler. 2000. "Unilateral Vibrissae Stimulation during Waking Induces Interhemispheric EEG Asymmetry during Subsequent Sleep in the Rat." *Journal of Sleep Research* 9 (4): 367–71. https://doi.org/10.1046/j.1365-2869.2000.00230.x.

Vyazovskiy, Vladyslav V., Chiara Cirelli, and Giulio Tononi. 2011. "Electrophysiological Correlates of Sleep Homeostasis in Freely Behaving Rats." *Progress in Brain Research* 193: 17–38. https://doi.org/10.1016/B978-0-444-53839-0.00002-8.

Vyazovskiy, Vladyslav V., and Kenneth D. Harris. 2013. "Sleep and the Single Neuron: The Role of Global Slow Oscillations in Individual Cell Rest." *Nature Reviews Neuroscience* 14 (6): 443–51. https://doi.org/10.1038/nrn3494.

Vyazovskiy, Vladyslav V., Umberto Olcese, Erin C Hanlon, Yuval Nir, Chiara Cirelli, and Giulio Tononi. 2011. "Local Sleep in Awake Rats." *Nature* 472 (7344): 443–47. https://doi.org/10.1038/nature10009.

Vyazovskiy, Vladyslav V., Umberto Olcese, Yaniv M. Lazimy, Ugo Faraguna, Steve K. Esser, Justin C. Williams, Chiara Cirelli, and Giulio Tononi. 2009. "Cortical Firing and Sleep Homeostasis." *Neuron* 63 (6): 865–78. https://doi.org/10.1016/j.neuron.2009.08.024.

Vyazovskiy, Vladyslav V., and Irene Tobler. 2012. "The Temporal Structure of Behaviour and Sleep Homeostasis." *PLoS ONE* 7 (12): 1–11. https://doi.org/10.1371/journal.pone.0050677.

Warnaby, Catherine E, Jamie W Sleigh, Darren Hight, Saad Jbabdi, and Irene Tracey. 2017. "Investigation of Slow-Wave Activity Saturation during Surgical Anesthesia Reveals a Signature of Neural Inertia in Humans." *Anesthesiology* 127 (4): 645–57. https://doi.org/10.1097/ALN.0000000000001759.

Washbourne, Philip, Peter M Thompson, Mario Carta, Edmar T Costa, James R Mathews, G Lopez-Bendito, Zoltán Molnár, et al. 2002. "Genetic Ablation of the T-SNARE SNAP-25 Distinguishes Mechanisms of Neuroexocytosis." *Nature Neuroscience* 5 (1): 19–26. https://doi.org/10.1038/nn783.

Weber, Franz, Shinjae Chung, Kevin T. Beier, Min Xu, Liqun Luo, and Yang Dan. 2015. "Control of REM Sleep by Ventral Medulla GABAergic Neurons." *Nature* 526 (7573): 435–38. https://doi.org/10.1038/nature14979.

Weber, Franz, and Yang Dan. 2016. "Circuit-Based Interrogation of Sleep Control." *Nature* 538 (7623): 51.

Werth, Esther, Peter Achermann, and Alexander A. Borbély. 1996. "Brain Topography of the Human Sleep EEG: Antero-Posterior Shifts of Spectral Power." *NeuroReport* 8 (1): 123–27. https://journals.lww.com/neuroreport/Fulltext/1996/12200/Brain_topography_of_the_human_sleep_EEG_.25.aspx.

———. 1997. "Fronto-Occipital EEG Power Gradients in Human Sleep." *Journal of Sleep Research* 6 (2): 102–12. https://doi.org/10.1046/j.1365-2869.1997.d01-36.x.

Wiegert, J Simon, Mathias Mahn, Matthias Prigge, Yoav Printz, and Ofer Yizhar. 2017. "Silencing Neurons: Tools, Applications, and Experimental Constraints." *Neuron* 95 (3): 504–29. https://doi.org/10.1016/j.neuron.2017.06.050.

Williams, Julie A, and Nirinjini Naidoo. 2020. "Sleep and Cellular Stress." *Current Opinion in Physiology* 15: 104–10. https://doi.org/https://doi.org/10.1016/j.cophys.2019.12.011.

Williams, Rhîannan H, Sarah W Black, Alexia M Thomas, Juliette Piquet, Bruno Cauli, and Thomas S Kilduff. 2019. "Excitation of Cortical NNOS/NK1R Neurons by Hypocretin 1 Is Independent of Sleep Homeostasis." *Cerebral Cortex* 29 (3): 1090–1108. https://doi.org/10.1093/cercor/bhy015.

Williams, Rhîannan H, Sarah W Black, Alexia M Thomas, Juliette Piquet, Bruno Cauli, Thomas S Kilduff, Jacqueline Vazquez-DeRose, et al. 2018. "Cortical NNOS/NK1 Receptor Neurons Are Regulated by Cholinergic Projections From the Basal Forebrain." *Cerebral Cortex* 28 (6): 1959–79. https://doi.org/10.1093/cercor/bhx102.

Wilson, Sue, Kirstie Anderson, David Baldwin, Derk-Jan Dijk, Audrey Espie, Colin Espie, Paul Gringras, et al. 2019. "British Association for Psychopharmacology Consensus Statement on Evidence-Based Treatment of Insomnia, Parasomnias and Circadian Rhythm Disorders: An Update." *Journal of Psychopharmacology* 33 (8): 923–47. https://doi.org/10.1177/0269881119855343.

Wisor, Jonathan P, Dmitry Gerashchenko, and Thomas S Kilduff. 2011. "Sleep-Active Neuronal Nitric Oxide Synthase-Positive Cells of the Cerebral Cortex: A Local Regulator of Sleep?" *Current Topics in Medicinal Chemistry* 11 (19): 2483–89. https://doi.org/10.2174/156802611797470367.

Xie, Lulu, Hongyi Kang, Qiwu Xu, Michael J Chen, Yonghong Liao, Meenakshisundaram Thiyagarajan, J. O'Donnell, et al. 2013. "Sleep Drives Metabolite Clearance from the Adult Brain." *Science* 342 (6156): 373–77. https://doi.org/10.1126/science.1241224.

Yamanaka, Akihiro, Carsten T Beuckmann, Jon T Willie, Junko Hara, Natsuko Tsujino, Michihiro Mieda, Makoto Tominaga, et al. 2003. "Hypothalamic Orexin Neurons Regulate Arousal According to Energy Balance in Mice." *Neuron* 38 (5): 701–13. https://doi.org/https://doi.org/10.1016/S0896-6273(03)00331-3.

Yao, Zizhen, Cindy T J van Velthoven, Thuc Nghi Nguyen, Jeff Goldy, Adriana E Sedeno-Cortes, Fahimeh Baftizadeh, Darren Bertagnolli, et al. 2021. "A Taxonomy of Transcriptomic Cell Types across the Isocortex and Hippocampal Formation." *Cell* 184 (12): 3222-3241.e26. https://doi.org/https://doi.org/10.1016/j.cell.2021.04.021.

Yasuda, Kyo, Lynn Churchill, Tadanobu Yasuda, Kelly Blindheim, Michael Falter, and James M Krueger. 2007. "Unilateral Cortical Application of Interleukin-1beta (IL1beta) Induces Asymmetry in Fos, IL1beta and Nerve Growth Factor Immunoreactivity: Implications for Sleep Regulation." *Brain Research* 1131 (1): 44–59. https://doi.org/10.1016/j.brainres.2006.11.051.

Yu, Xiao, Wei Ba, Guangchao Zhao, Ying Ma, Edward C Harding, Lu Yin, Dan Wang, et al. 2020. "Dysfunction of Ventral Tegmental Area GABA Neurons Causes Mania-like Behavior." *Molecular Psychiatry*. https://doi.org/10.1038/s41380-020-0810-9.

Yu, Xiao, Wen Li, Ying Ma, Kyoko Tossell, Julia J Harris, Edward C Harding, Wei Ba, et al. 2019. "GABA and Glutamate Neurons in the VTA Regulate Sleep and Wakefulness." *Nature Neuroscience* 22 (1): 106–19. https://doi.org/10.1038/s41593-018-0288-9.

Zhou, Mu, Zhihui Liu, Maxwell D Melin, Yi Han Ng, Wei Xu, and Thomas C Südhof. 2018. "A Central Amygdala to Zona Incerta Projection Is Required for Acquisition and Remote Recall of Conditioned Fear Memory." *Nature Neuroscience* 21 (11): 1515–19. https://doi.org/10.1038/s41593-018-0248-4.

Zhu, Hu, Dipendra K Aryal, Reid H.J. Olsen, Daniel J Urban, Amanda Swearingen, Stacy Forbes, Bryan L Roth, and Ute Hochgeschwender. 2016. "Cre-Dependent DREADD (Designer Receptors Exclusively Activated by Designer Drugs) Mice." *Genesis* 54 (8): 439–46. https://doi.org/10.1002/dvg.22949.

Zhu, Hu, Kristen E Pleil, Daniel J Urban, Sheryl S Moy, Thomas L Kash, and Bryan L Roth. 2014. "Chemogenetic Inactivation of Ventral Hippocampal Glutamatergic Neurons Disrupts Consolidation of Contextual Fear Memory." *Neuropsychopharmacology* 39 (8): 1880–92. https://doi.org/10.1038/npp.2014.35.